Wearable Chemo/bio-sensors for Sweat Sensing in Sports Applications: Combining Micro-fluidics and Novel Materials

Vincenzo Fabio Curto[1], M.Sc Eng

Thesis submitted for the Degree of Doctor of Philosophy

Supervisor: Prof. Dermot Diamond[1]

Dr. Fernando Benito-Lopez[1,2]

[1]CLARITY: Centre for Sensor Web Technologies, National Centre for Sensor Research, School of Chemical Sciences, Dublin City University, Dublin, Ireland;
[2]CIC microGUNE, Arrasate-Mondragón, Spain.

Dublin City University June 2013

Declaration

I hereby certify that this material, which I now submit for assessment on the programme of study leading to the award of Doctor of Philosophy is entirely my own work, and that I have exercised reasonable care to ensure that the work is original, and does not, to the best of my knowledge, breach any law of copyright, and has not been taken from the work of others save and to the extent that such work has been cited and acknowledged within the text of my work.

Signed: _____

(Vincenzo Fabio Curto)

ID No.: _____

Date: _____

Acknowledgements

First, I would like to thank Professor Dermot Diamond for giving me the opportunity to work in his group and to support all the scientific choices that I have made during these last three years. I really enjoyed my time working in your group at DCU and I will take beautiful memories with me, lifelong.

Special thanks must go to Fernando, who has been the perfect supervisor – no other PhD student could ask for better. For believing in me as a person and as a researcher – considering that I came as another Italian student with 110/110 *cum laude* grade. Thank you for all your support and all the confidence you put in me.

Thanks to all the collaborators I have been working with, starting form Dion, Xenofon, Professor Roisin Owens and Professor George Malliaras from the BEL department in France, Nuria from University of Granada, Vijay and Professor Douglas MacFarlane for Monash University and Anshika from University of Madras. The opportunity to collaborate with people of different backgrounds made my PhD more dynamic and fascinating.

Here I can't miss to thank all the people of the group: Bartosz, Larisa, Stefan, Alex, Cormac, Monika, Michele, Simon G., Andy, Giusy, Deirdre, Shirley, Kevin, Claudio, Simon C., Damien, John, Thomas, Fiachra, Dylan and all the other people who made this experience the best one ever.

To Viviana, who has been supporting and encouraging me during these three years of intense work; always there with me.

Mum and Dad, Filippo & Giusy, Claudia & Tommaso, Salvatore, Agatina, Luisa & Totò, you are a great family, thank you for all the support and love! My grandparents, aunties and uncles…you also made the person who I am today!

To Giuseppe and Roberta, real friends who has been and will be part of my life anywhere and anyway! Romeo *alias* "U Furmicula", Dario S. *alias* "U Sanfilì", Dario F. *alias* "Faccipò", Alessandro *alias* "Foca", Hilary, Giusy *alias* "Ciupina", Margherita, Enzo, Luciano *alias* "Barboncino", Jimmy, Ciccio, Antonino, "Il Tortorici" and hundreds more…companions of life experiences!!!

Now, let's hope for the best…

Ringraziamenti

Vorrei innanzitutto ringraziare Professor Dermot Diamond per avermi dato l'opportunità di lavorare nel suo gruppo di ricerca e per tutto il supporto nelle scelte scientifiche che ho preso durante questi ultimi tre anni. Ho trascorso tre bellissimi anni e porterò magnifici ricordi con me per tutta la vita.

Non posso che ringraziare a Fernando, che è stato un supervisore perfetto, nessun altro dottorato può chiedere di meglio. Per credere in me come persona e ricercatore, andando oltre allo stereotipo del neo-laureato italiano con voto 110/110 *cum laude*. Grazie per il tuo supporto e la fiducia che mi hai dato.

Grazie a tutti i collabboratori con cui ho attivamente lavorato in questi anni, Dion, Xenofon, Professor Roisin Owens e Professor George Malliaras del BEL department in Francia, Nuria dell'Università di Granada, Vijay e Professor Doug MacFarlane da Monash University e Anshika da University of Madras. L'opportunità di collaborare con voi ha reso il mio dottorato dinamico e affascinante.

Non posso che ringraziare tutte le persone del gruppo di ricerca: Bartosz, Larisa, Stefan, Alex, Cormac, Monika, Michele, Simon G., Andy, Giusy, Deirdre, Shirley, Kevin, Claudio, Simon C., Damien, John, Thomas, Fiachra, Dylan e tutti gli altri componenti che hanno reso questa esperienza indimenticabile.

A Viviana che mi ha supportato e incoraggiato durante questi tre anni di intenso lavoro. Presente in ogni momento.

Mamma e Papà, Filippo & Giusy, Claudia & Tommaso, Salvatore, Agatina, Luisa & Totò siete una famiglia magnifica, grazie per il sostegno e l'amore dimostratomi! Ai miei nonni, zii e zie…grazie anche a voi per aver cresciuto la persona che sono oggi!

A Giuseppe and Roberta, veri amici che sono stati e saranno parte della mia vita avunque e comunque! Romeo *alias* "U Furmicula", Dario S. *alias* "U Sanfilì", Dario F. *alias* "Faccipò", Alessandro *alias* "Foca", Hilary, Giusy *alias* "Ciupina", Margherita, Enzo, Luciano *alias* "Barboncino", Jimmy, Ciccio, Antonino, "Il Tortorici" e tutti gli altri…compagni di bellissime esperienze di vita!!!

E adesso, speriamo per il meglio…

List of Publications:

Peer-reviewed articles

1- **"Concept and Development of an Autonomous Wearable Micro-fluidic Platform for real time pH Sweat Analysis"** Vincenzo F. Curto, S. Coyle, R. Byrne, N. Angelov, D. Diamond, F. Benito-Lopez, *Sensors and Actuators B: Chemical*, 175 (2012) 263–270

2- **"Real-Time Sweat pH Monitoring Based on a Wearable Chemical Barcode Micro-fluidic Platform Incorporating Ionic Liquids"** Vincenzo F. Curto, Cormac Fay, Shirley Coyle, Robert Byrne, Corinne O'Toole, Caroline Barry, Sarah Hughes, Niall Moyna, Dermot Diamond, Fernando Benito-Lopez, *Sensors and Actuators B: Chemical*, 171–172 (2012) 1327–1334

3- **"Organic electrochemical transistor incorporating an ionogel as solid state electrolyte for lactate sensing"** Dion Khodagholy,* Vincenzo F. Curto,* Kevin J. Fraser, Moshe Gurfinkel, Robert Byrne, Dermot Diamond, George G. Malliaras, Fernando Benito-Lopez and Roisin M. Owens, *Journal of Material Chemistry*, 22 (2012) 4440-4443. (* Shared first author)

4- **"Optical sensing system based on wireless paired emitter detector diode device and ionogels for lab-on-a-disc water quality analysis"** M. Czugala, R. Gorkin, T. Phelan, J. Gaughran, Vincenzo F. Curto, J. Ducrée, D. Diamond and F. Benito-Lopez, *Lab on a Chip*, 12 (2012) 5069-5078

5- **"Sweat Analysis: Concept and Development of an Autonomous Wearable Micro-Fluidic Platform"** Vincenzo F. Curto, Shirley Coyle, Robert Byrne, Dermot Diamond, Fernando Benito-Lopez, *Procedia Engineering*, 25 (2012) 1561-1564

6- **" 'My Sweat my Health': Real Time Sweat Analysis Using Wearable Micro-fluidic Devices"** Vincenzo F. Curto, Nikolay Angelov, Shirley Coyle, Robert Byrne, Sarah Hughes, Niall Moyna, Dermot Diamond, Fernando Benito-Lopez, IEEE Conference publication related to the *"5th International Conference on Pervasive Computing Technologies for Healthcare (PervasiveHealth) and Workshops*", (2011), art. no. 6038789, 196-197. DOI 10.4108/icst.pervasivehealth.2011.246074.

7- **" 'Sweat-on-a-Chip': Analysing Sweat in Real Time with Disposable Micro-devices"** Fernando Benito-Lopez, Shirley Coyle, Robert Byrne, Vincenzo F. Curto, Dermot Diamond, IEEE Conference publication related to *"Sensors Conference, 2010"*, (2010) art. no, 5690681. DOI 10.1109/ICSENS.2010.5690681

8- **"Wearable Electrochemical Sensors for Monitoring Performance Athletes"**, K. J. Fraser, Vincenzo F. Curto, S. Coyle, B. Schazmann, R. Byrne, F. Benito-Lopez, R. M. Owens, G. G. Malliaras, D. Diamond, *Proceedings SPIE 8118*, 81180C-1, 2011; doi: 10.1117/12.895109.

9- **"Electrochemical Transistors with Ionic Liquids for Enzymatic Sensing"**, K. J. Fraser, S-Y. Yang, F. Cicoira, Vincenzo F. Curto, R. Byrne, F. Benito-Lopez, D. Khodagholy, R. M. Owens, G. G. Malliaras, D. Diamond, *Proceedings SPIE 8118 81180U-3*, 2011; doi: 10.1117/12.894412.

10- **"Fast prototyping of paper-based microfluidic devices by contact stamping using indelible ink"** Vincenzo F. Curto*, Nuria Lopez-Ruiz*, Luis F. Capitan-Vallvey, Alberto J. Palma, Fernando Benito-Lopez and Dermot Diamond, *Lab on a chip, submitted.* (* Shared first author)

11- **"Probing the specific ion effects of biocompatible hydrated choline ionic liquids on Lactate Oxidase biofunctionality"** *Vincenzo F. Curto*, Stefan Scheuermann, Roisin Owens, Vijayaraghavan Ranganathan, Douglas R. MacFarlane, Fernando Benito-Lopez and Dermot Diamond, *PCCP, submitted.*

Book Chapters

1. "**Properties and Customization of Materials for Bio- and Chemo-Sensing in Biomedical Applications**" Claudio Zuliani, Vincenzo F. Curto, Giusy Matzeu, Kevin Fraser, Dermot Diamond, book chapter – *Elsevier Publishing* - Book Series: Comprehensive Materials Processing, 2013, *accepted*.

Conference Presentations

Oral Presentations

1- **"Fast prototyping of paper-based microfluidic devices by contact stamping"**, Vincenzo F. Curto, Nuria Lopez-Ruiz, Luis F. Capitan-Vallvey, Alberto J. Palma, Fernando Benito-Lopez, Dermot Diamond, 17th International Conference on Miniaturized Systems for Chemistry and Life Sciences, Micro Total Analysis Systems μTAS, Freiburg, Germany, 27-31 October, 2013. (**abstract submitted**)

2- **"Continuous Multianalyte Detection Using an Organic Electrochemical Transistor"** Xenofon Strakosas, Dion Khodagholy, Vincenzo F. Curto, Moshe Gurfinkel, Dermot Diamond, George G. Malliaras, Fernando Benito-Lopez and Rosin Owens, 2013 MRS Spring Meeting, San Francisco, April 1-5.

3- **"Wearable Microfluidics: New Tools for In-situ Sweat Monitoring",** F. Benito-Lopez, VIncenzo F. Curto, S. Coyle, D. Diamond, Workshop on Wearable Sensors for Sports and Health, NCSR, Dublin City University, Ireland, 5 March, 2013.

4- **"Ionic Liquids in biosensors: influence of hydrated choline based ILs on the bio-functionality of Lactate Oxidase"** Vincenzo F. Curto, Stefan Scheuermann, Vijayaraghavan Ranganathan, Douglas R. MacFarlarne, Fernando Benito-Lopez and Dermot Diamond, 8th Annual International Electromaterials Science Symposium (ACES), North Wollongong, Australia, 13-15 Feb 2013. (**burster presentation**)

5- **"Functional Materials: Smart Solutions to Generate Useful Micro-fluidic Devices".** F. Benito-Lopez, L. Florea, Vncenzo F. Curto, M. Czugala, D. Diamond, 2nd International Symposium on Functional Nanomaterials, Dublin, Ireland, 6-7 September, 2012.

6- **"Micro-fluidic device for colorimetric analysis of sweat"**, Vincenzo F. Curto, Coyle Shirley, Diamond Dermot, Fernando Benito-Lopez, 4th International Conference "Smart Materials, Structures and Systems, Montecatini Terme, Italy, 10-12 June 2012.

7- **"Real-time analysis of sweat using integrated chemical sensors"**, Vincenzo F. Curto, Coyle Shirley, Diamond Dermot, Fernando Benito-Lopez, 4th International Conference "Smart Materials, Structures and Systems, Montecatini Terme, Italy, 10-12 June 2012.

8- **"Organic electrochemical transistor incorporating an ionogel as solid state electrolyte for lactate sensing"**, Vincenzo F. Curto, Dion Khodagholy, Kevin J. Fraser, Moshe Gurfinkel, Robert Byrne, George G. Malliaras, Roisin M. Owens, Dermot Diamond, Fernando Benito-Lopez, E-MRS spring meeting, Strasbourg, France, 8-14 May 2012.

9- **"Ionic Liquids for Enzymatic Sensing",** K. J Fraser, Vincenzo F. Curto, S. Scheuermann, F. Benito-Lopez, S. Warren, E. Dempsey, D. Diamond, ACS-Chemistry for Life, 243rd ACS National Meeting & Exposition, San Diego, California, USA, 25-29 March, 2012.

10- **"Photoswitchable Behaviour of New Spiropiran Derivatives",** D. Diamond, L. Florea, F. Benito-Lopez, Vincenzo F. Curto, SmartSurfaces2012: Solar & BioSensor Applications, Dublin, Ireland, 6-9 March, 2012.

11- **"Wearable Micro-Fluidic pH Sweat Sensing Device Based on Colorimetric Imaging Techniques"**, Vincenzo F. Curto, Shirley Coyle, Dermot Diamond, Fernando Benito-Lopez, Seminar in Micro-fluidics, University California Berkeley, California, USA, 10th October 2011 – **invited talk.**

12- **"Real-Time Sweat Analysis: Concept and Development of an Autonomous Wearable Micro-Fluidic Platform"**, Vincenzo F. Curto, Shirley Coyle, Robert Byrne, Dermot Diamond, Fernando Benito-Lopez, Eurosensors, Athens, Greece, 4-7 September, 2011.

13- **"Wearable Electrochemical Sensors for Monitoring High-performance Athletes"** K. J. Fraser, Vincenzo F. Curto, S. Coyle, B. Schazmann, R. Byrne, F. Benito-Lopez, R. M. Owens, G. G. Malliaras, D. Diamond, SPIE, San Diego, California, USA, 21-25 August, 2011.

14- **"Wearable Electrochemical Sensors for Monitoring High-performance Athletes"** K. J. Fraser, Vincenzo F. Curto, S. Coyle, B. Schazmann, R. Byrne, F. Benito-Lopez, R. M. Owens, G. G. Malliaras, D. Diamond, University California Berkeley, California, USA, 19 August, 2011– **invited talk.**

15- **"New Functional Materials for Fluid Control and Sensing in Microfluidic Devices",** F. Benito-Lopez, L. Florea, Vincenzo F. Curto, M. Czugala, K. J. Fraser, S. Coyle, R. Byrne, D. Diamond, University California Berkeley, California, USA14 July, 2011 – **invited talk.**

16- **"New Functional Materials for Fluid Control and Sensing in Microfluidic Devices",** L. Florea, V. F. Curto, M. Czugala, R. Byrne, S. Coyle, D. Diamond, F. Benito-Lopez, University of Granada, Spain, 10 June, 2011 – **invited talk.**

17- **" 'My Sweat my Health': Real Time Sweat Analysis with Wearable Micro-fluidic Devices",** F. Benito-Lopez, V. *F. Curto,* S. Coyle, R. Byrne, D. Diamond, ESPRIT Biosensing Workshop, Queen Mary, University of London, London, UK, 15 March, 2011 – **invited talk.**

Demo Presentations

18- **"Micro-fluidic device for colorimetric analysis of sweat"**, Vincenzo F. Curto, Shirley Coyle, Dermot Diamond, Fernando Benito-Lopez, Body Sensor Network Conference, London, UK, 10-13 May, 2012.

19- **" 'My Sweat my Health': Real Time Sweat Analysis Using Wearable Micro-fluidic Devices"**, Vincenzo F. Curto, Nikolay Angelov, Shirley Coyle, Robert Byrne, Sarah Hughes, Niall Moyna, Dermot Diamond, Fernando Benito-Lopez, 5th

International Conference on Pervasive Computing Technologies for Healthcare (PervasiveHealth) and Workshops, Dublin, Ireland, 23-26 May, 2011.

Poster Presentations

20- **"Multianalyte colourimetric water analysis, using a mobile phone, in a paper microfluidic"**, Nuria Lopez-Ruiz, Vincenzo F. Curto, Cormac Fay, Dermot Diamond, Fernando Benito-Lopez, Luis F. Capitan-Vallvey, Alberto J. Palma, 3rd International Conference on Bio–Sensing Technology, Sitges, Spain, 12-15 May, 2013.

21- **"Ionic Liquids in biosensors: influence of hydrated choline based ILs on the bio-functionality of Lactate Oxidase"** Vincenzo F. Curto, Stefan Scheuermann, Vijayaraghavan Ranganathan, Douglas R. MacFarlarne, Fernando Benito-Lopez and Dermot Diamond, 5th Congress on Ionic Liquids COIL-2013, Algarve, Portugal, 21-25 April, 2013.

22- **"Activation and Stabilisation of Lactate Oxidase in Ionic Liquids",** S. Scheuermann, Vincenzo F. Curto, D. Diamond, F. Benito-Lopez, MSE-2012 Materials Science Engineering, Darmstadt, Germany, 917, 25-27 September, 2012.

23- **"Ionic Liquids / Ionogels: New Materials for Inherently Biocompatble Molecular Sensors",** K. J. Fraser, Vincenzo F. Curto, D. Khodagholy, R. Byrne, F. Benito-Lopez, D. Diamond, G. Malliaras , R. Owens, Roisin, Irish Research Council Symposium, Dublin, Ireland, 22 September, 2012.

24- **"Label-free Metabolite Detection Using an Organic Electrochemical Transistor",** X. Strakosas, D. Khodagholy, Vincenzo F. Curto, K. J. Fraser, M. Gurfinkel, R. Byrne, D. Diamond, G. G. Malliaras, F. Benito-Lopez, R. M. Owens, E-MRS 2012 Spring Meeting, Strasbourg, France, 15-17 May, 2012.

25- **"Organic electrochemical transistor incorporating an ionogel as solid state electrolyte for lactate sensing"**, Vincenzo F. Curto, Dion Khodagholy, Kevin J. Fraser, Moshe Gurfinkel, Robert Byrne, George G. Malliaras, Roisin M. Owens, Dermot Diamond, Fernando Benito-Lopez, Smart Surface 2012, Dublin, Ireland, 6-9 March, 2012.

26- **"Electrochemical Transistors with Ionic Liquids for Enzymatic Sensing",** K. J. Fraser, R. Byrne, S.-Y- Yang, F. Cicoira, Vincenzo F. Curto, R. Byrne, F. Benito-Lopez, D. Khodagholy, R. M. Owens, G. G. Malliaras, D, Diamond, SPIE-2011, Optics and Photonics, San Diego, California, USA, 21 - 25 August, 2011.

27- **"Wearable Micro-Fluidic pH Sweat Sensing Device Based on Colorimetric Imaging Techniques"**, Vincenzo F. Curto, Cormac Fay, Shirley Coyle, Robert Byrne, Dermot Diamond, Fernando Benito-Lopez, 15th International Conference on Miniaturized Systems for Chemistry and Life Sciences, Seattle, Washington, USA, 2-6 October, 2011.

28- **"Phosphonium dicyanamide ionogel incorporating bromophenol blue dye as a versatile platform for monitoring pH in solution"**, Vincenzo F. Curto, Robert Byrne, Dermot Diamond, Fernando Benito-Lopez, 4th Congress on Ionic Liquids COIL-2011, Washington DC, 15-18 June, 2011.

29- **"Chemical barcodes for real-time sweat pH monitoring based on wearable microfluidic platforms incorporating ionic liquids"**, Vincenzo F. Curto, Shirley Coyle, Robert Byrne, Dermot Diamond, Fernando Benito-Lopez, Conference on Analytical Sciences Ireland 2011 - 6th CASi, Dublin, Ireland, 21-22 February, 2011.

Overall Aim and Thesis Structure

Overall Aim

The aim of this thesis is to explore the concept of wearable chemo/bio-sensing for real time sweat analysis during physical exercise. In order to fulfil this aim two different approaches have been followed, a technological one, which involves the fabrication of wearable micro-fluidic devices and a more fundamental approach, which investigates the capabilities of functional materials, ionogels and ionic liquids, in the realisation of wearable biosensors, *e.g.* lactic acid.

The fabrication and performance of wearable micro-fluidics devices, where the sensing active area is enclosed inside a micro-channel, are described in Chapter 3 and 4. The detection technique has been chosen with respect to the target analyte but taking into account the wearability of the whole system and the interrogation approach required to make the signal easily accessible to the user.

In Chapter 5 new approaches for the realisation of lactic acid biosensors have been investigated, giving priority to the flexibility and to the easy integration of the sensor into an electronic circuit (organic electrochemical transistor). In order to improve the life-time of the biosensor, novel matrix formulations for the lactic acid bio-receptor using ionic liquids have been meticulously investigated in Chapter 6.

In the last experimental chapter, Chapter 7, a new patterning technique is described for the realisation of micro-fluidic platforms based on capillary forces, describing its possible impact on the development of future wearable biosensors.

Selected publications and author contribution

This thesis includes one literature survey chapter, one book chapter accepted for publication, three original papers published in peer reviewed journals, two submitted publications and one future work and perspectives chapter. The core theme of the thesis is the development of wearable sensors using micro-fluidic devices. The ideas, development and writing up of all the papers in the thesis were the principal responsibility of myself, the candidate, working within CLARITY: Centre for Sensor Web Technologies, National Centre for Sensor Research, School of Chemical

Sciences, Dublin City University under the supervision of Professor Dermot Diamond and Dr. Fernando Benito-Lopez.

The inclusion of co-authors reflects the fact that part of the work came from active collaboration between researchers and acknowledges input into team-based research.

In the case of Chapters 2 to 7, my contribution to the work was as follows:

Thesis Chapter	Publication title	Publication status*	Nature and extent of candidate's contribution
2	**Properties and Customisation of Materials for Bio- and Chemo-Sensing in Biomedical Applications**	Accepted. book chapter – *Elsevier Science* (2013)	Author, manuscript development and writing up.
3	**Concept and development of an autonomous wearable micro-fluidic platform for real time pH sweat analysis**	Published. S*ensors and Actuators B: Chem.* 175 (2012) 263-270.	Main-author, key ideas, experimental design, data collection and analysis, manuscript development and writing up.
4	**Real-time sweat pH monitoring based on a wearable chemical barcode micro-fluidic platform incorporating ionic liquids**	Published. S*ensors and Actuators B: Chem.* 171-172(2012) 1327-1334.	Main-author, key ideas, experimental design, data collection and analysis, manuscript development and writing up.
5	**Organic electrochemical transistor incorporating an ionogel as a solid state electrolyte for lactate sensing**	Published. *Journal of Materials Chemistry* 22 (2012) 4440-4443.	Main-author, key ideas building on the previous electrochemical transistor concept, experimental design, data collection and analysis, manuscript development and writing up.
6	**Probing the specific ion effects of biocompatible hydrated choline ionic liquids on Lactate Oxidase biofunctionality**	Submitted. *Physical Chemistry Chemical Physics*	Main-author, key ideas, experimental design, data collection and analysis, manuscript development and writing up.
7	**Fast prototyping of paper-based microfluidic devices by contact stamping using indelible ink**	Submitted. *Lab on a chip*	Main-author, key ideas, experimental design, data collection and analysis, manuscript development and writing up.

Signed: …… ……

(Candidate) **(Principal Supervisor)**

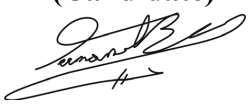

…… ……

(Co-Supervisor) **Date**

*For example, 'published'/ 'in press'/ 'accepted'/ 'returned for revision'/ 'submitted'

Chapter Overview

A detailed overview of each chapter together with the particular contributions from the research collaborators (where applicable), are given below:

Chapter 1: **Body Sensor Networks and Personal health management: An Overview**

This introductory chapter gives an overview of the reason behind the development of wearable sensor devices, giving particular attention to the concept of Wireless Sensor Network (WSN) and Body Sensor Network (BSN). Additionally, an overview of the integration of chemical/bio-sensors into wearable platforms is provided, as this is the core of the thesis.

Chapter 2: **Properties and Customisation of Materials for Bio- and Chemo-Sensing in Biomedical Applications**

This work, accepted as a book chapter, discusses the most recent examples of using novel material, such as Ionic Liquids, metal- and carbon-based nanoparticles and their composites, for the development of sensors in point-of-care devices. The possibilities of tuning the properties of these materials for sensing the target analytes is critically discussed, with a major focus on those systems that can have of immediate impact in the sensor market.

Chapter 3: **Concept and Development of an Autonomous Wearable Micro-fluidic Platform for Real Time pH Sweat Sensing**

This work, published as an original article, illustrates the development of a wearable colorimetric sensor for pH sensing. The two main focuses of the investigations are on the reduction of the electronic components dimensions in the detection system and on the micro-fluidic design and fabrication for performing real-time sweat analysis during physical exercise. This work has been done in collaboration with the engineering department at the NCSR, in particular with Dr. Shirley Coyle, who developed the electronic components of the detection system.

Chapter 4: **Real-Time Sweat pH Monitoring Based on a Wearable Chemical Barcode Micro-fluidic Platform Incorporating Ionic Liquids**

This work, published as an original article, illustrates a colorimetric micro-fluidic sensor for real-time pH detection. The sensor integrates four different sensing areas creating a barcode for wide pH spectrum detection, which can be detected by mean of a camera during cycling activity. This work has been done in collaboration with the engineering department at the NCSR, in particular with Mr. Cormac Fay, who developed the imaging processing algorithms.

Chapter 5: **Organic Electrochemical Transistor Incorporating an Ionogel as Solid State Electrolyte for Lactate Sensing**

This work, published as an original article, describes the integration of an ionogel (encapsulated Ionic Liquid in a polymeric matrix) in an organic electrochemical transistor (OECTs) for the detection of lactate. Moreover, an example of a flexible conformable OECTs is given as a futuristic prospective on wearable biosensing. This work has been done in collaboration with the Department of Bioelectronics (Ecole Nationale Superieure des Mines, Gardanne, France), in particular with Dr. Dion Khodagholy, who manufactured the OECTs and tested by myself during a research visit at the Department of Bioelectronics (France).

Chapter 6: **Probing the specific ion effects of biocompatible hydrated choline ionic liquids on Lactate Oxidase biofunctionality**

In this work, recently submitted as full research paper, describes the use of hydrated Ionic Liquids for the stabilisation of Lactate Oxidase (LOx) in solution. Spectroscopic techniques are employed in order to gain a better understanding of the ILs effects on the bioactivity LOx. This work has been done in collaboration with: the School of Chemistry of Monash University (Melbourne, Australia), in particular with Dr. Vijayaraghavan Ranganathan, who synthesised some of the Ionic Liquids used in this study and the Department of Bioelectronics (Ecole Nationale Superieure des Mines, Gardanne, France), in particular with Assistant Professor Roisin Owens, who gave relevant insight on the enzymatic activity of LOx.

Chapter 7: **Fast prototyping of paper-based microfluidic devices by contact stamping using indelible ink**

In this work, recently submitted as full research paper, presents the development of a single step technology for the realisation of paper-based micro-fluidic devices using just a indelible ink and a stamp, generating operative micro-fluidic structures in less than 10 seconds. This work has been carried out in collaboration with the Department of Electronics and Computer Technology (University of Granada, Spain), in particular with Miss Nuria Lopez-Ruiz, who came as visiting researcher to DCU and worked under my supervision, helping on the development of the technology.

Chapter 8: **Future Work and Perspectives**

This chapter suggests possible following paths of the work presented in this thesis. New strategies for the development of the electronic-free micro-fluidic pH sensor and novel approaches for the realisation of the wearable lactate sensor are presented.

Chapter 3

Chapter 4

Chapter 5

Chapter 6

Chapter 7

Chapter 8

Thesis Abstract

In the last decade, we have witnessed an exponential growth in the area of clinical diagnostic but surprisingly little has been done on the development of wearable chemo/bio-sensors in the field of sports science. In particular, the use of wearable wireless sensors capable of analysing sweat during physical exercise can provide access to new information sources that can be used to optimise and manage athletes' performance. Lab-on-a-Chip technology provides a fascinating opportunity for the development of such wearable sensors.

In this thesis two different colorimetric wearable microfluidic devices for real-time pH sensing were developed and used during athlete training activity. In one case a textile-based microfluidic platform employing cotton capillarity to drive sweat toward the pH sensitive area is presented that avoids the use of bulky fluid handling apparatus, *i.e.* pumps. The second case presents a wearable micro-fluidic device based on the use of pH responsive ionogels to obtain real-time sweat pH measurements through photo analysis of their colour variation.

The thesis also presents the first example of sweat lactate sensing using an organic electrochemical transistor incorporating an ionogel as solid-state electrolyte. In this chapter, optimization of the lactate oxidase stability when dissolved in number of hydrated ionic liquids is investigated. Finally, a new fabrication protocol for paper-based microfluidic technology is presented, which may have important implications for future applications such as low-cost diagnostics and chemical sensing technologies.

List of Abbreviations

$[C_2mIm][EtSO_4]$	1-ethyl-3-methyl imidazolium ethyl sulfate
$[P_{66614}]$ [dca]	Trihexyl(tetradecyl)phosphonium dicyanamide
4AAP	4-aminoantipyrine
ABS	Acrylonitrile Butadiene Styrene
BCG	Bromocresol Green
BCP	Bromocresol Purple
BPB	Bromophenol Blue
BSN	Body Sensor Network
BTB	Bromothymol Blue
CAAc	Choline Aminoacetate
CCl	Choline Chloride
CD	Circular Dichroism
CDHP	Choline Dihydrogenphosphate
CDHP/B	Choline Dihydrogenphosphate/Buffer
CF	Choline Formate
CG	Choline Gallate
CL	Choline Levulinate
CN	Choline Nitrate
CT	Choline Tartrate
CV	Choline Valporate
DMPA	2,2-Dimethoxy-2-phenylacetophenone
GO	Graphene Oxide
GOx	Glucose Oxidase
HBA	4-Hydroxybenzoic Acid
HRP	Peroxidase, from Horseradish
HSV	Hue Saturation Value
HT	High Tension
HyILs	Hydrated Ionic Liquids
k_{cat}	*turnover* number
K_M	Michaelis constant
LA	Lactic Acid

LOC	Lab on a Chip
LOx	Lactate Oxidase
MBAAm	*N,N′*-methylene bis(acrylamide)
MR	Methyl Red
MRE	Mean Residual Ellipticity
NIPAAm	N-isopropylacrylamide
OECTs	Organic Electrochemical Transistors
PDMS	Poly(dimethylsiloxale)
PEDOT:PSS	Poly(3,4-ethylenedioxythiophene) : poly(styrenesulfonate)
PMMA	Poly(methyl methacrylate)
POC	Point-of-Care
PSA	Pressure Sensitive Adhesive
RGB	Red Green Blue
rGO	Reduced Graphene Oxide
RTILs	Room Temperature Ionic Liquids
SM LEDs	Surface Mount Light Emitted Diodes
SSB	Sodium Sensor Belt
t_d	Delay time
t_r	Response time
v	*Enzymatic initial velocity*
v_0	*Enzymatic initial velocity day 0*
V_{max}	Max enzyme velocity
W	Designed stamp channel width
W_b	Percentage increment of the stamped border width
W_c	Percentage of the achieved channel width
W_{PDMS}	Width border employed PDMS stamp
W_{sb}	Stamped border width on the paper
W_{SC}	Stamped channel width on the paper
WSNs	Wireless Sensor Networks
μTAS	Micro-Total-Analysis-System

Chapter 1

Body Sensor Networks and Personal Health Management: an Overview

1.1 Wireless Sensor Networks and Personalised Health

Recent advances in the hi-tech sector and wireless network technologies have made worldwide access to low-cost, low-power multifunctional miniature sensor devices a reality. Each sensor represents a node that when inter-connected with other nodes can establish wireless sensor networks (WSNs).[1] WSNs have been recognised as a revolutionary way to perform ambient sensing in a wide range of application domains. This is because of the reliability, accuracy, flexibility, cost effectiveness and ease of deployment of wireless sensors using this communications infrastructure. WSNs can be used for military applications, habitat monitoring, infrastructure monitoring, agriculture and environmental monitoring. Another important field of application of WSNs is in healthcare monitoring and management.

Amongst others, one of the main challenges for modern healthcare is to provide improved services to an increasing number of people using limited financial and human resources. In this context pervasive healthcare is considered a solution to many existing problems. Pervasive healthcare can be defined as healthcare to anyone, anytime, and anywhere by removing locational, time and other restraints while increasing both its coverage and quality.[2]

The concept of pervasive health seeks to empower the individual with the ability to manage and assess its own state of health and healthcare needs. The use of point-of-care and/or wearable sensing devices could provide useful tools to overcome problems derived by infrequent clinical visits of patients to hospital structures and lack of data during daily activity and sleep time.[3] Long-term trend analysis will then reduce the potential severity of an illness if this is diagnosed during its early stage or when warning symptoms are manifesting. Moreover, in the case of rehabilitation a wearable sensing system could monitor the recovery process and detect complications as they arise.

1.2 Body Sensor Networks (BSN)

Body sensor network (BSN) technology refers to a sensor network made of devices that can be implantable and/or wearable devices capable of sensing biological

information from the body and transmitting it wirelessly to a base station device, such as mobile phone, personal computer, *etc.*[4]

A typical body sensor network is composed of tiny, lightweight, low-powered wireless sensors placed on/in patient's body to monitor vital signs, providing real-time feedback of chronic conditions, progress of recovery from illness, physiological condition during sport activities and other physiological conditions. The general idea of BSN is shown on Figure 1.1. The use of wireless technology can provide a significant improvement compared to conventional sensors used at the hospital level, which restrict the mobility of the patients because they are normally bulky and wired.[5]

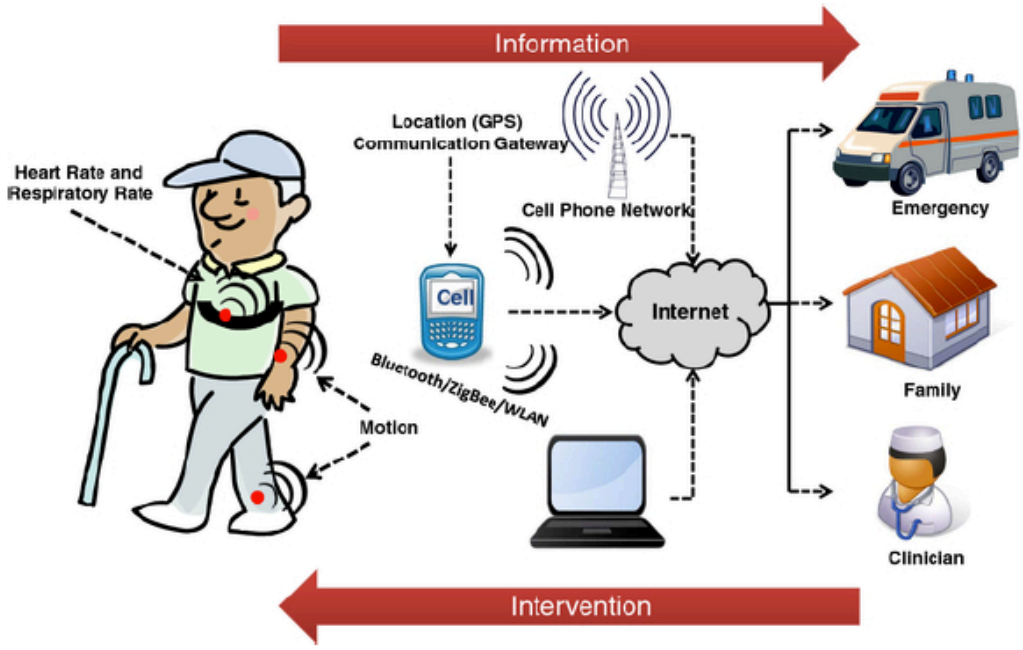

Figure 1.1. BSN based wearable personal health care system. (Adapted from reference [6])

To date one of the main areas of BSN research is the use of wearable sensors to sense physiological parameters such as heart or respiratory rate.[6] However, relatively little has been done on the development of wearable chemical sensors for real-time monitoring of diverse bodily fluids such as tears, sweat and urine. In the following sections of this Chapter, several examples of wearable systems presented in the literature are discussed, encompassing both physiological and chemo-/bio-sensors, with a particular focus on the latter.

1.2.1 Monitoring of Body Parameters

The majority of the existing wearable technologies are based on physical sensors (electrodes, thermistors and accelerometers) that respond to changes in their immediate environmental proximity, *e.g.* electric fields, heat and movement. Smart fabrics and interactive textiles are a relatively new area of research with many potential applications in the field of biomedical engineering and on future development of wearable sensors. The ability of smart textiles to interact with the body provides a novel means to sense the wearer's physiology and respond to the needs of the wearer. The advantage of this technology relies on the integration of sensors in the clothes that are worn on daily basis, providing the capacity to continuously monitor the physiology of the wearer.

The most common physiological parameters that have been studied using these kinds of sensors are electrocardiography (ECG),[7-9] electromyography (EMG),[10, 11] breathing,[12, 13] and body movements.[14-17]

ECG records the electrical activity of the heart from the skin surface and it is typically measured using silver chloride electrodes coupled to the skin with a gel. For instance, in clinical settings twelve electrodes are used, and these require wires and adhesive electrodes to be placed on the body. To overcome the limitations given by conventional ECG system, flexible conductive yarns, fully metal yarns, or natural/synthetics blended with conductive fibers have been knitted into garments to develop textile electrodes.[18] A study by Paradiso *et al.*[19] showed good correlation between fabric electrodes and traditional silver/silver chloride electrodes. Similar results were also obtained for the measurement of the electrical activity of muscles using surface EMG. In fact, it was shown that the signals from textile electrodes are in good agreement with traditionally measured surface EMG signals.[20]

Textile strain gauges and pressure sensors can also be integrated on textile to detect body movements such as breathing movements and foot pressure. Textile based strain sensors have been demonstrated using stretch fabrics modified with inherently conductive polymers[21] or carbon loaded rubbers.[22] Stretching of these textile sensors leads to a change in conductivity of the material, providing information about the breathing rate. Pang *et al.*[23] realised a skin-attachable strain

gauge sensor using two sandwiched layers of poly(dimethylsiloxane) (PDMS) modified with Platinum nanohairs (Figure 1.2-top). Within this system the interconnection and the electrical resistance of the nanohairs change upon the application of stimuli such as pressure, shear and torsion, as shown in Figure 1.2-bottom. The system was successfully applied for the measurement of heartbeat on the wrist.

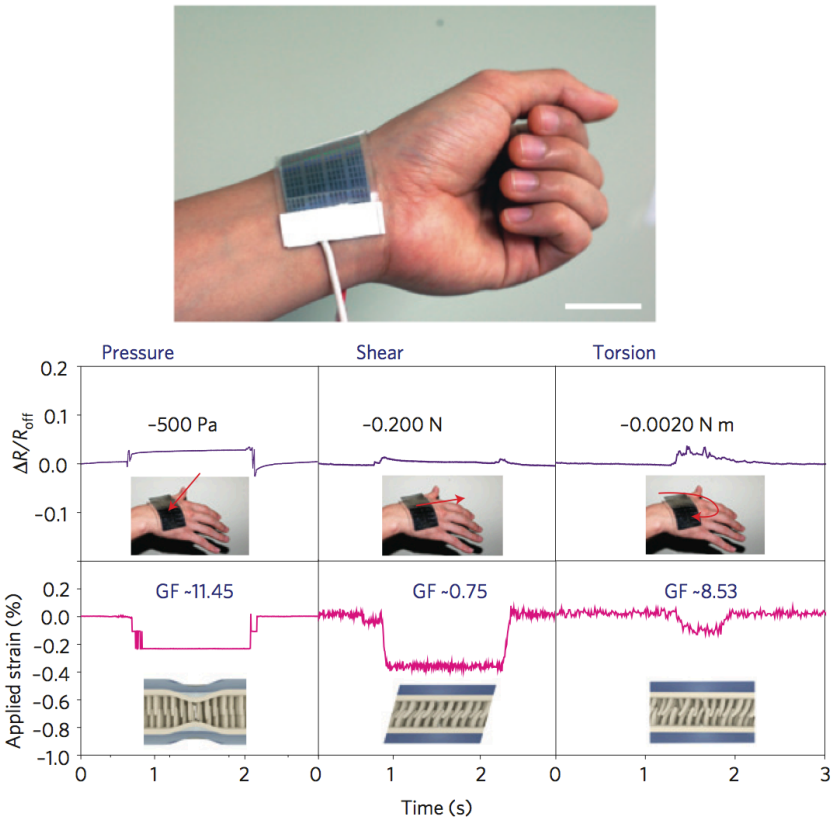

Figure 1.2. (top) Skin-attachable strain gauge sensor on human wrist. Scale bar 5 cm. (bottom) Detection and decoupling of pressure, shear and torsion loads with each time-dependent signal pattern of resistance ratio. (Adapted from reference [23])

The use of optical systems, for the realisation of smart textiles, is another common approach. For instance, blood oxygen saturation is normally estimated by pulse oximetry,[24] wherein the absorption of two different wavelengths of light through the tissue is measured. Photonic textiles using OLEDs can offer an alternative to conventional LEDs to create a textile based pulse oximetry system.[25] Sinusoidal shaped optical fibres stitched on textile have been employed for monitoring breathing.[26] Upon illumination of the fibres with a laser from one end, the light is detected using a photodiode placed on the other end of the fibres. The curvature of the bends affected the light attenuation through the fibre and the

analysis of the bending of these fibres was used to recognise the breathing movements of the wearer's upper body.

More recently the new trend on wearable sensors is the realisation of "conformal tattoo sensors", which adhere to the surface of the skin maximising the wearability of the sensor. Kim *et al.*[27] realised a stretchable epidermal electronics system (Figure 1.3-top) capable of sense a wide range of physiological parameters. The tattoo-like sensor showed reliable signals when tested for the measurement of ECG and EMG signals during simulated walking and standing activity. Moreover, the tattoo was also successfully applied for the remote control of a simple video game through movements of the neck using EMG signals. Additionally to this, the epidermal sensor presents high stretchability and adaptability to the body contours within different configurations (Figure 1.3-bottom), an important breakthrough for addressing future research.

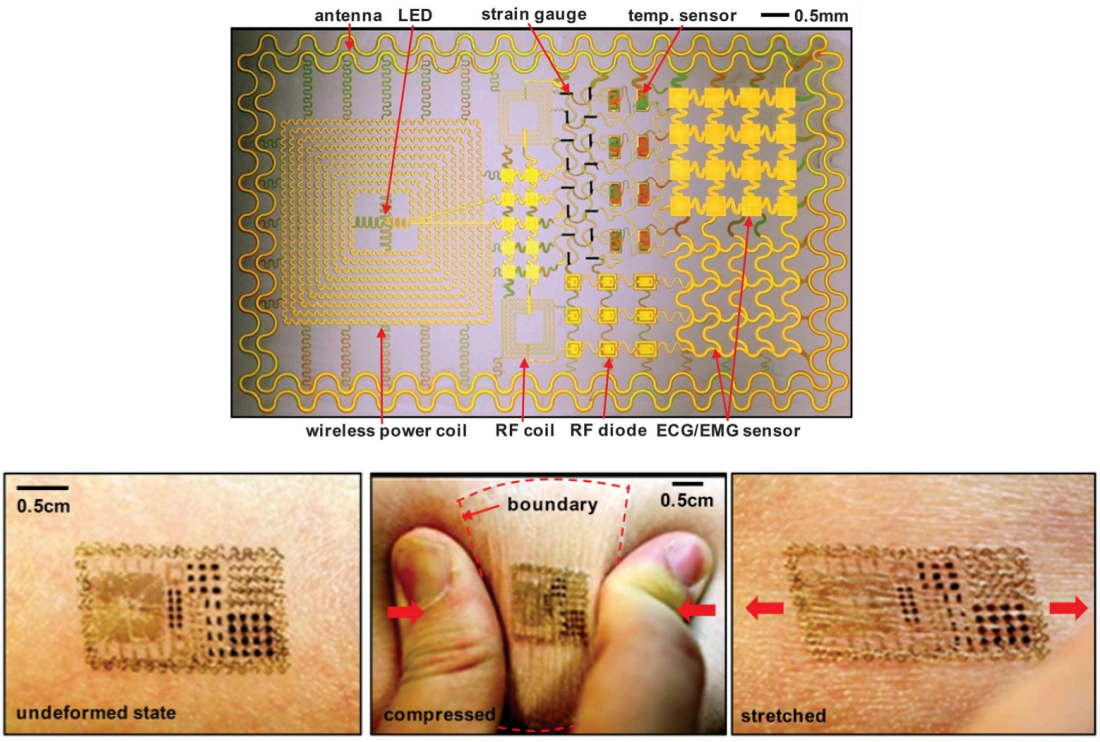

Figure 1.3. Image of the epidermal electronic sensor (top) and its application on skin when undeformed, compressed and stretched (bottom). (Adapted from reference [27])

Given the range of physiological signals that can be sensed, there are many scenarios and configurations to which wearable sensors can be applied. Therefore, an increasing interest on the field has brought a rapid growth in the number of EU

funded cooperative research projects on the development of these systems, such as MOBIHEALTH, WEALTHY, MYHEART, among others. [28]

1.2.2 On-body Chemosensing – Sweat Analysis

As previously stated, most of research to date in the field of wearable sensing focuses on physical transducers, mainly because of the technical barrier that wearable chemical sensors still need to overcome. These include sample collection and delivery, sensor calibration, ruggedness, lifetime and power consumption. Furthermore, wearability is probably the most important requirement that these sensors must fulfill without loosing functionality and, above all, compromising the wearer's comfort and/or safety.[3]

In a typical chemo-/biosensing scenario, samples must be delivered to the active surface on the sensor for a reaction to occur and the signal to be generated. For wearable chemo-/bio-sensors, the delivery of the sample is an issue closely related to the bodily fluid that has to be analysed. In most cases, the gold-standard fluid for diagnostics is blood. However, with wearable sensors the use of blood can be a limiting factor, for example, through drastic negative impact on the wearer's comfort. Although it is possible to find in the market wearable or semi-wearable sensing platforms for the detection of glucose[29] and lactate[30] in blood, much efforts, from the scientific community, have been put on the establishment of analytical methods wherein alternative bodily fluids can be employed, such as interstitial fluid,[31-33] tears,[34-36] saliva [37-41] and sweat.[42-47] The transition from blood analysis to other bodily fluids will provide less invasive approaches to sampling.

Integrated biosensors in contact lens can enable analyte targets in tears to be monitored, *e.g.* glucose, and this could represent a more convenient approach compared to conventional finger-picking sampling for glucose sensors. Badugu *et al.*[48] demonstrated the use of disposable contact lenses embedded with boronic acid-based fluorophores for the colorimetric detection of glucose. The contact lens changes colour according to the amount of sugar in tears, and is monitored by the wearer by simply looking into a mirror and comparing the colour to a pre-calibrated colour strip (Figure 1.4).

Electrochemical detection of tear biomarkers is also another common approach. Yao *et al.*[49] integrated a three-electrode electrochemical biosensor on a contact lens, while Kagie *et al.*[36] described a miniaturised flexible electrochemical biosensor suitable for insertion into the lacrimal canaliculus for amperometric detection. Although for the two systems the miniaturisation of the electronic components can be easily achieved, the integration into a wearable platform together with a battery for the supply of energy could compromise the effectiveness of the sensor.

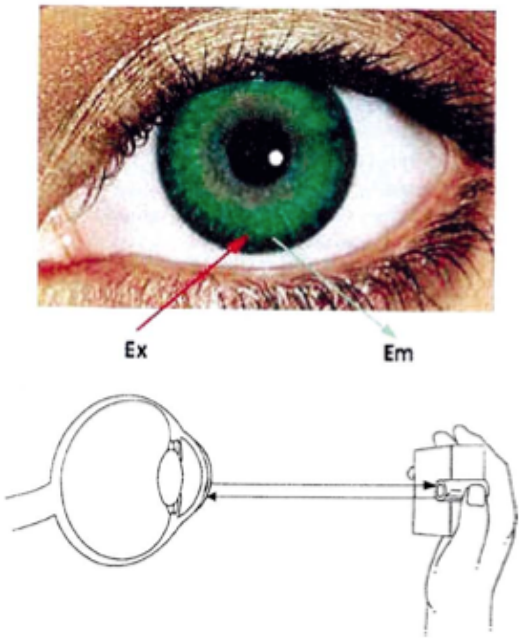

Figure 1.4. Potential methods for non-invasive continuous tear glucose monitoring using bore doped contact lenses (left) and schematic representation of the possible tear glucose sensing device (Bottom). (Adapted from reference [48])

Saliva is another interesting body fluid for monitoring different analytes and biomarkers, but no wearable chemo-sensors have been developed using saliva as the target fluid. However, the use of the saliva can be quite difficult due to the presence of mucus (making the sample viscous) and residual food and blood, which can induce misreading of the sensor.

Sweat is probably the most accessible fluid to be collected by a garment or from sensors integrated on smart vests.[50] Sweat is a body fluid naturally produced during physical exercise and emotional stress, and many relevant physiological analytes such as sodium, chloride, potassium, calcium, ammonia, glucose and lactate are normally dissolved in it.[51] Sweating is primarily a mechanism of body

thermoregulation to avoid dangerous increases in body temperature, related with an elevated metabolic rate of the individual.[52] For instance, sweat test of sodium and chloride concentration is the gold standard technique for the diagnosis of cystic fibrosis (CF).[50] Analysis of sweat loss and sweat composition can also offer valuable information regarding hydration status and electrolyte balance. The analysis of sweat composition can provide information regarding the physiological condition of the body and the health and well-being of the individual, especially during sports activities.[53]

Although several wearable real-time sweat sensors have been reported, to the best of our knowledge, no chemo-sensing platforms are commercially available in the market yet. The BIOTEX project was pioneering in the field of sweat analysis using wearable sensors.[54] The platform was developed using a textile-based system to collect, analyse and perform chemical measurements of sweat pH, sodium content and temperature (Figure 1.5-left).[55] This project will be briefly discussed in Chapter 3, where the second generation of such system is realised. Following a similar approach Salvo *et al.*[56] employed humidity sensors embedded on a textile to measure sweat rate. Recently, a sodium sensor belt (SSB) was developed by Schazmann *et al.*[43] to perform real-time measurements of sodium concentration in sweat using Ion Selective Electrode (ISE) technology, Figure 1.5-right. An application of the SSB was found for the comparison of sodium concentration in sweat in healthy and CF positive people during exercise.

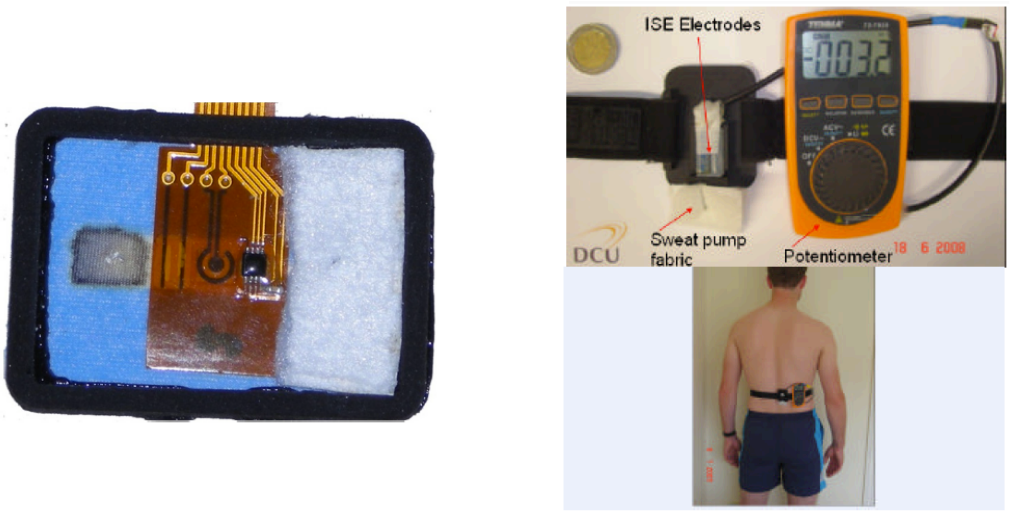

Figure 1.5. BIOTEX multiparametric patch containing pH indicator, conductivity, sodium, and temperature sensors (left) and the Sodium Sensor Belt (right). (Adapted from reference [55] and [43], respectively)

The development of suitable devices for continuous analysis of biomarkers dissolved in sweat, such as glucose and lactate has received relatively little attention. Wang *et al.*[57] demonstrated the possibility to print electrodes in clothing for the realisation of biosensors. Carbon strips were printed directly on the elastic waist of underwear, offering a tight and direct contact with the skin (Figure 1.6). The sensor was capable of maintaining its electrochemical behaviour after several cycles of folding or stretching of the supporting textile, indicating the potential application of this sensor configuration for the development of wearable electrochemical chemo-/biosensors. Moreover, a similar screen-printed electro-chemical sensor was also fabricated on underwater garments.[58]

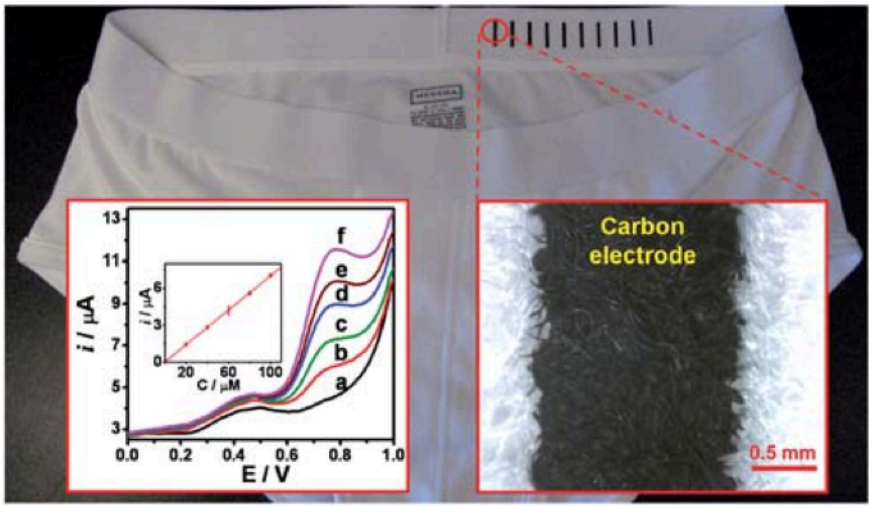

Figure 1.6. Image of screen-printed carbon electrodes on an underwear boxer. The two insets show the voltammetric response to different concentrations of NADH (left) and the morphology of a screen-printed electrode (right). (Adapted from reference [57])

It is clear that wearable chemical sensors have the potential to be employed for the continuous monitoring of the physiology of the wearer. This means that the wearer is kept informed of his/her well-being and can be actively involved in the management of their personal health, making pHealth (pervasive health) feasible. In this perspective, another field of impact for wearable technology is sports science, wherein diverse physiological conditions can exist during prolonged periods of training.[59] The opportunity to gather important information about the physiological status of the person during sport activities could potentially provide huge benefits for athletes, who can get personalised training regimes and rehydration/nutrition plans for future better performances. [60, 61]

1.3 Sweat Sampling: Micro-fluidics in Wearable Sensing

One of the main challenges regarding of sweat analysis is the difficulty of obtaining a valid sample, in particular when real-time information of sweat content needs to be gained during physical exercise. Difficulties arise from the high risk of cross-contamination of the samples during collection, handling and post-run analysis. Different sweat collection techniques have been employed over the years. Most common sweat collection techniques involve the use of patches (Figure 1.7-left) [62] and capsules made from flexible adhesive membranes using Parafilm.[63] A commercially available technique involves the use of pilocarpine intophoresis, in which a macroduct system is used to collect the sweat.[64] Shiffers *et al.*[65] proposed the whole body wash down technique (Figure 1.7-right), in which sweat loss from the whole body is determined by weighing the subject before and after exercise and collection of all fluid lost during the training period. However, the main limitation for these techniques is a substantial sampling to analysis delay (which can be from several hours to days in the case of the patches), with lack of real-time data of the body condition during physical efforts. Clearly, real-time information would give better understanding of the athletes' physiological state during training.

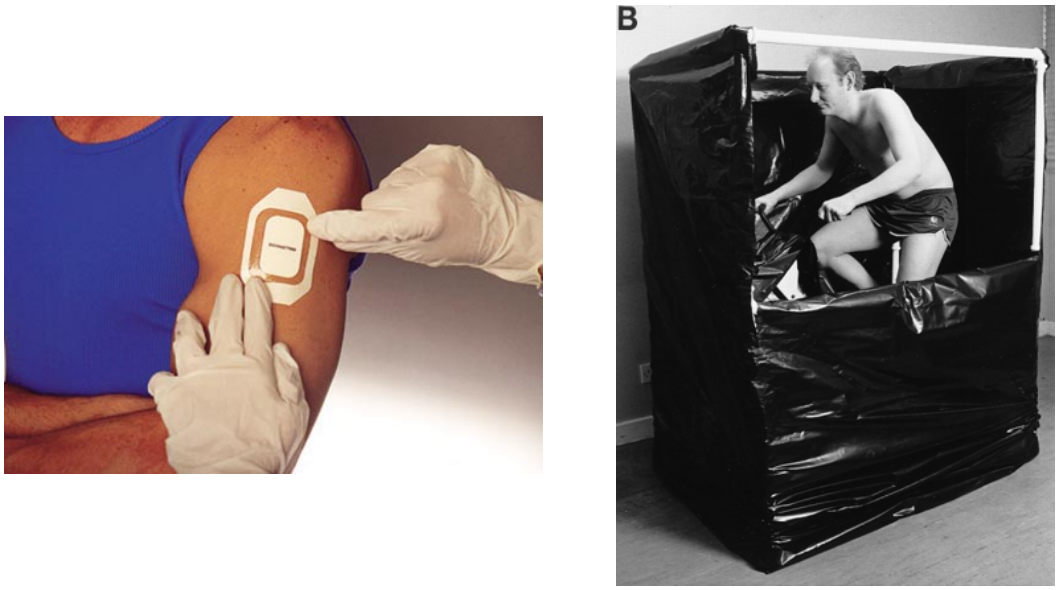

Figure 1.7. Commercially available patch for sweat collection (left) and set-up for sweat collection using the wash down technique (right). (Adapted from references [66] and [65], respectively)

In order to design viable autonomous wearable chemosensors, different factors need to be considered in order to achieve reliable systems capable of monitoring physical and/or bio-chemical conditions in real time. As already mentioned, sampling is crucial since the sample needs to be collected and delivered to the active sensing area where the analytical signal will be generated. Another important requirement to take into account is the flexibility of the device in order to be wearable and adaptable to the body contours (minimising the discomfort to the wearer), with respect to the integrated detection system. Therefore, real-time sweat analysis when performed during exercise is a great challenge for sensor fabrication due to the need for on-body fluid handling, sensor deployment and data management. If all these issues can be accomplished, the obtained devices will be capable of providing immediate feedback on fluid loss and variations of sweat analytes, giving prompt and reliable information of athlete performance and/or general health.

Micro-fluidics is an emerging area that is impacting in several fields, especially on the development of personalised health care and point-of-care diagnostic devices.[67] Amongst others, the main advantage of using micro-fluidic system is given by the possibility to deal with micro-volumes of the target sample, obtaining exactly the same information that is provided by standard analytical techniques.[68] Despite this, sweat is still a largely unexplored bodily fluid for analysis using micro-fluidic systems.

Although the realisation of a system capable of fulfilling all the required specifications will not be easy to achieve, in this thesis it is proposed that the employment of micro-fluidic technology is an effective means to succeed where other methods have failed or showed limitations on the sampling of sweat. In particular, because micro-liter volumes of sweat are needed to perform these measurements, the fluid handling system of the sensor can be simplified and the size reduced. However, the main advantage relies on the possibility of integrating the sensing active area inside the micro-fluidic channel, thereby minimising delay between sampling and analysis of the specimen.

With regard to the sensing materials, a more detailed overview will be given in the next chapter, in which emerging materials recently used for the development of chemo/bio-sensors are discussed in detail.

1.4 References

1. Tubaishat, M.; Madria, S., Sensor networks: an overview. *Potentials, IEEE* **2003,** *22*, 20-23.
2. Varshney, U., Pervasive Healthcare and Wireless Health Monitoring. *Mobile Networks and Applications* **2007,** *12*, 113-127.
3. Diamond, D.; Coyle, S.; Scarmagnani, S.; Hayes, J., Wireless Sensor Networks and Chemo-/Biosensing. *Chemical Reviews* **2008,** *108*, 652-679.
4. Yang, G.-Z., *Body Sensor Networks*. Springer-Verlag New York, Inc.: 2006.
5. Darwish, A.; Hassanien, A. E., Wearable and Implantable Wireless Sensor Network Solutions for Healthcare Monitoring. *Sensors* **2011,** *11*, 5561-5595.
6. Patel, S.; Park, H.; Bonato, P.; Chan, L.; Rodgers, M., A review of wearable sensors and systems with application in rehabilitation. *Journal of NeuroEngineering and Rehabilitation* **2012,** *9*, 21.
7. Oresko, J. J.; Zhanpeng, J.; Jun, C.; Shimeng, H.; Yuwen, S.; Duschl, H.; Cheng, A. C., A Wearable Smartphone-Based Platform for Real-Time Cardiovascular Disease Detection Via Electrocardiogram Processing. *Information Technology in Biomedicine, IEEE Transactions on* **2010,** *14*, 734-740.
8. Finlay, D. D.; Nugent, C. D.; Donnelly, M. P.; McCullagh, P. J.; Black, N. D., Optimal Electrocardiographic Lead Systems: Practical Scenarios in Smart Clothing and Wearable Health Systems. *Information Technology in Biomedicine, IEEE Transactions on* **2008,** *12*, 433-441.
9. Ueno, A.; Akabane, Y.; Kato, T.; Hoshino, H.; Kataoka, S.; Ishiyama, Y., Capacitive Sensing of Electrocardiographic Potential Through Cloth From the Dorsal Surface of the Body in a Supine Position: A Preliminary Study. *Biomedical Engineering, IEEE Transactions on* **2007,** *54*, 759-766.
10. Yuwei, C.; Ruizhi, C.; Xiang, C.; Wei, C.; Qian, W. In *Wearable electromyography sensor based outdoor-indoor seamless pedestrian navigation using motion recognition method*, Indoor Positioning and Indoor Navigation (IPIN), 2011 International Conference on, 21-23 Sept. **2011**, 1-9.
11. Akita, J.; Shinmura, T.; Sakurazawa, S.; Yanagihara, K.; Kunita, M.; Toda, M.; Iwata, K., Wearable electromyography measurement system using cable-free network system on conductive fabric. *Artificial Intelligence in Medicine* **2008,** *42*, 99-108.
12. Paradiso, R.; Loriga, G.; Taccini, N., A wearable health care system based on knitted integrated sensors. *Information Technology in Biomedicine, IEEE Transactions on* **2005,** *9*, 337-344.
13. Di Rienzo, M.; Rizzo, F.; Meriggi, P.; Castiglioni, P.; Mazzoleni, P.; Parati, G.; Bordoni, B.; Brambilla, G.; Ferratini, M., MagIC system. *Engineering in Medicine and Biology Magazine, IEEE* **2009,** *28*, 35-40.
14. Bartalesi, R.; Lorussi, F.; Tognetti, A.; Tesconi, M.; Zupone, G.; Carbonaro, N.; De Rossi, D., Wearable Kinesthetic Sensors For Body Posture and Movement Analysis. *Journal of Biomechanics* **2007,** *40, Supplement 2*, S425-S427.
15. Lin, C.-S.; Hsu, H. C.; Lay, Y.-L.; Chiu, C.-C.; Chao, C.-S., Wearable device for real-time monitoring of human falls. *Measurement* **2007,** *40*, 831-840.
16. Ermes, M.; Parkka, J.; Mantyjarvi, J.; Korhonen, I., Detection of Daily Activities and Sports With Wearable Sensors in Controlled and Uncontrolled Conditions. *Information Technology in Biomedicine, IEEE Transactions on* **2008,** *12*, 20-26.
17. Aylward, R.; Paradiso, J. A. In *A Compact, High-Speed, Wearable Sensor Network for Biomotion Capture and Interactive Media*, Information Processing in Sensor

Networks, 2007. IPSN 2007. 6th International Symposium on, 25-27 April **2007**, 380-389.

18. Catrysse, M.; Puers, R.; Hertleer, C.; Van Langenhove, L.; Van Egmond, H.; Matthys, D.; Leuven, K. U. In *Fabric sensors for the measurement of physiological parameters* Transducers '03,12th International Conference on Solid-State Sensors, Actuators and Microsystems, Boston, U.S.A., **2003**, 1758 - 1761.
19. Paradiso, R.; Belloc, C.; Loriga, G.; Taccini, N., Wearable healthcare systems, new frontiers of e-textile. In *Studies in Health Technology and Informatics, Volume 117, 2005, Personalised Health Management Systems - The Integration of Innovative Sensing, Textile, Information and Communication Technologies*, Nugent, C. D.; McCullagh, P. J.; McAdams, E. T.; Lymberis, A., Eds. **2005**.
20. Finni, T.; Hu, M.; Kettunen, P.; Vilavuo, T.; Cheng, S., Measurement of EMG activity with textile electrodes embedded into clothing. *Physiological Measurement* **2007,** *28*, 1405–1419.
21. Rovira Carlos, W. T., McCoy Aaron, Shirley Coyle, Brian Corcoran, Florin Stroiescu, Kieran Daly,Dermot Diamond, In *Web-based Wearable Sensor Streaming for Respiratory Monitoring Applications.*, IEEE Sensors, Limerick, Ireland, **2011**.
22. Tognetti, A.; Lorussi, F.; Tesconi, M.; Bartalesi, R.; Zupone, G.; De Rossi, D. In *Wearable kinesthetic systems for capturing and classifying body posture and gesture*, Engineering in Medicine and Biology 27th Annual Conference, Shanghai, China, September 1-4, **2005**.
23. Pang, C.; Lee, G.-Y.; Kim, T.-i.; Kim, S. M.; Kim, H. N.; Ahn, S.-H.; Suh, K.-Y., A flexible and highly sensitive strain-gauge sensor using reversible interlocking of nanofibres. *Nat Mater* **2012,** *11*, 795-801.
24. WHO; World; Health; Organization, http://www.who.int/patientsafety/safesurgery/pulse_oximetry/en/. **June 12th 2013**.
25. Rothmaier, M.; Selm, B.; Spichtig, S.; Haensse, D.; Wolf, M., Photonic textiles for pulse oximetry. *Optics Express* **2008,** *16*, 12973-12986.
26. D'Angelo, L. T.; Weber, S.; Honda, Y.; Thiel, T.; Narbonneau, F.; Luth, T. C. In *A system for respiratory motion detection using optical fibers embedded into textiles*, Engineering in Medicine and Biology Society, 2008. EMBS 2008. 30th Annual International Conference of the IEEE, 20-25 Aug. 2008, 2008; 2008; pp 3694-3697.
27. Kim, D.-H.; Lu, N.; Ma, R.; Kim, Y.-S.; Kim, R.-H.; Wang, S.; Wu, J.; Won, S. M.; Tao, H.; Islam, A.; Yu, K. J.; Kim, T.-i.; Chowdhury, R.; Ying, M.; Xu, L.; Li, M.; Chung, H.-J.; Keum, H.; McCormick, M.; Liu, P.; Zhang, Y.-W.; Omenetto, F. G.; Huang, Y.; Coleman, T.; Rogers, J. A., Epidermal Electronics. *Science* **2011,** *333*, 838-843.
28. CORDIS http://cordis.europa.eu/home_en.html.
29. Medtronic http://www.medtronicdiabetes.com/products/guardiancgm.
30. HaBdirect http://www.habdirect.com.au/Lactate_Scout_Solo_Lactate_Analyser_p/lacsc.htm.
31. Woderer, S.; Henninger, N.; Garthe, C.-D.; Kloetzer, H. M.; Hajnsek, M.; Kamecke, U.; Gretz, N.; Kraenzlin, B.; Pill, J., Continuous glucose monitoring in interstitial fluid using glucose oxidase-based sensor compared to established blood glucose measurement in rats. *Analytica Chimica Acta* **2007,** *581*, 7-12.
32. Facchinetti, A.; Sparacino, G.; Cobelli, C., Reconstruction of Glucose in Plasma from Interstitial Fluid Continuous Glucose Monitoring Data: Role of Sensor Calibration. *Journal of Diabetes Science and Technology* **2007,** *1*, 617-623.

33. Rebrin, K.; NF, N. S.; Steil, G., Use of subcutaneous interstitial fluid glucose to estimate blood glucose: revisiting delay and sensor offset. *Journal of Diabetes Science and Technology* **2010,** *4*, 1087-1098.

34. Iguchi, S.; Kudo, H.; Saito, T.; Ogawa, M.; Saito, H.; Otsuka, K.; Funakubo, A.; Mitsubayashi, K., A flexible and wearable biosensor for tear glucose measurement. *Biomedical Microdevices* **2007,** *9*, 603-609.

35. Chu, M.; Shirai, T.; Takahashi, D.; Arakawa, T.; Kudo, H.; Sano, K.; Sawada, S.-i.; Yano, K.; Iwasaki, Y.; Akiyoshi, K.; Mochizuki, M.; Mitsubayashi, K., Biomedical soft contact-lens sensor for <i>in situ</i> ocular biomonitoring of tear contents. *Biomedical Microdevices* **2011,** *13*, 603-611.

36. Kagie, A.; Bishop, D. K.; Burdick, J.; La Belle, J. T.; Dymond, R.; Felder, R.; Wang, J., Flexible Rolled Thick-Film Miniaturized Flow-Cell for Minimally Invasive Amperometric Sensing. *Electroanalysis* **2008,** *20*, 1610-1614.

37. Papacosta, E.; Nassis, G. P., Saliva as a tool for monitoring steroid, peptide and immune markers in sport and exercise science. *Journal of Science and Medicine in Sport* **2011,** *14*, 424-434.

38. Ljungberg, G.; Ericson, T.; Ekblom, B.; Birkhed, D., Saliva and marathon running. *Scandinavian Journal of Medicine & Science in Sports* **1997,** *7*, 214-219.

39. Ghimenti, S.; Lomonaco, T.; Onor, M.; Murgia, L.; Paolicchi, A.; Fuoco, R.; Ruocco, L.; Pellegrini, G.; Trivella, M. G.; Di Francesco, F., Measurement of Warfarin in the Oral Fluid of Patients Undergoing Anticoagulant Oral Therapy. *PLoS ONE* **2011,** *6*, e28182.

40. Yang, C.-Y.; Brooks, E.; Li, Y.; Denny, P.; Ho, C.-M.; Qi, F.; Shi, W.; Wolinsky, L.; Wu, B.; Wong, D. T. W.; Montemagno, C. D., Detection of picomolar levels of interleukin-8 in human saliva by SPR. *Lab on a Chip* **2005,** *5*, 1017-1023.

41. Yoda, K.; Shimazaki, K.; Ueda, Y., Analysis of Glycolysis Relevant Compounds in Saliva by Microbiosensors. *Annals of the New York Academy of Sciences* **1998,** *864*, 600-604.

42. Souza, A. P. R. d.; Lima, A. S.; Salles, M. O.; Nascimento, A. N.; Bertotti, M., The use of a gold disc microelectrode for the determination of copper in human sweat. *Talanta* **2010,** *83*, 167-170.

43. Schazmann, B.; Morris, D.; Slater, C.; Beirne, S.; Fay, C.; Reuveny, R.; Moyna, N.; Diamond, D., A wearable electrochemical sensor for the real-time measurement of sweat sodium concentration. *Analytical Methods* **2010,** *2*, 342-348.

44. Cai, X.; Yan, J. L.; Chu, H. H.; Wu, M. S.; Tu, Y. F., An exercise degree monitoring biosensor based on electrochemiluminescent detection of lactate in sweat. *Sensors and Actuators B-Chemical* **2009,** *143*, 655-659.

45. Mebazaa, R.; Rega, B.; Camel, V. r., Analysis of human male armpit sweat after fenugreek ingestion: Characterisation of odour active compounds by gas chromatography coupled to mass spectrometry and olfactometry. *Food Chemistry* **2011,** *128*, 227-235.

46. Hirokawa, T.; Okamoto, H.; Gosyo, Y.; Tsuda, T.; Timerbaev, A. R., Simultaneous monitoring of inorganic cations, amines and amino acids in human sweat by capillary electrophoresis. *Analytica Chimica Acta* **2007,** *581*, 83-88.

47. Kidwell, D. A.; Holland, J. C.; Athanaselis, S., Testing for drugs of abuse in saliva and sweat. *Journal of Chromatography B: Biomedical Sciences and Applications* **1998,** *713*, 111-135.

48. Badugu, R.; Lakowicz, J. R.; Geddes, C. D., A Glucose Sensing Contact Lens: A Non-Invasive Technique for Continuous Physiological Glucose Monitoring. *Journal of Fluorescence* **2003,** *13*, 371-374.

49. Yao, H.; Shum, A. J.; Cowan, M.; L√§hdesm√§ki, I.; Parviz, B. A., A contact lens with embedded sensor for monitoring tear glucose level. *Biosensors and Bioelectronics* **2011,** *26*, 3290-3296.
50. Coyle, S.; Benito-Lopez, F.; Radu, T.; Lau, K. T.; Diamond, D., Fibers and fabrics for chemical and biological sensing. *J. Text. App.* **2010,** *14*.
51. Whitehouse, A. G. R., The Dissolved Constituents of Human Sweat. *Proceedings of the Royal Society of London. Series B, Biological Sciences* **1935,** *117*, 139-154.
52. Wilke, K.; Martin, A.; Terstegen, L.; Biel, S. S., A short history of sweat gland biology. *International Journal of Cosmetic Science* **2007,** *29*, 169-179.
53. Morris, D.; Schazmann, B.; Wu, Y.; Coyle, S.; Brady, S.; Fay, C.; Hayes, J.; Lau, K.; Wallace, G.; Diamond, D., Wearable technology for bio-chemical analysis of body fluids during exercise. **2008**, 5741 - 5744.
54. BIOTEX http://www.biotex-eu.com/.
55. Coyle, S.; King-Tong, L.; Moyna, N.; O'Gorman, D.; Diamond, D.; Di Francesco, F.; Costanzo, D.; Salvo, P.; Trivella, M. G.; De Rossi, D. E.; Taccini, N.; Paradiso, R.; Porchet, J. A.; Ridolfi, A.; Luprano, J.; Chuzel, C.; Lanier, T.; Revol-Cavalier, F.; Schoumacker, S.; Mourier, V.; Chartier, I.; Convert, R.; De-Moncuit, H.; Bini, C., BIOTEX - Biosensing Textiles for Personalised Healthcare Management. *Information Technology in Biomedicine, IEEE Transactions on* **2010,** *14*, 364-370.
56. Salvo, P.; Di Francesco, F.; Costanzo, D.; Ferrari, C.; Trivella, M. G.; De Rossi, D., A Wearable Sensor for Measuring Sweat Rate. *Sensors Journal, IEEE* **2010,** *10*, 1557-1558.
57. Yang, Y.-L.; Chuang, M.-C.; Lou, S.-L.; Wang, J., Thick-film textile-based amperometric sensors and biosensors. *Analyst* **2010,** *135*, 1230-1234.
58. Malzahn, K.; Windmiller, J. R.; Valdes-Ramirez, G.; Schoning, M. J.; Wang, J., Wearable electrochemical sensors for in situ analysis in marine environments. *Analyst* **2011,** *136*, 2912-2917.
59. Taylor, N.; Machado-Moreira, C., Regional variations in transepidermal water loss, eccrine sweat gland density, sweat secretion rates and electrolyte composition in resting and exercising humans. *Extreme Physiology & Medicine* **2013,** *2*, 4.
60. Maughan, R. J.; Shirreffs, S. M., Development of individual hydration strategies for athletes. *International journal of sport nutrition and exercise metabolism* **2008,** *18*, 457-472.
61. Skolnik, H.; Chernus, A., *Nutrient Timing for Peak Performance*. Human Kinetics: **2010**.
62. Hayden, G.; Milne, H.; Patterson, M.; Nimmo, M., The reproducibility of closed-pouch sweat collection and thermoregulatory responses to exercise–heat stress. *European Journal of Applied Physiology* **2004,** *91*, 748-751.
63. Brisson, G.; Boisvert, P.; Péronnet, F.; Perrault, H.; Boisvert, D.; Lafond, J., A simple and disposable sweat collector. *European Journal of Applied Physiology and Occupational Physiology* **1991,** *63*, 269-272.
64. Wescor, http://www.wescor.com/biomedical/cysticfibrosis/macroduct.html. **June 12th 2013**.
65. Shirreffs, M. S.; Maughan, J. R., *Whole body sweat collection in humans : an improved method with preliminary data on electrolyte content*. American Physiological Society: Bethesda, MD, ETATS-UNIS, 1997; Vol. 82.
66. PREMIER http://www.premierintegrity.com/SweatTesting.aspx.
67. Gubala, V.; Harris, L.; Ricco, A.; Tan, M.; Williams, D., Point of care diagnostics: status and future. *Analytical Chemistry* **2012,** *84*, 487-1002.
68. Whitesides, G., Solving problems. *Lab on a Chip* **2010,** *10*, 2317-2318.

Chapter 2

Properties and Customisation of Materials for Bio- and Chemo-sensing in Biomedical Applications

Claudio Zuliani[1*], Vincenzo F. Curto[1], Giusy Matzeu[1], Kevin J. Fraser[1], Dermot Diamond[1]

Comprehensive Materials Processing - Sensor Materials and Technologies (Sensor Materials)

Elsevier Science 2013 - ISBN-13: 978-0080965321

Accepted for publication

[1]CLARITY: Centre for Sensor Web Technologies, National Centre for Sensor Research, School of Chemical Sciences, Dublin City University, Dublin 9, Ireland

* Author to whom correspondence should be addressed;

Abstract

The great challenge in the bio- and chemo-sensors field is the fabrication and delivery of devices that must be reliable, low-cost, minimally invasive, little to no calibration and with extended operational lifetime. In recent years materials science has offered appealing means to tailor the desired properties and challenges of these sensors. This chapter reviews exciting developments in materials science including the use of ionic Liquids (ILs), ionogels, conducting polymers (CPs), metal nanoparticles (NPs), carbon nanotubes (CNTs), graphene and nanocomposites in the preparation of (bio)chemical sensors.

Keywords: Sensors, biosensors, biomedical devices, wearable sensors, ionic liquids, conducting polymers, nanoparticles, carbon nanotubes, graphene, nanocomposites, ionogels.

2.1 Key Challenges in Molecular Sensing for Biomedical Applications

Low power chemo/biosensing devices capable of monitoring clinically important parameters in real-time, represent a great challenge in the analytical field as the issue of sensor calibration pertaining to keeping the response within an accurate calibration domain is particularly significant.[1-4] Diagnostics, personal health and related costs will also benefit from the introduction of sensors technology.[5-7] In addition, with the introduction of REACH regulation, (acronym for Registration, Evaluation, Authorisation and Restriction of Chemical Substances) unraveling the cause-effect relationships in the epidemiology studies will be of outmost importance in order to help establishing reliable environmental policies aimed at protecting the health of individuals and communities.[8-10] For instance, the effect of low concentration of toxic elements is seldom investigated as physicians do not have means to access the data.[11]

Implantable devices, which in the past brought much hope for continuous monitoring of chronic medical conditions, have made little progress in the last twenty years. The major mechanism of failure is the biodegradation of the sensing layer and the changing diffusional barrier that arises from the host's response towards the implanted sensor.[12] Current devices cannot be used for prolonged periods of measurement because of endogenous interferences, fouling *etc*.[13-15] However, there are few examples of commercially available sensors that are suitable for short-term continuous monitoring of clinical relevant markers. For instance, the Abbott Freestyle Navigator, which continuously monitors glucose, has been successfully applied for over five days in trials.[16] In addition, recent work has demonstrated continuous performance of indwelling glucose biosensors for up to four months in rats and up to one year in pigs.[12] However, the ultimate goal of an implantable sensor that would automatically trigger the release of insulin remains very far from realisation.[17]

From this point of view it is significant to note that glucose sensors account for approximately 85 % of the biosensor industry, and that these sensors are based on the employment of enzymes.[16] In this regard, the physical and chemical stability of

enzymes and their cost represent often a major hurdle in the sensors development. Therefore, materials, which provide a stabilisation of the enzymes or which can work as selective catalysts mimicking the proteins function, are of outmost importance. In addition, sampling represents another important aspect of consideration in order to deliver minimally invasive sensors and, in this regard, easily accessible body fluids, *i.e.*, sweat, saliva and interstitial fluids, rather than blood offer a paradigmatic shift in the sampling strategy.[18-25] For instance, sweating may assist the removal of toxic elements, *e.g.*, heavy metals, from the body,[11] and the design of robust trials for accessing the analytical levels of these elements in the sweat would help establishing therapeutic protocols.

Interstitial fluids have also received attention because of the advantages that this media offers compared to blood, *i.e.*, easily accessible, painless sampling and reduced risk of infection.[12, 26-29] However, an important fact often overlooked is that the sample volume of the harvested interstitial fluids is low, *i.e.*, 10 μL h^{-1}. Few examples based on the sampling of interstitial fluids have actually been reported and, even for glucose, a commercial device which can reliably monitor its concentration appears elusive. To date, there is no unanimous agreement on the typical delay between the glucose levels measured in interstitial fluids and whole blood samples.[14, 28-30] Microspikes and hollow microneedles have been employed to harvest the interstitial fluids, and the integration of these structures with a sensor in a micro-fluidic device is an attractive possibility. For example, Trzebinski *et al.*[27] functionalised the top layer of a microspike array suitable for piercing the skin with an enzyme layer allowing the detection of glucose or lactate in buffered solutions. However, using functionalised solid microneedles array for *in vivo* sensing is challenging because of the potential structural deformation upon their insertion into the skin, which, for instance, may drastically change the sampling dynamics thereby introducing an unpredictable delay in the time from sampling to detection.

The integration of on-body sensors into textiles allows monitoring physiological parameters in a non-invasive fashion and it has generated considerable research activity across many important biomedical applications such as sports, exercises and personal health.[31] At present, only wearable electrodes to monitor heart rate[32] and wearable respiration devices are commercially available and the goal of producing reliable chemical sensing garments seems largely unmet.[33] Producing wearable chemical sensors, which must be comfortable during daily

activities, reliable and available at affordable cost is a challenging task.[34] In addition to these challenges, population growth and ageing population profiles will significantly affect the cost of health care systems and the future sustainability of healthcare services will rely on the adoption of new low-cost technologies, with the shift to much more personalised and home/community-based healthcare systems.[19, 35-38]

2.2 An Outline of Clinical Markers

2.2.1 Molecular Clinical Markers

The concentration of ethanol in blood is strictly regulated and the breath analysers market has successfully matured in order to enforce drink-driving legislation. However, it is interesting to note that the ethanol level in sweat has a significant clinical relevance as it correlates well with its concentration in blood.[31] Lactate concentration in blood is a fundamental parameter for the diagnosis of clinical disorders such as hypoxia, and drug toxicity.[39] It also gives information on the extent of hemorrhagic shock in trauma patients[12] and of myocardial ischemia.[10, 13, 40-42] In Sports Science lactate levels in blood are measured in order to determine the so-called anaerobic threshold which is a fundamental aspect in optimising the athletes training.[10, 43-45] Therefore, there is considerable interest in developing less-invasive, real-time devices for the measurement of lactate in sweat and saliva, as the lactate concentration correlates with that of blood.[10, 31, 43] While sensors for the determination of lactate in saliva have been reported in the literature,[10] a key challenge is their integration in a wearable platform which allows real-time analysis. One example of such a wearable sensor would be the integration into gum shields.

Cholesterol[46] and urea[47] have been standard parameters for the diagnosis of cardiovascular disorders. The development of low-cost sensors for these analytes has received remarkable attention in the literature. Similarly, ammonia sensors have been investigated especially for point-of-care applications, as high levels of ammonia, which is a product of the urea degradation, is associated with renal dysfunction[48] and other pathologies.[49] Interestingly, ammonia concentrations in

human breath correlate well with the levels of urea found in blood.[50] However, commercial sensors for home-testing or point-of-care are not common and tend to be relatively expensive. For instance, portable ammonia detectors cost more than 400 euro (www.gasmonitor-point.co.uk/ammonia-gas-detectors, www.draeger.com).

In addition, some molecules of interest are difficult to detect, such as bilirubin and nitric oxide. Bilirubin is a tetrapyrrole formed from the breakdown of the heme in red blood cells, whose concentration in blood serum is normally in the 1-10 μM range and is associated with liver functionality.[51, 52] Nitric oxide (NO) has multiple critical functions in biological systems, *e.g.*, as a neurotransmitter, cytostatic agent, blood pressure regulator and it is thought to be implicated in the pathogenesis of several diseases, *e.g.*, gastric tumor. Spectroscopic measurements of bilirubin in blood are difficult because of interferences such as pH effects, and biosensors based on bilirubin oxidase are hampered by the relative instability of the enzyme.[51] Studies on NO are further complicated by its chemical reactivity with hemoglobin, oxygen and other biological species which results in a half-life ranging from 6 to 50 seconds.[53]

2.2.2 Ionic Clinical Markers

Monitoring of pH has received attention because of its clinical relevance. For example, pH in sweat may be related to acid build-up in muscle cells during exercise, and pH in wounds maybe associated with the wound healing process.[54] On-skin pH meters and electrodes can be obtained from Hanna instruments (www.hannainst.co.uk) but they are not designed for continuous monitoring. Levels of sodium, potassium and chloride in sweat have been used for diagnostics of cystic fibrosis.[19, 36, 55, 56] Real time monitoring of the sweat electrolyte content could also be important for regulating hydration/dehydratation issues, an issue which can be fatal in some cases.[57, 58] The so called dietary minerals, *e.g.*, Ca^{2+}, Cl^{-}, K^{+}, Mg^{2+}, *etc.* have an important physiological role and when present at excessively high and low levels can be harmful for human beings.[59-61] For example, calcium has an important role in key biological processes such as the coagulation cascade, regulation of muscular activity and hypercalcemia is an indicator of the possible presence of malignant tumors.[62] Lithium in saliva can be used to regulate lithium

carbonate intake during treatment of manic depression and hyperthyroidism disorders.[63] Li-Ion Selective Electrodes (ISEs) are generally sensitive to high sodium concentration[64] but in saliva the sodium levels are three orders of magnitude lower than in blood.[65] There is an interest in monitoring ammonium and trace metals in sweat.[66] As an example, people affected by Wilson's disease, where copper is absorbed through the intestines and reduced excretion by the liver causes an accumulation of the metal in the body.[66] In addition, copper accumulation maybe connected not only to liver damage[67] but also to Alzheimer's disease.[68]

2.3 Opportunities for Materials Science in Biomedical Sensing

A holistic approach is required to solve the multi-disciplinary challenges associated with the preparation of the next generation biomedical devices which must be low-cost, low-power, reliable and easy-to-operate. Materials science plays a significant role of delivering suitable materials for such devices as discussed below.[69-71] Self-powered sensors will have a key role in the biomedical field. For instance, micro-fluidic paper analytical devices show promise as low-cost and disposable devices, more so when coupled with paper-based batteries. Liu and Crooks[72] demonstrated the detection of glucose on a paper-based micro-electrochemical sensing platform where the battery is activated by the contact with the sample. The read-out is based on the change of colour of the electrochromic Prussian Blue spot deposited on the ITO surface as shown in Figure 2.1.[72] Such devices would benefit from research in material science as their performance can be optimised, *e.g.*, the paper can be loaded with ionic liquids which may influence the stability of enzyme, or ITO may be replaced by other conductive surfaces, *e.g.*, conductive polymers (CPs), to deal with the forecasted short supply of indium. Perhaps the most important challenge is to understand how to reduce biofouling in implanted sensors. The mechanism of biofouling of implanted systems seems to be related to the denaturation of extracellular matrix proteins, which triggers the inflammatory cascade.[73] Materials should be designed to stop or inhibit this initial step.

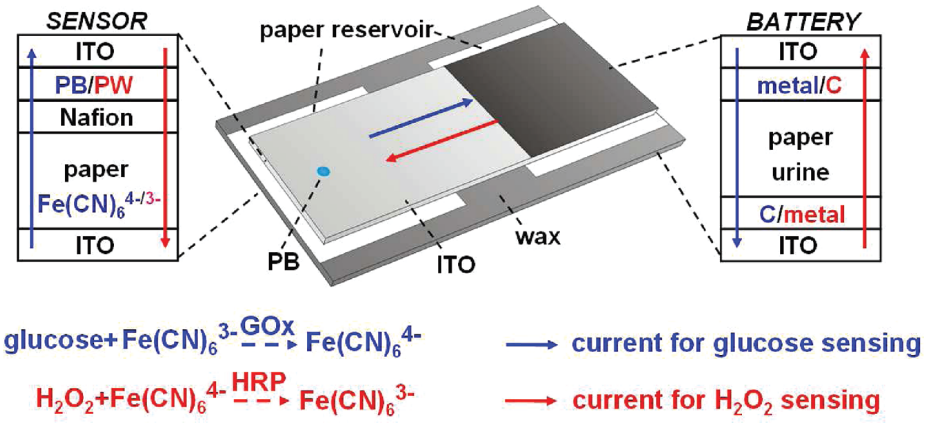

Figure 2.1. The operational principles of a device consisting of a sensor and an Al/air battery separated by a wax barrier. The paper reservoir of the sensor is preloaded with dried glucose oxidase (GOx) and $Fe(CN)_6^{3-}$. The catalytic oxidation of glucose by GOx results in the conversion of $Fe(CN)_6^{3-}$ to $Fe(CN)_6^{4-}$ which is then oxidised back to its original state on the lower ITO electrode resulting in the reduction of Prussian Blue to colourless Prussian White on the upper ITO electrode. (adapted from reference [72])

Phenylboronic acid and derivatives have been extensively exploited as glucose receptors in "smart" hydrogels as the binding induces a change in the optical diffraction thus making it possible to monitor minute changes in the hydrogel volume of a microscale device.[74] For instance, it was shown that these hydrogels can be used as holographic glucose sensors in simulated tear fluids with negligible interferences from lactate and pH.[74] This seems a fascinating approach for non-invasive real time analysis and this research seems to have addressed the optimisation of the response kinetics.

Stimuli-driven recognition, transportation and translocation processes perfected by nature over millions of years is surely a source of inspiration.[75] For instance, polymer brushes based on a photo-responsive polymers have received a lot of interest as colorimetric sensors due to their ability to report colorimetrically the presence or absence of the ion-ligand complex.[76] A photochemically and electrochemically triggered gold nanoparticle sponge has been prepared in Willner's group by attaching spiropyran and thioaniline moieties to the particles.[77, 78] Interestingly, it was reported that this composite can be used as an imprinted matrix for a zwitterionic electron acceptor whose uptake and release is controlled electrochemically and photochemically through the conductive polymer and the spiropyran moieties, respectively.[77]

Materials that may provide the much sought-after control of structure at the nanoscale in order to obtain, for instance, larger surface areas, improve electron communication with enzymes and enhance surface plasmon effects are of particular interest.[79] Ionic liquids, conducting polymers, metal nanoparticles, hydrogels, and hybrids of these materials are appealing from this point of view and they will be discussed in the upcoming sections.

2.4 Ionic Liquids and Sensing.

2.4.1 Introduction to Ionic Liquids.

According to current convention, a salt that melts below the normal boiling point of water is known as an 'ionic liquid' (IL) or by one of many synonyms including low/ambient/room temperature molten salt, ionic fluid, liquid organic salt, fused salt, and neoteric solvent.[80] ILs have been used for a wide range of applications, ranging across catalysis reactions, electrochemistry, separation science, polymer chemistry, formulation of pharmaceutical drugs, amongst others.[81, 82] Several reviews available in the literature as for example, Hapiot and Lagrost[83] and Buzzeo *et al.*[84] focused on the electrochemical reactivity of ILs, and their properties in relation to fundamental electrochemical studies. MacFarlane and co-workers discussed the chemistry of ILs and how this affects their physico-chemical properties.[80, 85] Wei and Ivaska[86] discussed the application of ILs in electrochemical sensors. Erdemenger *et al.*[87] described the use of ILs for controlling polymerisation reactions, while Armand *et al.*[88] outlined future trends of ILs use and applications.

ILs are typically characterised by a bulky unsymmetrical cation combined with a poorly coordinating anion in order to impede tight packing of the ionic lattice[89] and hence the resulting melting point is dramatically decreased compared to conventional salts.[90] ILs can be classified within seven different families on the basis of the ionic structure[91] and typical cations are shown in Figure 2.2. Their properties depend dramatically on the cation-anion combination[83] and in this sense can be thought as "designer" or "fine-tunable"[92] as polarity, viscosity, thermal stability, conductivity and solvent capacity can be tailored by thoughtful choice of

cations and anions.[85, 93] The variation in properties between salts, even those with a common cation but different anions, is dramatic. For example, butylmethylimidazolium hexafluoro-phosphate [C_4mIm] [PF_6] is immiscible with water, whereas butylmethylimidazolium tetrafluoroborate [C_4mIm][BF_4] is water soluble.[94]

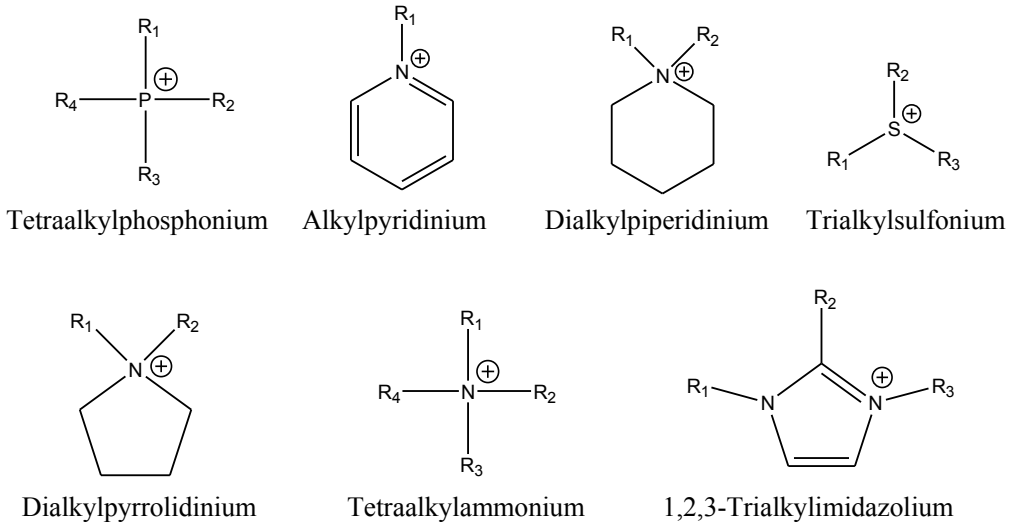

Figure 2.2. Common cations used for preparation of ILs. Popular side chains include: CH_3 (Me), C_2H_5 (Et), n-C_3H_7 (Pr), n-C_4H_9 (Bu), n-C_6H_{13} (Hex), n-C_8H_{17} (Oct), n-$C_{10}H_{21}$ (Dec), n-$C_{16}H_{33}$ (Hexde), $CH_2(OH)CH_2$ (HydroPr), CH_3OCH_2 (MeOMe), $CH_3OC_2H_4$ (MeOEt). The most commonly used anions are: BF_4^-, $CF_3BF_3^-$, $CF_3SO_3^-$, $(CF_3SO_2)_2N^-$, PF_6^-, $(CN)_2N^-$, $(CN)_3N^-$, SCN^-, Cl^-, Br^-, $EtSO_3^-$, NO_3^-, $H_2PO_4^-$. Adapted from reference [91].

There are several motivations to consider ILs as particularly appealing in the development of biosensors. For example, the existence of nanoscale structural heterogeneities in ILs and in particular the presence of H-bonded nanostructured networks with polar and non-polar regions has been associated with the stabilisation of enzymes.[95] This very relevant characteristic will be discussed more in details in the next section. In addition, ILs have received attention as they offer good media for the dispersion of carbon nanotubes, (CNTs) [96] and examples of successful applications of IL-CNTs composites in sensing will be discussed in Section 2.4.2. Hybrid MWNTs-ionogel monoliths (from a silica matrix), show a mixed ionic and electronic conductivity which makes them potential candidates as electrode materials or electron-to-ion transducers in ion-selective electrodes.[96] In some cases, ILs in

their solid state, have conductivities comparable to the liquid phase, *e.g.,* ethylammonium dicyanamide, which in connection to their plasticity makes them valuable materials as solid-state electrolytes in sensor designing.[97] Other properties often mentioned are their low-volatility, high ionic density and conductivity (up to 100 mS cm^{-1}), as well as excellent chemical and electrochemical stability (potential windows up to 7 V have been reported).[98]

It is worthwhile mentioning some of the drawbacks of ILs as material for sensing to give the reader a wider background. Often overlooked in the ILs literature is their complex chemo-physical nature, currently not fully understood, which may complicate prediction and tuning of their role in a sensor. For instance, theoretical models to describe the non-ideal conductivity and of the double-layer charging behaviours are yet to be implemented.[83, 99] Secondly, problems can stem from their relatively high viscosity, cost and in some cases, toxicity.[83, 84, 99] For instance, high viscosity impedes the diffusion of solutes and charge transport[83, 84, 99, 100] and the ion-transport in ILs is limited by the availability of channels of suitable size within the structure. Thirdly, the liquid nature of ILs is a limiting factor in the preparation of point-of-care biosensors because of the additional degree of complexity that liquid sampling brings. On this regard, the introduction of ionogels, confined ILs in a polymer matrix, may offer some solutions as discussed in Section 2.5.

2.4.2 Ionic Liquids and Biomedical Sensing

2.4.2.1 Ionic Liquids in Biosensors

ILs can be employed as a new class of solvents as many biological molecules (proteins, amino acids, DNA, sugars and polysaccharides) can be solubilised in them without loss of their bioactivity.[103] This specific property seems to be particularly relevant for the field of biosensing because ILs can provide an effective way to overcome the stability limitations of these sensors related to the limited temperature range and the very narrow pH range for protein stability in water.[88] An increase in the stability and activity of enzymes has been observed using certain ILs compared to common aqueous media such as PBS.[89, 101] For instance, it was reported that

cytochrome-c can be stored in hydrated choline dihydrogenphosphate for up to 18 months without losing its activity.[102] Moreover, lysozyme was stabilised against denaturation during thermal cycles in aqueous media containing an equal mass fraction of ethylammonium nitrate while the unfolding/refolding of the protein is not possible when the IL was not added.[103] Yang *et al.*[104] first demonstrated the use of ILs as electrolytes for the development of organic electrochemical transistors (OECTs) for glucose sensing. These plastic-based devices [105] coupled with ILs offer potential advantages for the preparation of low-cost, reliable and long-term stable biosensors. The mechanism of protein stabilisation in ILs is still under debate, but it seems that hydrogen bonding and electrostatic interactions between the IL and the enzyme may increase the kinetic barrier for the unfolding of enzymes.[86, 101, 106-109] It is important to note that this is not a general trend in ILs and that some ILs are known to denature proteins. [83]

ILs such as *n*-octyl-pyridinium hexafluorophosphate (*n*OPPF$_6$), which is solid at room temperature, have been employed as a binding agent and mixed with graphite and enzymes to prepare new generations of biosensors. It was found that the carbon to IL ratio strongly influences the performance of the electrode, in that it controls the capacitive current through reduction of water content and it can regulate the electrode conductivity.[110] For example, Ping *et al.*[111] used *n*OPPF$_6$ as a binder to create screen-printed graphite ink for the selective detection of dopamine with low interference from ascorbic acid and uric acid. These screen-printed electrodes, after the electrochemical deposition of exfoliated graphene oxide and after electrode modification with coating containing glucose oxidase, were used to detect glucose in buffer solutions, linear range 5.0 μM - 10.0 mM and sensitivity of 22.8 μA mM^{-1} cm^{-2}.[112] Authors found that the graphene oxide layer enhance the sensor sensitivity compared to the case in which this layer is not present.

Santafé *et al.*[113] studied the effect of 1-ethyl-3-methylimidazolium ethylsulfate [C$_2$mIm][EtSO$_4$] on copper-catalysed luminol chemiluminescence (CL). A clear difference in the light emission was observed that was ascribed to a strong interaction between Cu^{2+} and the imidazolium ring of the IL. Interesting effects of [C$_2$mIm][EtSO$_4$] on glucose oxidase activity were also noticed, and this enhancement was employed to perform sensitive chemiluminescent glucose detection (LOD = 4 μM) at pH 8.0.[113]

ILs have been used in the detection of volatile biologically relevant compounds such as NO. In one example, 1-hexyl-3-methylimidazolium hexafluorophosphate has been used in combination with a double chain surfactant to replace Nafion® as an antifouling layer on top of electrodes modified with poly(eosin-b). The results showed that the IL composite modified electrode exhibited excellent anti-interference behavior against nitrite, for example, and a wide linear relationship over a NO concentrations ranging from 36 nM to 0.13 mM.[53]

Before concluding this section, it is worthwhile to note that electrochemical sensors in the literature often rely on the use of stable and reliable standard reference electrodes, *e.g.,* Ag/AgCl with an inner filling solution, typically KCl. However, ideally, the reference electrodes should be mass produced, *e.g.,* prepared from a scalable automatic process like screen printing, and they should be maintenance-free, or at least require minimal maintenance. These demands are driving the increasing trend towards solid-state functional components.[114] As novel designs for reference electrodes that, for example, do not rely on an inner-filling solution, are much needed, IL related developments emerging from materials science research may offer advantages. For instance, Cicmil *et al*.[115, 116] reported on the use of ILs in poly(vinyl chloride) (PVC) matrices for the preparation of disposable reference electrodes in which the partitioning of the ions into the liquid phase defines the interfacial potential. After comparing several ILs, the authors found that reference electrodes prepared with 1-Ethyl-3-methylimidazolium bis(trifluoromethanesulfonyl) imide $[C_2mIm][NTf_2]$ were least sensitive to changes in the concentration of common alkali metal chlorides. The authors successfully employed these reference electrodes for the potentiometric measurement of Pb^{2+} solutions, cyclic voltammetry of a solution phase redox probe and impedance spectroscopy of a polymer membrane. Results comparable to standard reference electrodes have been obtained with hydrophobic ionic liquids, such as 1-methy-3-octylimidazolium bis-(trifluoromethylsulfonyl)imide which was jellified and saturated with AgCl.[117, 118] The electrodes suffered from component leaching and signal deviations (in the mV range) due for example to phthalate ions or chloride interference at concentrations larger than 0.1 M.[117, 118]

2.4.2.2 Ionic Liquids for Sensing Ions.

There are various motivations for developing novel membrane materials in ion-selective electrodes. These include the need for biocompability, elimination of plasticisers, minimise leaching, miniaturisation, increasing the selectivity and stability and improving detection limits.[119] An attractive advantage of ILs, is the ability to use them to tailor or tune the properties of a material, such as the solvation environment which determines ion-extraction and complexation equilibrium within a membrane.[85, 119] It may be that ILs will replace conventional ion-exchangers [119-122], plasticisers or even the ionophore in ISEs, but this area seems still in its infancy and only a few examples have been published in the literature.[119, 120, 123, 124]

When using ILs as plasticisers, the mechanical properties of the membranes formed have to be taken into consideration. For example, it was found that imidazolium-based ILs plasticise poly(methyl metacrylate) (PMMA) but not PVC, *i.e.*, membranes plasticised with PVC are found to be brittle and inductile.[120] In addition, it should be noted that ILs influence the fluidity of the membrane, thus determining the diffusion coefficient of the ions and therefore the sensor response time and detection limits.[119]

In addition, ILs are known to have larger dielectric constants, which on turn influences the ISEs selectivity.[119] For instance, Wardak *et al.*[124, 125] applied ILs as a solid-contact in ISEs to study the effect of three different alkyl chains situated on the methylimidazolium cation, while keeping the anion constant (Cl^-). Authors observed that the substituents in the imidazolium ring affected the limit of detection of the sensors and the best results were obtained with 1-butyl-3-methylimidazolium. However, no explanation of the underlying reasons for this behavior was given. The optimised sensors could detect 40 ppm of lead in spiked tap, river and waste water using the standard addition method, which was in good correlation with data obtained from anodic stripping voltammetry.

Beyond ion-selective electrodes, ILs may be employed as electrocatalyst for the detection of ionic species of clinical importance. For instance, a new iron(III)-containing ionic liquid $[(C_4H_9)_2\text{-bim}][FeCl_4]$ (Fe-IL, bim = benzimidazolium) was developed as an electrocatalyst for nitrite and bromate detection[126] which are

classified as carcinogens.[127, 128] A conductive carbon paste electrode (Fe-IL/CPE) comprised of Fe-IL and carbon powder was fabricated and the Fe-IL had the advantage of being both a binder and the electrocatalyst. The detection limit and the sensitivity were found to be 0.01 μM and 100.58 μA μM^{-1} for nitrite, and 0.01 μM and 83.11 μA μM^{-1} for bromate detection, respectively.

2.5 Recent Trends in Sensing with Conducting Polymers

2.5.1 Introducing Conducting Polymers

Conducting polymers are organic polymers with intrinsically high electrical conductivities. They have received ever-increasing attention since the seminal contribution of Heeger, MacDiarmid and Shirakawa, who jointly received the Nobel Prize for Chemistry in 2000.[129-132] While they were initially investigated as substitutes for metals, their range of applications quickly expanded covering several research fields such as electrocatalysis, energy storage and sensing.[133] Today's conductive polymer workhorses are primarily derivatives of polypyrrole, polythiophene, polyaniline and poly(3,4-ethylenedioxythiophene), see Figure 2.3.

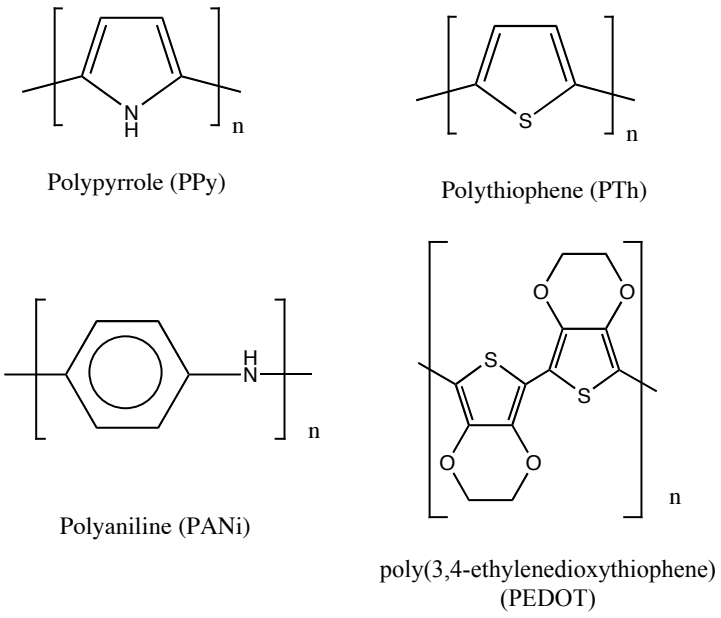

Figure 2.3. The most common CPs in the undoped form including polypyrrole (PPy), polythiophene (PTh), polyaniline (PANi) and poly(3,4-ethylenedioxythiophene) (PEDOT).

Below it is presented a brief overview on conducting polymers with references available if the reader wishes to explore further. Some particularly important contributions are summarised below.

Chujo,[134] and Leclerc and Morin[135] focused their attention on the synthetic aspects of the preparation of CPs. A book containing several contributions which span from the fundamental aspects of CPs, *e.g.*, mechanism of growth and electrochemical characterisation, to their recent applications in sensing, in energy storage and as artificial muscles is available by Cosnier and Karyakin.[136] Wallace and co-authors[100] compiled a concise but detailed book which describes their wide range of applications and gives a brief insight into the preparation and characterisation of the most common CPs employed in the literature, *i.e.*, polypyrroles, polyanilines, and polythiophenes. Eftekhari[137] presented some recent methods to control the morphology of conducting polymers at the nanoscale. Skotheim and Reynolds[138] provided a detailed coverage of recent advances in the chemistry, physics, and materials science of conjugated and conducting organic polymers. Gerard *et al.*[135] presented a review that describes the salient features of conducting polymers and their wide applications in health care, food industries and environmental monitoring. Lin *et al*.[139] published an overview of organic thin-film transistors as chemical and biological sensors describing in detail the sensing mechanisms and the detection limits of these devices. Nambiar *et al.*[140] focused on the use of CP-based sensing devices as tools in clinical diagnosis and for assisting surgical interventions, *e.g.,* electrochemical biosensor, tactile sensing 'skins', and thermal sensors. Ates and Sarac[139] reported on the electrochemical deposition of conducting polymers on carbon substrates for biosensor preparation while Rozlosnik[136] focused on the use of PEDOT in biosensing.

Amongst the most popular CPs being investigated for sensing applications are PPy and PEDOT derivatives. PPy is known for its good mechanical properties but this is counterbalanced by low ion accessibility due to its dense films, relatively low conductivity (10 - 50 S cm^{-1}) and chemical instability (*e.g.,* oxygen).[141] PEDOT is the most popular CP among the polythiophene family. Compared to PPy, PEDOT has ten times greater conductivity (300 - 500 Scm^{-1}), greater chemical and thermal stability, and higher optical transparency. [136, 141, 142] The green emeraldine salt form of PANi has conductivity in the range 1–10 Scm^{-1}.

Furthermore, PANi has the ability to form a broad range of nanostructures without the use of a template.[143]

A general feature of CPs is that they change their properties, such as conductivity or optical properties, depending on the doping state which has been used as transducing principle, *i.e.*, when the analyte changes the doping state of the polymer. Another attractive feature of CPs in the preparation of disposable and low-cost sensors is their compatibility with ink-jet printing[144, 145] or electrospinning.[143] In addition, polymer based organic electronics based on CPs may open the way to the creation of inexpensive flexible devices and offer the possibility of integration of sensing/electronic devices with wearable fabrics.[146-148]

In recent years, there have been considerable efforts to improve the phisiochemical characteristics of CPs. Of particular interest has been the possibility of improving the mechanical, physical and chemical properties of CPs by integrating ILs during their electropolymerisation.[84, 87, 142, 149-151] For instance, control of the water content during the electropolymerisation seems to affect the conductivity of the CP layers. This was observed during the electropolymerisation of thiophene in an aqueous electrolyte, and it resulted in the formation of a non-conducting polymer film.[97, 152] In addition, the choice of IL cation/anion is important as it affects the stabilisation of the radical produced during IL electrochemical oxidation and regulates the degree of electrostatic interaction between the anion and the polymer backbone.[83, 97] In addition, ILs may affect chemical doping of the polymer film, the polymer film thickness, and film morphology.[83] For example, pyrrolidinium based NTf_2-ILs led to polythiophene films that were smoother and denser than those produced using imidazolium-based NTf_2 ILs.[83, 146] While these differences were ascribed primarily to the different viscosities and conductivity of the ILs, effects arising from the cation during the electropolymerisation cannot be totally excluded. In certain cases ILs may affect the structuring of the polymer chains at the nano scale, as demonstrated by Ahmad *et al.*[142, 146] who showed that 1-ethyl-3-methylimidazolium bis(perfluoroethylsulfonyl)imide assisted fibre growth in PEDOT films. These nanostructures tend to shorten diffusion distance for ion transport which affects the polymer charge/discharge capacities and rates[153] while also increasing electrocatalytic activity.[146] Interestingly, co-deposition of PPy and PEDOT has been demonstrated in ILs.[141] This particular study highlighted that co-

deposition resulted in a more porous film due to entanglement and mismatch of PPy and PEDOT chains.[141]

Finally, it is important to acknowledge some issues that may arise with CPs, such as concerns over thermal and chemical stability, the mechanical ruggedness, and tolerance to high field electric fields of CPs.[73, 140], all of which may affect the performance of CP-based sensors. Recent research has focused on finding solutions to some of these issues, and the electrochemical growth of CPs in new media like ILs, as highlighted above, has offered some improvements. In addition, while CPs are generally regarded as non-cytotoxic to mammalian cells, there is still concern about their long term impact, and therefore there is considerable interest in producing new types of biodegradable CPs.[73]

2.5.2 Customisation of Conducting Polymers for Biomedical Applications

2.5.2.1 Conducting Polymers in Biosensors

CPs have been successfully used in the preparation of biosensors in order to entrap enzymes *in situ*; however, in certain cases, the high enzyme loading has proven to impede the electropolymerisation of the CP.[154] It should also be noted that when hydrogen peroxide is developed as a by-product of the oxidase enzymatic substrate conversion during the sensor activity, this compound can cause the overoxidation of the CP and limit the lifetime of the sensor.[12] Therefore, the sensor requires careful designing in order to minimise H_2O_2 formation.

A few examples of the use of CPs in the fabrication of biosensors are detailed below. Two polythiophene derivatives, poly(4,7-di(2,3)-dihydrothienol[3,4-b][1,4]dioxin-5-yl[1,2,5]thiadiazole and poly(4,7-di(2,3)-dihydrothienol[3,4-b][1,4]dioxin-5-yl-2,1,3-benzoselenadiazole, have been employed in order to increase the stability of the adsorbed glucose oxidase (GOx) enzyme thanks to enhanced π-π stacking and electrostatic interactions.[155] The modified electrodes were capable of detecting glucose in real human serum samples although these were diluted with buffer solutions to coincide with the limited sensor dynamic range, *i.e.*, 0.05 - 1.0 mM.[155] In addition, the immobilisation of GOx on top of the CP layers

with glutaraldehyde seems to be a serious limitation as this compound may cause the denaturation of enzymes.

Rahman *et al.*[51] showed that poly-5,2'-5',2''-terthiophene-3-carboxylic acid (TTCA) electrochemically grown at gold electrodes can be used to complex Mn^{2+} through the carboxylic groups of the CP. The resulting film was used as biocatalyst for the oxidation of bilirubin and, with the addition of an anti-interference layer, the biosensor could detect bilirubin in a human serum sample, although this was diluted with a buffer.[51] The bilirubin content was measured to be 5.2 ± 0.7 μM, which is reasonably consistent with the result obtained from a spectrophotometric method (4.9 ± 0.2 μM). TTCA polymer was also used for the preparation of NO sensors. In fact, the polymer was electrochemically grown on platinum microelectrodes and the CP was covalently attached to cytochrome-c.[156] After coating with Nafion®, the modified microelectrode showed a linear response for NO in the range 2.4 - 55 μM allowing the detection of NO *in vivo* in rat brain tissue.[156]

Polyaniline has been polymerised by the hydrogen peroxide produced enzymatically by GOx in the presence of glucose.[157] The gluconic acid produced enzymatically, causes a pH drop which triggers the catalytic polymerisation of aniline.[157] Interestingly, in this manner, the physically adsorbed enzyme could be encapsulated within a polyaniline layer which limits the rate of leakage of the enzyme.[157] Polyaniline nanoparticles and urease have been successfully incorporated onto a flexible substrate using ink-jet printing in the preparation of urea sensors.[144] The biosensor could measure urea in the range of 2 - 12 mM but the data obtained for the urea content in fifteen human serum samples showed a positive bias, against a spectrophotometric assay. Polyaniline, thanks to its pH dependent doping states, seems to be a popular material for the preparation of ammonia sensors that have been successfully applied in the monitoring of human breath samples. For instance, an amperometric sensor was created by electropolymerising aniline onto gold nanoelectrodes.[158] By increasing the concentration of ammonia, the current decreased due to de-doping of the conducting polymer. Tests with real breath samples correlated well with a laboratory standard colorimetric technique for ammonia detection with a discrepancy of 12 %, possibly due to experimental differences in the sample handling.[158]

Nanostructures based on CPs have been also applied to sensing.[137] For example, poly(toluidine blue) nanowires, prepared from a template-directed electrochemical deposition, have been used to load and stabilise Horseradish Peroxidase (HRP).[159] The resulting sensor showed good linear response to H_2O_2 over a wide substrate concentration range, although the template deposition method can be cumbersome and may suffer from the potential leaking of the adsorbed enzyme. With regards to template-less polymerisation, for instance, pyrrole has received a lot of attention due to the possibility of producing nanostructures during its electrodeposition. Fibrillar, rod and worm-like structures can be prepared using carbonate or phosphate salt solutions.[160-164] The mechanism behind the formation of the nanostructures is still controversial but it has been hypothesised it may be due to the low density of the charge carriers during the polymer growth and alignment of PPy chains bridged by the phosphate or carbonate anions.[160, 165]

CPs may be tailored to introduce chemical functionalities into the polymer backbone, as this can provide anchoring sites for specific sensing tasks such as binding aptamers for the development of highly sensitive aptasensors. For instance, the extended π-conjugation along the backbone of poly(*m*-phenylenediamine) (PMPD) allows the physical adsorption of a dye-labeled thrombin aptamer onto the surface of PMPD rods.[166] Indeed, the presence of these aptamers on the surface of the rods induced substantial quenching of the fluorescence dye, which was recovered only in the presence of thrombin, due to the formation of the quadruplex-trombin complex. Luo *et al.*[167] covalently attached the immunoglobulin E (*IgE*) aptamer to the amino groups of the polyaniline (PANi) backbone. Using this approach it was possible to prepare a conductometric and label free aptasensor for *IgE* which relates to cancer pathologies.[168] The detection principle is based on the notion that the high surface-to-volume ratio of the nanostructures is markedly affected by minor perturbations of their electrical field induced upon binding of *IgE*.[169]

2.5.2.2 Sensing Ions and Conducting Polymers

In solid-contact ion-selective electrodes (SC-ISEs), the internal reference electrode and inner filling solutions can be replaced by solid materials.[114, 170-174] SC-ISEs are more convenient for remote monitoring than liquid filled ISEs as they are more

compatible with microfabrication technologies.[114, 170-174] While CPs have been extensively used as a solid contact material it is important to note that the choice of the conducting polymer is imperative in the ISE's longevity as it will affect the stability over time and the limit of detection (LOD).[114, 129, 170-181] In addition, the type of CP to be used as a solid contact can also depend on the ion analyte.[182] Poly(3-octylthiophene) (POT) has been used as a solid contact due to its hydrophobicity as this improves membrane adhesion and limits water uptake[173, 183]. PANi was also used as SC layer in potassium-ISEs which have been used for the detection of potassium in artificial serum, with a linear range between 10^{-5} M and 10^{-1} M and no pH interference under physiological conditions.[184]

While PANi, PPy and PEDOT have been extensively investigated as solid contacts in ISEs, the possibility of improving SC-ISE performance using other CPs or by CPs nanostructuring seems to be relatively unexplored.[185] For instance, polypyrrole microcapsules have previously been employed as solid contacts in calcium-ISEs.[186, 187] Authors claim that through this, they can control the electrolyte composition of the microcapsules, thus providing a means to fine-tune the LOD.

The use of neat CPs or CPs doped with selected ionophores as a sensing layer is an interesting approach. However, thus far, such sensors suffer from poor sensitivity and high LODs.[136, 185, 188, 189] PANi deposited on plastic substrates by means of ink-jet printing was used to detect pH changes both potentiometrically and spectrophotometrically[188] but the selectivity factor hampered their use in real-sample scenarios.[188] A stripping voltammetric sensor based on an overoxidised PPy film was developed for the detection of copper in human hair.[190] The device had a sensitive range from 2 to 250 ng mL^{-1}, and experimental results were in agreement with results obtained from Atomic Absorption Spectroscopy. This particular sensor could be regenerated by washing with EDTA solutions, without appreciable differences in response characteristics before and after the washing step. Finally, PEDOT drop-cast nanorods produced by interfacial polymerisation on a glassy carbon electrode showed high electrocatalytic activity for nitrite oxidation.[191] The amperometric sensor showed a linear response in the range 0.6 to 40 μM and a sensitivity of 22.8 μA mM^{-1}. However, the sensor was not tested with real samples.

A recent nice example of a CP-based sensor employed poly(9,9-bis(6'-benzimidazole)hexyl) fluorine-*alt*-1,4-phenylene. This is a water soluble fluorescent polymer that has been used for the detection of phosphates in blood serum.[192] The phenyl benzimidazole group of the polymer is able to bind selectively Fe^{3+}which in turns quenches approximately 97 % of its fluorescence. However, phosphates restore more than 95 % of the polymer fluorescence as they bind to the Fe^{3+}. Because of the control of the polymer fluorescence exerted by $Fe^{3+}$and the phosphates, the authors were able to use the polymer to detect phosphates in blood serum samples. The sensor-determined levels of phosphate were in the range 4.24 – 4.37 mg dL^{-1} which was in good agreement with the value of 4.46 mg dL^{-1} obtained by standard spectrometric and potentiometric assays employed in clinical practices.[192]

2.6 Recent Developments in Nanomaterial-based Sensors

2.6.1 Metal Nanoparticles

2.6.1.1 Introduction to Metal Nanoparticles

Metal nanoparticles (NPs) date back in time since their first applications in glass staining to create colour-changing effects.[193] Faraday gave the first scientific explanation of their optical properties suggesting that the interaction of the light with the colloids is at the basis of their colour. Nowadays, this behavior is understood as originating from localised surface plasmons which oscillate with a characteristic frequency which is sensitive to the changes in the local dielectric environment.[193] In recent years, nanoparticles have been at the centre of tremendous research attention, most notably through the work by Brust *et al.*[194] who developed an easy pathway to their chemical synthesis and stabilisation. Chemical synthesis is still one of the best approaches for their preparation, although other methods such as evaporation under vacuum or laser ablation[195] have also proven effective. Nanoparticles have been prepared using different metals, such as gold, silver, platinum, palladium, with each metal imparting specific catalytic and optical properties.[196, 197] In NP chemical synthesis, the choice of ligands, the metal to reducing agent ratio, time, and temperature all play an important role in determining the morphological aspects and properties of the resulting NPs.[195] While a detailed

discussion is beyond the scope of this chapter, the reader can find valuable information in several excellent references, which are summarised below.

Kelly *et al.*[198] described how size, shape and dielectric environment influence the optical properties of metal NPs; Narayanan and El-Sayed[199] described the use of NPs as electrocatalysts, and Murray[200] discussed the electrochemical properties of metal NPs and their incorporation in electrochemical devices. Schmid[193] edited a comprehensive book introducing the booming field of the "nanoworld" and covering aspects of nanoparticles from their fundamental principles to their use in novel applications. Rotello[201], from a chemical standpoint, described the diverse structures and properties of nanoparticles, presenting also fundamental studies and pragmatic applications ranging from materials research to device fabrication. Nagarajan and Hatton[202] published a book covering recent advances in the synthesis, stabilisation, passivation and functionalisation of nano-objects made from a wide range of materials, such as metals and metal oxides. Methods to control the number of functional groups and to attain aqueous dispersibility, the impact of stabilisers on Surface-enhanced Raman spectroscopy (SERS) activity and ways to tune plasmon resonance *via* nanoparticle shapes were also presented.

An attractive advantage of nanoparticles is the possibility to tune the plasmon resonance in order to match a biological window of tissue transparency, so as to coincide with an emitter excitation or to match a laser source.[203, 204] For this reason, nanoparticles have been extensively used for analytical purposes, in particular, as labeling components for biological compounds such as DNA, enzymes, and antibodies.[205] Another useful property of metal NPs is that they quench fluorescence. For instance, fluorescent polymer conjugates coupled with gold nanoparticles have been prepared for sensing of proteins such as bovine serum albumin, β-galactosidase, or phosphatase.[206] Indeed, the presence of proteins disrupts the NP-polymer interaction producing distinct fluorescence response patterns which are characteristic of individual proteins at nanomolar concentration.[206]

Synthetic methods to functionalise NPs have achieved great level of control and sophistication such that NPs can be prepared with an innumerable number of different ligands and coatings, offering therefore enormous opportunities in tailoring specific properties for sensing applications. For instance, the problem of the

electrochemical stability of the solid contact material in SC-ISEs is well documented and CPs have been employed to tackle it as discussed in the previous section.[207] Nanoparticles may also have a role to play in solving this issue, thanks to their chemical stability and tunable properties, for example through control of the ligands and the core materials used in their fabrication.[207]

A core goal of nanotechnology is the ability to manipulate materials at the nano-scale. In this regard, control over the shape and alloy spatial distribution, at the nano and micro scale that can be obtained through the use of nanoparticles is striking. In fact, it is possible to carve metal nanoparticles in an aqueous medium at room temperature[208, 209] or to control their spatial network distribution by means of external stimuli in order to create tailored architectures.[210, 211] NPs may also offer advantages for the customisation of low-cost optical sensors integrated in lab-on-a-chip platforms[212], paper-based sensors and micro-fluidics, and in point-of-care devices[213-215].

2.6.1.2 Metal Nanoparticles for Biomedical Applications.

The conjugation of DNA or aptamers with NPs has opened new routes in biosensing because it combines the selectivity and the affinity of these proteins with the advantageous spectroscopic properties of NPs.[216] For instance, the shift in surface plasma resonance (SPR) upon the specific binding of the target analyte to the aptamer has been exploited for the detection of cocaine.[217] Zhang *et al.*[218] developed a selective cocaine aptasensor where two sequences of cocaine aptamer stabilised the Au-NPs upon salt addition if no cocaine was present. In the presence of cocaine, aggregation occurred and the SPR of Au-NPs shifts, producing a colour change from red to blue. Willner *et al.*[219] worked on the use of aptamers to create smart surfaces, which respond to a desired target analyte. For instance a cocaine aptasensor was developed using two anti-cocaine aptamer subunits; one subunit was assembled on a gold support, acting as an electrode or a SPR-active surface, and the second aptamer subunit was labeled with Pt-NPs or Au-NPs. The addition of cocaine resulted in the formation of supramolecular complexes between the NPs-labeled aptamer subunits and cocaine on the metallic surface. Depending on the type of nanoparticles, cocaine could be detected from the reduction current of H_2O_2

electrocatalysed by the Pt-NPs or from the reflectance changes stimulated by the electronic coupling between the localised plasmon of the Au-NPs and the surface plasmon wave. The detection limit for cocaine was at best 1 μM. A long response time, ~ 30 min, and the need to control the ionic strength of the solution seemed to be the major hurdles for this sensor configuration.[219] Visual detection of cocaine was performed using a DNA modified linear polyacrylamide polymer, which was crosslinked with a cocaine aptamer and loaded with Au-NPs. In presence of cocaine the hydrogel dissolves and Au-NPs are released in solution, turning its colour from colourless to red and thus allowing its detection.[220]

Au-NPs have been largely employed as a colorimetric transducer due to their attractive optical properties such as high extinction coefficient and marked colour change accompanying aggregation.[221, 222] For example, a colorimetric assay for the detection of cerebral glucose was reported by coupling Au-NPs modified with adsorbed single stranded DNA (ssDNA).[223] The hydroxyl radicals provided by the reaction between the enzymatically produced H_2O_2 and Fe^{2+}, both added to the solution containing the NPs, caused the cleavage of the adsorbed ssDNA. The addition of sodium chloride caused aggregation and therefore a change in colour from red to blue. Similarly, bare Au-NPs and cationic conjugated polyelectrolytes were employed for the detection of DNA, cocaine, and thrombin.[224] Interestingly, the latter method provides a simple and rapid way to visually detect thrombin at a concentration as low as 10 nM.

In the field of immunosensors, Au-NPs have found application in the detection of cancer biomarkers.[225] In fact, it has been shown that for the detection of CA15-3-antigen, a known breast cancer biomarker, the application of Au-NPs labeled with Horseradish Peroxidase (HRP) and CA15-3-antibody enhanced the sensitivity and shortened the incubation time of a commercially available ELISA immunoassay from 30 to only 5 min.[226] Stevens *et al*.[227] developed a colorimetric prostate specific antigen (PSA) nanosensor, using gold nanostars. An antibody was tagged to GOx which in the presence of PSA caused the formation of the antibody-antigen-labeled antibody complex. In the presence of glucose and silver ions (both added to the solution), GOx converted glucose to gluconolactone and H_2O_2, which then reduced silver ions around the gold nanostars.[227] When the concentration of GOx was as low as 10^{-20} g ml^{-1}, a homogenous silver coating on the nanostars was observed causing a large blue-shift of the SPR of the nanostar.[227]

This resulted in an exceptional detection limit of 40 femtomolar for the PSA cancer biomarker in whole blood serum.

Khlebtsov *et al.*[228] introduced a multiplexed colorimetric dot immunoassay on a nitrocellulose membrane strip for simultaneous detection of rabbit anti-chicken, anti-rat and anti-mouse antibodies. Ag nanocubes, Ag/Au alloy nanoparticles and Ag/Au nanocages probes, Figure 2.4, were labeled with chicken, rat and mouse immune-gamma globulin (*IgG*) in order to generate spots of yellow, red and blue colours, respectively.[228] Upon spiking known concentrations of the target analytes on top of the nitrocellulose membrane, the latter was exposed to a solution containing a mixture of the three nano-probes and the analyte-probe pair specifically formed. The resulting stained the nitrocellulose membrane as shown in Figure 2.4.[228] Using this approach, concentrations as low as 20 fM of the target analyte could be detected by the human eye.

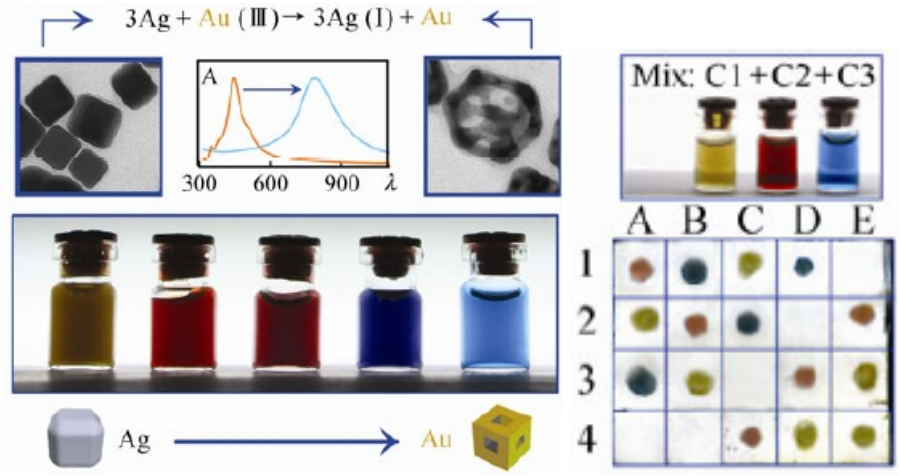

Figure 2.4. On the left side, TEM images of Ag cubes and of Au/Ag alloy nanocages together with pictures of vials containing their colloidal suspensions. On the right side, results obtained with the multiplexed dot immunoassay for the three target analytes on the nitrocellulose membrane. (adapted from reference [228])

The NPs developed by Strömberg *et al.*[229] were used in an optode for the detection of ammonia in porcine skeletal muscle tissue. The signal was analysed by image processing and a limit of detection of 2 nM was achieved without any other ionic interference from the sample. The sensor was based on a hydrogel loaded with Au-NPs, 2-(dodecyloxy)benzonitrile, merocyanine and nonactin which acts as the ammonium carrier.[229] As the porcine skeletal muscle tissue was sandwiched between a silicone sheet and the gas permeable membrane, the ammonia released

was protonated to ammonium within the hydrogel which in turns changed the fluorescence of the nanoparticles.[229] This device may be implemented in breath diagnostic devices for patients with metabolic disorders or in artificial nose and tongue devices. Detection of Ca^{2+} in animal and human serum samples was achieved by functionalising the nanoparticles with calsequestrin which is a protein of the sarcoplasmatic reticulum able to reversibly bind calcium.[62] The electrostatic interaction between calcium and calsequestrin caused nanoparticle aggregation which in turn produced a visible colour change from red to purple.[62] Zhang *et al.*[230] developed a colorimetric assay for iodine using a nanoalloy particle of a copper core surrounded by a gold shell. The iodine caused a colour change from purple to red which was proposed to be due to a transformation of the interconnected, irregularly shaped nanoparticles to the single, separated, and nearly spherical ones. The sensor was able to monitor iodine concentrations (6 μM), with interferences from other ions occurring only when their concentrations were in the mM range. However, the colour change was relatively slow, taking around 20 min.[230]

2.6.2 Carbon Nanotubes and Graphene.

2.6.2.1 Carbon Nanotubes and Graphene - An Overview

Carbon nanotubes (CNTs) exist mainly in two forms, single- and multi-wall, respectively termed SW-CNTs and MW-CNT. SW-CNTs can be considered as a long wrapped graphene sheet consisting of two separate regions (side and end cap) with very different physical and chemical properties.[231, 232] For instance, certain studies imply that the tips of CNTs are more reactive than the cylindrical parts.[231] MW-CNTs consist of concentric SW-CNTs of different diameter, in which the shells of carbon are closely separated.[231] The lengths of CNTs play an important role in determining the electrical, optical and mechanical properties.[232]

CNTs have received particular attention not only for their electrical properties but also because they seem to promote electron transfers to and from immobilised biomolecules, which is appealing for preparing biosensors.[231, 233] For example, enzymes have been immobilised on CNTs [234], although, it has also been reported

that the activity of enzymes may decrease considerably after their adsorption onto surfaces modified with CNTs.[235] In this regard, the use of appropriate dispersant agents, *e.g*. ILs, may avoid the denaturation issue.[235] It is perhaps worthwhile to note that the CNTs electrocatalytic properties are somewhat controversial. In fact, it has been suggested that it is the presence of metal impurities introduced during the preparation of CNTs, rather than the CNTs themselves, which provides the basis of the electrocatalytic behavior.[205, 236, 237] In addition, there is still not unanimous agreement regarding the cytotoxicity of CNTs, although some authors support that functionalisation of CNTs can control it.[236, 237] Finally, an important aspect to consider is the relatively high cost of producing and purifying CNTs, (although this is decreasing over time), which may someway explain the delay in their uptake by the industry.[231, 236]

Graphene is an unique material in which carbon atoms are arranged in a regular hexagonal pattern similar to graphite but in a one-atom thick sheet.[16] It is a zero bandgap semiconductor having conductivity akin to metals, which, in the opinion of some researchers, could provide the basis of materials with exceptional electrocatalytic abilities.[16] Large-scale patterned growth of graphene is still problematic but progress is happening.[238] For example, electrolytic exfoliation is particularly promising for producing graphene nanosheets in aqueous solution at low-cost.[145]

2.6.2.2 Applications of Carbon Nanotubes and Graphene in Biomedical Sensing

Carbon nanomaterials are particular suitable for use in biosensors due to their high surface/volume ratios and the possibility of immobilising target molecules, e.g., bio-receptors, with high density. Thanks to their high conductivity and large surface-to-volume ratio, small changes on the conformation or displacement of the immobilised bio-receptors can be detected.[239, 240] This transduction mechanism has been reported in field-effect transistors (FET) [2, 69, 241, 242] and may provide the basis of future devices like sensor based bioelectronic noses and tongues[114, 232, 243] although, at present, the response patterns obtained by these devices are not stable over time.[2] This is a serious limitation in bioelectronic tongues and noses although

their potential to extract complex information from the sensor array seems very powerful.[2]

Dextran modified single-walled CNTs were employed as glucose biosensors in a FET configuration.[244] In this sensor, concanavalin A, which was bound to the dextran layer, was displaced in the presence of glucose producing a change in conductance.[244] An *et al.*[245] reported a FET for the detection of thrombin using aptamer-modified single-walled CNTs. The sensor had a linear sensitivity in the thrombin physiological range, *i.e.,* from 70 pM to 70 nM. FETs based on carbon nanomaterials also have been reported to be responsive to pH [246] and sodium.[247, 248] For instance, sodium levels in the range from 1 nM to 1 mM were detected in serum samples. The operating mechanism is not fully understood, but it was suggested that the sodium ions bind to the carboxylic groups on the graphene layer and the change of the sodium concentration modulates the current into the transistor.[248] However, no tests with real body fluids were reported which raises questions about their use in real scenarios.

Building precise sub-micron scaled scaffoldings and networks is important in order to impart certain functions to the sensing interface. Rusling *et al.*[249] employed SW-CNTs forests for the electrochemiluminescent detection of interleukin-6 (IL-6) and PSA, two cancer biomarker proteins. A CCD camera was then used for the detection of the light generated by the silica NPs labeled with a ruthenium dye and the specific antibody, achieving detection limits of 1 pg ml^{-1} for PSA and 0.25 pg ml^{-1} for IL-6.[250, 251] CNTs forests allow ample space in between the pillars, but their preparation can be cumbersome.[231, 252] In this sense, a novel bucky-paper material prepared by Lard *et al.*[252] seems promising as it shows high surface adhesion and tunable electrical conductivity while maintaining separation of the individual tubes.[252] The key material is a polymer with lamellar crystal structure. The polymer is perpendicular to the tubes and its size tunes the porosity, surface roughness, and conductivity of the bucky-paper.[252]

Graphene offers excellent electron transfer properties, and this can play a key role in the performance of sensors.[253] For example, ssDNA segments physically adsorbed on graphene quantum dots (GQDs) were reported for the detection of thrombin.[254] The specific binding of the ssDNA with the target analyte generated an electron transfer between the electro-active species $[Fe(CN)_6]^{3-/4-}$ and the GQDs modified electrode, which would have otherwise been blocked by the adsorbed

ssDNA. Nitrite sensors were also reported, based on immobilisation of hemoglobin on graphene sheets functionalised with tetrasodium 1,3,6,8-pyrenetetrasulfonic acid[255] which binds to the positive domains of myoglobin.[256] Graphene enhanced the electron transfer kinetics of the protein, and nitrite levels could be amperometrically quantified in the range of 0.01 mM - 2.5 mM. However, it was found that the signal was pH dependent, which limits the practical applicability of the sensor. Graphene may also improve the solid contact characteristics of ion-selective electrodes due to its exceptional electrochemical properties and hydrophobicity. In this regard, MW-CNTs employed as the solid contact in ion-selective electrodes have been reported to result in improved stability compared to CPs.[257]

Graphene-based fluorescence quenching has been employed as the basis of several sensors. For instance, potassium was detected by immobilising a DNAzyme (deoxyribozymes) on graphene and then intercalating a commercial fluorophore within the DNA structure. [258, 259] It was found that the fluorescence emission was quenched by the graphene layer, but the addition of Cu^{2+} ions generated a fluorescence signal proportional to the metal concentration in the range 2 - 250 nM.[259]

2.6.3 Nanocomposites.

2.6.3.1 Introduction and Properties of Nanocomposites.

Nanocomposites are formed by combining nanoscaled-materials in order to obtain synergetic effects,[260, 261] such as improvements in the sensitivity and limit of detection of sensors, and to limit bio-fouling[236]. Nanocomposites have been also investigated as a means to create a suitable microenvironment for the stabilisation of biomolecules,[262]. In this respect, the combination of ILs and nanoparticles appears to present particular promise.[83, 263] CPs loaded with NPs have also proven effective in enhancing the electron transfer between entrapped enzymes and the electrode.[205] In SC-ISEs the ion-to-electron transduction may result either from a Faradic redox process either from a double-layer charging process.[264, 265]

In case of a capacitive contribution the use of nanocomposite as solid contact

may be beneficial in order to increase the surface area and therefore the overall capacitance which in turns has proven to improve the sensor stability.[264] For a commercial perspective, the possibility of preparing nanocomposites at a low-cost, and the feasibility of using these materials in common industrial processes will be important. In this regard, it is worth remembering that graphene and PEDOT can be printed together using ink-jet printing.[145]

2.6.3.2 Tailoring Nanocomposites for Biomedical Applications.

Nanomaterials have been used in a combined manner in order to improve the stability of enzymes [266-268]. For example, platinum NPs and CNTs were used to modify glassy carbon electrodes in order to improve the deposition of oxidase-enzymes.[267] The glucose oxidase-based biosensor built using these two materials showed a linear response up to 10 mM glucose, with a detection limit of 250 nM and a response time of 5s but it was not tested with real samples. Wu *et al.*[269] prepared multifunctional micro-gel particles for optically sensing glucose and simultaneous self-regulation of insulin. This was achieved by co-polymerisation of a gel layer of 2-(dimethylamino)ethyl acrylate and with 4-vinylphenylboronic acid onto Ag nanoparticle. The microgel layer swells as a function of glucose concentration resulting in a change of the local refractive index around the inorganic core and a marked decrease of the photoluminescence intensity of the Ag cores, which provided means to monitor the glucose concentration in solution. At the same time, the swelling of the microgel particles, which depends from the glucose concentration, was used to regulate the release of the insulin loaded within the particles as shown in Figure 2.5.[269]

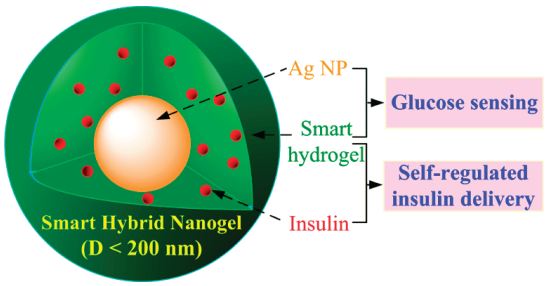

Figure 2.5. Schematic illustration of smart hybrid nano-gels that integrate optical glucose detection and self-regulated insulin delivery at physiological pH into a single nano-object. (adapted from reference [269])

Serafin *et al*.[270] used a 1-butyl-3-methylimidazolium hexafluorophosphate IL in order to solubilise alcohol oxidase and 3,4-ethylenedioxylthiophene (EDOT). The polymerisation of the EDOT on carbon screen printed electrodes (SPEs) modified with gold nanoparticles that resulted in the entrapment of the enzyme.[270] The measured current for ethanol was 30 % larger in cases where SPEs were modified with NPs. The sensor showed a linear range between 5 and 100 μM and a detection limit of 2 μM. Mixtures of colloidal gold modified graphite powder with a solid RTIL, *n*-octyl-pyridinium hexafluorophosphate, were combined with glucose oxidase to prepare paste electrodes.[89, 271, 272] The proposed biosensor responded to glucose linearly over concentrations ranging from 5.0 μM to 2.6 mM, with a fast response (10 s), and the life time was reported to be over two months.[271] The effects of electroactive interferents, such as ascorbic acid and uric acid, were significantly reduced using a Nafion® coating and the electrodes were used to analyse blood serum samples with good correlation with HPLC results, *i.e.,* relative errors < ± 5 %. These results are interesting as perhaps the graphite/ILs composite could be employed in ink formulations for the preparation of disposable glucose sensors.

Chitosan, which is a linear hydrophilic polysaccharide obtained by deacetylation of natural chitin, is attractive because of its biocompability, bioavailability, non-toxicity, and film-forming ability.[101, 273] It is pH sensitive and at pH values below its pK_a , *i.e.* pH < 4.5, it exists as a water-soluble cationic polyelectrolyte while at higher pH, *i.e.* ~ 7, it becomes neutral and insoluble.[101, 273] It has been largely used in nanocomposites for biosensing applications as it is thought to provide a good environment for enzyme stabilisation.[101, 273]

Chitosan was electrochemically deposited at an electrode surface by lowering the local pH using a proton-consumer reaction (reduction of water or other oxidants in solution).[101, 273] This deposition method provided good reproducibility of the film thickness and high surface area for the three-dimensional chitosan gel.[101, 273] During the biopolymer deposition 1-butyl-3methyl-imidazolium tetrafluoroborate [C_4mIm][BF_4] and GOx were also entrapped.[101, 273] The sensor thus prepared had a linear response for glucose in the 3 μM to 9 mM range. It was also able to detect glucose in serum samples showing a good correlation to the measurements with standard commercial biochemical analysers.[101] A nanocomposite based on assembled layers of MWCNTs, gold nanoparticles, 1-butyl-

3-methylimidazolium tetrafluoroborate and chitosan has been investigated as a means to immobilise cholesterol oxidase.[274] The resulting sensor demonstrated good sensitivity with a dynamic linear range up to 5 mM and cholesterol levels in serum samples were accurately measured using the standard addition method.[274] NPs in chitosan-IL composite gels have also proven beneficial in biosensing.[275] For instance, Au/Pt-NPs deposited within a chitosan/1-butyl-3-methylimidazolium chloride gel immobilised on a glassy carbon electrode, coated with cholesterol oxidase using glutaraldehyde has been successfully used for cholesterol monitoring.[276] The biosensor exhibited two wide linear ranges of responses to cholesterol, 0.05 – 6.2 mM and 6.2 –11.2 mM. The sensitivity of the biosensor was 90.7 μA mM^{-1} cm^{-2}, the limit of detection was 10 μM of cholesterol and the response time was less than 7 s. Levels of cholesterol in serum samples determined by the sensor agreed with the those obtained by a standard clinical method, showing relative percentage errors smaller than 3 %.[276] However, the samples had to be pre-treated with cholesterol esterase to convert fully the esterified cholesterol before the measurements were made.

CPs have been combined with other nanomaterials to enhance sensor performance, *e.g.,* enzyme immobilisation and sensitivity. Nanofibrous PEDOT has been deposited on glassy carbon electrodes by a micellar assisted soft template approach using $[C_4mIm][BF_4]$, and sodium dodecyl sulfate.[277] The IL works as a co-surfactant and as a dopant for PEDOT. Palladium nanoparticles were then deposited on the CP layer, followed by a potential-triggered deposition of GOx and encapsulation using Nafion®.[277] The sensor had a high sensitivity, 1.6 mA M^{-1} cm^{-2}, and was linear over a wide range of concentration, (0.5 to 30 mM). Besides, the sensor was able to detect glucose in diluted human serum samples showing small difference in relative percentage error (< 3 %) against values obtained with a standard reference method.[277]

Poly-5,2'-5',2'',terthiophene-3'-carboxylic acid was electropolymerised in the presence of MWCNTs on gold electrodes, followed by chemical coupling of lactate dehydrogenase and its co-factor nicotinamide adenine dinucleotide, NAD^+, to the conductive polymer -COOH groups. The sensor showed a linear response in the range from 5 to 90 μM and it retained 98 % of its sensitivity after a period of 30 days[39]. It should be noted, however, that commercial lactate test-strips can last up to one year. The sensor could detect lactate in human serum, however, samples had

to be diluted 1000 times, and the standard addition method was employed, which is not a feasible practice in ready-to-use sensors.

Non-enzymatic sensors for the detection of molecules such as glucose, lactate or ethanol is another important area of research due to the stability issues of enzymes when incorporated into biosensors. Certain conditions such as pH and temperature play a pivotal role in the stability of the enzyme and therefore these sensors sometimes have a small operational window.[16, 278] Enzymatic approaches remain commercially unchallenged thanks to their reliability and low-cost, *i.e.* few Euros per strip (http://www.novabiomedical.com/products/lactate-plus/). Research into enzyme mimicking materials is typically focused on addressing significant issues, such as fouling and selectivity.[16] In this regard, combinations of ILs, CNTs or graphene with metal nanomaterials seems a promising approach for the non-enzymatic detection of glucose [16, 205, 279-283]

Zhu *et al.*[284] studied the role of ILs in composites prepared by embedding Au-NPs in Bucky-gels. The composite functioned as an electrocatalyst for the conversion of glucose. The authors gave evidence that imidazolium cations facilitate both the stability of sensor and the efficiency of NPs and CNTs in catalysing glucose conversion, while non-imidazolium-based ILs work against the dispersion of CNTs and GNPs in the gel, reducing the detection sensitivity. It was also reported that the response to glucose could be improved by increasing the hydrophilicity of the anion. For example ions such as sulphonate gave better results than BF_4^- and PF_6^-. Copper nanocubes deposited on vertically aligned MW-CNTs arrays were developed for the non-enzymatic detection of glucose, and the resulting sensors showed minimal interference from oxidisable interfering species such as fructose, ascorbic and uric acid.[285] Results returned from human blood serum were close (within 5 % relative error) to those obtained via standard tests. However, the requirement to add 0.1 M NaOH to the samples (dilution factor 1 : 1000)[285] may be a limiting factor in the preparation of ready-to-use sensors. Gold nanoparticles grown on CNTs were also reported for the electrocatalytic conversion of bilirubin, although the experiments were done in buffer solutions[52] rather than real samples, which limits the value of this output.

The use of magnetic nanomaterials offers certain advantages as magnetic separation is easy to implement and the composite can be easily collected for further analysis.[222, 286, 287] Fe_3O_4 magnetic nanoparticles have been found to mimic the

activity of peroxidases.[288] This catalytic behavior, in combination with bio-separation and recycling, perhaps may be a plausible and exciting feature for the preparation of non-enzyme based sensing strategies in which the sensing surface is newly generated each time, *i.e*. similarly to the hanging mercury drop technique. Tang *et al.*[289] introduced a micro-fluidic device for an immunoassay for simultaneous determination of carcinoembryonic (CEA) and alpha-fetoprotein (AFP) in biological fluids. The immunoassay was realised using anti-CEA and anti-AFP antibodies, immobilised on the Fe_3O_4 nanoparticle-coated graphene nanosheets. The magnetic composite allowed an easy separation from the biological specimen by application of a local magnetic field, avoiding the need of washing steps. In addition, authors employed as antibody labels nanogold hollow microsphere which provided higher loading capacity of the electrochemical active species (HRP-thionine and HRP-ferrocene) and larger surface coverage than bulk-AuNPs. The final immunosensor achieved an LOD equal to 1.0 pg mL^{-1} for both the target analytes.

This section concludes reporting on a number of nanocomposites which have been used to modify electrode surface in order to improve sensor performance compared to bare surfaces.[290-294] For example, simultaneous detection of NO_2^-, dopamine and ascorbic acid was achieved using a nanostructured glassy carbon electrode modified with a graphene/MW-CTNs mixture dispersed in β-cyclodextrin and and cyclodextrin prepolymer.[295] As cyclodextrin exhibits different interactions with the three molecules, it was possible to differentiate them using differential pulse voltammetry.[295] A linear range from 1.65 μM to 6.75 mM was achieved for NO_2^- and the sensor was successfully applied to the analysis of diluted urine samples spiked with the analyte of interest.[295] Nanostructured polyaniline has been chemically synthesised using graphene oxide nanosheets as a polymerisation template for adapting the surface of glassy carbon electrodes.[296] Using this approach, it was possible to simultaneously differentiate between ascorbic acid, dopamine and uric acid. NiO nanoparticles have been used as seeds for the polymerisation of pyrrole, which was triggered by addition of $HAuCl_4$ after monomer adsorption on the NiO core. The nanocomposite worked as an electro-catalyst for the oxidation of bio-thiols, with the polypyrrole layer improving the composite adhesion to the electrode surface.[297] Sensors developed using this method showed a linear response in the range from 0.35 to 9 μM for the detection of

cysteine in saliva using the standard additions method, with almost no interference from other biological thiols like homocysteine and glutathione reported.

2.7 Ionogels: Diverse Materials for Sensing Platforms.

2.7.1 Introduction to Ionogels.

Ionogels are polymer gels in which an ionic liquid is integrated to the polymeric network. In these materials, the IL can often retain its specific properties within the polymer/gel environment. The employment of ILs as a replacement for water in gel-based polymers has led to the emergence of ionogels as a relatively new sub-class of materials. To date, ionogels have been the subject of reviews detailing their preparation and applications in sensor science.[95, 298] The ionogel template is an ideal matrix as the properties of the IL is hybridised within those of the polymer component combining the favorable characteristics of both independent phases in one material. An excellent review by Bideau *et al.*[299] discusses ionogels, in which the properties of the ILs are hybridised with those of various components. These may be organic (low molecular weight gelator, polymer), inorganic (*e.g.* carbon nanotubes, silica *etc.*) or organic–inorganic (e.*g.* polymer and inorganic fillers) as shown in Figure 2.6.

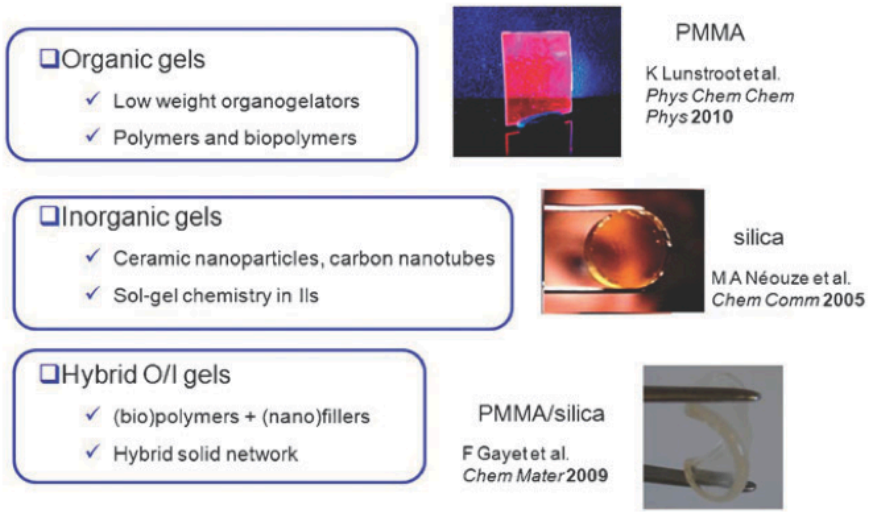

Figure 2.6. Types of Ionogels synthesised as outlined by Bideau *et al.* (adapted form reference [299])

Another approach for the preparation of ionogels is to use ILs in which the cation or the anion is polymerised, *e.g.* via vinyl groups. These ionogels are normally denoted as poly-ILs (PILs). This approach can be particularly effective in reducing the leaching of IL components into a sample.[300] The use of ionogels in electrochemical sensors and biosensors is an ever-growing field. An intrinsic advantage of ionogels compared to redox polymers is that their ion-conductivity is de-coupled from segmental motion, *i.e*. movement of polymer branches, providing high conductivity even below their glass transition temperature.[301]

As discussed in Section 2.2, in certain cases, ILs may exhibit favorable biocompatibility behavior, and stabilise biomolecules and enzymes, leading to enhanced sensor stability and shelf-life. Some examples are based on the immobilisation of enzyme-IL systems with hyaluronic acid[302] or Nafion®.[303] Ionogels may also assist in the preparation of stable conductive-textile yarns, maximising contact surface, and improving skin-adhesion during sweating [32, 34, 304]. This is an attractive proposition for the field of wearable textile (bio)-sensors. These materials should be capable of retaining the favorable properties of the base IL in a solid, semi-solid gel-like structure.[305]

2.7.2 Biomedical Applications of Ionogels.

Perhaps, the most common use of ionogels is to provide a suitable solid-state matrix for a stable encapsulation of nanostructured materials, such as proteins and enzymes.[86, 231, 261] For instance, PILs have been used for the electrochemical sensing of glucose. In fact, hydrophilic microparticles were prepared by emulsion polymerisation of 1-vinyl-3-ethylimidazolium bromide in presence of a cross-linker and GOx.[306] This method allowed the entrapment of the enzyme within the microparticles which were then immobilised at the electrode interface.[306] Using amperometry, glucose levels in serum human sample were validated and the sensor showed storage stability up to 150 days when stored in frozen PBS at -4 °C.[307] A polyethylenimine functionalised IL (PFILs) was successfully used as a matrix in aqueous solution to synthesise Au-NPs (*ca.* 2.4 nm) and simultaneously stabilise MW-CNTs.[308] The nanocomposite (AuNPS / MWCNTs / PFILs) once deposited onto glassy carbon electrodes could successfully “wire” the glucose oxidase, which

was physisorbed onto the nanocomposite. The sensor response was linear in glucose buffer solutions ranging from 2 to 12 mM which is suitable for its practical application in determining blood sugar although this was not demonstrated with the analysis of real samples. Similarly, graphene sheets were stabilised by a mixture of poly(vinyl-pyrrolidone) and PFILs, providing direct "wiring" of GOx, and they were successfully used in the sensing of glucose in aqueous solution.[309] In another interesting example, methyl-imidazolium moieties were grafted on MW-CNTs in order to confine redox-active ferricyanide thanks to the strong electrostatic interactions.[310] The nanocomposite was then coated with GOx (through crosslinking with glutaraldehyde) and developed as a glucose sensor.[310] Fonseca *et al*.[311] explored the application of new biocompatible materials by developing colorimetric glucose sensor strips. Imidazolium based ILs paired with a gelling agent (gelatin type A) formed an ionogel, defined by the authors as Ion Jelly®, which provided a stable environment for the GOx enzyme for up to 2 weeks of storage with 30 % loss of stability.[311] By incorporating GOx, HRP and the chromogenic dye precursors into the Ion Jelly®, (in which IL was $[C_2mIm][EtSO_4]$), authors realised a colorimetric glucose sensing strip. This work is surely exciting, however, the accuracy of the colorimetric assay in determining the glucose level together with the short shelf-life of such sensor (limited by the stability of the enzyme in the Ion Jelly®) seem to be two major hurdles in the system.

In recent years, developments in the field of organic electronics have led to novel approaches for producing flexible electronics using organic semiconductors.[312] Among others CPs, PEDOT:PSS can be patterned on a wide variety of substrates such as glass, flexible plastic and textiles, opening the way for the development of wearable biosensors. Such biosensors can be incorporated into fabrics such as T-shirts, sweat bands or shorts allowing for real-time measurements of the target analyte. In this respect, Khodagholy *et al.*[313] used a PEDOT:PSS organic electrochemical transistor (OECT) in which a pNIMAm/$[C_2mIm][EtSO_4]$ ionogel was integrated as a solid-state electrolyte for the detection of lactate in the sweat physiological range (between 9 and 23 mM), as will be discussed in chapter 5 of this thesis. As proof of concept, it was also demonstrated for the use of the OECTs in an array with a "tattoo-like" format using a flexible substrate, *i.e*., parylene, as shown in Figure 2.7.

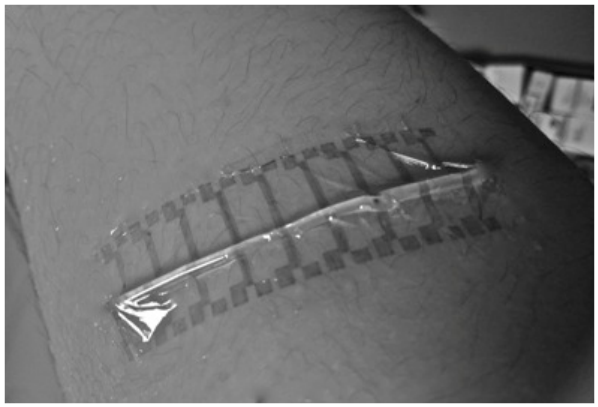

Figure 2.7. Concept of a flexible and conformal OECTs/ionogel array worn on the forearm. (adapted from reference [313])

Regarding wearable sensors, ionogels may offer a route to generating simple colorimetric devices. For instance, chapter 4 and 8 will discuss the development of a colorimetric wearable micro-fluidic barcode for the real-time monitoring of pH in sweat, Figure 2.8.[314] The barcode contain ionogels which are doped with several pH chromogenic dyes (having different pK_a) such that the device is capable of monitoring the pH in the range 4.5 – 7.5. It was reported that the pNIPAAm/$[P_{6,6,6,14}]$[dca] ionogel provides a convenient matrix to immobilise the pH responsive dyes, as it reduces leaching of the dyes through electrostatic interactions within the IL. The device was integrated into a commercially available plaster, and was successfully used for measuring the pH of an athlete during a 50 min training session.

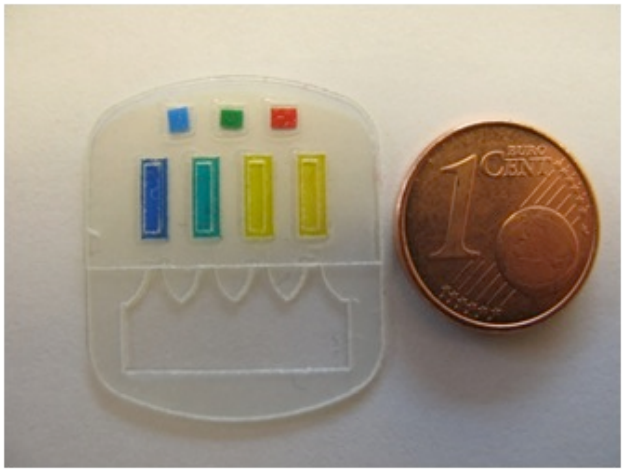

Figure 2.8. Flexible and wearable micro-fluidic barcode for real-time pH sweat analysis through the use of four pH sensitive phosphonium based ionogels. (adapted from reference [315])

Mixture of carbon nanotubes (or graphene) and ionic liquids have been combined for generation of interesting sensing material, bucky-gel.[316] For example, a MW-CNTs and 1-octyl-3-methylimidazolium hexafluorophosphate bucky-gel was decorated with ternary alloy nanoparticles based on Pt, Ru and Ni.[317] The sensor was applied to alcohol detection in aqueous solutions up to a concentration of 38 mM. Graphene mixed with 1-butyl-3methyl imidazolium hexafluorophosphate has been used in the fabrication of gels for the detection of NO in aqueous solutions.[318] The sensor exhibited a fast response of less than 4 s, and a low detection limit of 16 nM, which is superior than that of NO sensing platforms based on carbon nanotubes and gold nanoparticles.[318]

Ionogels represent an interesting approach also for the detection of ions and metal oxides by voltammetric methods such as stripping voltammetry[319], thanks to their solvation properties.[320] For example, Wan *et al.*[316] incorporated thiols to improve the stability of bucky-gels on carbon electrodes and then used the modified electrodes to detect lead ions by means of stripping voltammetry. The authors reported the detection of lead at the femtomolar level and successfully measured lead content in lake water. Ionogels have been reported to provide a stable double layer capacitance and therefore overall stable sensor response in solid contact electrodes.[124] The possibility of tuning the characteristics of an ionogel by varying the IL is an attractive proposition. For example, this has been used to control the hydrophobicity of ionogels and therefore the degree of swelling, which is critical for the realisation of polymer actuators. It should be noted that hydrogels are not effective as materials for solid contact electrodes because of their natural tendency to absorb water.[321] In contrast, using ionogels rather than hydrogels as the solid contact material in ISEs can reduce this problem, and this may improve the long term response and the storage stability of these sensors.

2.8 Future Trends

2.8.1 Evolutionary and Revolutionary Materials

The grand challenge for enzyme based sensors is to control the enzyme orientation in the responsive material such that the enzyme response characteristics are not affected.[322] One of the most effective biosensor configurations reported thus far is

an enzymatic glucose sensor developed by Heller *et al.* in collaboration with Abbott Diabetes Care. In this configuration an osmium hydrogel entraps the glucose dehydrogenase at one electrode.[14, 16] The sensor is functional over the range 20 - 500 mg dL^{-1}, with a correlation coefficient of $R^2 = 0.99$ against the Yellow Spring (YSI) glucose analyser.[323] This is regarded as an example of a third generation biosensor, *i.e.*, in which the enzyme is directly wired to a conductive diffusionless network. Research is now focused on materials that can improve the enzyme stability and the sensor sensitivity for other analytes, lactate for example. It is also important to note that, with some exceptions, sensors described in the literature fail when challenged with complex samples, such as interstitial fluid, sweat and saliva. To date, the goal of a reagentless, real-time implantable sensor remains largely unmet.[324, 325] As nature can carry out these complex reactions successfully, one can be inspired to continue to research, as natural ligand-biomolecule interactions are highly specific and signal transduction is fast and reversible.[324]

Another challenge is presented by solid waste generation, able to dictate a shift from traditional polymers to "green nanocomposites", based on bio-polymers matrices such as cellulose nanowhiskers or metal-chitosan nanocomposites.[237, 326] In this regard, it is worthwhile to note the ability of ILs to solubilise biopolymers such as chitosan, agarose, keratin, dextran, pectin and cellulose is of considerable interest.[93, 327] For instance, Ion-Jelly® may represent a valid route for the preparation of electrochemical sensors in which the matrix stabilises the enzyme whilst also providing good mechanical and electrical properties.[93] In addition, research into bio-polymers may be beneficial for providing new materials for ISEs membranes (compared to the traditional PVC and poly-acrylates).

Research in polymer chemistry may also provide novel materials that can allow control over the chemical, physical and mechanical properties of sensors, and also incorporate biofunctionality.[328] The combination of ILs with block polymers is particularly appealing as it should allow better control at the nanoscale, which may improve control over phase transitions, and mechanical and chemical properties.[329] In addition, research into supramolecular polymers networks may help in obtaining intelligent sensors by means of non-covalent interactions via a bottom-up approach.[330, 331] For example, rubbery-metallo supramolecular polymers have shown self-healing by exposure to UV light, which may be an interesting feature for biosensing materials capable of self-regeneration or repair.

[330] Research is ongoing into skin-like gel behavior, wherein the signal is amplified throughout the system in response to an environmental stress or chemical input. While these studies are at early stage, far from real applications, they may pave the way to the creation of 'artificial skin'.[332]

Surface chemistry and nanostructuring will also be two important players in addressing the biofouling issue in biomedical applications.[260, 333, 334] In order to produce long-term biocompatible coatings, the ability to trap-air at the solid–liquid interface may be important.[334] Nanostructured electrode materials will also represent a significant area of interest for kinetically controlled, surface bound reactions, *e.g.,* glucose oxidation, which in turn will be beneficial for the development of non-enzymatic sensors.[16]

2.8.2 Future Trends in Biomedical Sensing

An important challenge for materials chemistry will be the integration of sensors into wearable systems. Wearable sensors should allow the continuous monitoring of a person's physiology in a natural setting, thus decreasing the demand on local health care systems. At present, health-monitoring using electronic textiles are targeting applications based upon physiological parameters, such as body movements or electrocardiography (ECG). Several products are already commercially available, such as the Lifeshirt®, developed by Vivometrics®, the body monitoring system developed by BodyMedia® and the Nike-Apple iPod Sports kit which facilitates individualised feedback control of performance during exercise periods. The use of wearable systems such as these for personalised exercise regimes for health and rehabilitation is particularly interesting. However, due to their relative complexity, there is very little activity in the development of real-time wearable chemo/bio sensing for sports applications.

These sensors require that the desired sample of analysis, usually a body fluid such as sweat or interstitial fluid is delivered to the sensor's active surface, whereupon a reaction happens and a signal is generated. Moreover the system must be low cost, while still being robust, miniature flexible, washable, reusable or disposable.[335] All these requirements point to micro-fluidic devices as the key for improving wearable chemo-/bio-sensing.[336] Chemical measurements on bodily

fluids such as blood, sweat, and urine are needed. This area of research is still hardly developed due to the difficulty in sampling such fluids and in particular obtaining uncontaminated samples. The BIOTEX project tackled some of these problems, such as fluid handling, by developing a textile-based system to collect and analyse sweat using a textile-based sensor capable of performing chemical measurements.[335]

Textile fibers such as cellulose or cotton can be made conductive by coating with carbon nanotubes [337] and anti-microbial coatings can be grafted onto textiles and plastics.[338] Flexible/stretchable and transparent electronics that can be intimately associated with human skin and tissues is likely to play a significant role in future applications involving chemical sensing.[232, 339-343] Currently wearable sensors are mainly applied to the measurement of electrical activity produced by the brain and heart of humans non-invasively.[340] Recently, Windmiller *et al*.[342] showed that on-skin tattoo electrodes can be fabricated and employed for electroanalytical measurements, though no real-time body-sensing measurements were reported. The combination of tattoo-based electrochemical sensors with wearable electronics may, in the future, assist with the realisation of fully-functional electronic skin.[342, 343]. This is a very interesting, and also challenging research subject, as, in principle, it may allow important parameters related to personal health to be continuously monitored in a non- or minimally invasive manner.[56]

2.9 Concluding Remarks

Chapter 1 presented the most recent and noteworthy scientific contributions to the realisation of wearable physiological and chemo/bio-sensors, with particular emphasis on the application of materials science. For instance, devices such as that described in figure 1.3 provide ground-breaking solutions that have the potential to enable multi-parameter measurements through the use of a conformal and stretchable epidermal electronic sensor. Although this approach has a great significance for the realisation of wearable devices, the significant challenges still remains with respect to the development of platforms capable of sensing chemically and biologically relevant species present in bodily fluids, such as sweat.

Another valuable approach for the realisation of wearable chemo/bio-sensors is provided by their integration into fabrics, as shown in figure 1.6. In fact, conformal

fabric based sensors can be integrated into clothes, for instance in sport applications in which tight lycra suits are worn, facilitating effective contact of the resulting flexible sensor platforms with the body contours. Electronic integration of these devices can be readily achieved using electric circuits connected with conducting threads and fibres.

Novel sensing materials play a critical role in the realisation of these novel wearable sensing platforms. Therefore a wide variety of materials and their potential for use in on-body sensing is presented and discussed in this chapter. In section 1.3 the use of micro-fluidic technology was proposed as an effective alternative to overcome several limitations present in existing sampling techniques, *e.g.* adhesive plasters during the performing of sweat analysis. Additionally, as previously highlighted, another advantage of the use of micro-fluidic technology lies in the possibility of integrating the sensing close to the sample input to the micro-fluidic structure, decreasing the sampling to analysis time. Therefore, the choice of the sensing material to be integrated inside the micro-fluidic channels becomes crucial as it has to present specific characteristics compatible both with wearable applications and with the technique employed for the generation of the analytical signal.

In the following chapters of this thesis materials such as ILs, ionogels and CPs are investigated for use in wearable chemo/bio-sensors. ILs are extensively investigated in chapters 4, 5 and 6. The results show that IL behaviour is strongly influenced by the choice of the anion/cation pair, which can significantly change the resulting properties of the ILs (see section 2.4). For instance, in the case of the wearable micro-fluidic device for real-time analysis of sweat pH (Chapter 4), the chosen ionic liquid provided a suitable immobilisation medium for the chromogenic dyes, without altering their pH-sensitive characteristics.

Furthermore, the immobilisation of the ILs in a polymer matrix (ionogels) facilitates the incorporation of the sensing materials in wearable platforms, reducing the complexity of the sensor and, at the same time, improving its overall performance. This approach has been used in Chapter 5, for the realisation of a lactic acid sensor using organic electrochemical transistors based on CPs. In this system, the choice of the IL was dictated by its compatibility with the bio-receptor substrate, while the ionogel physical characteristics were influenced by the requirements of future integration of the sensor in a micro-fluidic device. In Chapter 6, the preparation of stable ILs/enzyme formulations designed to improve the performance

of a lactic acid sensor are discussed in more detail, while chapter 7 introduces a novel method for the realisation of paper-based micro-fluidics for biosensing applications.

Finally, Chapter 8 presents a preliminary investigation into the fabrication of a wearable fabric based biosensor in which the use of graphene nanomaterials appear to open new scenarios for the development of stable and flexible wearable chemo/bio-sensors.

2.10 References

1. Byrne, R.; Diamond, D., Chemo/bio-sensor networks. *Nature Materials* **2006,** *5*, 421-424.
2. Diamond, D.; Collins, F.; Cleary, J.; Zuliani, C.; Fay, C., Distributed Environmental Monitoring. In *Autonomous Sensor Networks, Collective Sensing Strategies for Analytical Purposes*, Filippini, D., Ed. Springer: Due by January **2013**, 13.
3. Byrne, R.; Ventura, C.; Benito Lopez, F.; Walther, A.; Heise, A.; Diamond, D., Characterisation and analytical potential of a photo-responsive polymeric material based on spiropyran. *Biosensors and Bioelectronics* **2010,** *26*, 1392-1398.
4. De Marco, R.; Clarke, G.; Pejcic, B., Ion-Selective Electrode Potentiometry in Environmental Analysis. *Electroanalysis* **2007,** *19*, 1987-2001.
5. Diamond, D.; Coyle, S.; Scarmagnani, S.; Hayes, J., Wireless Sensor Networks and Chemo/Biosensing. *Chemical Reviews* **2008,** *108*, 652-679.
6. Diamond, D.; Lau, K. T.; Brady, S.; Cleary, J., Integration of analytical measurements and wireless communications. Current issues and future strategies. *Talanta* **2008,** *75*, 606-612.
7. Farré, M.; Kantiani, L.; Pérez, S.; Barceló, D., Sensors and biosensors in support of EU Directives. *Trends in Analytical Chemistry* **2009,** *28*, 170-185.
8. Yantasee, W.; Lin, Y.; Hongsirikarn, K.; Fryxell, G. E.; Addleman, R.; Timchalk, C., Electrochemical Sensors for the Detection of Lead and Other Toxic Heavy Metals: The Next Generation of Personal Exposure Biomonitors. *Environ Health Perspect* **2007,** *115*, 1683-1690.
9. Zhuiykov, S., Solid-state sensors monitoring parameters of water quality for the next generation of wireless sensor networks. *Sensors and Actuators B Chemistry* **2012,** *161*, 1-20.
10. Ballesta Claver, J.; Valencia Miron, M. C.; Capitan-Vallvey, L. F., Disposable electrochemiluminescent biosensor for lactate determination in saliva. *Analyst* **2009,** *134*, 1423-1432.
11. Sears, M. E.; Kerr, K. J.; Bray, R. I., Arsenic, Cadmium, Lead, and Mercury in Sweat: A Systematic Review. *Journal of Environmental and Public Health* **2012,** *2012*, 1-10.
12. Kotanen, C. N.; Moussy, F. G.; Carrara, S.; Guiseppi-Elie, A., Implantable enzyme amperometric biosensors. *Biosensors and Bioelectronics* **2012,** *35*, 14-26.
13. Guiseppi-Elie, A., An implantable biochip to influence patient outcomes following trauma-induced hemorrhage. *Analytical and Bioanalytical Chemistry* **2011,** *399*, 403-419.
14. Heller, A.; Feldman, B., Electrochemical Glucose Sensors and Their Applications in Diabetes Management. *Chemical Reviews* **2008,** *108*, 2482-2505.

15. Justin, G.; Finley, S.; Abdur Rahman, A.; Guiseppi-Elie, A., Biomimetic hydrogels for biosensor implant biocompatibility: electrochemical characterization using micro-disc electrode arrays (MDEAs). *Biomedical Microdevices* **2009,** *11*, 103-115.
16. Toghill, K. E.; Compton, R. G., Electrochemical Non-enzymatic Glucose Sensors: A Perspective and an Evaluation. *Int. J. Electrochem. Sci.* **2010,** *5*, 1246-1301.
17. Steiner, M.-S.; Duerkop, A.; Wolfbeis, O. S., ChemInform Abstract: Optical Methods for Sensing Glucose. *ChemInform* **2011,** *42*.
18. Hassan, S. S. M.; Badr, I. H. A.; Kamel, A. H.; Mohamed, M. S., A Novel Poly(vinyl chloride) Matrix Membrane Sensor for Batch and Flow-Injection Determinations of Thiocyanate, Cyanide and Some Metal Ions. *Analytical Sciences* **2009,** *25*, 911-917.
19. Schazmann, B.; Morris, D.; Slater, C.; Beirne, S.; Fay, C.; Reuveny, R.; Moyna, N.; Diamond, D., A wearable electrochemical sensor for the real-time measurement of sweat sodium concentration. *Analytical Methods* **2010,** *2*, 342-348.
20. Katsu, T.; Tsunamoto, Y.; Hanioka, N.; Komagoe, K.; Masuda, K.; Narimatsu, S., S,S,S-Tris(2-ethylhexyl) phosphorotrithioate as an effective solvent mediator for a mexiletine-sensitive membrane electrode. *Analytical and Bioanalytical Chemistry* **2007,** *387*, 2057-2064.
21. Singh, P.; Singh, A., Determination of thiocyanate ions at nanolevel in real samples using coated graphite electrode based on synthesised macrocyclic Zn(II) complex. *Analytical and Bioanalytical Chemistry* **2011,** *400*, 2261-2269.
22. Opydo-Szymaczek, J.; Opydo, J., Salivary Fluoride Concentrations and Fluoride Ingestion Following Application of Preparations Containing High Concentration of Fluoride. *Biological Trace Element Research* **2010,** *137*, 159-167.
23. Al-Naimi, O.; Itota, T.; Hobson, R.; McCabe, J., Fluoride release for restorative materials and its effect on biofilm formation in natural saliva. *Journal of Materials Science: Materials in Medicine* **2008,** *19*, 1243-1248.
24. Singh, A. K.; Singh, U. P.; Mehtab, S.; Aggarwal, V., Thiocyanate selective sensor based on tripodal zinc complex for direct determination of thiocyanate in biological samples. *Sensors and Actuators B: Chemical* **2007,** *125*, 453-461.
25. Meyer, E.; Laitano, O.; Bar-Or, O.; McDougall, D.; Heigenhauser, G. J. F., Effect of age and gender on sweat lactate and ammonia concentrations during exercise in the heat. *Brasilian Journal of Medical and Biological Research* **2007,** *40*, 135-143.
26. Venugopal, M.; Feuvrel, K. E.; Mongin, D.; Bambot, S.; Faupel, M.; Panangadan, A.; Talukder, A.; Pidva, R., Clinical Evaluation of a Novel Interstitial Fluid Sensor System for Remote Continuous Alcohol Monitoring. *Sensors Journal, IEEE* **2008,** *8*, 71-80.
27. Trzebinski, J.; Sharma, S.; Radomska-Botelho Moniz, A.; Michelakis, K.; Zhang, Y.; Cass, A. E. G., Microfluidic device to investigate factors affecting performance in biosensors designed for transdermal applications. *Lab on a Chip* **2012,** *12*.
28. Cengiz, E.; Tamborlane, W. V., A Tale of Two Compartments: Interstitial Versus Blood Glucose Monitoring. *Diabetes Technology & Therapeutics* **2009,** *11*, S11-S16.
29. Rebrin, K.; Sheppard, N. F.; Steil, G. M., Use of subcutaneous interstitial fluid glucose to estimate blood glucose: revisiting delay and sensor offset. *Journal of diabetes science and technology* **2010,** *4*, 1087-1098.
30. Windmiller, J. R.; Zhou, N.; Chuang, M.-C.; Valdes-Ramirez, G.; Santhosh, P.; Miller, P. R.; Narayan, R.; Wang, J., Microneedle array-based carbon paste amperometric sensors and biosensors. *Analyst* **2011,** *136*, 1846-1851.
31. Yang, Y.-L.; Chuang, M.-C.; Lou, S.-L.; Wang, J., Thick-film textile-based amperometric sensors and biosensors. *Analyst* **2010,** *135*, 1230-1234.
32. Seoane, F.; Marquez, J. C.; Ferreira, J.; Buendia, R.; Lindecrantz, K., The Challenge of the Skin-Electrode Contact in Textile-enabled Electrical Bioimpedance

Measurements for Personalized Healthcare Monitoring Applications. In *Biomedical Engineering, Trends in Materials Science*, Laskovski, A. N., Ed. In-Tech: **2011**.

33. Marchand, G.; Rat, V.; Guillemaud, R.; Vinet, F.; Antonakios, M.; David, N.; Bourgerette, A. In *Development of a Dehydration Sensor Integrated on Fabric*, BSN 2009. Sixth International Workshop on Wearable and Implantable Body Sensor Networks., Berkeley, USA, 3-5 June **2009**, 230-233.
34. Paradiso, R.; Loriga, G.; Taccini, N., A wearable health care system based on knitted integrated sensors. *IEEE Transactions on Information Technology in Biomedicine* **2005,** *9*, 337-344.
35. Aguilera-Herrador, E.; Cruz-Vera, M.; Valcarcel, M., Analytical connotations of point-of-care testing. *Analyst* **2010,** *135*, 2220-2232.
36. Gonzalo-Ruiz, J.; Mas, R.; de Haro, C.; Cabruja, E.; Camero, R.; Alonso-Lomillo, M. A.; Muñoz, F. J., Early determination of cystic fibrosis by electrochemical chloride quantification in sweat. *Biosensors and Bioelectronics* **2009,** *24*, 1788-1791.
37. Li, C.; Shutter, L. A.; Wu, P.-M.; Ahn, C. H.; Narayan, R. K., Potential of a simple lab-on-a-tube for point-of-care measurements of multiple analytes. *Lab on a Chip* **2010,** *10*, 1476-1479.
38. Heinrich, S.; Luppa, M.; Matschinger, H.; Angermeyer, M. C.; Riedel-Heller, S. G.; Koenig, H.-H., Service utilization and health-care costs in the advanced elderly. *Value In Health* **2008,** *11*, 611-620.
39. Rahman, M. M.; Shiddiky, M. J. A.; Rahman, M. A.; Shim, Y.-B., A lactate biosensor based on lactate dehydrogenase/nictotinamide adenine dinucleotide (oxidized form) immobilized on a conducting polymer/multiwall carbon nanotube composite film. *Analytical Biochemistry* **2009,** *384*, 159-165.
40. Ges, I. A.; Baudenbacher, F., Enzyme-coated microelectrodes to monitor lactate production in a nanoliter microfluidic cell culture device. *Biosensors and Bioelectronics* **2010,** *26*, 828-833.
41. Lupu, S.; Lakard, B.; Hihn, J.-Y.; Dejeu, J.; Rougeot, P.; Lallemand, S., Morphological characterization and analytical application of poly(3,4-ethylenedioxythiophene)–Prussian blue composite films electrodeposited in situ on platinum electrode chips. *Thin Solid Films* **2011,** *519*, 7754-7762.
42. Romero, M. R.; Ahumada, F.; Garay, F.; Baruzzi, A. M., Amperometric Biosensor for Direct Blood Lactate Detection. *Analytical Chemistry* **2010,** *82*, 5568-5572.
43. Schabmueller, C. G. J.; Loppow, D.; Piechotta, G.; Schütze, B.; Albers, J.; Hintsche, R., Micromachined sensor for lactate monitoring in saliva. *Biosensors and Bioelectronics* **2006,** *21*, 1770-1776.
44. Romero, M. R.; Garay, F.; Baruzzi, A. M., *Sensors and Actuators B: Chemical* **2008,** *131*, 590-595.
45. Yashina, E. I.; Borisova, A. V.; Karyakina, E. E.; Shchegolikhina, O. I.; Vagin, M. Y.; Sakharov, D. A.; Tonevitsky, A. G.; Karyakin, A. A., Sol−Gel Immobilization of Lactate Oxidase from Organic Solvent: Toward the Advanced Lactate Biosensor. *Analytical Chemistry* **2010,** *82*, 1601-1604.
46. Gomathi, P.; Ragupathy, D.; Choi, J. H.; Yeum, J. H.; Lee, S. C.; Kim, J. C.; Lee, S. H.; Ghim, H. D., Fabrication of novel chitosan nanofiber/gold nanoparticles composite towards improved performance for a cholesterol sensor. *Sensors and Actuators B: Chemical* **2011,** *153*, 44-49.
47. Lakard, B.; Magnin, D.; Deschaume, O.; Vanlancker, G.; Glinel, K.; Demoustier-Champagne, S.; Nysten, B.; Jonas, A. M.; Bertrand, P.; Yunus, S., Urea potentiometric enzymatic biosensor based on charged biopolymers and electrodeposited polyaniline. *Biosensors and Bioelectronics* **2011,** *26*, 4139-4145.

48. Wolfe, R. A.; Ashby, V. B.; Daugirdas, J. T.; Agodoa, L. Y. C.; Jones, C. A.; Port, F. K., Bosy size, dose of hemodialysis, and mortality. *American Journal of Kidney Diseases* **2000,** *36*, 1025.

49. Hibbard, T.; Killard, A. J., Breath Ammonia Analysis: Clinical Application and Measurement. *Critical Reviews in Analytical Chemistry* **2011,** *41*, 21-35.

50. Kumar, C.; Patel, N., Sensitive analysis of breath gases for bloodless blood tests. *Gases Technology* **2002,** *1*, 24-30.

51. Rahman, M. A.; Lee, K.-S.; Park, D.-S.; Won, M.-S.; Shim, Y.-B., An amperometric bilirubin biosensor based on a conductive poly-terthiophene–Mn(II) complex. *Biosensors and Bioelectronics* **2008,** *23*, 857-864.

52. Wang, C.; Wang, G.; Fang, B., Electrocatalytic oxidation of bilirubin at ferrocenecarboxamide modified MWCNT-gold nanocomposite electrodes. *Microchimica Acta* **2009,** *164*, 113-118.

53. Peng, Y.; Ji, Y.; Zheng, D.; Hu, S., In situ monitoring of nitric oxide release from rat kidney at poly(eosin b)-ionic liquid composite-based electrochemical sensors. *Sensors and Actuators B: Chemical* **2009,** *137*, 656-661.

54. Phair, J.; Newton, L.; McCormac, C.; Cardosi, M. F.; Leslie, R.; Davis, J., A disposable sensor for point of care wound pH monitoring. *Analyst* **2011,** *136*, 4692-4695.

55. Lynch, A.; Diamond, D.; Leader, M., Point-of-need diagnosis of cystic fibrosis using a potentiometric ion-selective electrode array. *Analyst* **2000,** *125*, 2264-2267.

56. Coyle, S.; Lau, K. T.; Moyna, N.; O'Gorman, D.; Diamond, D.; Di Francesco, F.; Costanzo, D.; Salvo, P.; Trivella, M. G.; De Rossi, D. E.; Taccini, N.; Paradiso, R.; Porchet, J. A.; Ridolfi, A.; Luprano, J.; Chuzel, C.; Lanier, T.; Revol-Cavalier, F.; Schoumacker, S.; Mourier, V.; Chartier, I.; Convert, R.; De-Moncuit, H.; Bini, C., BIOTEX-Biosensing Textiles for Personalised Healthcare Management. *Ieee Transactions on Information Technology in Biomedicine* **2010,** *14*, 364-370.

57. Munaron, L.; Scianna, M., Multilevel complexity of calcium signalling: modelling angiogenesis. *World Journal of Biological Chemistry* **2012,** *3*, 121.

58. Titze, J.; Machnik, A., Sodium sensing in the interstitium and relationship to hypertension. *Current Opinion in in Nephrology and Hypertension* **2010,** *19*.

59. Brugnara, C., Iron deficiency and erythropoiesis: new diagnostiv approaches. *Clinical Chemistry* **2003,** *10*, 1573.

60. Spielmann, N.; Wong, D. T., Saliva: diagnostics and therapeutic perspectives. *Oral diseases* **2011,** *17*, 345-354.

61. Malongo, T. K.; Patris, S.; Macours, P.; Cotton, F.; Nsangu, J.; Kauffmann, J.-M., Highly sensitive determination of iodide by ion chromatography with amperometric detection at a silver-based carbon paste electrode. *Talanta* **2008,** *76*, 540-547.

62. Kim, S.; Park, J. W.; Kim, D.; Kim, D.; Lee, I.-H.; Jon, S., Bioinspired Colorimetric Detection of Calcium(II) Ions in Serum Using Calsequestrin-Functionalized Gold Nanoparticles. *Angewandte Chemie International Edition* **2009,** *48*, 4138-4141.

63. Makarychev-Mikhailov, S.; Shvarev, A.; Bakker, E., New Trends in Ion-Selective Electrodes. In *Electrochemical sensors, biosensors and their biomedical applications*, Zhang, X.; Ju, H.; Wang, J., Eds. Academic Press: US, **2007**, 72-114.

64. Lewenstam, A., Clinical analysis of blood gases and electrolytes by ion-selective sensors. In *Comprehensive Analytical Chemistry*, Alegret, S.; Merkoçi, A., Eds. Elsevier: 2007; Vol. 49, pp 5-24.

65. Harvey, C. J.; LeBouf, R. F.; Stefaniak, A. B., Formulation and stability of a novel artificial human sweat under conditions of storage and use. *Toxicology in Vitro* **2010,** *24*, 1790-1796.

66. Souza, A. P. R. d.; Lima, A. S.; Salles, M. O.; Nascimento, A. N.; Bertotti, M., The use of a gold disc microelectrode for the determination of copper in human sweat. *Talanta* **2010,** *83*, 167-170.

67. Zietz, B. P.; Dieter, H. H.; Lakomek, M.; Schneider, H.; Keßler-Gaedtke, B.; Dunkelberg, H., Epidemiological investigation on chronic copper toxicity to children exposed via the public drinking water supply. *Science of The Total Environment* **2003,** *302*, 127-144.

68. Rivera-Mancía, S.; Pérez-Neri, I.; Ríos, C.; Tristán-López, L.; Rivera-Espinosa, L.; Montes, S., The transition metals copper and iron in neurodegenerative diseases. *Chemico-Biological Interactions* **2010,** *186*, 184-199.

69. Schuhmann, W.; Bonsen, E. M., Biosensors. In *Encyclopedia of Electrochemistry: Instrumentation and electroanalytical chemistry*, Bard, A. J.; Stratmann, M.; Unwin, P. R., Eds. Wiley-VCH: Weinheim, Germany, **2003**, 350-383.

70. Bard, A. J.; Faulkner, L. R., Electrochemical Instrumentation. In *Electrochemical methods: fundamentals and applications*, Wiley India Pvt. Ltd.: 2006; pp 632-658.

71. Wipf, D., Analog and Digital Instrumentation. In *Handbook of Electrochemistry*, Zoski, C. G., Ed. Elsevier: 2007; pp 24-50.

72. Liu, H.; Crooks, R. M., Paper-Based Electrochemical Sensing Platform with Integral Battery and Electrochromic Read-Out. *Analytical Chemistry* **2012,** *84*, 2528-2532.

73. Guiseppi-Elie, A., Electroconductive hydrogels: Synthesis, characterization and biomedical applications. *Biomaterials* **2010,** *31*, 2701-2716.

74. Yang, X.; Pan, X.; Blyth, J.; Lowe, C. R., Towards the real-time monitoring of glucose in tear fluid: Holographic glucose sensors with reduced interference from lactate and pH. *Biosensors and Bioelectronics* **2008,** *23*, 899-905.

75. Martinez-Manez, R.; Sancenon, F.; Biyikal, M.; Hecht, M.; Rurack, K., Mimicking tricks from nature with sensory organic-inorganic hybrid materials. *Journal of Materials Chemistry* **2011,** *21*, 12588-12604.

76. Fries, K. H.; Driskell, J. D.; Sheppard, G. R.; Locklin, J., Fabrication of Spiropyran-Containing Thin Film Sensors Used for the Simultaneous Identification of Multiple Metal Ions. *Langmuir* **2011,** *27*, 12253-12260.

77. Balogh, D.; Tel-Vered, R.; Freeman, R.; Willner, I., Photochemically and Electrochemically Triggered Au Nanoparticles "Sponges". *Journal of the American Chemical Society* **2011,** *133*, 6533-6536.

78. Yehezkeli, O.; Tel-Vered, R.; Reichlin, S.; Willner, I., Nano-engineered Flavin-Dependent Glucose Dehydrogenase/Gold Nanoparticle-Modified Electrodes for Glucose Sensing and Biofuel Cell Applications. *ACS Nano* **2011,** *5*, 2385-2391.

79. Gamero, M.; Pariente, F.; Lorenzo, E.; Alonso, C., Nanostructured rough gold electrodes for the development of lactate oxidase-based biosensors. *Biosensors and Bioelectronics* **2010,** *25*, 2038-2044.

80. Fraser, K. J.; MacFarlane, D. R., Phosphonium-Based Ionic Liquids: An Overview. *Australian Journal of Chemistry* **2009,** *62*, 309-321.

81. Hough, W. L.; Smiglak, M.; Rodriguez, H.; Swatloski, R. P.; Spear, S. K.; Daly, D. T.; Pernak, J.; Grisel, J. E.; Carliss, R. D.; Soutullo, M. D.; Davis, J. J. H.; Rogers, R. D., The third evolution of ionic liquids: active pharmaceutical ingredients. *New Journal of Chemistry* **2007,** *31*, 1429-1436.

82. Forsyth, S. A.; Pringle, J. M.; MacFarlane, D. R., Ionic liquids - An overview. *Australian Journal of Chemistry* **2004,** *57*, 113-119.

83. Hapiot, P.; Lagrost, C., Electrochemical Reactivity in Room-Temperature Ionic Liquids. *Chemical Reviews* **2008,** *108*, 2238-2264.

84. Buzzeo, M. C.; Evans, R. G.; Compton, R. G., Non-Haloaluminate Room-Temperature Ionic Liquids in Electrochemistry—A Review. *ChemPhysChem* **2004,** *5*, 1106-1120.

85. MacFarlane, D. R.; Pringle, J. M.; Johansson, K. M.; Forsyth, S. A.; Forsyth, M., Lewis base ionic liquids. *Chemical Communications* **2006**, 1905-1917.

86. Wei, D.; Ivaska, A., Applications of ionic liquids in electrochemical sensors. *Analytica Chimica Acta* **2008,** *607*, 126-135.

87. Erdmenger, T.; Guerrero-Sanchez, C.; Vitz, J.; Hoogenboom, R.; Schubert, U. S., Recent developments in the utilization of green solvents in polymer chemistry. *Chemical Society Reviews* **2010,** *39*.

88. Armand, M.; Endres, F.; MacFarlane, D. R.; Ohno, H.; Scrosati, B., Ionic-liquid materials for the electrochemical challenges of the future. *Nature Materials* **2009,** *8*, 621-629.

89. Franzoi, A. C.; Migowski, P.; Dupont, J.; Vieira, I. C., Development of biosensors containing laccase and imidazolium bis(trifluoromethylsulfonyl)imide ionic liquid for the determination of rutin. *Analytica Chimica Acta* **2009,** *639*, 90-95.

90. Keskin, S.; Kayrak-Talay, D.; Akman, U.; Hortacsu, O., A review of ionic liquids towards supercritical fluid applications. *Journal of Supercritical Fluids* **2007,** *43*, 150-180.

91. Torimoto, T.; Tsuda, T.; Okazaki, K.; Kuwabata, S., New Frontiers in Materials Science Opened by Ionic Liquids. *Advanced Materials* **2010,** *22*, 1196-1221.

92. Ohno, H., Electrochemical Aspects of Ionic Liquids. In John Wiley & Sons, Inc.: 2005.

93. Singh, T.; Trivedi, T. J.; Kumar, A., Dissolution, regeneration and ion-gel formation of agarose in room-temperature ionic liquids. *Green Chemistry* **2010,** *12*, 1029-1035.

94. Chujo, Y., *Conjugated Polymer Synthesis*. Wiley: **2011**.

95. Le Bideau, J.; Viau, L.; Vioux, A., Ionogels, ionic liquid based hybrid materials. *Chemical Society Reviews* **2011,** *40*, 907-925.

96. Ducros, J. B.; Buchtova, N.; Magrez, A.; Chauvet, O.; Le Bideau, J., Ionic and electronic conductivities in carbon nanotubes - ionogel solid device. *Journal of Materials Chemistry* **2011,** *21*, 2508-2511.

97. MacFarlane, D. R.; Forsyth, M.; Howlett, P. C.; Pringle, J. M.; Sun, J.; Annat, G.; Neil, W.; Izgorodina, E. I., Ionic Liquids in Electrochemical Devices and Processes: Managing Interfacial Electrochemistry. *Accounts of Chemical Research* **2007,** *40*, 1165-1173.

98. Suarez, P. A. Z.; Selbach, V. M.; Dullius, J. E. L.; Einloft, S.; Piatnicki, C. M. S.; Azambuja, D. S.; de Souza, R. F.; Dupont, J., Enlarged electrochemical window in dialkyl-imidazolium cation based room-temperature air and water-stable molten salts. *Electrochimica Acta* **1997,** *42*, 2533-2535.

99. Taylor, A. W.; Licence, P.; Abbott, A. P., Non-classical diffusion in ionic liquids. *Physical Chemistry Chemical Physics* **2011,** *13*, 10147-10154.

100. Wallace, G. G.; Spinks, G. M.; Kane-Maguire, L. A. P., *Conductive Electroactive Polymers: Intelligent Polymer Systems*. CRC Press: **2009**.

101. Zeng, X.; Li, X.; Xing, L.; Liu, X.; Luo, S.; Wei, W.; Kong, B.; Li, Y., Electrodeposition of chitosan–ionic liquid–glucose oxidase biocomposite onto nano-gold electrode for amperometric glucose sensing. *Biosensors and Bioelectronics* **2009,** *24*, 2898-2903.

102. Fujita, K.; MacFarlane, D. R.; Forsyth, M.; Yoshizawa-Fujita, M.; Murata, K.; Nakamura, N.; Ohno, H., Solubility and Stability of Cytochrome c in Hydrated Ionic Liquids: Effect of Oxo Acid Residues and Kosmotropicity. *Biomacromolecules* **2007,** *8*, 2080-2086.

103. Byrne, N.; Wang, L.-M.; Belieres, J.-P.; Angell, C. A., Reversible folding-unfolding, aggregation protection, and multi-year stabilization, in high concentration protein solutions, using ionic liquids. *Chemical Communications* **2007**, 2714-2716.

104. Yang, S. Y.; Cicoira, F.; Byrne, R.; Benito-Lopez, F.; Diamond, D.; Owens, R. M.; Malliaras, G. G., Electrochemical transistors with ionic liquids for enzymatic sensing. *Chemical Communications* **2010,** *46*.

105. Berggren, M.; Nilsson, D.; Robinson, N. D., Organic materials for printed electronics. *Nat Mater* **2007,** *6*, 3-5.

106. Zhao, H., Methods for stabilizing and activating enzymes in ionic liquids - a review. *Journal of Chemical Technology and Biotechnology* **2010,** *85*, 891-907.

107. Moniruzzaman, M.; Kamiya, N.; Goto, M., Activation and stabilization of enzymes in ionic liquids. *Organic & Biomolecular Chemistry* **2010,** *8*, 2887-2899.

108. Weingartner, H.; Cabrele, C.; Herrmann, C., How ionic liquids can help to stabilize native proteins. *Physical Chemistry Chemical Physics* **2012,** *14*, 415-426.

109. Yang, Z., Hofmeister effects: an explanation for the impact of ionic liquids on biocatalysis. *Journal of Biotechnology* **2009,** *144*, 12-22.

110. Musameh, M. M.; Kachoosangi, R. T.; Xiao, L.; Russell, A.; Compton, R. G., Ionic liquid-carbon composite glucose biosensor. *Biosensors and Bioelectronics* **2008,** *24*, 87-92.

111. Ping, J.; Wu, J.; Ying, Y., Development of an ionic liquid modified screen-printed graphite electrode and its sensing in determination of dopamine. *Electrochemistry Communications* **2010,** *12*, 1738-1741.

112. Ping, J.; Wang, Y.; Fan, K.; Wu, J.; Ying, Y., Direct electrochemical reduction of graphene oxide on ionic liquid doped screen-printed electrode and its electrochemical biosensing application. *Biosensors and Bioelectronics* **2011,** *28*, 204-209.

113. Santafé, A. l. A. M.; Doumèche, B.; Blum, L. J.; Girard-Egrot, A. s. P.; Marquette, C. A., 1-Ethyl-3-Methylimidazolium Ethylsulfate/Copper Catalyst for the Enhancement of Glucose Chemiluminescent Detection: Effects on Light Emission and Enzyme Activity. *Analytical Chemistry* **2010,** *82*, 2401-2404.

114. Zuliani, C.; Diamond, D., Opportunities and challenges of using ion-selective electrodes in environmental monitoring and wearable sensors. *Electrochimica Acta* **2012,** *84*, 29-34.

115. Cicmil, D.; Anastasova, S.; Kavanagh, A.; Diamond, D.; Mattinen, U.; Bobacka, J.; Lewenstam, A.; Radu, A., Ionic Liquid-Based, Liquid-Junction-Free Reference Electrode. *Electroanalysis* **2011,** *23*, 1881-1890.

116. Zhang, T.; Lai, C.-Z.; Fierke, M. A.; Stein, A.; Bühlmann, P., Advantages and Limitations of Reference Electrodes with an Ionic Liquid Junction and Three-Dimensionally Ordered Macroporous Carbon as Solid Contact. *Analytical Chemistry* **2012,** *84*, 7771-7778.

117. Guth, U.; Gerlach, F.; Decker, M.; Oelßner, W.; Vonau, W., Solid-state reference electrodes for potentiometric sensors. *Journal of Solid State Electrochemistry* **2009,** *13*, 27-39.

118. Kakiuchi, T.; Yoshimatsu, T.; Nishi, N., New Class of Ag/AgCl Electrodes Based on Hydrophobic Ionic Liquid Saturated with AgCl. *Analytical Chemistry* **2007,** *79*, 7187-7191.

119. Gourishetty, R.; Crabtree, A. M.; Sanderson, W. M.; Johnson, R. D., Anion-selective electrodes based on ionic liquid membranes: effect of ionic liquid anion on observed response. *Analytical and Bioanalytical Chemistry* **2011,** *400*, 3025-3033.

120. Shvedene, N. V.; Chernyshov, D. V.; Khrenova, M. G.; Formanovsky, A. A.; Baulin, V. E.; Pletnev, I. V., Ionic Liquids Plasticize and Bring Ion-Sensing Ability to Polymer Membranes of Selective Electrodes. *Electroanalysis* **2006,** *18*, 1416-1421.

121. Marciniak, A., The Solubility Parameters of Ionic Liquids. *International Journal of Molecular Sciences* **2010,** *11*, 1973-1990.

122. Coll, C.; Labrador, R. H.; Manez, R. M.; Soto, J.; Sancenon, F.; Segui, M. J., Ionic liquids promote selective responses towards the highly hydrophilic anion sulfate in PVC membrane ion-selective electrodes. *Chemical Communications* **2005**, 3033-3035.

123. Chernyshov, D. V.; Egorov, V. M.; Shvedene, N. V.; Pletnev, I. V., Low-Melting Ionic Solids: Versatile Materials for Ion-Sensing Devices. *ACS Applied Materials & Interfaces* **2009,** *1*, 2055-2059.

124. Wardak, C., A highly selective lead-sensitive electrode with solid contact based on ionic liquid. *Journal of Hazardous Materials* **2011,** *186*, 1131-1135.

125. Wardak, C., A Comparative Study of Cadmium Ion-Selective Electrodes with Solid and Liquid Inner Contact. *Electroanalysis* **2012,** *24*, 85-90.

126. Wang, K. F.; Zhang, L.; Zhuang, R. R.; Jian, F. F., An iron(III)-containing ionic liquid: characterization, magnetic property and electrocatalysis, Transition Metal Chemistry. *Transition Metal Chemistry* **2011,** *36*, 785.

127. Delker, D.; Hatch, G.; Allen, J.; Crissman, B.; George, M.; Geter, D.; Kilburn, S.; Moore, T.; Nelson, G.; Roop, B.; Slade, R.; Swank, A.; Ward, W.; DeAngelo, A., Molecular biomarkers of oxidative stress associated with bromate carcinogenicity. *Toxicology* **2006,** *221*, 158-165.

128. Bryan, N. S.; Alexander, D. D.; Coughlin, J. R.; Milkowski, A. L.; Boffetta, P., Ingested nitrate and nitrite and stomach cancer risk: An updated review. *Food and Chemical Toxicology* **2012,** *50*, 3646-3665.

129. Plieth, W., Instrincally Conducting Polymers. In *Electrochemistry for materials science*, Elsevier: Hungary, 2008; pp 323-363.

130. Bidan, G., Electropolymerized Films of pi-conjugated Polymers. A Tool for Surface Functionalization: a Brief Historical Evolution and Recent Trends. In *Electropolymerization: Concepts, Materials and Applications*, Cosnier, S.; Karyakin, A., Eds. John Wiley & Sons: Germany, **2010**, 1-26.

131. Otero, T. F.; Arias-Pardilla, J., Electrochemical Devices: Artificial Muscles. In *Electropolymerization: Concepts, Materials and Applications*, Cosnier, S.; Karyakin, A., Eds. John Wiley & Sons: Germany, **2010**, 241-245.

132. Vorotyntsev, M. A.; Zinovyeva, V. A.; Konev, D. V., Mechanims of Electropolyemrization and Redox Activity: Fundamental Aspects. In *Electropolymerization: Concepts, Materials and Applications*, Cosnier, S.; Karyakin, A., Eds. John Wiley & Sons: Germany, **2010**, 27-50.

133. Campbell, J. S., History of Conductive Polymers. In *Nanostructured Conductive Polymers*, Eftekhari, A., Ed. Wiley: Great Britain, **2011**, 1-17.

134. Ates, M.; Sarac, A. S., Conducting polymer coated carbon surfaces and biosensor applications. *Progress in Organic Coatings* **2009,** *66*, 337-358.

135. Leclerc, M.; Morin, J. F., *Design and Synthesis of Conjugated Polymers*. Wiley: **2010**.

136. Rozlosnik, N., New directions in medical biosensors employing poly(3,4-ethylenedioxy thiophene) derivative-based electrodes. *Analytical and Bioanalytical Chemistry* **2009,** *395*, 637-645.

137. Eftekhari, A., *Nanostructured Conductive Polymers*. Wiley: **2011**.

138. Skotheim, T. A.; Reynolds, J. R., *Handbook of Conducting Polymers*. CRC: **2007**.

139. Lin, P.; Yan, F., Organic Thin-Film Transistors for Chemical and Biological Sensing. *Advanced Materials* **2012,** *24*, 34-51.

140. Nambiar, S.; Yeow, J. T. W., Conductive polymer-based sensors for biomedical applications. *Biosensors and Bioelectronics* **2011,** *26*, 1825-1832.

141. Snook, G. A.; Best, A. S., Co-deposition of conducting polymers in a room temperature ionic liquid. *Journal of Materials Chemistry* **2009,** *19*, 4248-4254.

142. Ahmad, S.; Deepa, M.; Singh, S., Electrochemical Synthesis and Surface Characterization of Poly(3,4-ethylenedioxythiophene) Films Grown in an Ionic Liquid. *Langmuir* **2007,** *23*, 11430-11433.

143. Marjanovic, G. C., Polyaniline Nanostructures. In *Nanostructured Conductive Polymers*, Eftekhari, A., Ed. Wiley: **2011**, 19-98.

144. Suman; O'Reilly, E.; Kelly, M.; Morrin, A.; Smyth, M. R.; Killard, A. J., Chronocoulometric determination of urea in human serum using an inkjet printed biosensor. *Analytica Chimica Acta* **2011,** *697*, 98-102.

145. Sriprachuabwong, C.; Karuwan, C.; Wisitsorrat, A.; Phokharatkul, D.; Lomas, T.; Sritongkham, P.; Tuantranont, A., Inkjet-printed graphene-PEDOT:PSS modified screen printed carbon electrode for biochemical sensing. *Journal of Materials Chemistry* **2012,** *22*, 5478-5485.

146. Ahmad, S.; Carstens, T.; Berger, R.; Butt, H.-J.; Endres, F., Surface polymerization of (3,4-ethylenedioxythiophene) probed by in situ scanning tunneling microscopy on Au(111) in ionic liquids. *Nanoscale* **2011,** *3*, 251-257.

147. Long, Y.-Z.; Li, M.-M.; Gu, C.; Wan, M.; Duvail, J.-L.; Liu, Z.; Fan, Z., Recent advances in synthesis, physical properties and applications of conducting polymer nanotubes and nanofibers. *Progress in Polymer Science* **2011,** *36*, 1415-1442.

148. Wan, M., A Template-Free Method Towards Conducting Polymer Nanostructures. *Advanced Materials* **2008,** *20*, 2926-2932.

149. Lu, W.; Fadeev, A. G.; Qi, B.; Smela, E.; Mattes, B. R.; Ding, J.; Spinks, G. M.; Mazurkiewicz, J.; Zhou, D.; Gordon, G. W.; MacFarlane, D. R.; Forsyth, S. A.; Forsyth, M., Use of Ionic Liquids for π-Conjugated Polymer Electrochemical Devices. *Science* **2002,** *297*, 983-987.

150. Winterton, N., Solubilization of polymers by ionic liquids. *Journal of Materials Chemistry* **2006,** *16*, 4281-4293.

151. Jiang, Y.; Wang, A.; Kan, J., Selective uricase biosensor based on polyaniline synthesized in ionic liquid. *Sensors and Actuators B: Chemical* **2007,** *124*, 529-534.

152. Ahmad, S.; Yum, J.-H.; Xianxi, Z.; Gratzel, M.; Butt, H.-J.; Nazeeruddin, M. K., Dye-sensitized solar cells based on poly (3,4-ethylenedioxythiophene) counter electrode derived from ionic liquids. *Journal of Materials Chemistry* **2010,** *20*, 1654-1658.

153. Li, Y.; Wang, B.; Chen, H.; Feng, W., Improvement of the electrochemical properties via poly(3,4-ethylenedioxythiophene) oriented micro/nanorods. *Journal of Power Sources* **2010,** *195*, 3025-3030.

154. Nien, P.-C.; Tung, T.-S.; Ho, K.-C., Amperometric Glucose Biosensor Based on Entrapment of Glucose Oxidase in a Poly(3,4-ethylenedioxythiophene) Film. *Electroanalysis* **2006,** *18*, 1408-1415.

155. Emre, F. B.; Ekiz, F.; Balan, A.; Emre, S.; Timur, S.; Toppare, L., Conducting polymers with benzothiadiazole and benzoselenadiazole units for biosensor applications. *Sensors and Actuators B: Chemical* **2011,** *158*, 117-123.

156. Alvin Koh, W. C.; Rahman, M. A.; Choe, E. S.; Lee, D. K.; Shim, Y.-B., A cytochrome c modified-conducting polymer microelectrode for monitoring in vivo changes in nitric oxide. *Biosensors and Bioelectronics* **2008,** *23*, 1374-1381.

157. Kausaite-Minkstimiene, A.; Mazeiko, V.; Ramanaviciene, A.; Ramanavicius, A., Enzymatically synthesized polyaniline layer for extension of linear detection region of amperometric glucose biosensor. *Biosensors and Bioelectronics* **2010,** *26*, 790-797.

158. Aguilar, A. D.; Forzani, E. S.; Nagahara, L. A.; Amlani, I.; Tsui, R.; Tao, N. J., A Breath Ammonia Sensor Based on Conducting Polymer Nanojunctions. *Sensors Journal, IEEE* **2008,** *8*, 269-273.

159. Lu, L.-M.; Wang, S.-P.; Qu, F.-L.; Zhang, X.-B.; Huan, S.; Shen, G.-L.; Yu, R.-Q., Synthesis and Characterization of Poly(toluidine blue) Nanowires and Their Application in Amperometric Biosensors. *Electroanalysis* **2009,** *21*, 1152-1158.

160. Wang, J.; Mo, X.; Ge, D.; Tian, Y.; Wang, Z.; Wang, S., Polypyrrole nanostructures formed by electrochemical method on graphite impregnated with paraffin. *Synthetic Metals* **2006,** *156*, 514-518.

161. Zang, J.; Li, C. M.; Bao, S.-J.; Cui, X.; Bao, Q.; Sun, C. Q., Template-Free Electrochemical Synthesis of Superhydrophilic Polypyrrole Nanofiber Network. *Macromolecules* **2008,** *41*, 7053-7057.

162. Özcan, L.; Şahin, Y.; Türk, H., Non-enzymatic glucose biosensor based on overoxidized polypyrrole nanofiber electrode modified with cobalt(II) phthalocyanine tetrasulfonate. *Biosensors and Bioelectronics* **2008,** *24*, 512-517.

163. Zang, J.; Bao, S.-J.; Li, C. M.; Bian, H.; Cui, X.; Bao, Q.; Sun, C. Q.; Guo, J.; Lian, K., Well-Aligned Cone-Shaped Nanostructure of Polypyrrole/RuO2 and Its Electrochemical Supercapacitor. *The Journal of Physical Chemistry C* **2008,** *112*, 14843-14847.

164. Debiemme-Chouvy, C., Template-free one-step electrochemical formation of polypyrrole nanowire array. *Electrochemistry Communications* **2009,** *11*, 298-301.

165. Zhang, X.; Wang, J.; Wang, Z.; Wang, S. c., Preparation/Property Relationships for a Nitrate Amperometric Sensor: Effect of Nanowires Polymerization Parameters. *Journal of Macromolecular Science, Part B* **2006,** *45*, 475-483.

166. Zhang, Y.; Sun, X., A novel fluorescent aptasensor for thrombin detection: using poly(m-phenylenediamine) rods as an effective sensing platform. *Chemical Communications* **2011,** *47*, 3927-3929.

167. Luo, X.; Lee, I.; Huang, J.; Yun, M.; Cui, X. T., Ultrasensitive protein detection using an aptamer-functionalized single polyaniline nanowire. *Chemical Communications* **2011,** *47*.

168. Bluth, M., IgE and chemotherapy. *Cancer Immunology, Immunotherapy* **2012,** *61*, 1585-1590.

169. Wanekaya, A. K.; Chen, W.; Myung, N. V.; Mulchandani, A., Nanowire-Based Electrochemical Biosensors. *Electroanalysis* **2006,** *18*, 533-550.

170. Bobacka, J.; Ivaska, A., Ion sensors with conducting polymers as ion-to-electron transducers. In *Comprehensive Analytical Chemistry*, Alegret, S.; Merkoçi, A., Eds. Elsevier: **2007**, 49, 73-86.

171. Bobacka, J., Conducting Polymer-Based Solid-State Ion-Selective Electrodes. *Electroanalysis* **2006,** *18*, 7-18.

172. Bobacka, J.; Ivaska, A.; Lewenstam, A., Potentiometric Ion Sensors. *Chemical Reviews* **2008,** *108*, 329-351.

173. Lindner, E.; Gyurcsányi, R., Quality control criteria for solid-contact, solvent polymeric membrane ion-selective electrodes. *Journal of Solid State Electrochemistry* **2009,** *13*, 51-68.

174. Pawlak, M.; Grygolowicz-Pawlak, E.; Bakker, E., Ferrocene Bound Poly(vinyl chloride) as Ion to Electron Transducer in Electrochemical Ion Sensors. *Analytical Chemistry* **2010,** *82*, 6887-6894.

175. Amemiya, S., Potentiometric Ion-Selective Electrodes. In *Handbook of electrochemistry*, Zoski, C. G., Ed. Elsevier: **2007**, 261-294.

176. Vázquez, M.; Danielsson, P.; Bobacka, J.; Lewenstam, A.; Ivaska, A., Solution-cast films of poly(3,4-ethylenedioxythiophene) as ion-to-electron transducers in all-solid-state ion-selective electrodes. *Sensors and Actuators B: Chemical* **2004,** *97*, 182-189.

177. Lindfors, T.; Höfler, L.; Jágerszki, G.; Gyurcsányi, R. E., Hyphenated FT-IR-Attenuated Total Reflection and Electrochemical Impedance Spectroscopy Technique

to Study the Water Uptake and Potential Stability of Polymeric Solid-Contact Ion-Selective Electrodes. *Analytical Chemistry* **2011,** *83*, 4902-4908.

178. Lindfors, T.; Szücs, J. l.; Sundfors, F.; Gyurcsányi, R. E., Polyaniline Nanoparticle-Based Solid-Contact Silicone Rubber Ion-Selective Electrodes for Ultratrace Measurements. *Analytical Chemistry* **2010,** *82*, 9425-9432.
179. Radu, A.; Diamond, D., Ion-selective electrodes in trace level analysis of heavy metals: Potentiometry for the XXI century. In *Comprehensive Analytical Chemistry*, Alegret, S.; Merkoçi, A., Eds. Elsevier: **2007**, 49, 25-52.
180. Guo, J.; Amemiya, S., Voltammetric Heparin-Selective Electrode Based on Thin Liquid Membrane with Conducting Polymer-Modified Solid Support. *Analytical Chemistry* **2006,** *78*, 6893-6902.
181. Michalska, A.; Wojciechowski, M.; Bulska, E.; Maksymiuk, K., Experimental study on stability of different solid contact arrangements of ion-selective electrodes. *Talanta* **2010,** *82*, 151-157.
182. Michalska, A.; Wojciechowski, M.; Jędral, W.; Bulska, E.; Maksymiuk, K., Silver and lead all-plastic sensors—polyaniline vs. poly(3,4-ethyledioxythiophene) solid contact. *Journal of Solid State Electrochemistry* **2009,** *13*, 99-106.
183. Chumbimuni-Torres, K. Y.; Rubinova, N.; Radu, A.; Kubota, L. T.; Bakker, E., Solid Contact Potentiometric Sensors for Trace Level Measurements. *Analytical Chemistry* **2006,** *78*, 1318-1322.
184. Han, W. S.; Lee, Y. H.; Jung, K. J.; Ly, S. Y.; Hong, T. K.; Kim, M. H., Potassium Ion-selective polyaniline solid-contact electrodes based on 4',4''(5'')- Di-tert-butyldibenzo-18-crown-6-ether ionophore. *Journal of Analytical Chemistry* **2008,** *63*, 987.
185. Lisak, G.; Wagner, M.; Kvarnstrom, C.; Bobacka, J.; Ivaska, A.; Lewenstam, A., Electrochemical Behaviour of Poly(benzopyrene) Films Doped with Eriochrome Black T as a Pb2+-Sensitive Sensors. *Electroanalysis* **2010,** *22*, 2794-2800.
186. Kisiel, A.; Mazur, M.; Kuśnieruk, S.; Kijewska, K.; Krysiński, P.; Michalska, A., Polypyrrole microcapsules as a transducer for ion-selective electrodes. *Electrochemistry Communications* **2010,** *12*, 1568-1571.
187. Kijewska, K.; Blanchard, G. J.; Szlachetko, J.; Stolarski, J.; Kisiel, A.; Michalska, A.; Maksymiuk, K.; Pisarek, M.; Majewski, P.; Krysinski, P.; Mazur, M., Photopolymerized Polypyrrole Microvessels. *Chemistry-a European Journal* **2012,** *18*, 310-320.
188. Malinowski, P.; Grzegrzółka, I.; Michalska, A.; Maksymiuk, K., Dual potentiometric and UV/Vis spectrophotometric disposable sensors with dispersion cast polyaniline. *Journal of Solid State Electrochemistry* **2010,** *14*, 2027-2037.
189. Garcia-Cordova, F.; Valero, L.; Ismail, Y. A.; Otero, T. F., Biomimetic polypyrrole based all three-in-one triple layer sensing actuators exchanging cations. *Journal of Materials Chemistry* **2011,** *21*, 17265-17272.
190. Mohadesi, A.; Taher, M. A., Overoxidized polypyrrole doped with 4,5-Dihydroxy-3-(p-sulphophenylazo)-2,7-naphthalene disulfonic acid as a selective and regenerable film for the stripping detection of copper(II). *Analytical Sciences* **2007,** *23*, 969.
191. Mao, H.; Liu, X.; Chao, D.; Cui, L.; Li, Y.; Zhang, W.; Wang, C., Preparation of unique PEDOT nanorods with a couple of cuspate tips by reverse interfacial polymerization and their electrocatalytic application to detect nitrite. *Journal of Materials Chemistry* **2010,** *20*, 10277.
192. Dwivedi, A. K.; Saikia, G.; Iyer, P. K., Aqueous polyfluorene probe for the detection and estimation of Fe3+ and inorganic phosphate in blood serum. *Journal of Materials Chemistry* **2011,** *21*, 2502-2507.
193. Schmid, G., *Nanoparticles: From Theory to Application*. Wiley: **2011**.

194. Brust, M.; Walker, M.; Bethell, D.; Schiffrin, D. J.; Whyman, R., Synthesis of thiol-derivatised gold nanoparticles in a two-phase Liquid-Liquid system. *Journal of the Chemical Society, Chemical Communications* **1994,** *0*, 801-802.

195. Rao, C. N. R.; Kulkarni, G. U.; Thomas, P. J.; Edwards, P. P., Metal nanoparticles and their assemblies. *Chemical Society Reviews* **2000,** *29*, 27-35.

196. Jia, C.-J.; Schuth, F., Colloidal metal nanoparticles as a component of designed catalyst. *Physical Chemistry Chemical Physics* **2011,** *13*, 2457-2487.

197. Haes, A. J.; Zou, S.; Schatz, G. C.; Van Duyne, R. P., A Nanoscale Optical Biosensor: The Long Range Distance Dependence of the Localized Surface Plasmon Resonance of Noble Metal Nanoparticles. *The Journal of Physical Chemistry B* **2003,** *108*, 109-116.

198. Kelly, K. L.; Coronado, E.; Zhao, L. L.; Schatz, G. C., The Optical Properties of Metal Nanoparticles: The Influence of Size, Shape, and Dielectric Environment. *The Journal of Physical Chemistry B* **2002,** *107*, 668-677.

199. Narayanan, R.; El-Sayed, M. A., Catalysis with Transition Metal Nanoparticles in Colloidal Solution: Nanoparticle Shape Dependence and Stability. *The Journal of Physical Chemistry B* **2005,** *109*, 12663-12676.

200. Murray, R. W., Nanoelectrochemistry: Metal Nanoparticles, Nanoelectrodes, and Nanopores. *Chemical Reviews* **2008,** *108*, 2688-2720.

201. Rotello, V. M., *Nanoparticles*. Kluwer Academic Pub: 2004.

202. Nagarajan, R.; Hatton, T. A.; Colloid, A. C. S. D. o.; Chemistry, S.; Meeting, A. C. S., *Nanoparticles: synthesis, stabilization, passivation, and functionalization*. American Chemical Society: **2008**.

203. Anderson, L. J. E.; Payne, C. M.; Zhen, Y.-R.; Nordlander, P.; Hafner, J. H., A Tunable Plasmon Resonance in Gold Nanobelts. *Nano Letters* **2011,** *11*, 5034-5037.

204. Strong, L. E.; West, J. L., Thermally responsive polymer–nanoparticle composites for biomedical applications. *Wiley Interdisciplinary Reviews: Nanomedicine and Nanobiotechnology* **2011,** *3*, 307-317.

205. Campbell, F.; Compton, R., The use of nanoparticles in electroanalysis: an updated review. *Analytical and Bioanalytical Chemistry* **2010,** *396*, 241-259.

206. You, C.-C.; Miranda, O. R.; Gider, B.; Ghosh, P. S.; Kim, I.-B.; Erdogan, B.; Krovi, S. A.; Bunz, U. H. F.; Rotello, V. M., Detection and identification of proteins using nanoparticle-fluorescent polymer /chemical nose/ sensors. *Nature Nano* **2007,** *2*, 318-323.

207. Jaworska, E.; Wójcik, M.; Kisiel, A.; Mieczkowski, J.; Michalska, A., Gold nanoparticles solid contact for ion-selective electrodes of highly stable potential readings. *Talanta* **2011,** *85*, 1986-1989.

208. González, E.; Arbiol, J.; Puntes, V. F., Carving at the Nanoscale: Sequential Galvanic Exchange and Kirkendall Growth at Room Temperature. *Science* **2011,** *334*, 1377-1380.

209. Zhou, Y.-G.; Rees, N. V.; Compton, R. G., Nanoparticle–electrode collision processes: The electroplating of bulk cadmium on impacting silver nanoparticles. *Chemical Physics Letters* **2011,** *511*, 183-186.

210. Wojcik, M.; Lewandowski, W.; Matraszek, J.; Mieczkowski, J.; Borysiuk, J.; Pociecha, D.; Gorecka, E., Liquid-Crystalline Phases Made of Gold Nanoparticles. *Angewandte Chemie International Edition* **2009,** *48*, 5167-5169.

211. Zhao, Y.; Thorkelsson, K.; Mastroianni, A. J.; Schilling, T.; Luther, J. M.; Rancatore, B. J.; Matsunaga, K.; Jinnai, H.; Wu, Y.; Poulsen, D.; Frechet, J. M. J.; Paul Alivisatos, A.; Xu, T., Small-molecule-directed nanoparticle assembly towards stimuli-responsive nanocomposites. *Nature Materials* **2009,** *8*, 979-985.

212. Sia, S. K.; Kricka, L. J., Microfluidics and point-of-care testing. *Lab on a Chip* **2008,** *8*, 1982-1983.

213. Martinez, A. W.; Phillips, S. T.; Butte, M. J.; Whitesides, G. M., Patterned Paper as a Platform for Inexpensive, Low-Volume, Portable Bioassays. *Angewandte Chemie International Edition* **2007,** *46*, 1318-1320.

214. Schilling, K. M.; Lepore, A. L.; Kurian, J. A.; Martinez, A. W., Fully Enclosed Microfluidic Paper-Based Analytical Devices. *Analytical Chemistry* **2012,** *84*, 1579-1585.

215. Songjaroen, T.; Dungchai, W.; Chailapakul, O.; Henry, C. S.; Laiwattanapaisal, W., Blood separation on microfluidic paper-based analytical devices. *Lab on a Chip* **2012,** *12*, 3392-3398.

216. Li; Rothberg, L. J., Label-Free Colorimetric Detection of Specific Sequences in Genomic DNA Amplified by the Polymerase Chain Reaction. *Journal of the American Chemical Society* **2004,** *126*, 10958-10961.

217. Sharon, E.; Freeman, R.; Tel-Vered, R.; Willner, I., Impedimetric or Ion-Sensitive Field-Effect Transistor (ISFET) Aptasensors Based on the Self-Assembly of Au Nanoparticle-Functionalized Supramolecular Aptamer Nanostructures. *Electroanalysis* **2009,** *21*, 1291-1296.

218. Zhang, J.; Wang, L.; Pan, D.; Song, S.; Boey, F. Y. C.; Zhang, H.; Fan, C., Visual Cocaine Detection with Gold Nanoparticles and Rationally Engineered Aptamer Structures. *Small* **2008,** *4*, 1196-1200.

219. Golub, E.; Pelossof, G.; Freeman, R.; Zhang, H.; Willner, I., Electrochemical, Photoelectrochemical, and Surface Plasmon Resonance Detection of Cocaine Using Supramolecular Aptamer Complexes and Metallic or Semiconductor Nanoparticles. *Analytical Chemistry* **2009,** *81*, 9291-9298.

220. Zhu, Z.; Wu, C.; Liu, H.; Zou, Y.; Zhang, X.; Kang, H.; Yang, C. J.; Tan, W., An Aptamer Cross-Linked Hydrogel as a Colorimetric Platform for Visual Detection. *Angewandte Chemie International Edition* **2010,** *49*, 1052-1056.

221. Yu, C.; Tseng, W., Colorimetric Detection of Mercury(II) in a High-Salinity Solution Using Gold Nanoparticles Capped with 3-Mercaptopropionate Acid and Adenosine Monophosphate. *Langmuir* **2008,** *24*, 12717.

222. Zhou, Y.; Wang, S.; Zhang, K.; Jiang, X., Visual Detection of Copper(II) by Azide- and Alkyne-Functionalized Gold Nanoparticles Using Click Chemistry. *Angewandte Chemie International Edition* **2008,** *47*, 7454-7456.

223. Jiang, Y.; Zhao, H.; Lin, Y.; Zhu, N.; Ma, Y.; Mao, L., Colorimetric Detection of Glucose in Rat Brain Using Gold Nanoparticles. *Angewandte Chemie International Edition* **2010,** *49*, 4800-4804.

224. Xia, F.; Zuo, X.; Yang, R.; Xiao, Y.; Kang, D.; Valle-Belisle, A.; Gong, X.; Yuen, J. D.; Hsu, B. B. Y.; Heeger, A. J.; Plaxco, K. W., Colorimetric detection of DNA, small molecules, proteins, and ions using unmodified gold nanoparticles and conjugated polyelectrolytes. *Proceedings of the National Academy of Sciences* **2010,** *107*, 10837-10841.

225. Liu, X.; Dai, Q.; Austin, L.; Coutts, J.; Knowles, G.; Zou, J.; Chen, H.; Huo, Q., A One-Step Homogeneous Immunoassay for Cancer Biomarker Detection Using Gold Nanoparticle Probes Coupled with Dynamic Light Scattering. *Journal of the American Chemical Society* **2008,** *130*, 2780-2782.

226. Ambrosi, A.; Airò, F.; Merkoci, A., Enhanced Gold Nanoparticle Based ELISA for a Breast Cancer Biomarker. *Analytical Chemistry* **2009,** *82*, 1151-1156.

227. Rodriguez-Lorenzo, L.; de la Rica, R.; Alvarez-Puebla, R. A.; Liz-Marzan, L. M.; Stevens, M. M., Plasmonic nanosensors with inverse sensitivity by means of enzyme-guided crystal growth. *Nat Mater* **2012,** *11*, 604-607.

228. Panfilova, E.; Shirokov, A.; Khlebtsov, B.; Matora, L.; Khlebtsov, N., Multiplexed dot immunoassay using Ag nanocubes, Au/Ag alloy nanoparticles, and Au/Ag nanocages. *Nano Research* **2012,** *5*, 124-134.

229. Strömberg, N.; Hakonen, A., Plasmophore sensitized imaging of ammonia release from biological tissues using optodes. *Analytica Chimica Acta* **2011,** *704*, 139-145.

230. Zhang, J.; Xu, X.; Yang, C.; Yang, F.; Yang, X., Colorimetric Iodide Recognition and Sensing by Citrate-Stabilized Core/Shell Cu@Au Nanoparticles. *Anal. Chem.* **2011,** *83*, 3911.

231. Feng, M.; Han, H.; Zhang, J.; Tachikawa, H., Electrochemical sensors based on carbon nanotubes. In *Electrochemical Sensors, Biosensors and Their Biomedical Applications*, Zhang, X.; Ju, H.; Wang, J., Eds. Academic Press: **2007**, 459-500.

232. Cao, Q.; Rogers, J. A., Ultrathin Films of Single-Walled Carbon Nanotubes for Electronics and Sensors: A Review of Fundamental and Applied Aspects. *Advanced Materials* **2009,** *21*, 29-53.

233. Goran, J. M.; Lyon, J. L.; Stevenson, K. J., Amperometric Detection of l-Lactate Using Nitrogen-Doped Carbon Nanotubes Modified with Lactate Oxidase. *Analytical Chemistry* **2011,** *83*, 8123-8129.

234. Jönsson-Niedziolka, M.; Kaminska, A.; Opallo, M., Pyrene-functionalised single-walled carbon nanotubes for mediatorless dioxygen bioelectrocatalysis. *Electrochimica Acta* **2010,** *55*, 8744-8750.

235. Zeng, X.; Li, X.; Liu, X.; Liu, Y.; Luo, S.; Kong, B.; Yang, S.; Wei, W., A third-generation hydrogen peroxide biosensor based on horseradish peroxidase immobilized on DNA functionalized carbon nanotubes. *Biosensors and Bioelectronics* **2009,** *25*, 896-900.

236. Vashist, S. K.; Zheng, D.; Al-Rubeaan, K.; Luong, J. H. T.; Sheu, F.-S., Advances in carbon nanotube based electrochemical sensors for bioanalytical applications. *Biotechnology Advances* **2011,** *29*, 169-188.

237. Inamdar, N.; Mourya, V. K., Composite of chitosan for biomedical applications. In *Recent developments in bio-nanocomposites for biomedical applications*, Tiwari, A., Ed. Nova Science Publishers: New York, **2011**, 277-343.

238. Kim, K. S.; Zhao, Y.; Jang, H.; Lee, S. Y.; Kim, J. M.; Ahn, J. H.; Kim, P.; Choi, J. Y.; Hong, B. H., Large-scale pattern growth of graphene films for stretchable transparent electrodes. *Nature* **2009,** *457*, 706-710.

239. Tlili, C.; Myung, N. V.; Shetty, V.; Mulchandani, A., Label-free, chemiresistor immunosensor for stress biomarker cortisol in saliva. *Biosensors and Bioelectronics* **2011,** *26*, 4382-4386.

240. Ohno, Y.; Maehashi, K.; Matsumoto, K., Label-Free Biosensors Based on Aptamer-Modified Graphene Field-Effect Transistors. *Journal of the American Chemical Society* **2010,** *132*, 18012-18013.

241. Grieshaber, D.; MacKenzie, R.; Vörös, J.; Reimhult, E., Electrochemical Biosensors - Sensor Principles and Architectures. *Sensors* **2008,** *8*, 1400-1458.

242. Janata, J.; Josowicz, M., Conducting polymers in electronic chemical sensors. *Nat Mater* **2003,** *2*, 19-24.

243. Goldsmith, B. R.; Mitala, J. J.; Josue, J.; Castro, A.; Lerner, M. B.; Bayburt, T. H.; Khamis, S. M.; Jones, R. A.; Brand, J. G.; Sligar, S. G.; Luetje, C. W.; Gelperin, A.; Rhodes, P. A.; Discher, B. M.; Johnson, A. T. C., Biomimetic Chemical Sensors Using Nanoelectronic Readout of Olfactory Receptor Proteins. *ACS Nano* **2011,** *5*, 5408-5416.

244. Cella, L. N.; Chen, W.; Myung, N. V.; Mulchandani, A., Single-Walled Carbon Nanotube-Based Chemiresistive Affinity Biosensors for Small Molecules:

Ultrasensitive Glucose Detection. *Journal of the American Chemical Society* **2010,** *132*, 5024-5026.

245. An, T.; Kim, K. S.; Hahn, S. K.; Lim, G., Real-time, step-wise, electrical detection of protein molecules using dielectrophoretically aligned SWNT-film FET aptasensors. *Lab on a Chip* **2010,** *10*, 2052-2056.
246. Lee, D.; Cui, T., Low-cost, transparent, and flexible single-walled carbon nanotube nanocomposite based ion-sensitive field-effect transistors for pH/glucose sensing. *Biosensors and Bioelectronics* **2010,** *25*, 2259-2264.
247. Ohno, Y.; Maehashi, K.; Yamashiro, Y.; Matsumoto, K., Electrolyte-Gated Graphene Field-Effect Transistors for Detecting pH and Protein Adsorption. *Nano Letters* **2009,** *9*, 3318-3322.
248. Sofue, Y.; Ohno, Y.; Maehashi, K.; Inoue, K.; Matsumoto, K., Highly Sensitive Electrical Detection of Sodium Ions Based on Graphene Field-Effect Transistors. *Japanese Journal of Applied Physics* **2011,** *50*, 1.
249. Sardesai, N. P.; Barron, J. C.; Rusling, J. F., Carbon Nanotube Microwell Array for Sensitive Electrochemiluminescent Detection of Cancer Biomarker Proteins. *Analytical Chemistry* **2011,** *83*, 6698-6703.
250. Malhotra, R.; Patel, V.; Vaqué, J. P.; Gutkind, J. S.; Rusling, J. F., Ultrasensitive Electrochemical Immunosensor for Oral Cancer Biomarker IL-6 Using Carbon Nanotube Forest Electrodes and Multilabel Amplification. *Analytical Chemistry* **2010,** *82*, 3118-3123.
251. Chikkaveeraiah, B. V.; Bhirde, A.; Malhotra, R.; Patel, V.; Gutkind, J. S.; Rusling, J. F., Single-Wall Carbon Nanotube Forest Arrays for Immunoelectrochemical Measurement of Four Protein Biomarkers for Prostate Cancer. *Analytical Chemistry* **2009,** *81*, 9129-9134.
252. Laird, E. D.; Wang, W.; Cheng, S.; Li, B.; Presser, V.; Dyatkin, B.; Gogotsi, Y.; Li, C. Y., Polymer Single Crystal-Decorated Superhydrophobic Buckypaper with Controlled Wetting and Conductivity. *ACS Nano* **2012,** *6*, 1204-1213.
253. Zeng, G.; Xing, Y.; Gao, J.; Wang, Z.; Zhang, X., Unconventional Layer-by-Layer Assembly of Graphene Multilayer Films for Enzyme-Based Glucose and Maltose Biosensing. *Langmuir* **2010,** *26*, 15022-15026.
254. Zhao, J.; Chen, G.; Zhu, L.; Li, G., Graphene quantum dots-based platform for the fabrication of electrochemical biosensors. *Electrochemistry Communications* **2011,** *13*, 31-33.
255. Liu, P.; Zhang, X.; Feng, L.; Xiong, H.; Wang, S., Direct Electrochemistry of Hemoglobin on Graphene Nanosheet-based Modified Electrode and Its Electrocatalysis to Nitrite. *American Journal of Biomedical Sciences* **2011,** *3*, 69.
256. Yue, R.; Lu, Q.; Zhou, Y., A novel nitrite biosensor based on single-layer graphene nanoplatelet–protein composite film. *Biosensors and Bioelectronics* **2011,** *26*, 4436-4441.
257. Rius-Ruiz, F. X.; Crespo, G. A.; Bejarano-Nosas, D.; Blondeau, P.; Riu, J.; Rius, F. X., Potentiometric Strip Cell Based on Carbon Nanotubes as Transducer Layer. Towards Low-Cost Decentralized Measurements. *Analytical Chemistry* **2011,** *83*, 5783-5788.
258. Zhao, X.; Kong, R.; Zhang, X.; Meng, H.; Liu, W.; Tan, W.; Shen, G.; Yu, R., Graphene_DNAzyme Based Biosensor for Amplified Fluorescence "Turn-On" Detection of Pb2+ with a High Selectivity. *Anal. Chem.* **2011,** *83*, 5062.
259. Liu, M.; Zhao, H.; Chen, S.; Yu, H.; Zhang, Y.; Quan, X., Label-free fluorescent detection of Cu(II) ions based on DNA cleavage-dependent graphene-quenched DNAzymes. *Chemical Communications* **2011,** *47*, 7749.

260. Bucio, E.; Melendez-Ortiz, H. I.; Isoshima, T.; Macossay, J., Synthesis of novel stimuli responsive nanocomposite for biomedical applications. In *Recent Developments in Bio-Nanocomposites for Biomedical Applications*, Tiwari, A., Ed. Nova Science Pub Incorporated: **2010**, 207-231.

261. Campuzano, S.; Wang, J., Nanobioelectroanalysis Based on Carbon/Inorganic Hybrid Nanoarchitectures. *Electroanalysis* **2011,** *23*, 1289-1300.

262. Wang, Y. T.; Yu, L.; Wang, J.; Lou, L.; Du, W. J.; Zhu, Z. Q.; Peng, H.; Zhu, J. Z., A novel l-lactate sensor based on enzyme electrode modified with ZnO nanoparticles and multiwall carbon nanotubes. *Journal of Electroanalytical Chemistry* **2011,** *661*, 8-12.

263. Gao, R.; Zheng, J.; Zheng, X., Direct electrochemistry of myoglobin in a layer-by-layer film on an ionic liquid modified electrode containing CeO₂ nanoparticles and hyaluronic acid. *Microchimica Acta* **2011,** *174*, 273-280.

264. Mattinen, U.; Rabiej, S.; Lewenstam, A.; Bobacka, J., Impedance study of the ion-to-electron transduction process for carbon cloth as solid-contact material in potentiometric ion sensors. *Electrochimica Acta* **2011,** *56*, 10683-10687.

265. Bühlmann, P.; Chen, L. D., Ion-Selective Electrodes With Ionophore-Doped Sensing Membranes. In *Supramolecular Chemistry*, John Wiley & Sons, Ltd: **2012**.

266. Li, J.; Yu, J.; Zhao, F.; Zeng, B., Direct electrochemistry of glucose oxidase entrapped in nano gold particles-ionic liquid-N,N-dimethylformamide composite film on glassy carbon electrode and glucose sensing. *Analytica Chimica Acta* **2007,** *587*, 33-40.

267. Male, K. B.; Hrapovic, S.; Luong, J. H. T., Electrochemically-assisted deposition of oxidases on platinum nanoparticle/multi-walled carbon nanotube-modified electrodes. *Analyst* **2007,** *132*, 1254-1261.

268. Song, M.-J.; Kim, J.-H.; Lee, S.-K.; Lim, D.-S.; Hwang, S. W.; Whang, D., Analytical Characteristics of Electrochemical Biosensor Using Pt-Dispersed Graphene on Boron Doped Diamond Electrode. *Electroanalysis* **2011,** *23*, 2408-2414.

269. Wu, W.; Mitra, N.; Yan, E. C. Y.; Zhou, S., Multifunctional Hybrid Nanogel for Integration of Optical Glucose Sensing and Self-Regulated Insulin Release at Physiological pH. *Acs Nano* **2010,** *4*, 4831-4839.

270. Serafín, V.; Agüí, L.; Yáñez-Sedeño, P.; Pingarrón, J. M., A novel hybrid platform for the preparation of disposable enzyme biosensors based on poly(3,4-ethylenedioxythiophene) electrodeposition in an ionic liquid medium onto gold nanoparticles-modified screen-printed electrodes. *Journal of Electroanalytical Chemistry* **2011,** *656*, 152-158.

271. Liu, X. Y.; Zeng, X. D.; Mai, N. N.; Liu, Y.; Kong, B.; Li, Y. H.; Wei, W. Z.; Luo, S. L., Amperometric glucose biosensor with remarkable acid stability based on glucose oxidase entrapped in colloidal gold-modified carbon ionic liquid electrode. *Biosensors & Bioelectronics* **2010,** *25*, 2675-2679.

272. Kachoosangi, R. T.; Musameh, M. M.; Abu-Yousef, I.; Yousef, J. M.; Kanan, S. M.; Xiao, L.; Davies, S. G.; Russell, A.; Compton, R. G., Carbon Nanotube-Ionic Liquid Composite Sensors and Biosensors. *Analytical Chemistry* **2009,** *81*, 435-442.

273. Xi, F.; Liu, L.; Wu, Q.; Lin, X., One-step construction of biosensor based on chitosan–ionic liquid–horseradish peroxidase biocomposite formed by electrodeposition. *Biosensors and Bioelectronics* **2008,** *24*, 29-34.

274. Gopalan, A. I.; Lee, K.-P.; Ragupathy, D., Development of a stable cholesterol biosensor based on multi-walled carbon nanotubes–gold nanoparticles composite covered with a layer of chitosan–room-temperature ionic liquid network. *Biosensors and Bioelectronics* **2009,** *24*, 2211-2217.

275. Xiao, F.; Zhao, F.; Zhang, Y.; Guo, G.; Zeng, B., Ultrasonic Electrodeposition of Gold-Platinum Alloy Nanoparticles on Ionic Liquid-Chitosan Composite Film and Their Application in Fabricating Nonenzyme Hydrogen Peroxide Sensors. *The Journal of Physical Chemistry C* **2008,** *113*, 849-855.

276. Safavi, A.; Farjami, F., Electrodeposition of gold–platinum alloy nanoparticles on ionic liquid–chitosan composite film and its application in fabricating an amperometric cholesterol biosensor. *Biosensors and Bioelectronics* **2011,** *26*, 2547-2552.

277. Santhosh, P.; Manesh, K. M.; Uthayakumar, S.; Komathi, S.; Gopalan, A. I.; Lee, K. P., Fabrication of enzymatic glucose biosensor based on palladium nanoparticles dispersed onto poly(3,4-ethylenedioxythiophene) nanofibers. *Bioelectrochemistry* **2009,** *75*, 61-66.

278. Huang, H.-Y.; Chen, P.-Y., PdNi- and Pd-coated electrodes prepared by electrodeposition from ionic liquid for nonenzymatic electrochemical determination of ethanol and glucose in alkaline media. *Talanta* **2010,** *83*, 379-385.

279. Yang, M. H.; Choi, B. G.; Park, H.; Park, T. J.; Hong, W. H.; Lee, S. Y., Directed Self-Assembly of Gold Nanoparticles on Graphene-Ionic Liquid Hybrid for Enhancing Electrocatalytic Activity. *Electroanalysis* **2011,** *23*, 850-857.

280. Wu, H.-X.; Cao, W.-M.; Li, Y.; Liu, G.; Wen, Y.; Yang, H.-F.; Yang, S.-P., In situ growth of copper nanoparticles on multiwalled carbon nanotubes and their application as non-enzymatic glucose sensor materials. *Electrochimica Acta* **2010,** *55*, 3734-3740.

281. Ping, J.; Ru, S.; Fan, K.; Wu, J.; Ying, Y., Copper oxide nanoparticles and ionic liquid modified carbon electrode for the non-enzymatic electrochemical sensing of hydrogen peroxide. *Microchimica Acta* **2010,** *171*, 117-123.

282. Bo, X.; Bai, J.; Yang, L.; Guo, L., The nanocomposite of PtPd nanoparticles/onion-like mesoporous carbon vesicle for nonenzymatic amperometric sensing of glucose. *Sensors and Actuators B: Chemical* **2011,** *157*, 662-668.

283. Fang, Y.; Guo, S.; Zhu, C.; Zhai, Y.; Wang, E., Self-Assembly of Cationic Polyelectrolyte-Functionalized Graphene Nanosheets and Gold Nanoparticles: A Two-Dimensional Heterostructure for Hydrogen Peroxide Sensing. *Langmuir* **2010,** *26*, 11277-11282.

284. Zhu, H.; Liang, X.; Chen, J.; Li, M.; Zhu, Z., The influence of ionic liquids on the fabrication of nonenzymatic glucose electrochemical sensor. *Talanta* **2011,** *85*, 1592-1597.

285. Yang, J.; Zhang, W.-D.; Gunasekaran, S., An amperometric non-enzymatic glucose sensor by electrodepositing copper nanocubes onto vertically well-aligned multi-walled carbon nanotube arrays. *Biosensors and Bioelectronics* **2010,** *26*, 279-284.

286. Liu, X.; Zhu, H.; Yang, X., An amperometric hydrogen peroxide chemical sensor based on graphene-Fe3O4 multilayer films modified ITO electrode. *Talanta* **2011,** *87*, 243-248.

287. Lizeng, G.; Jie, Z.; Leng, N.; Jinbin, Z.; Yu, Z.; Ning, G.; Taihong, W.; Jing, F.; Dongling, Y.; Perrett, S.; Xiyun, Y., Intrinsic peroxidase-like activity of ferromagnetic nanoparticles. *Nature Nanotechnology* **2007,** *2*, 577-583.

288. Gao, L.; Zhuang, J.; Nie, L.; Zhang, J.; Zhang, Y.; Gu, N.; Wang, T.; Feng, J.; Yang, D.; Perrett, S.; Yan, X., Intrinsic peroxidase-like activity of ferromagnetic nanoparticles. *Nature Nano* **2007,** *2*, 577-583.

289. Tang, J.; Tang, D.; Niessner, R.; Chen, G.; Knopp, D., Magneto-Controlled Graphene Immunosensing Platform for Simultaneous Multiplexed Electrochemical Immunoassay Using Distinguishable Signal Tags. *Analytical Chemistry* **2011,** *83*, 5407-5414.

290. Zhang, L.; Yi, M., Electrochemical nitrite biosensor based on the immobilization of hemoglobin on an electrode modified by multiwall carbon nanotubes and positively charged gold nanoparticle. *Bioprocess and Biosystems Engineering* **2009,** *32*, 485.

291. Eguílaz, M.; Agüí, L.; Yáñez-Sedeño, P.; Pingarrón, J. M., A biosensor based on cytochrome c immobilization on a poly-3-methylthiophene/multi-walled carbon nanotubes hybrid-modified electrode. Application to the electrochemical determination of nitrite. *Journal of Electroanalytical Chemistry* **2010,** *644*, 30-35.

292. Liu, S.; Tian, J.; Wang, L.; Luo, Y.; Sun, X., Production of stable aqueous dispersion of poly(3,4-ethylenedioxythiophene) nanorods using grapheme oxide as a stabilizing agent and their application for nitrite detection. *Analyst* **2011,** *136*, 4898.

293. Han, D.; Han, T.; Shan, C.; Ivaska, A.; Niu, L., Simultaneous Determination of Ascorbic Acid, Dopamine and Uric Acid with Chitosan-Graphene Modified Electrode. *Electroanalysis* **2010,** *22*, 2001-2008.

294. Xue, Y.; Zhao, H.; Wu, Z.; Li, X.; He, Y.; Yuan, Z., The comparison of different gold nanoparticles/graphene nanosheets hybrid nanocomposites in electrochemical performance and the construction of a sensitive uric acid electrochemical sensor with novel hybrid nanocomposites. *Biosensors and Bioelectronics* **2011,** *29*, 102-108.

295. Zhang, Y.; Yuan, R.; Chai, Y.; Li, W.; Zhong, X.; Zhong, H., Simultaneous voltammetric determination for DA, AA and NO2− based on graphene/poly-cyclodextrin/MWCNTs nanocomposite platform. *Biosensors and Bioelectronics* **2011,** *26*, 3977-3980.

296. Bao, Y.; Song, J.; Mao, Y.; Han, D.; Yang, F.; Niu, L.; Ivaska, A., Graphene Oxide-Templated Polyaniline Microsheets toward Simultaneous Electrochemical Determination of AA/DA/UA. *Electroanalysis* **2011,** *23*, 878-884.

297. Jia, D.; Ren, Q.; Sheng, L.; Li, F.; Xie, G.; Miao, Y., Preparation and characterization of multifunctional polypyrrole–Au coated NiO nanocomposites and study of their electrocatalysis toward several important bio-thiols. *Sensors and Actuators B: Chemical* **2011,** *160*, 168-173.

298. Kavanagh, A.; Byrne, R.; Diamond, D.; Fraser, K. J., Stimuli Responsive Ionogels for Sensing Applications—An Overview. *Membranes* **2012,** *2*, 16-39.

299. Le Bideau, J.; Viau, L.; Vioux, A., Ionogels, ionic liquid based hybrid materials. *Chemical Society Reviews* **2011**.

300. He, Y.; Lodge, T. P., A thermoreversible ion gel by triblock copolymer self-assembly in an ionic liquid. *Chemical Communications* **2007**, 2372-2734.

301. Ueki, T.; Watanabe, M., Macromolecules in Ionic Liquids: Progress, Challenges, and Opportunities. *Macromolecules* **2008,** *41*, 3739-3749.

302. Zhang, Y.; Zheng, J., Direct electrochemistry and electrocatalysis of myoglobin immobilized in hyaluronic acid and room temperature ionic liquids composite film. *Electrochemistry Communications* **2008,** *10*, 1400-1403.

303. Zhang, J.; Lei, J.; Liu, Y.; Zhao, J.; Ju, H., Highly sensitive amperometric biosensors for phenols based on polyaniline-ionic liquid-carbon nanofiber composite. *Biosensors and Bioelectronics* **2009,** *24*, 1858-1863.

304. Usakli, A. B., Improvement of EEG Signal Acquisition: An Electrical Aspect for State of the Art of Front End. *Computational Intelligence and Neuroscience* **2010,** *2010*.

305. Torimoto, T.; Tsuda, T.; Okazaki, K.-i.; Kuwabata, S., New Frontiers in Materials Science Opened by Ionic Liquids. *Advanced Materials* **2010,** *22*, 1196-1221.

306. Marcilla, R.; Sanchez-Paniagua, M.; Lopez-Ruiz, B.; Lopez-Cabarcos, E.; Ochoteco, E.; Grande, H.; Mecerreyes, D., Synthesis and characterization of new polymeric ionic liquid microgels. *Journal of Polymer Science Part A: Polymer Chemistry* **2006,** *44*, 3958-3965.

307. Lopez, M. S.-P.; Mecerreyes, D.; Lopez-Cabarcos, E.; Lopez-Ruiz, B., Amperometric glucose biosensor based on polymerized ionic liquid microparticles. *Biosensors and Bioelectronics* **2006,** *21*, 2320-2328.

308. Jia, F.; Shan, C.; Li, F.; Niu, L., Carbon nanotube/gold nanoparticles/polyethylenimine-functionalized ionic liquid thin film composites for glucose biosensing. *Biosensors and Bioelectronics* **2008,** *24*, 945-950.

309. Shan, C.; Yang, H.; Song, J.; Han, D.; Ivaska, A.; Niu, L., Direct Electrochemistry of Glucose Oxidase and Biosensing for Glucose Based on Graphene. *Analytical Chemistry* **2009,** *81*, 2378-2382.

310. Xiang, L.; Zhang, Z.; Yu, P.; Zhang, J.; Su, L.; Ohsaka, T.; Mao, L., In situ cationic ring-opening polymerization and quaternization reactions to confine ferricyanide onto carbon nanotubes: A general approach to development of integrative nanostructured electrochemical biosensors. *Analytical Chemistry* **2008,** *80*, 6587-6593.

311. Lourenco, N. M. T.; Osterreicher, J.; Vidinha, P.; Barreiros, S.; Afonso, C. A. M.; Cabral, J. M. S.; Fonseca, L. P., Effect of gelatin-ionic liquid functional polymers on glucose oxidase and horseradish peroxidase kinetics. *Reactive and Functional Polymers* **2011,** *71*, 489-495.

312. Nilsson, D.; Kugler, T.; Svensson, P.-O.; Berggren, M., An all-organic sensor-transistor based on a novel electrochemical transducer concept printed electrochemical sensors on paper. *Sensors and Actuators B: Chemical* **2002,** *86*, 193-197.

313. Khodagholy, D.; Curto, V. F.; Fraser, K. J.; Gurfinkel, M.; Byrne, R.; Diamond, D.; Malliaras, G. G.; Benito-Lopez, F.; Owens, R. M., Organic electrochemical transistor incorporating an ionogel as a solid state electrolyte for lactate sensing. *Journal of Materials Chemistry* **2012,** *22*, 4440-4443.

314. Curto, V. F.; Fay, C.; Coyle, S.; Byrne, R.; O'Toole, C.; Barry, C.; Hughes, S.; Moyna, N.; Diamond, D.; Benito-Lopez, F., Real-time sweat pH monitoring based on a wearable chemical barcode micro-fluidic platform incorporating ionic liquids. *Sensors and Actuators B: Chemical* **2012,** *171-172*, 1327-1334.

315. Curto, V. F.; Fay, C.; Coyle, S.; Byrne, R.; Diamond, D.; Benito-Lopez, F., Wearable Microfluidic pH Sweat Sensing Device based on Colorimetric Imaging Techniques. In *The 15th International Conference on Miniaturized Systems for Chemistry and Life Sciences, μTAS 2011 (MicroTAS) Conference*, Seattle, USA, **2011**.

316. Wan, Q.; Yu, F.; Zhu, L.; Wang, X.; Yang, N., Bucky-gel coated glassy carbon electrodes, for voltammetric detection of femtomolar leveled lead ions. *Talanta* **2010,** *82*, 1820-1825.

317. Xiao, F.; Zhao, F.; Zeng, J.; Zeng, B., Novel alcohol sensor based on PtRuNi ternary alloy nanoparticles–multi-walled carbon nanotube–ionic liquid composite coated electrode. *Electrochemistry Communications* **2009,** *11*, 1550-1553.

318. Ng, S. R.; Guo, C. X.; Li, C. M., Highly Sensitive Nitric Oxide Sensing Using Three-Dimensional Graphene/Ionic Liquid Nanocomposite. *Electroanalysis* **2011,** *23*, 442-448.

319. Ohtani, T.; Nishi, N.; Kakiuchi, T., Differential pulse stripping voltammetry of moderately hydrophobic ions based on hydrophobic ionic liquid membranes supported on the Ag/AgCl electrode. *Journal of Electroanalytical Chemistry* **2011,** *656*, 102-105.

320. Jia, J.; Cao, L.; Wang, Z.; Wang, T., Properties of Poly(sodium 4-styrenesulfonate)-Ionic Liquid Composite Film and Its Application in the Determination of Trace Metals Combined with Bismuth Film Electrode. *Electroanalysis* **2008,** *20*, 542-549.

321. Michalska, A., All-Solid-State Ion Selective and All-Solid-State Reference Electrodes. *Electroanalysis* **2012,** *24*, 1253-1265.

322. Ash, P. A.; Vincent, K. A., ChemInform Abstract: Spectroscopic Analysis of Immobilized Redox Enzymes under Direct Electrochemical Control. *ChemInform* **2012,** *43*.

323. Alva, S., FreeStyle Lite—A Blood Glucose Meter That Requires No Coding. *Journal of Diabetes Science and Technology* **2008,** *2*, 546-551.

324. Vallée-Bélisle, A.; Plaxco, K. W., Structure-switching biosensors: inspired by Nature. *Current Opinion in Structural Biology* **2010,** *20*, 518-526.

325. Justino, C. I. L.; Rocha-Santos, T. A.; Duarte, A. C., Review of analytical figures of merit of sensors and biosensors in clinical applications. *TrAC Trends in Analytical Chemistry* **2010,** *29*, 1172-1183.

326. Mishra, A. K.; Mishra, S. B.; Tiwari, A.; Rai, R. S., Fabrication of bionanocomposites from natural biopolymer matrices and inorganic nanofillers. In *Recent Developments in Bio-Nanocomposites for Biomedical Applications*, Tiwari, A., Ed. Nova Science Pub Incorporated: **2010**.

327. Kadokawa, J.-i.; Murakami, M.-a.; Kaneko, Y., A facile preparation of gel materials from a solution of cellulose in ionic liquid. *Carbohydrate Research* **2008,** *343*, 769-772.

328. Kopecek, J., Hydrogels: From soft contact lenses and implants to self-assembled nanomaterials. *Journal of Polymer Science Part A: Polymer Chemistry* **2009,** *47*, 5929-5946.

329. Lodge, T. P., Materials science - A unique platform for materials design. *Science* **2008,** *321*, 50-51.

330. Seiffert, S.; Sprakel, J., Physical chemistry of supramolecular polymer networks. *Chemical Society Reviews* **2012,** *41*, 909-930.

331. Pasparakis, G.; Vamvakaki, M., Multiresponsive polymers: nano-sized assemblies, stimuli-sensitive gels and smart surfaces. *Polymer Chemistry* **2011,** *2*, 1234-1248.

332. Kuksenok, O.; Yashin, V. V.; Balazs, A. C., Global signaling of localized impact in chemo-responsive gels. *Soft Matter* **2009,** *5*, 1835-1839.

333. Magin, C. M.; Cooper, S. P.; Brennan, A. B., Non-toxic antifouling strategies. *Materials Today* **2010,** *13*, 36-44.

334. Scardino, A. J.; de Nys, R., Mini review: Biomimetic models and bioinspired surfaces for fouling control. *Biofouling* **2010,** *27*, 73-86.

335. Diamond, D.; Coyle, S.; Scarmagnani, S.; Hayes, J., Wireless Sensor Networks and Chemo-/Biosensing. *Chemical Reviews* **2008,** *108*, 652-679.

336. Bhandari, P.; Narahari, T.; Dendukuri, D., 'Fab-Chips': a versatile, fabric-based platform for low-cost, rapid and multiplexed diagnostics. *Lab on a Chip* **2011,** *11*, 2493-2499.

337. Hu, L.; Pasta, M.; Mantia, F. L.; Cui, L.; Jeong, S.; Deshazer, H. D.; Choi, J. W.; Han, S. M.; Cui, Y., Stretchable, Porous, and Conductive Energy Textiles. *Nano Letters* **2010,** *10*, 708-714.

338. Dhende, V. P.; Samanta, S.; Jones, D. M.; Hardin, I. R.; Locklin, J., One-Step Photochemical Synthesis of Permanent, Nonleaching, Ultrathin Antimicrobial Coatings for Textiles and Plastics. *ACS Applied Materials & Interfaces* **2011,** *3*, 2830-2837.

339. Lee, S.-K.; Kim, B. J.; Jang, H.; Yoon, S. C.; Lee, C.; Hong, B. H.; Rogers, J. A.; Cho, J. H.; Ahn, J.-H., Stretchable Graphene Transistors with Printed Dielectrics and Gate Electrodes. *Nano Letters* **2011,** *11*, 4642-4646.

340. Kim, D. H.; Lu, N. S.; Ma, R.; Kim, Y. S.; Kim, R. H.; Wang, S. D.; Wu, J.; Won, S. M.; Tao, H.; Islam, A.; Yu, K. J.; Kim, T. I.; Chowdhury, R.; Ying, M.; Xu, L. Z.; Li, M.; Chung, H. J.; Keum, H.; McCormick, M.; Liu, P.; Zhang, Y. W.; Omenetto, F. G.;

Huang, Y. G.; Coleman, T.; Rogers, J. A., Epidermal Electronics. *Science* **2011,** *333*, 838-843.

341. Carta, R.; Jourand, P.; Hermans, B.; Thoné, J.; Brosteaux, D.; Vervust, T.; Bossuyt, F.; Axisa, F.; Vanfleteren, J.; Puers, R., Design and implementation of advanced systems in a flexible-stretchable technology for biomedical applications. *Sensors and Actuators A: Physical* **2009,** *156*, 79-87.
342. Windmiller, J. R.; Bandodkar, A. J.; Valdes-Ramirez, G.; Parkhomovsky, S.; Martinez, A. G.; Wang, J., Electrochemical sensing based on printable temporary transfer tattoos. *Chemical Communications* **2012,** *48*, 6794-6796.
343. Bandodkar, A. J.; Hung, V. W. S.; Jia, W.; Valdes-Ramirez, G.; Windmiller, J. R.; Martinez, A. G.; Ramirez, J.; Chan, G.; Kerman, K.; Wang, J., Tattoo-based potentiometric ion-selective sensors for epidermal pH monitoring. *Analyst* **2013**, In Press.

Chapter 3

Concept and Development of an Autonomous Wearable Micro-fluidic Platform for Real Time pH Sweat Analysis

Vincenzo F. Curto[1], S. Coyle[1], R. Byrne[1], N. Angelov[1], D. Diamond[1], F. Benito-Lopez[1*]

Sensors and Actuators B: Chemical 175 (2012) 263–270

ISSN: 0925-4005; http://dx.doi.org/10.1016/j.snb.2012.02.010

[1]CLARITY: Centre for Sensor Web Technologies, National Centre for Sensor Research, School of Chemical Sciences, Dublin City University, Dublin 9, Ireland

* Author to whom correspondence should be addressed;

Abstract

In this chapter, the development of an autonomous, robust and wearable micro-fluidic platform capable of performing on-line analysis of pH in sweat is discussed. Through the means of an optical detection system based on a surface mount light emitting diode (SMD LED) and a light photo sensor as a detector, a wearable system was achieved in which real-time monitoring of sweat pH was performed during 55 minutes of cycling activity. It is shown how through systems engineering, integrating miniaturised electrical components, and by improving the micro-fluidic chip characteristics, the wearability, reliability and performance of the micro-fluidic platform was significantly improved.

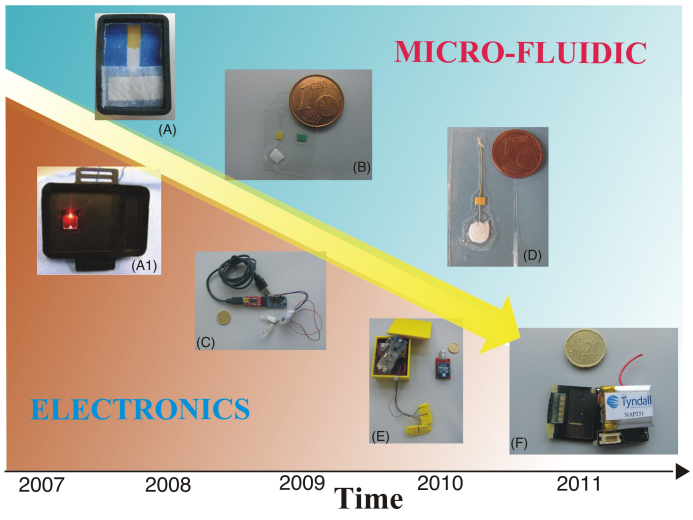

Keywords: micro-fluidic; pH; SMD LED; light photo sensor; wearable system; sweat analysis

3.1 Introduction

Sweat is a body fluid naturally produced during physical exercise and emotional stress, and it is essentially a filtrate of blood plasma containing many substances such as sodium, chloride, potassium, bicarbonate, calcium, ammonia and organic compounds, such as glucose and lactate.[1] Sweating is primarily a mechanism of body thermoregulation to avoid dangerous rise in body temperature that correlates with the increases in metabolic rate of the individual. During this physiological process, electrolytes and liquid are excreted by sweat glands via a duct to the outer skin surface.[2] Through the analysis of its composition, it is possible to obtain useful information regarding the physiological condition of the body and provides information about the health and well-being of the individual as well, especially during sport activities.

In section 1.3 of Chapter 1, different sampling techniques for the performing of sweat analysis were presented, such as the whole body wash down technique[3] and the use of epidermal patches[4] or capsule.[5] However, these techniques are not able to give real-time information and it is very likely to cross-contaminate the collected samples. Therefore, real-time sweat analysis when performed during exercise is a great challenge for sensor fabrication due to the need for on-body fluid handling, sensor deployment and data management. If all these issues can be accomplished, the obtained devices will be capable of provide immediate feedback of fluid loss and variations of sweat analytes, giving prompt and reliable information of athlete performance and/or general health.

Sweat analysis has been employed in the diagnosis of diseases,[6] drug abuse[7] and in the optimisation of the performance of athletes.[8] Using a gold disc microelectrode De Souza *et al.*[9] developed a rapid and straightforward method for copper ions detection for clinical diagnosis of Wilson disease. Also, inorganic cations, amines and amino acids in human sweat were detected by capillary electrophoresis,[10] while odour active compounds of human male armpit sweat, after fenugreek ingestion, were investigated by gas chromatography coupled to mass spectrometry and olfactometry.[11] Real-time measurements of sodium concentration in sweat was developed by Schazmann *et al.*[12] using a sodium sensor belt (SSB) based on Ion Selective Electrodes (ISE). An application of this

SSB was found for the diagnosis of Cystic Fibrosis (CF) disease.

The present study investigates changes of pH in sweat since it is a very important, but at the same time, easy to measure physiological parameter in sweat. Many research groups have been interested in the analysis of pH in sweat, showing that there are several factors that correlate pH of sweat with health. For instance, Patterson *et al.*[13] found a correlation between sweat pH and sodium and chloride concentration in sweat, suggesting that decreasing of sodium and chloride concentrations in sweat is followed by a decrease of its pH. Furthermore, it was demonstrated that the ingestion of sodium bicarbonate led to the increase in blood and sweat pH's.[14] In addition, it was found that changes in the pH of the skin play a role in the pathogenesis of skin diseases, such as dermatitis and acne.[15]

Autonomous wearable sensors to monitor sport activities should consist of reliable systems capable of monitoring physical and/or bio-chemical conditions in real time so different factors need to be considered during the design of these systems. Firstly, sampling is crucial since sample needs to be collected and delivered to the sensing active area where a signal will be generated. A failure at this stage will compromise the performance and reliability of the whole sensor. Moreover, other important requirements to take into account are: (1) low cost of manufacture, (2) affordable market price, (3) flexibility of the device in order to be wearable and adaptable to the body contours (minimising the discomfort to the wearer), (4) easy transfer of signal to wearer interface and (5) long term stability.

Prior this research, as part of BIOTEX (Biosensing textile for health management) project (http://www.biotex-eu.com/), the first generation of a wearable and wireless sweat analysis system was successfully fabricated and tested.[16] This sensor was integrated into a wearable platform consisting of a black masked case containing a fluid-handing system and an optical detector.

A textile-based fluidic system was used to draw and deliver sweat to the sensing area where a pH sensitive dye was incorporated in one end of the polyester/lycra® blends wicking textile. The colorimetric response of the pH sensitive dye was detected using Light Emitting Diodes (LEDs) integrated and positioned over the fabric channel into the device holder.

In this chapter, the technological achievements in performing real-time pH sweat analysis in real time coming from the basic concept of the textile-based fluid handling device towards a miniaturised wearable micro-fluidic device is presented.

Two main investigation streams are described: the size reduction of the electronic components that compose the detection system of the device and a smart micro-fluidic chip design and fabrication, capable of improving sample collection, minimising dead volumes, sample cross-contamination and detection times. The development of a fully autonomous and functional wearable micro-fluidic platform for real-time sweat analysis based on both approaches will be described in the following sections.

3.2 Experimental

3.2.1 Materials

The fabrication of the micro-fluidic devices was carried out using a laser ablation system-excimer/CO_2 laser (Optec LaserMicromachining Systems, Belgium) and a thermal roller laminator (Titan-110, GBC Films, USA). Poly(methyl-methacrylate) (PMMA) 50 μm slides were purchased from Goodfellow, UK. 80 μm double-sided pressure sensitive adhesive film (PSA-AR8890) was obtained from Adhesives Research, Ireland.

Artificial sweat was prepared according to the standard ISO 3160-2 (20 g L^{-1} NaCl, 17.5 g L^{-1} NH_4OH, 5 g L^{-1} acetic acid and 15 g L^{-1} lactic acid) (Sigma-Aldrich, St. Louis, USA). Bromocresol purple dye (BCP), hydrochloric acid, sodium hydroxyde and tetraoctyl ammonium bromide were obtained from Sigma-Aldrich, St. Louis, USA. Cotton gauze was purchased from Boots Pharmaceuticals, Ireland.
Yellow surface mount LEDs (SMD LEDs) of peak wavelength 590 nm, (KP 2012SYC, Kingbright) and surface mount light photo sensor modules (APDS-9004, Avago Technologies) were purchased from Farnell Ireland. Temperature sensors (Analog Devices, ADT 7301) and humidity sensors (Sensirion, SHT 11) were purchased from Radionincs. Arduino microcontrollers and Xbee wireless modules were purchased from Sparkfun Electronics, Boulder, Colorado, USA. The in-house-designed case and micro-fluidic holder of wired and wireless detectors were fabricated using a 3D printer (Stratasys, USA) in acrylonitrile butadiene styrene co-polymer (ABS) plastic in order to protect the electronics from moisture and liquid and to minimise interferences from ambient light during the operation of the device. The printed parts were designed using ProEngineer CAD/CAM software package®.

3.2.2 Textile-based Fluid Handling Device

The textile-based fluid handling device used a fabric based fluidic system, where sweat entered and flowed through a channel by capillary action and collected by an absorbent patch at the end of the channel. The channel was created by coating regions of the fabric with hydrophobic materials. The channel width was 8 mm and overall length was over 30 mm. This was designed to accommodate multiple sensors. A cover was held 5 mm above the fabric layer by means of a rubber gasket. The fabric patch covered an area of 40 x 50 mm. pH sensitive BCP dye was applied to the fabric channel and optical sensing components were positioned in the plastic cover. A paired emitter-detector LED configuration was used to measure the colour change of the fabric. Two red LED's (λ = 660 nm) were positioned at an angle above the fabric in a reflectance mode configuration. Black silicone was placed around the sides of the detector LED to block ambient light (Figure 3.3-a). The LEDs were chosen because they have a narrow viewing angle (34 º) to help focus the light on a smaller sensing region. A minimum sensing region of 5 x 5 mm was needed, based on the height and angles that the LEDs were positioned. As the fabric channel was 8 mm wide, based on the requirements of other sensors placed on the channel, the pH dye was printed onto a 8 x 7 mm area.[17]

3.2.3 Micro-fluidic Platform

All the micro-fluidic chips (Figure 3.1 a and c) were fabricated using multilayer lamination protocol. In brief, a CO_2 laser system was used to cut the various polymer layers. Micro-fluidic channels were cut from 80 μm thick layer of PSA and laminated onto PMMA 50 μm thick, using the thermal roller laminator. Figure 3.1-b shows the fabrication of the two generations of the micro-fluidic chips. The sensing area is a piece of nylon lycra® textile (3 x 3 mm) embedded in the middle of the device with a pH sensitive dye, bromocresol purple (BCP), which varies colour according to the pH of the sweat. The immobilisation of BCP is performed in an ethanol solution containing tetraoctyl ammonium bromide to avoid leaching of the dye during the contact with aqueous solutions and sweat. BCP dye colour range varies in the physiological pH range of sweat (pH 5-7).

The first generation of the micro-fluidic chip consists of a small structure of 20 by 10 mm, as shown in Figure 3.1-a. A round inlet of 2 mm in diameter is placed at the top of the channel that has an overall length of 8 mm. The first part of the channel is characterised by a drop shape (length of 6 mm) structure, which acts as a collector of fresh sweat coming from the skin. The collector is followed by a 2 mm length channel, while the channel following the sensing area (exhaustion channel) presents a length of 2 mm. Both channels have a width and depth equal to 400 µm and 80 µm, respectively. At the end of the channel, a 5 mm diameter chamber contains the absorbent material (4 x 3 mm).

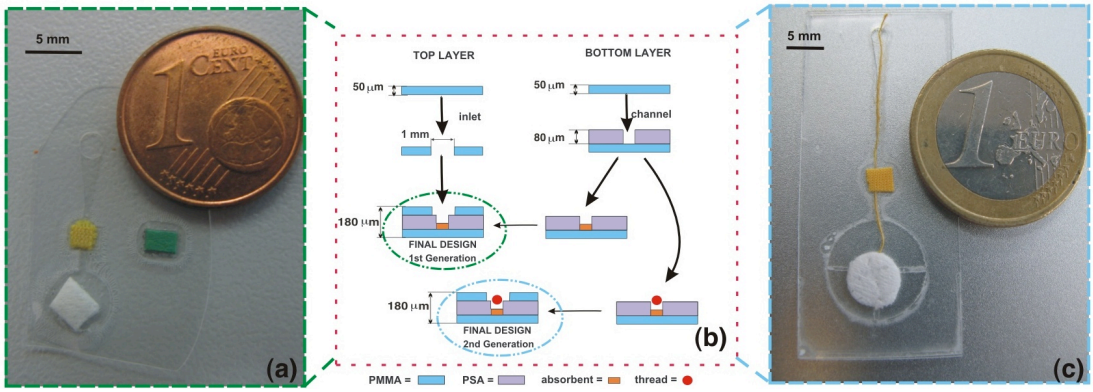

Figure 3.1. First generation of the micro-fluidic chip *(a)*. Schematic representation of the fabrication steps for first and second generation of the micro-fluidic chip *(b)*. Second generation of the micro-fluidic chip *(c)*.

The design of the second generation of the micro-fluidic chip takes into consideration other parameters like long-term operability and flow control by the integration of a cotton thread inside the micro-channel to ensure a homogeneous sweat flow rate through the channels (Figure 3.1 b, c). The overall dimensions of the micro-fluidic chip are 45 x 20 mm. Inlet diameter, channel width, depth and collector are the same as in the first generation, while the exhaustion channel has a length of 4 mm. The absorbent material has a diameter of 6 mm and it is placed into a round chamber of 12 mm in diameter (see Figure A1 in appendix A).

3.2.4 Detection System

3.2.4.1 Textile-based Fluid Handling Device

The LEDs were controlled by a central control unit that was supplied by CSEM. The detector LED was reverse-biased at +5 V, which charges the capacitance across it. This is discharged by the photocurrent generated upon incident light. The discharge rate is proportional to the intensity of the light reaching the detector. A digital output can be obtained by using a basic detection/timer circuit, which measures the time it takes the photocurrent to discharge the voltage from +5 V (logic 1) to +1.7 V (logic 0). Data was wirelessly transmitted to a laptop for analysis via Bluetooth. The detector case is shown in Figure 3.3-a.

3.2.4.2 Wired Device

By reducing the fluidic channel from a width of 8 mm to 400 μm and reducing the sensing region from 56 mm^2 to 4 mm^2 the optical detection components also needed to be miniaturised and be aligned to focus on a smaller region. For this reason super-bright yellow SMD LEDs (λ = 590 nm) were chosen.

Wired System 1 (not shown here)

The first miniaturised system used the same principle as the textile-based fluid handling device and a pair of SMD LEDs was placed above and below the sensing area of the microfluidic chip in a transmission configuration. In first trials black masking tape was used to position the SMD LEDs and also to block ambient light. One of the SMD LEDs acted as light source while the other was reverse biased and acted as a detector. A resistor was connected in series with the source SMD LED to attenuate the light to prevent saturation of the detector. Both SMD LEDs were controlled by a microcontroller platform, Lilypad Arduino, which is designed for wearable applications. The detector SMD LED was connected to the digital I/O pin of the Arduino and a timing routine was used to measure the discharge time from logic ‘1’ to ‘0’. Data was sampled at 2 Hz and transferred to a laptop by an RS232 serial link.

Wired System 2

In this system, SMD LED was used as light source, while surface mount light photo sensor (APDS-9004, Avago Technologies) was chosen as a detector. The circuit diagram of the detector is shown in Figure 3.2. The SMD LED intensity was controlled by a current limiting resistor (R_1). The 30 awg wire leads were soldered to the pins of the components and the devices subsequently coated in silicone (Dow Corning, Sylgard 184) to protect the components and also to prevent short circuits between the pins. The output pin of the light photo sensor module was connected to the analogue input channel of the microcontroller. A capacitor (C) was used as a low pass filter to remove high frequency noise, and a load resistor (R_2) was used to control the current to voltage output signal of the light photo sensor.

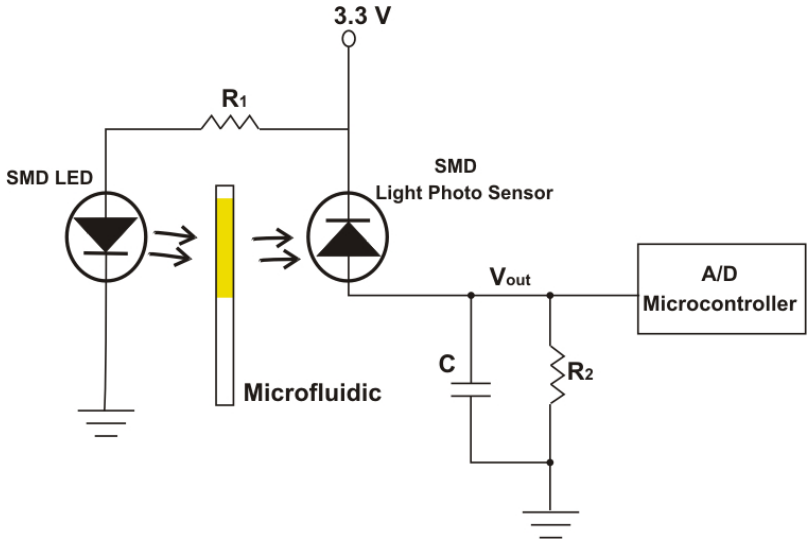

Figure 3.2. Circuit diagram of the detection system in transmittance mode

A transmission configuration was used, where the light passes directly through the sensing material. The SMD LED and light photo sensor were placed on either side of the chip. For the on-body trials a robust system was required to position the optical components onto the microfluidic chip. Plastic 3D printed case was designed to hold the components in place, as shown in Figure 3.3-b. The data was sampled at 2 Hz using either an Arduino Lilypad or Arduino Pro and transferred to a laptop by an RS232 serial link.

3.2.4.3 *Wireless Device*

In this system, the wired connection to the laptop was replaced with a wireless link. One option was to attach a Bluetooth® modem (BlueSMiRF silver) to the Arduino device. At the time of development a new Arduino Funnel IO was released, which presents an Xbee socket. This device provided a more compact solution rather than adding a separate modem to the existing configuration. There is also an option of a longer range using Xbee Pro modules and lower power consumption for shorter ranges compared to Bluetooth. However, this system requires an Xbee base-station to be connected to a laptop, while many devices would have Bluetooth capability in-built. In the end, an Xbee module was chosen.

The optical components and associated electronics were assembled in the same way as the previous wired system (Figure 3.2). In addition, a temperature sensor and humidity sensor were integrated into the device to measure skin temperature and the humidity of the surrounding environment. Digital sensors were used as these could be easily configured using the Arduino FIO. A plastic holder was made using a 3D printer to hold the temperature sensor (Analog Devices, ADT 7301), humidity sensor (Sensirion, SHT 11) sensors, SMD light photo sensor and LED and the pH microfluidic chip. A separate box was designed to hold the Arduino funnel, battery and control circuitry (Figure 3.3-c).

3.2.4.4 *Portable Device*

The portable device was designed to improve the wearability of the system by reducing the size of the overall design and customise a wireless system based on the sweat sensor requirements. The sampling point, sensing elements and associated electronics were combined into a single device, Figure 3.3-d. The device once again uses a transmission mode configuration with a SMD LED and light photo sensor to detect colour changes related to pH. A temperature sensor was included in the device to measure skin temperature. The wireless capability is based on the Tyndall 25 mm mote. This device operates in the 2.4 GHz ISM Band and uses ZigBee protocols for communication. A base-station mote is connected to a laptop to receive the transmitted data and log this for analysis.

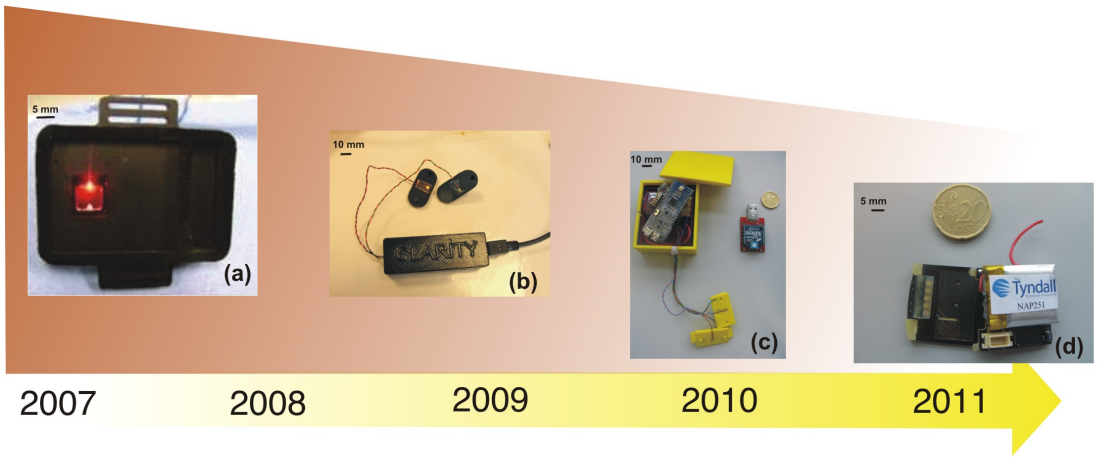

Figure 3.3. Development of the electronics in the autonomous wearable micro-fluidic platform for sweat pH analysis. Textile-based fluid handling device (a), Wired detection system 2 (b), Wireless detection system (c) and miniaturised wearable micro-fluidic detector (d).

3.3 Results and Discussion

3.3.1 Detection System

Colorimetric detection is performed as the sensing material changes colour according to the pH of sweat. A light source is needed to illuminate the fabric and an optical detector is needed to measure the transmitted or reflected light. In the textile-based fluid handling device, the optical sensing configuration used a reflectance measurement where the light source and the detector were positioned at an angle above the sensing layer, as shown in Figure 3.4-a. This meant that an adequate sensing region (56 mm^2) was needed to ensure accurate measurements, so that the detector LED would only receive light reflected from the sensing region of the fabric and not from the surrounding textile. This was important considering possible movement effects during wear. 3 mm LEDs were used and were encased in clear silicone to avoid the effects of sweat condensation. A reverse-biased LED was used as a detector. This arrangement used the inherent capacitance of the LED and measured the discharge time using a microcontroller. The discharge rate is proportional to the intensity of the light reaching the detector.

Despite the good performance obtained by the textile-based fluid handling device, the bulkiness of the LED-LED system made it difficult to place and adapt the sensor to different parts of the body. Therefore, we decided to miniaturise the

detection system by replacing the 3 mm LEDs by SMD LEDs. This reduced the bulkiness of the detection system considerably since the SMD LED is 1 x 1 mm and flat (500 µm) ensuring a more compact and compatible detector for wearable applications.

The first detector realised using SMD LED was the *wired system 1*, where a reverse biased SMD LED in transmittance was used as detector. During preliminary experiments this system demonstrated good response for changes in pH from pH 4 to pH 7. However, the detection system did not have sufficient sensitivity when calibrations were performed using artificial sweat solutions between these pH ranges.[18] Therefore, a SMD light photo sensor (APDS-9004, Avago Technologies) was chosen as detector, with the aim to increase its sensitivity compared to the reverse biased SMD LED. The SMD LED and light photo sensor were placed above and below the sensing area of the micro-fluidic chip in a tidy and compact structure as shown in Figure 3.4-b.

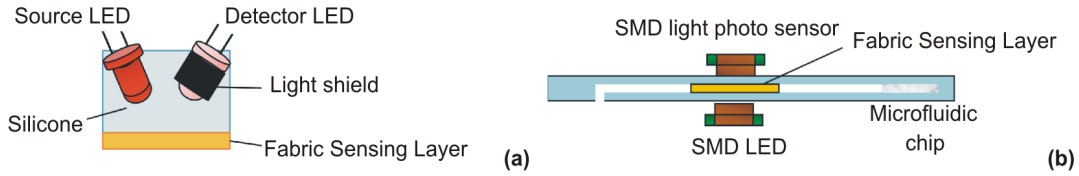

Figure 3.4. Schematic representation of the alignment of LED-LED detector system in textile-based fluid handling device (a), and the alignment of SMD LED and light photo sensor in the transmittance detectors (b).

The light emitted by the SMD LED is attenuated as it passes through the textile that presents different colour depending on the pH of the sample. This change in light intensity is sensed by the light photo-sensor operating in photoconductive mode where the V_{out} (Figure 3.2) is proportional to the photocurrent generated by the transmitted light.[19] A black plastic holder for the wired system 2 was made using the 3D printer to align the SMD LED and the light photo sensor. Initially, the SMD LED and the light photo sensor were integrated in a wired configuration (Figure 3.3-b), wherein both were controlled by an Arduino Pro platform, which uses the ATmega168 microcontroller. Therefore, in the second generation of the device the replacement of an Arduino Pro by an Arduino Funnel IO, which uses the ATmega328P and contains an Xbee socket, enabled a wireless system to be realised

through which data was wirelessly transmitted to an Xbee base-station connected to a remote laptop via a USB serial link. With this configuration it was possible to provide more freedom of movements to the wearer and increasing the spatial operation of the system.

In spite of the good performance of the detector, its packaging was performed in such a way that it was too big and uncomfortable to carry during the exercise period. A more compact structure will provide a better adaptability of the whole system to the body contours. That is why we decided to work in the fabrication of a miniaturised system.

Figure 3.3-d shows the third generation of the wearable detector device, in which all the electronic components are integrated in a much smaller cordless platform (2.5 x 3 cm) capable of wireless transmission of pH sweat data directly to a laptop. This device is based on the Tyndall 25 mm mote, which is a modular stackable layer solution (http://www.tyndall.ie/mai/).[20, 21] This design opens the possibility of performing real-time sweat analysis, minimising the discomfort of the wearer while simultaneously providing information about the wearer's physiological conditions during exercise session. Moreover, due to its small dimensions, several devices could be used in different parts of the body simultaneously, to map pH sweat composition over the whole body.

3.3.2 Micro-fluidic Chip Fabrication

The employment of a micro-fluidic chip to perform sweat analysis gives several advantages over previous systems presented in literature.[3, 17] For instance, in the textile-based fluid handling device it is employed as *"fluid handling system"* based on fabrics with inherent moisture wicking properties. Despite the good performance and the inherent capability of the system to collect fresh sample over a period of time, the system needs high volume of liquid (milliliter) to carry out the analysis and activate the passive pump system prior use. These factors limit the continuous operability of the sensor; in fact, a decrease in the sweat rate compromises its real-time operation.

To overcome these limitations, the development of micro-fluidic systems allows a substantially reduction of the volume that is needed to monitor certain analytes in sweat, *i.e.* pH, because of the drastic reduction of channel width and

length and therefore the sensing area. Moreover, since the sensing area is enclosed inside the micro-fluidic device, cross-contamination from other skin areas and the surrounding environment is very unlikely.

In section 3.3, two generations of micro-fluidic chips were described, where the main advantage was the reduction of the sample volume to less than 10µL.[18] In both micro-fluidic chip configurations the sweat is drawn into the sensing area by an absorbent fiber placed at the end of the channel that acts as a passive pump system. Figure 3.5 shows four pump-less micro-fluidic devices and the relation of channel length with the time necessary for the fluid to reach the sensing area. The channel of 2 mm ensures fast sensor response reducing the delay time (t_d) between the generation of the sweat in the skin and the sensor response to less than 20 s.

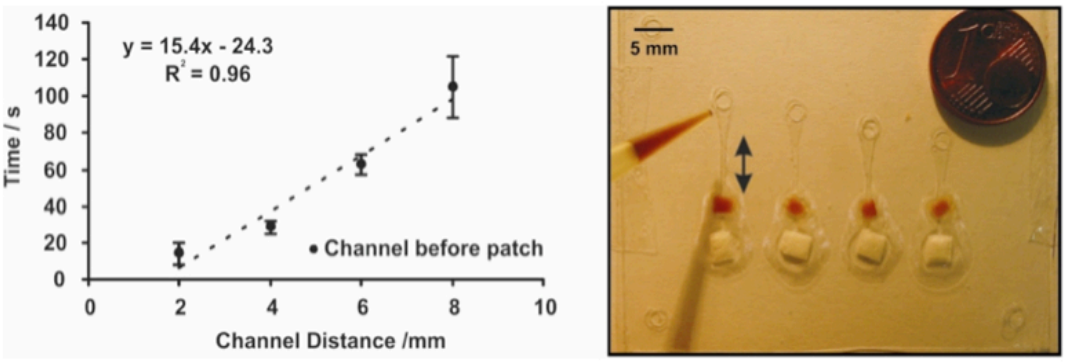

Figure 3.5. Relation between channel length and the time that sweat needs to reach the sensing area using the passive pump in the chip *(left)* (n = 5), picture of four micro-fluidic devices with different channel length

Nevertheless, a better control of the flow rate in the microfluidic was obtained by the integration of a cotton thread inside the micro-channel. The use of cotton threads textiles into micro-fluidic systems has been explored by Li *et al.*[22], who demonstrated that using the intrinsic capillarity action of a thread textile it is possible to fabricate low-cost and easy-to-use devices for sensor purposes. Here the wicking property of a thread was used to transport sweat along the micro-fluidic channel, ensuring a homogeneous sweat flow rate, improving response time and robustness of the micro-fluidic device. Although it was previously shown that the first generation of the micro-fluidic chip presents a good performance using a channel length of 2 mm, in the second generation the length of the channel was increased seven times. The reason for this new design was mainly to ensure better flexibility and body

adaptability of the inlet of the micro-fluidic chip when in contact with the skin with respect to the sensor electronics. A defined distance of 14 mm was necessary to avoid inlet detachment from the skin due to the tight position between micro-fluidic chip and electronics.

3.3.3 Micro-fluidic Chip Performance

3.3.3.1 Passive Pump

Figure 3.6 shows the autonomous pumping rate of the second generation of the micro-fluidic chip over time. The flow rate was calculated by adding a 10 μL drop of DI water on the inlet of the micro-fluidic chip and recording the time the water is completely absorbed by the passive pump (absorbent). According to Morris *et al*.[17], it is possible to define three operative regimes where the fluid rate is consistently different. When the system is in its dry state, the rate of fluid transports through the channel is due to the natural adsorption of the cotton thread placed into the channel. In our experiments is in the range of 1 μL min^{-1}. Considering the volume of the micro-channel from the inlet to the sensing material (approximately 0.928 μL) and assuming a linear increment of the pumping rate during the first ten minutes, it has been calculated that the average time for the fluid to reach the sensing area is around 3 min. The second regime is characterised by an increasing of the pumping rate when the fluid reaches the super absorbent. The flow is controlled by the absorbing capacity of the absorbent material placed at the end of the channel. The pumping rate presents a maximum value of 2.37 μL min^{-1} after 20 min, although the whole range of operation at this regime can be defined between minutes 15 and 40, as shown in Figure 3.6. A quite large variation of the pumping rate occurs over time according to the error shown in Figure 3.6, *e.g.* ± 1 μL min^{-1} for the worst scenario. The error is the average of four independent micro-fluidic chips and it can be attributed to the differences in the fabrication of the device since this is manual. We have observed that the position of the thread in the channel is of extreme importance for the homogeneous flow behavior during testing.

Finally the last regime found during passive pumping starts when the absorbent gets saturated and so the flow rate slows down considerably, stabilising a flow rate of around 0.5 μL min^{-1} through to full absorbent saturation.

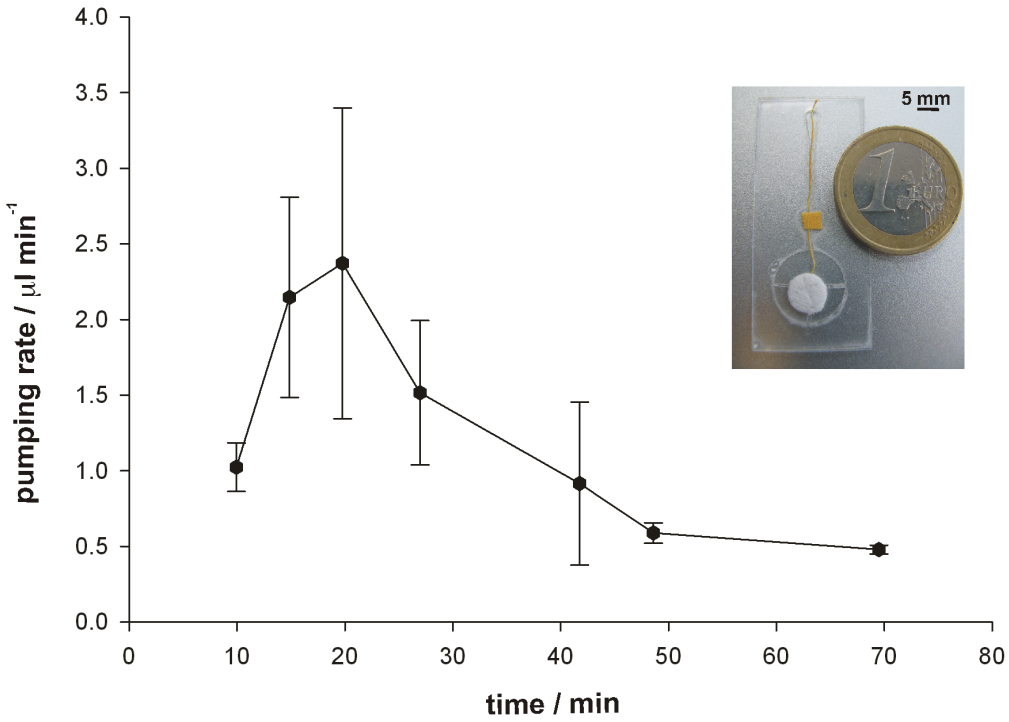

Figure 3.6. Average of the pumping rate of the passive pumping system, n = 4.

3.3.3.2 Loading Capacity of the Micro-fluidic Chip

The loading capacity of the micro-fluidic chip, which is the maximum amount of sweat that the absorbent can uptake before the passive flow reaches zero, was calculated to be 68.7 ± 6 µL. Therefore, the calculated life-time of the device, taking into account an average of sweat flow (1.29 ± 0.4 µL min^{-1}) was found to be around 53 minutes. Since in a healthy individual the sweating process starts between 10-15 minutes from the beginning of the exercise activity, [17] the whole operation time of the device can be approximately considered as one hour in continuous mode. Moreover, due to the easy fabrication protocol of the device, multiple copies can be prepared in a single batch and replacement of an exhausted chip by a new fully operative device will increase the operation time.

However, when longer life-times are required, a careful redesign of the micro-fluidic can be performed to extend the device operation time. For example, by changing the amount of the absorbent material placed at the end of the channel, the

second operative regime can be easily extended.

These results suggested that the passive pump system is able to provide fresh sweat into the channel toward the sensing area without using any mechanical components, which makes this device an effective low-cost pumping system for wearable applications.

3.3.4 Sensor Response

The dynamic response of the sensing area of the micro-fluidic chip was investigated using solutions of different pH's. A 40 μL drop of HCl ($[H^+]$ = 0.1 M) and NaOH ($[OH^-]$ = 0.01 M) were alternatively placed in the inlet and they were allowed to flow till the sensing area was reached, then the colour variation generated by the pH was recorded using the SMD LED-light photo sensor system.

Figure 3.7 shows the response when the system is alternatively exposed to pH 1 and 12 for four times. Briefly, the low voltage output of the light photo sensor corresponds to a less intense light due to a darker colour of the sensing material. Because BCP dye changes colour from yellow (acidic form) to blue (basic form), the lower value of ~ 0.8 V has to be interpreted as the high pH, *i.e.* 12. Conversely, the higher value of ~ 2.35 V corresponds to acidic pH.

The results show that the sensing platform generates reproducible signals for both acidic and basic pH conditions. Two main parameters can be obtained from Figure 3.7, the "delay time" and the "response time" summarised in Table 1.

The "delay time" (t_d) corresponds to the time that sweat takes to reach the sensor area (textile), flat regions in Figure 3.7. The "response time" (t_r) corresponds to the time that sweat of certain pH fills the full sensing area and generates a stable signal in the detector, half parabolic regions in Figure 3.7.

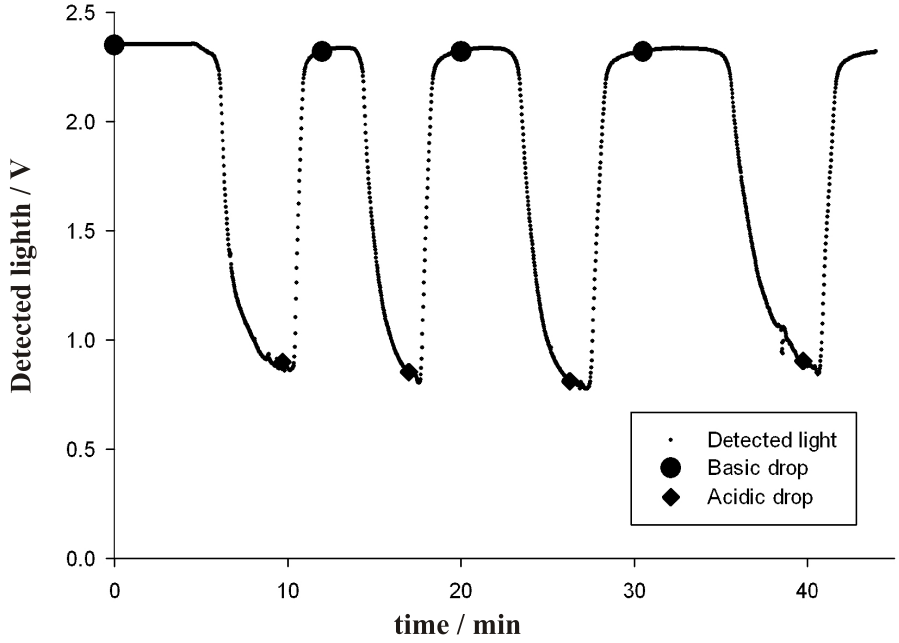

Figure 3.7. Dynamic response of the micro-fluidic chip when alternatively is exposed to pH 1 and pH 12 solutions.

Table 3.1. Basic/acidic delay and response times of the micro-fluidic chip

	Basic t_d / min	**Acidic t_d / min**	**Basic t_r / min**	**Acidic t_r / min**
Cycle 1	4.74	0.60	4.96	1.7
Cycle 2	1.77	0.69	3.21	2.28
Cycle 3	2.37	1.13	3.97	3.06
Cycle 4	3.70	1.29	5.30	3.17

As it is possible to observe in Table 3.1, both basic t_d and t_r in cycle 1, showed substantial higher values than in the rest of the cycles. These results are in accordance with the pumping rate data presented in Figure 3.6. In fact, when the system is on its first flow regime, the micro-fluidic chip is dry, the flow rate is slow because the passive pump system is not still active and the thread needs to hydrate. In the subsequent cycles acidic and basic t_d are found to be lower than the first basic t_d (cycle 1) but the values are progressively increasing with the number of cycles. This expected behaviour is following the trend of Figure 3.6 where the pumping flow, once it has reached its maximum rate, starts to decrease gradually till regime three where the absorbent is completely full with sweat and the passive flow stops.

It is interesting to point out that since concentrations of acid and base are not equal ($HCl_{sol,}$ 0.1 M and $NaOH_{sol}$ 0.01 M) the sensor was able to provide the two

different t_d coming from the response to the acid and the basic solution. The acidic solution has a proton concentration ten times bigger than the hydroxide concentration of the basic solution, so neutralisation of the excess of acid in the textile needs to be performed before the sensor area starts to change colour and so to be observed by the SMD LED-light photo sensor. In addition, experiments carried out with the same acidic and basic concentrations solutions showed that the t_d is equal for a defined passive flow rate. With regard to t_r, a similar trend to t_d was observed. In fact, during the last basic cycle t_r, the micro-fluidic chip is approaching the last regime where the passive pump flow is reduced significantly.

In short, these results confirm the reproducibility of the colorimetric detection over several cycles and the capability of the thread to draw the fluid toward the sensing area, generating a stable signal.

3.3.5 Sensor Calibration

Figure 3.8 shows the calibration curve of the fabric textile containing the pH sensitive dye embedded as explained in section 3.1. The sensor material was tested using artificial sweat as standard solutions, where its pH was systematically varied from 1 to 14 adding an exact amount of 1 M NaOH solution. The textile exhibits a colour change from yellow to blue in this pH region and the change in colour was detected by the SMD LED-light photo sensor detector. The absorbed light is plotted as the inverse of the detected voltage. The experimental data are fitted by a sigmoidal curve following the equation 3.1.

$$I = [a / (1+e^{\,b\,(pH-z)})] + c \qquad \text{eq. 3.1}$$

where I is the detected light intensity, a is the peak height, b is the slope coefficient, z is the point of inflection and c accounts for a baseline offset. The sensor presents a pK_a of 6.8 which is slightly higher than the one from literature for the same dye in solution, pK_a 6.2.[23] However, this effect has been previously observed by others who concluded that immobilised dye in a solid support varies the pK_a value due to a change of the microenvironment where the dye is immobilised.[24]

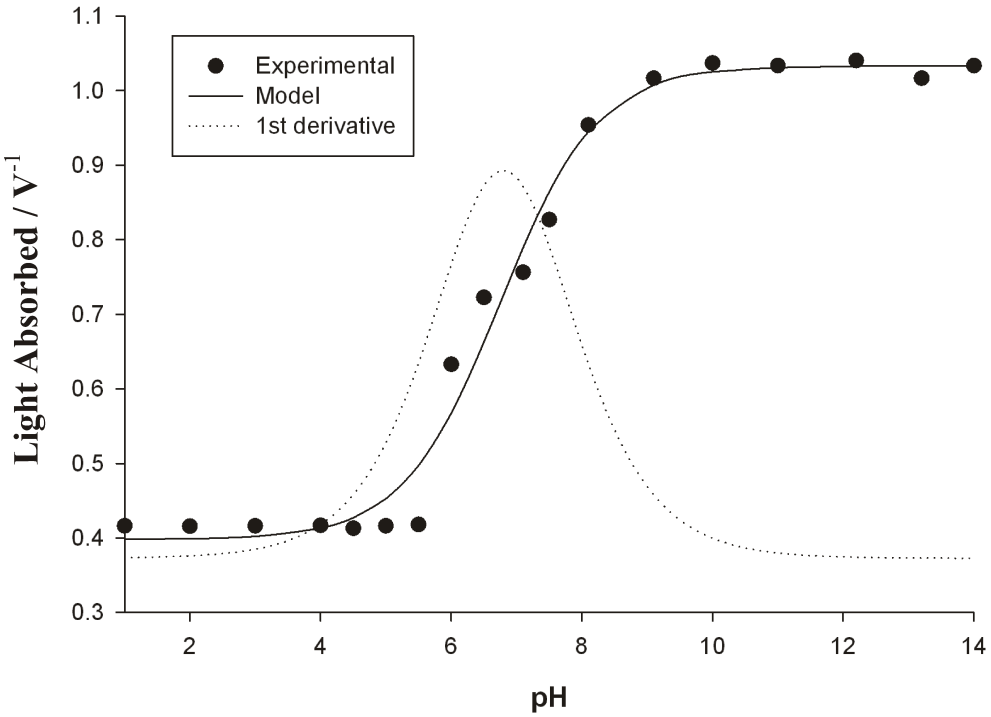

Figure 3.8. Calibration curve of the fabric textile immobilised BCP dye.

3.3.6 On-body Trial

During on-body-trials the athlete was equipped with a Velcro belt located around the pelvis and the micro-fluidic device was fixed to the lumbar region of his back, as shown in the picture of Figure 3.9. The trial was carried out using the wireless detector (located in a pocket) and the micro-fluidic chip containing the thread. The pH of sweat was monitored in real-time for 55 min during a cycling trial. To verify the reliability of the measurements of the micro-fluidic device, a conventional glass pH electrode was used to carry out reference measurements.

In the trial the athlete worked at three different loading intensities: light, moderate and high. During the warm-up period (between 0 – 10 minutes) the athlete cycled in a moderate intensity mode for the first 5 min, changing to a high intensity regime with the aim of generating sweat as fast as possible. In this time interval, it is possible to appreciate a drastic increase of the pH, from 2.5 to 6.2 as shown in Figure 3.9. Considering that the chip was placed on the body without any previous precondition, the first 5 min reading was generate by a dry chip, in its acidic state.

After the initial 5 warm-up minutes the athlete started to sweat, therefore sweat is drawn from the skin to the reservoir by the passive pump system working in its first regime (Figure 3.6).

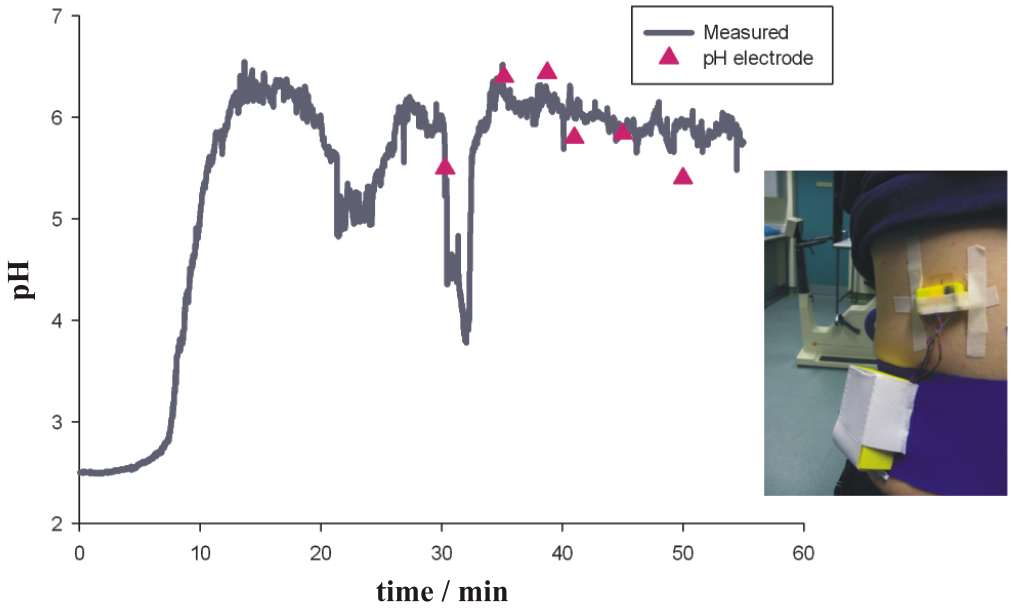

Figure 3.9. pH of sweat data recorded during 55 min of cycling exercise using the wireless detector and the micro-fluidic chip containing the thread.

From minutes 5 to 8 there is an increase in pH towards a stable value of 6.2. This reading is in accordance with the estimation made in section 3.3.3.1, where it was calculated that the average time for the fluid to reach the sensing area is around 3 minutes. Finally, the 6.2 pH value is reached when fresh sweat is covering the entire sensing area and a homogeneous colour was generated giving a stable signal.

In Figure 3.9 two big drops of the pH value can be seen. During these time intervals the athlete changed alternatively the work intensity from high to moderate and a substantial increase in the sweat rate occurred. The reason why these two big drops in pH value were generated can be attributed to several sources, including physiological reasons, the increase of sweat flow rate, or a malfunction by the detector. At present, the reason of this large drop in pH cannot be definitely ascribed to any particular source, and further investigations will be carried out in our laboratories to clarify this behaviour.

Lastly, comparing the real-time measurements and the ones made thorough a skin pH electrode a good correlation is observed, suggesting that the micro-fluidic

sensor was capable of measuring real events of pH changes in sweat. However, the last pH meter reading value differs ~0.5 pH units with the pH electrode value. This can be attributed to a decreasing of the fluid flow rate in the micro-fluidic chip when the absorbent material started to be saturated and the system was working on the last regime.

3.4 Conclusions

In this chapter, significant improvements in the realisation of a fully autonomous wearable sensor capable of performing real-time chemical analysis of sweat composition, in particular pH, during exercise events has been presented. The micro-fluidic system was developed using low-cost and flexible materials, and the passive pump system was developed through an absorbent material and a cotton thread inside the channel, improving robustness and dynamic response. Improvements in the detection system were gained through miniaturisation of its components as such detection system, wireless platform, battery and package. All these improvements have been made in order to have a platform that was physically compatible with the needs of wearable applications, while still providing a chemical analysis capability through the monitoring of reactive indicator colour (pH in this case) using a SMD LED- light photo sensor detector.

Future work will be focused on the extension of the life-time of the micro-fluidic chip and on the use of the portable device and its possible integration into a T-shirt, avoiding the use of external belt used for the placement of the whole system.

Acknowledgements

This work was supported by Science Foundation Ireland under grant 07/CE/I1147 and a Research Career Start Programme 2010 fellowship from Dublin City University. Thanks to TEXSUS Spa (Italy) for supplying the CCAEP571LL absorbent material, Eng. Philip Angove and Mr. Javier Torres from Tyndall institute involved in the National Access Programme (NAP-251). Finally, Dr. Damien Maher who realised the 3D printing projects and work.

Appendix A. Supporting information

Figure A1 of appendix A shows the three layers of the micro-fluidic device.

3.5 References

1. Whitehouse, A. G. R., The Dissolved Constituents of Human Sweat. *Proceedings of the Royal Society of London. Series B, Biological Sciences* **1935,** *117*, 139-154.
2. Wilke, K.; Martin, A.; Terstegen, L.; Biel, S. S., A short history of sweat gland biology. *International Journal of Cosmetic Science* **2007,** *29*, 169-179.
3. Shirreffs, M. S.; Maughan, J. R., *Whole body sweat collection in humans : an improved method with preliminary data on electrolyte content*. American Physiological Society: Bethesda, MD, ETATS-UNIS, 1997; Vol. 82.
4. Hayden, G.; Milne, H.; Patterson, M.; Nimmo, M., The reproducibility of closed-pouch sweat collection and thermoregulatory responses to exercise–heat stress. *European Journal of Applied Physiology* **2004,** *91*, 748-751.
5. Brisson, G.; Boisvert, P.; Péronnet, F.; Perrault, H.; Boisvert, D.; Lafond, J., A simple and disposable sweat collector. *European Journal of Applied Physiology and Occupational Physiology* **1991,** *63*, 269-272.
6. Webster, L.; Lochlin, H., *Cystic fibrosis screening by sweat analysis: a critical review of techniques*. 1977; Vol. 1, p 923-927.
7. Kidwell, D. A.; Holland, J. C.; Athanaselis, S., Testing for drugs of abuse in saliva and sweat. *Journal of Chromatography B: Biomedical Sciences and Applications* **1998,** *713*, 111-135.
8. Maughan, R. J.; Shirreffs, S. M., Development of individual hydration strategies for athletes. *International journal of sport nutrition and exercise metabolism* **2008,** *18*, 457-472.
9. Souza, A. P. R. d.; Lima, A. S.; Salles, M. O.; Nascimento, A. N.; Bertotti, M., The use of a gold disc microelectrode for the determination of copper in human sweat. *Talanta* **2010,** *83*, 167-170.
10. Hirokawa, T.; Okamoto, H.; Gosyo, Y.; Tsuda, T.; Timerbaev, A. R., Simultaneous monitoring of inorganic cations, amines and amino acids in human sweat by capillary electrophoresis. *Analytica Chimica Acta* **2007,** *581*, 83-88.
11. Mebazaa, R.; Rega, B.; Camel, V. r., Analysis of human male armpit sweat after fenugreek ingestion: Characterisation of odour active compounds by gas chromatography coupled to mass spectrometry and olfactometry. *Food Chemistry* **2011,** *128*, 227-235.
12. Schazmann, B.; Morris, D.; Slater, C.; Beirne, S.; Fay, C.; Reuveny, R.; Moyna, N.; Diamond, D., A wearable electrochemical sensor for the real-time measurement of sweat sodium concentration. *Analytical Methods* **2010,** *2*, 342-348.
13. Patterson*, M. J.; Galloway, S. D. R.; Nimmo, M. A., Variations in regional sweat composition in normal human males. *Experimental Physiology* **2000,** *85*, 869-875.
14. Patterson, M. J.; Galloway, S. D. R.; Nimmo, M. A., Effect of induced metabolic alkalosis on sweat composition in men. *Acta Physiologica Scandinavica* **2002,** *174*, 41-46.
15. Schmid-Wendtner, M. H.; Korting, H. C., The pH of the Skin Surface and Its Impact on the Barrier Function. *Skin Pharmacology and Physiology* **2006,** *19*, 296-302.

16. Coyle, S.; King-Tong, L.; Moyna, N.; O'Gorman, D.; Diamond, D.; Di Francesco, F.; Costanzo, D.; Salvo, P.; Trivella, M. G.; De Rossi, D. E.; Taccini, N.; Paradiso, R.; Porchet, J. A.; Ridolfi, A.; Luprano, J.; Chuzel, C.; Lanier, T.; Revol-Cavalier, F.; Schoumacker, S.; Mourier, V.; Chartier, I.; Convert, R.; De-Moncuit, H.; Bini, C., BIOTEX - Biosensing Textiles for Personalised Healthcare Management. *Information Technology in Biomedicine, IEEE Transactions on* **2010,** *14*, 364-370.
17. Morris, D.; Coyle, S.; Wu, Y.; Lau, K. T.; Wallace, G.; Diamond, D., Bio-sensing textile based patch with integrated optical detection system for sweat monitoring. *Sensors and Actuators B: Chemical* **2009,** *139*, 231-236.
18. Benito-Lopez, F.; Coyle, S.; Byrne, R.; Smeaton, A.; O'Connor, N. E.; Diamond, D., Pump Less Wearable Microfluidic Device for Real Time pH Sweat Monitoring. *Procedia Chemistry* **2009,** *1*, 1103-1106.
19. Fraden, J., *Handbook of Modern Sensors: Physics, Designs, and Applications*. Springer: **2010**.
20. O'Flynn; Brendan; Bellis; S.; Mahmood; K.; Morris; M.; Duffy; G.; Delaney; K.; O'Mathuna; C., *A 3D miniaturised programmable transceiver*. MCB University Press: Bradford, ROYAUME-UNI, **2005**,22 , 5.
21. Barton, J.; Hynes, G.; O'Flynn, B.; Aherne, K.; Norman, A.; Morrissey, A., 25 mm sensor-actuator layer: a miniature, highly adaptable interface layer. *Sensors and Actuators A: Physical* **2006,** *132*, 362-369.
22. Li, X.; Tian, J.; Shen, W., Thread as a Versatile Material for Low-Cost Microfluidic Diagnostics. *Acs Applied Materials & Interfaces* **2009,** *2*, 1-6.
23. Sabnis, R. W., *Handbook of Acid-Base Indicators*. Taylor & Francis: **2007**.
24. Soller, B. R., Design of intravascular fiber optic blood gas sensors. *Engineering in Medicine and Biology Magazine, IEEE* **1994,** *13*, 327-335.

Chapter 4

Real-Time Sweat pH Monitoring Based on a Wearable Chemical Barcode Micro-fluidic Platform Incorporating Ionic Liquids

Vincenzo F. Curto[1], C. Fay[1], S. Coyle[1], R. Byrne[1], C. O'Toole[1], C. Barry[1], S. Hughes[2], N. Moyna[2], D. Diamond[1], F. Benito-Lopez[1*]

Sensors and Actuators B: Chemical 171-172 (2012) 1327–1334

ISSN: 0925-4005; http://dx.doi.org/10.1016/j.snb.2012.06.048

[1]CLARITY: Centre for Sensor Web Technologies, National Centre for Sensor Research, School of Chemical Sciences, Dublin City University, Dublin 9, Ireland

[2]School of Health and Human Performance, Dublin City University, Dublin, Ireland

* Author to whom correspondence should be addressed;

Abstract

This chapter presents the fabrication, characterisation and the performance of a wearable, robust, flexible and disposable chemical barcode device based on a micro-fluidic platform that incorporates ionic liquid polymer gels (ionogels). The device has been applied to the monitoring of the pH of sweat in real time during an exercise period. The device is an ideal wearable sensor for measuring the pH of sweat since it does not content any electronic part for fluidic handle or pH detection and because it can be directly incorporated into clothing, head- or wristbands, which are in continuous contact with the skin. In addition, due to the micro-fluidic structure, fresh sweat is continuously passing through the sensing area providing the capability to perform continuous real time analysis. The approach presented here ensures immediate feedback regarding sweat composition. Sweat analysis is attractive for monitoring purposes as it can provide physiological information directly relevant to the health and performance of the wearer without the need for an invasive sampling approach.

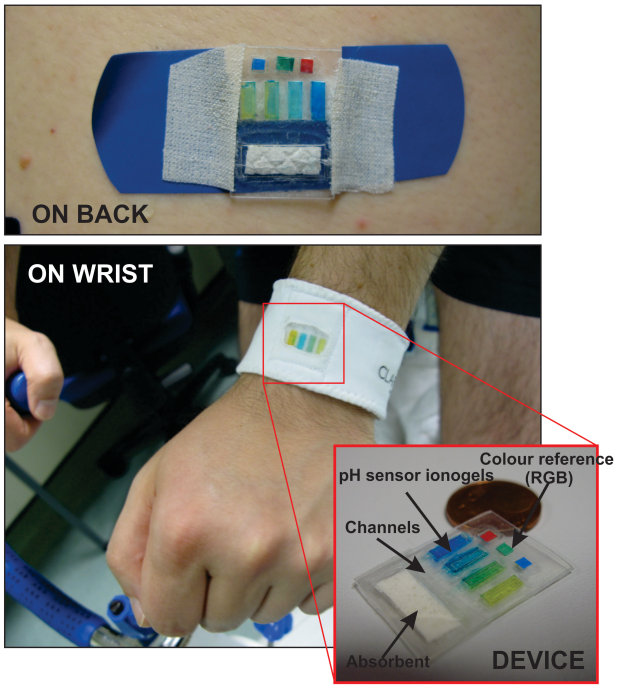

Keywords: Sweat analysis; Ionic liquid; Ionogel; pH; Wearable micro-fluidic

4.1 Introduction

Wearable sensors such as heart rate monitors and pedometers are in common use by people involved in sports and exercise activities. This area is growing exponentially, and while it is mainly driven by interest from health/sports enthusiasts, it will increasingly expand into health monitoring, as the economics of healthcare will force trends towards remote (home based) monitoring of patient status, rather than the current hospital focused model. In particular, the true potential of wearable chemical sensors for the real-time ambulatory monitoring of bodily fluids such as tears, sweat, urine and blood has not been realised due to difficulties associated with sample generation, collection and delivery, sensor calibration and reliability, wearability and safety issues.[1]

Sweat is naturally generated during exercise; thus, the possibility of monitoring its contents provides very rich information about the physiological condition of the individual.[2] Sweat analysis is known to be used to identify pathological disorders such as cystic fibrosis.[3] Moreover, real-time sweat analysis, particularly during exercise,[4] potentially opens a route to gathering valuable information on dehydration and the detection of conditions related to changes in the concentrations of important biomolecules and ions, such as hyponatremia (low sodium concentration). This information can be used to optimise approaches to rehydration and re-mineralisation[5] which can enhance athletic performance and general health.
There are several factors that correlate the pH of sweat and health. Changes in the pH of the skin are reported to play a role in the pathogenesis of skin diseases like irritant contact dermatitis and acne, among others.[6] Patterson *et al.*[7] showed that inducing metabolic alkalosis through the ingestion of sodium bicarbonate led to increased blood and sweat pH. Furthermore, it has been reported that sweat pH will rise in response to an increased sweat rate.[8] A relationship was also observed between pH and sodium (Na^+) levels in isolated sweat glands in that the greater the concentration of Na^+, the higher the sweat pH will be.[9] As exercising in a dehydrated condition has been shown to lead to increased levels of Na^+, it can be seen that such changes can be measured directly (using a Na^+ selective sensor) or indirectly by monitoring the pH of sweat.[10]

Micro-Total-Analysis (μTAS) or Lab-on-a-Chip (LOC) is an important concept for the development of personalised healthcare and point of care diagnostic devices, and it has the potential to improve the performance and capabilities of many commercial products that are already available in the market.[11] Important technological barriers such as miniaturisation, low cost production, reusability or disposability, robustness, flexibility and adaptability are continuously being overcome using this approach. However, sweat, which is easily accessible using non-invasive means, remains largely unexplored as a sample medium for tracking personal health status using the LOC approach.[12]

The use of optical pH sensors offer several advantages such as freedom from electrical noise, possibility of miniaturisation, ability to monitor status without physical contact, and flexibility in interrogation approaches (human eye, LED-sensors, cameras, spectrometers).[13] Also, optical pH sensors are suitable for applications where conventional electrodes cannot be used because of their size or because of the risk of electric shock, such as during in vivo measurements. To provide optical pH sensors with good sensitivity, selectivity and stability, various support materials, methods and reagents, and immobilisation techniques for pH indicator dyes have been employed.[14, 15] In particular, ionic liquids (ILs) have been rarely employed in optical sensors despite their excellent chemical and thermal stabilities, low vapour pressure, high ionic conductivity properties, and tuneable hydrophobic and hydrophilic nature.[16-22] The incorporation of ILs into polymer gels to form so-called 'ionogels' is a particularly attractive strategy as it may generate materials that maintain the inherent advantages of ILs within a solid or semi-solid gel-type structure.[23-26]

This chapter presents a simple, autonomous, wearable, robust, flexible and disposable micro-fluidic platform based on ionogels that can be used for monitoring the pH of sweat generated during an exercise period in real-time. Accurate pH values can be obtained by simply observing the barcode colour variation in comparison to a standard colour chart or through more sophisticated methods such as photo or video analysis of the colour changes. A significant advantage of these approaches is that the on-body sensor consumes no power, does not require any electronics for signal acquisition or communication, and therefore does not need a battery. On the other hand, remote interrogation by eye or by camera requires direct line of sight of the

sensor status by the observer or camera. However, the colorimetric response can also be monitored on-line using simple opto-electronic components integrated into the device, along with wearable communications electronics (mote, dedicated platforms, mobile phones, *etc*.), providing continuous feed-back of the sweat composition to remote locations via a local base-station, as shown in the previous chapter.[12,26,27]

4.2 Experimental

4.2.1 Materials

N-isopropylacrylamide (NIPAAm, Wako) was purified by recrystallisation in a mixed solution of hexane and toluene and dried under a vacuum. *N,N*-methylene-bis(acrylamide) (MBAAm, Sigma-Aldrich), 2,2-dimethoxy-2-phenyl acetophenone (DMPA, Sigma-Aldrich, St. Louis, USA), methyl red (MR), bromophenol blue (BPB), bromocresol green (BCG), bromocresol purple (BCP) and bromothymol blue (BTB) (Sigma-Aldrich, St. Louis, USA), were used without further purification. Trihexyltetradecyl-phosphonium dicyanoamide $[P_{6,6,6,14}][dca]$ were obtained with compliments of Cytec Industries. The IL was purified thoroughly by column chromatography,[28] dried under vacuum at 40 °C for 48 h, and stored under argon at 20 °C. Artificial sweat was prepared according to the standard ISO 3160-2 (20 g L^{-1} NaCl, 17.5 g L^{-1} NH_4OH, 5 g L^{-1} acetic acid and 15 g L^{-1} lactic acid) (Sigma-Aldrich, St. Louis, USA). Super-absorbent non-woven textiles (Absortex) were purchased from Texsus SpA, Italy. Hansaplast commercially available plasters were used to encapsulate the micro-fluidic platforms.

Devices were fabricated using multilayer lamination. A CO_2 laser (Laser Micro-machining Light Deck, Optec, Belgium) system was used to cut the various polymer layers. Connecting holes and micro-fluidic channels were cut from an 80 μm thick layer of pressure-sensitive adhesive (PSA - AR9808, Adhesives Research, Ireland) and laminated onto a 125 μm poly(methylmethacrylate), PMMA, support layer (GoodFellow, UK) using a thermal roller laminator (Titan-110, GBC Films, USA).

Photographs were taken using a Canon PowerShot G7 camera. The skin pH sensor was purchased from Hanna Instruments, India. The UV light source used for

photo-polymerisation was a BONDwand UV-365 nm obtained from Electrolyte Corporation, USA. UV light intensity was measured with a Lutron (Taiwan) UV-340A UV light meter. The pictures were processed and analysed using the Open Computer Vision (OpenCV) image processing libraries.

4.2.2 Micro-fluidic Platform Fabrication

The micro-fluidic platform (23 x 17 mm), Figure 4.1-a, consists of four independent reservoirs and channels, fabricated in six layers of poly(methyl methacrylate) and PSA using CO_2 ablation laser and lamination. Figure 4.1-b shows the fabrication protocol that starts with a 125 µm thick PMMA base layer followed by two layers of PSA (160 µm), containing the micro-channels (5 x 1 mm and 160 µm in depth), four rectangular ionogel reservoirs and an absorbent reservoir. Then an additional layer of PMMA (125 µm), which contains only the four rectangular reservoirs (2 x 6 mm) and the absorbent reservoir, was laminated over the PSA layers. The incorporation of the four ionogels inside of the microfluidic was performed as describe in section 4.2.3. To seal the system, a lid consisting of two more layers, PSA and PMMA (205 µm), was laminated over the previous four layers. The lid contains four rectangular holes (1 x 5 mm) fabricated using the CO_2 laser. The holes were carefully arranged to site directly over the polymerised ionogels. The micro-channels connect the four rectangular independent ionogel/dyes reservoirs with a common reservoir (15 x 5 mm and 285 µm depth), where an absorbent fiber drives the sweat from the sensing area through the channels by capillary action. This ensured that fresh sweat from the skin is continuously drawn into contact with the ionogel/dyes sensors. More details on the barcode dimensions are provided in Figure B1 of Appendix B.

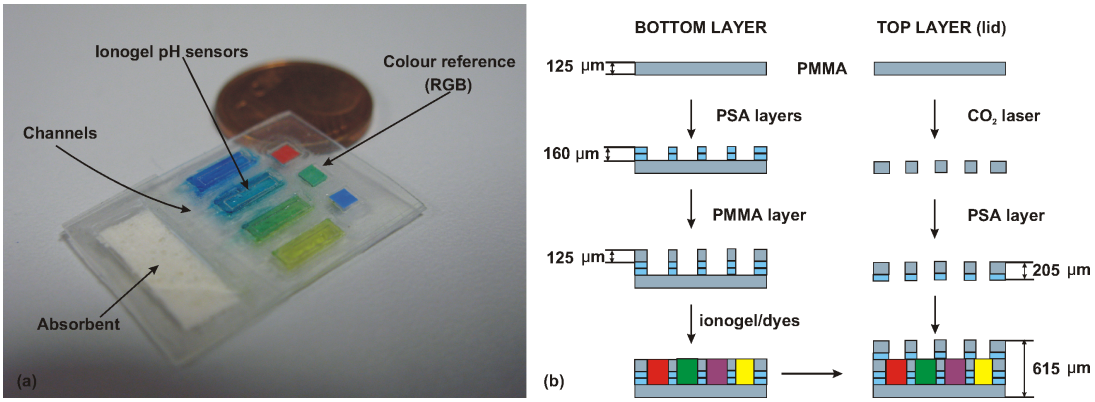

Figure 4.1. (a) Picture of the micro-fluidic device. (b) Micro-fluidic platform fabrication steps

4.2.3 Preparation of the Phosphonium Based Ionogel with Integrated pH Sensitive Dyes

The ionogel consisted of two monomeric units: *N*-isopropylacrylamide and *N,N'*-methylene-bis(acrylamide) in the ratio 100:5, respectively. The reaction mixture was prepared by dissolving the NIPAAm monomer (4.0 mmol), the MBAAm (0.2 mmol) and the photo-initiator 2,2-dimethoxy-2-phenylacetophenone DMPA (0.11 mmol) (Figure 4.2a) into 1.5 mL of $[P_{6,6,6,14}][dca]$ ionic liquid, shown in Figure 4.2-b. 7 μL of the reaction mixture was placed in each of the reservoirs after mixing at 45 °C for 10 minutes. The monomers were then photo-polymerised within the ionic liquid matrix using a UV irradiation source (365 nm) placed 5 cm from the monomers for 30 minutes (UV intensity ~ 630 μW cm^{-2}). 365 nm UV irradiation source is necessary to have the correct radical polymerisation process and obtain the desired ionogel structure and physical consistence. When the polymerisation was complete, the ionogels were washed with de-ionised water and subsequently with ethanol for 1 min each, and the procedure was repeated three times to remove any unpolymerised monomer and any excess of ionic liquid. Finally the ionogels were left to fully dry for five hours at room temperature. 5 μL ethanol solution of each of the dyes (10^{-3} M) was pipetted over the ionogel and left until dry. This process was repeated three times. Then, the barcode system was washed in ethanol and in water several times until no leaching of the dyes was observed. The lid was placed on top of the barcode and laminated to form the final structure. Finally the device was dried at room temperature for five hours. The stability of the micro-fluidic barcode against pH was carried out following the same protocol than that in Benito-Lopez *et al.*.[26]

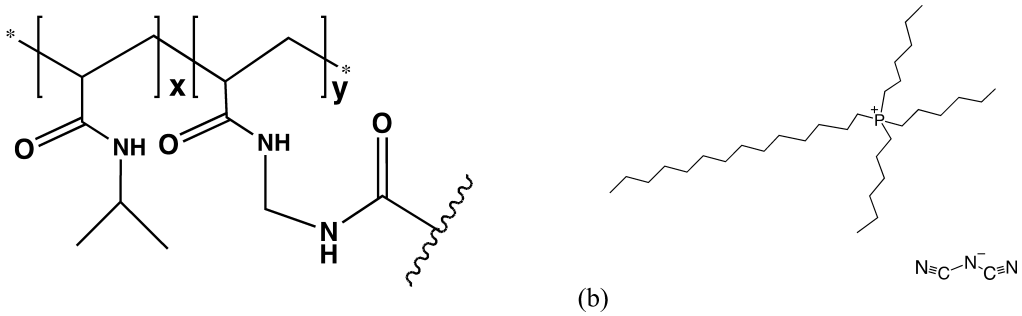

(a) (b)

Figure 4.2. The molecular structure of the two components that make up the ionogel material. (a) *N*-isopropylacrylamide and *N,N*-methylene-bis(acrylamide) crosslinked polymer in the ratio 100(x):5(y), and (b) the ionic liquid $[P_{6,6,6,14}][dca]$ structure.

4.2.4 pH Sensor and Optical Detection

A colorimetric approach was employed to quantitatively determine the concentration of pH of sweat by means of a digital colour camera (Canon PowerShot G7). The approach involved the use of four pH sensitive dyes (methyl red, bromocresol green, bromocresol purple and bromothymol blue), which change in colour over a pH range defined by their respective pKa's. Figure 4.3 visually shows colour changes in the dyes in a pH range from 4.5 to 8, which covers the typical pH range of a human's sweat during exercise, *i.e*. from 5-7. Although this range was sufficiently covered, it was important to ascertain how the dyes respond over the full pH scale for later analysis. Therefore a calibration routine was carried out, where the platform was exposed to artificial sweat at different pH, from *ca*. 1 to *ca.* 14, within 0.5 pH unit steps. A photograph of each event was captured with the parameters of the camera set to manual, 1/16 and at optimum resolution. For each capture, the camera was fixed at a distance of 5 cm from the barcode's planar surface along with ensuring that the barcode platform was captured in its entirety within the camera's field of view. In addition, a light source (60 W, Philips, 30°*8L, Sportline R63, 240V, Holland) was placed at a 45 ° angle for illumination and minimisation of background visual effects. Later, each captured image was processed by employing a standard set of algorithms using OpenCV. Firstly, each image region of interest (4 dyes and 3 reference patches) was identified through the creation of a binary mask image. This involved creating a copy of the original image, applying noise reduction filtering techniques (Gaussian blurring, median and erosion/dilation morphological algorithms) to aid in the segmentation step and then applying a connected component algorithm to the image. This resulted in a binary image with neighbouring pixels of similar colour being grouped together and identified as separate image regions. Next, the regions representing the 4 dyes and 3 reference patches were identified based on their location within the original image and stored in memory while the rest (misclassified regions) were omitted. After this, the resulting binary image was applied to the original image, removing the background (unwanted pixels) and leaving only pixel regions representing the ionogel/dye regions and reference patches. Subsequently, each region was considered in turn where the dominant colour component was calculated (*i.e.* the mean value) on each of the region's colour

channel components (RGB). Next, the colour components of the dyes regions were normalised with respect to the reference patches to account for potential ambient lighting effects. A calibration plot for each dye was ascertained and the camera response (R') was calculated by: R' = R/(R+G+B) using the normalised response of the RGB channels. Finally, a sigmoidal regression analysis (Boltzmann) was applied to achieve a calibration model.

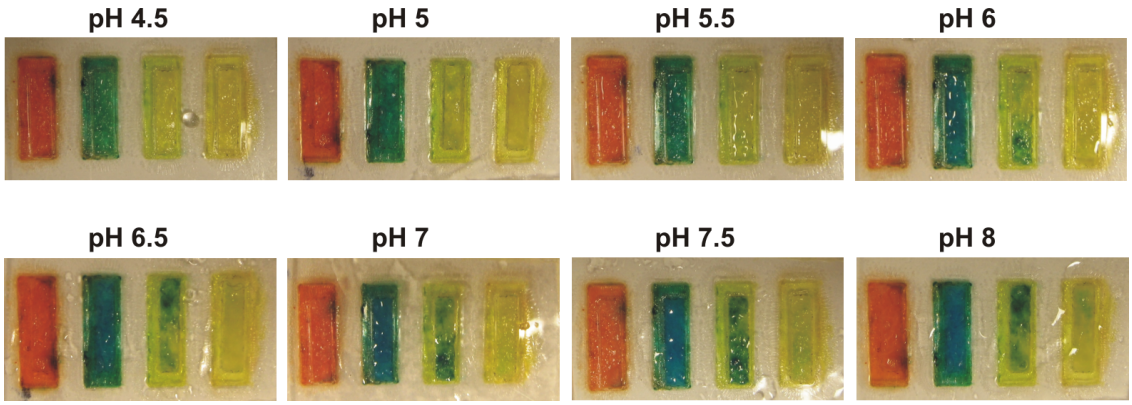

Figure 4.3. Photographs of the micro-fluidic system at different pH's tested with artificial sweat (ISO 3160-2).

4.2.5 On-Body Trials

The micro-fluidic system was incorporated into an adhesive plaster to avoid direct contact of the ionogels with the skin, see Figure 4.4-a. The plaster was placed in the lower back region of the body where the sweat rate is approximately 0.85 ± 0.41 mg min^{-1} cm^{-2}.[9] Reference measurements were taken manually at fixed time intervals (10 min) using a commercial pH probe. At the same time three pictures of the barcode were taken in order to measure the pH of the sweat and for comparison with the reference values as explained above. The exercise protocol involved indoor cycling (room temperature 18 ºC) using a bicycle ergometer. Elite athletes participated in the study, who cycled for one hour at a self-selected pace.

4.3 Results and Discussion

4.3.1 Why a Barcode pH sensor Micro-fluidic Platform?

Several methods for measuring the pH of sweat are already established, which are based mainly on glass electrodes and ion-sensitive field-effect transistors (ISFET's). The most popular are planar-tipped conventional pH-probes, which can be placed directly in contact with the skin in order to measure the pH. The drawback to this approach is that it is physically difficult to maintain contact between the probe and the skin over a prolonged period of time and it tends to suffer from drift and motion artefacts.

Moreover they are typically planar glass electrodes, which can cause skin damage when broken. The micro-fluidic platform is more fit-for-purpose as a wearable pH sensor since it can be directly incorporated into clothing or attached as an adhesive strip in continuous contact with the skin. Furthermore, due to the micro-fluidic structure, fresh sweat is continuously passing through the sensing area providing a real-time monitoring capability.

The ionogel matrix provides an ideal platform for the pH indicators dyes. This is because of, firstly, ion-pair interactions between the different pH indicators and the ionic liquid that forms the ionogel structure, and secondly, there is no leaching of the pH dyes during the experiments.[29] Furthermore, it was observed that the ionogel material is impressively robust under harsh conditions (pH ranges from 0 to 14).[26]

4.3.2 Micro-fluidic Platform Fabrication and Performance

The micro-fluidic system was fabricated using six thin PMMA and PSA layers (615 μm, total thickness). This ensures that the whole device is flexible and can easily adapt to the body contours. In addition, it is comfortable to wear providing an unobtrusive and non-invasive method for the analysis of sweat during exercise. The micro-fluidic system can be encapsulated into an adhesive plaster, Figure 4.4-a, integrated in the sport clothes or into a sweat band worn on the head or the wrist, in order to directly obtain pH information of sweat during an exercise period, Figure 4.4-b.

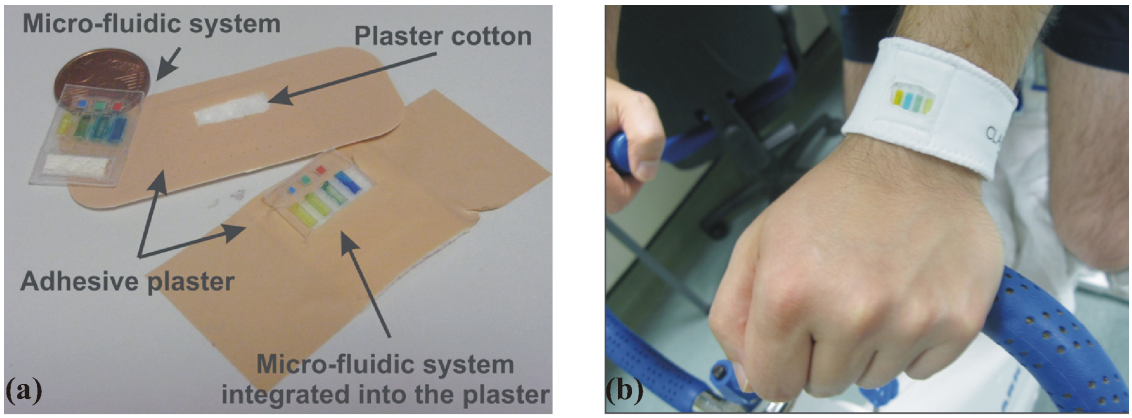

Figure 4.4. Picture of the micro-fluidic system integrated into a plaster *(left)* and into a wrist-band *(right)*.

The micro-fluidic structure ensures that fresh sweat is continuously sampled from the skin and flows past the ionogels during the entire training period. The performance of the micro-fluidic platform is presented schematically in Figure 4.5-a. Sweat is absorbed by the fabric of the clothes/adhesive plaster cotton and comes in contact with the barcode sensor. The dyes react with sweat and change colour according to their respective pKa values. Sweat is continuously drawn through the microfluidic device by the super-absorbant material, which acts as a passive pump.

To test the performance of the microfluidic platform, artificial sweat was used to calculate the flow rate in the channels generated by the device. Snap-shot pictures of the channels were taken over time (see Figure 4.5-b) and then analysed. The flow rate of the device was found to be initially ca. 6.4 ± 2 µL min^{-1} (n = 12) but once the micro-fluidic channel was filled up by the artificial sweat, the flow rate decreased gradually to 1.1 ± 0.8 µL min^{-1} (n = 12) in the steady state. At this point, the flow rate remains constant until the absorbent reaches its maximum loading capacity, 148 ± 2 µL (n = 20). This gives the device an operational lifetime of *ca.* 135 min, in the current manifestation. However, since the device is easy to fabricate, and multiple replicates can be prepared in a single batch, the design can be easily modified for applications involving longer exercise periods. For example, the amount of absorbent material can be increased, or the channel dimensions varied to reduce the device flow rate, both of which would extend the useful operational time.

In addition, due to the inherent micro-sampling capability of the platform, the area of the skin that is sampled is much smaller than commercially available sweat collection systems, *i.e.* patches. Considering the total exposed sensing areas, equal to

the four lid holes (4 x 0.05 cm^2), the flow rate per unit area of the whole device is determined by the average steady state flow rate per unit area of each channel, 22 µL min^{-1} cm^{-2}, times four. This gives a total device flow rate of 88 µL min^{-1} cm^{-2}. This value is much larger than typical skin sweat flow rates, *e.g.* lower back 0.85 ± 0.41 µL min^{-1} cm^{-2} (assuming sweat density equal to 1 g mL^{-1}). This ensures that all the generated fresh sweat is always sampled by the device during operation.

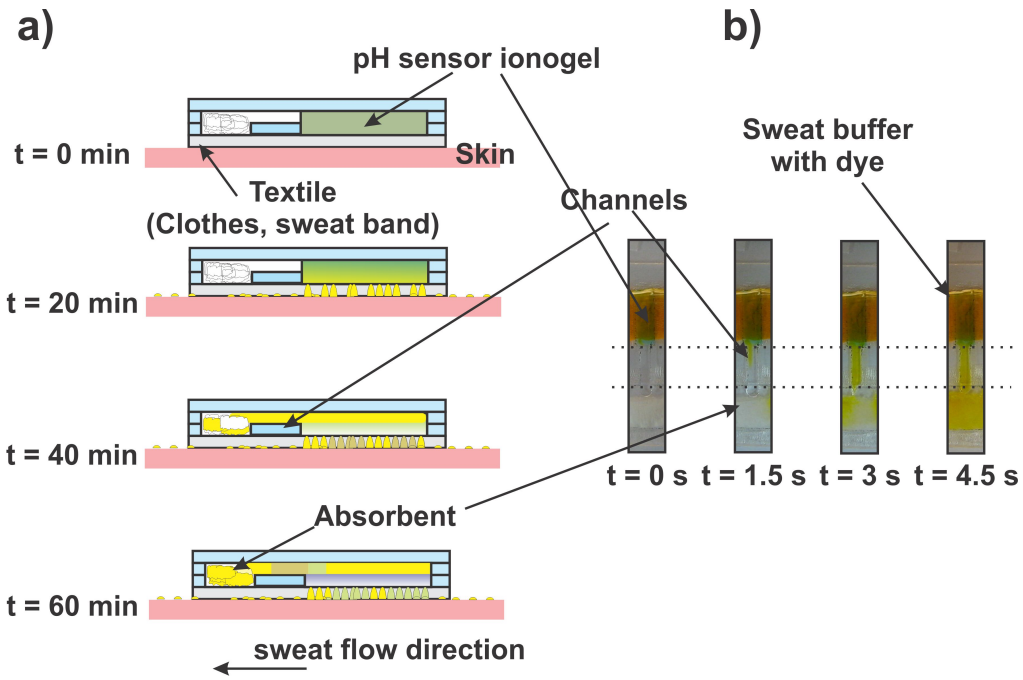

Figure 4.5. a) Schematic representation of the micro-fluidic system's performance over time. b) Series of pictures showing the channel performance in the micro-fluidic system (artificial sweat with dye), Pictures like these were used to estimate the sweat flow rate through the device.

The response of the four immobilised dyes in the ionogel matrixes was evaluated through a calibration routine using buffer solutions, as explained in detail in section 4.2.4 of this chapter. The results show that the dyes exhibited a colour change depending on the pH and are shown in Figure 4.6. The change in colour intensity of each of the pH indicators was plotted against the pH value. A sigmoidal regression analysis (Boltzmann technique) was then applied to the calibration points and resulted in a calibration model for each dye.

Figure 4.6 shows the calibration curves for the indicators BCG and BCP and as an example. The pKa of MR was not determined since its colour did not vary over the experimental pH range conditions. This could be due to the fact that the anion of

the ionic liquid $[dca]^-$, is known to show characteristics of a Lewis base,[30] and this could interfere with the acid/base chemistry of the methyl red dye. For the other ionogel/dyes the experimental values for the pKa values were estimated to be: bromocresol green BCG: 3.4; bromocresol purple BCP: 7.6 and bromothymol blue BTB: 8.8, which slightly varied with respect to the literature values (BCG: 4.6, BCP: 6.4 and BTB: 7.1).

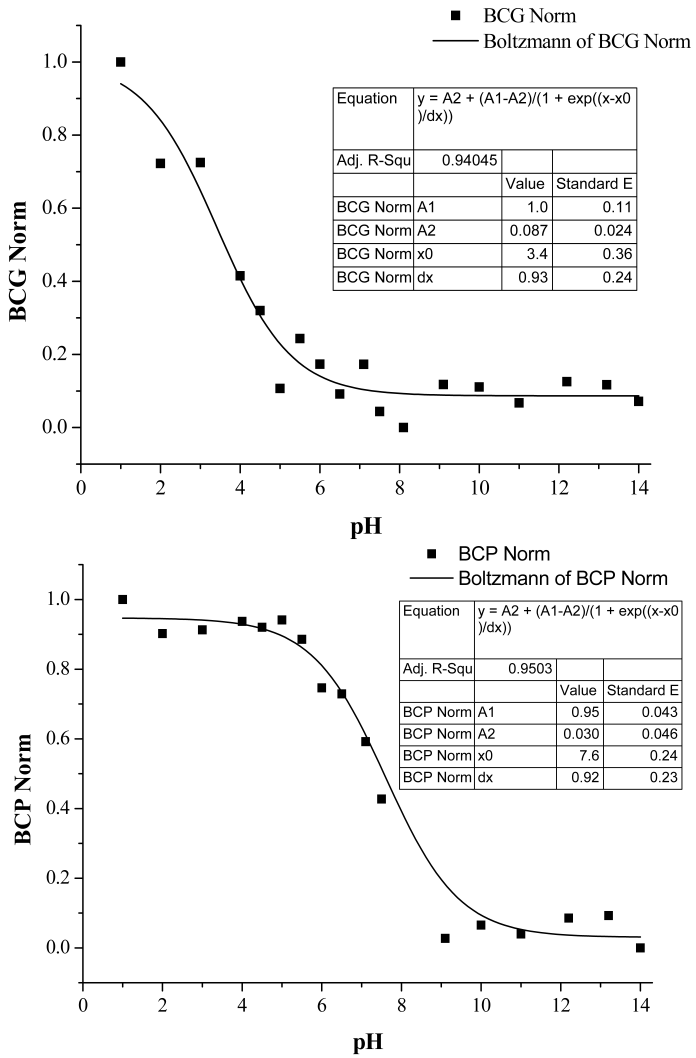

Figure 4.6. Calibration curves showing pH *vs.* R' = R/(R+G+B) normalised [0,1] bromocresol green (*top*) and bromocresol purple (*bottom*).

The variations are not surprising, as it has been shown that immobilisation of acidochromic dyes leads to variations in pKa due to a change of local micro-environment.[31]

Moreover, the stability of the barcode was demonstrated by performing three calibrations using three different barcode platforms. Calibration showed good

repeatability with relative standard deviation (R.S.D.) typically within 4 % (n = 3). This indicated that the pH indicator dyes are fully reversible to pH changes and that no significant dye leaching occurred during the experiments. Signal intensity is reproducible after three calibrations using the same barcode with relative standard deviation (R.S.D.) typically within 6 % (n = 3).[26]

4.4 On-body Trials

Sweat flow rate and fluid losses vary for individuals and are generally dependent on body size, gender, exercise intensity, environmental conditions and individual metabolism.[32] For on-body trials, the subject was equipped with a micro-fluidic platform on the low back region. The micro-fluidic platform was activated before with a hydrochloric acid solution at pH 2 for 5 min. After a period of 20 minutes, following the approach used by Morris *et al.*[33] where it was shown that it takes approximately 10 - 15 min to produce an appreciable amount of sweat during exercise, sweat reached the sensors and it was possible to begin monitoring the pH of the sweat. This delay arises firstly from the fact that sweat does not commence immediately upon exercise and that the device has a small but finite dead volume that must be filled before the sample reaches the sensors and a colour change is gained. Then a picture of the micro-fluidic platform was taken every 10 min along with parallel manual reference measurements using a pH electrode for specific use (Hanna Instruments HI-1413B/50). The results are presented in Figure 4.7-a. In the micro-fluidic platform, continuous fresh sweat is passed through the ionogel matrix, and the conditioning of the activation solution is quickly flushed away from the sensing area. After twenty minutes of a training period, no activation solution is observed in bromocresol green and bromocresol purple doped ionogels. For instance, the bromocresol green ionogel is yellow at times from 0 to 10 corresponding to a pH 2 (*i.e.* that of the conditioning solution), after a 20 minute training period, the ionogel is blue in colour (pH 6) and it varies from dark to light blue, *i.e.* pH 5.5-6.5, during the rest of the experiment. Therefore, the pH of the two ionogels compared reasonably well with the commercial pH probe reference measurements.

As previously described, the ionogel incorporating the methyl red indicator did not perceptibly change over the whole pH range of study even though it has a pK_a of 5, (red to yellow). Therefore the dye was replaced by bromophenol blue that has a

similar pK_a (~ 4) and it changes colour during the calibration process. Unfortunately, since the pH range of the dye is 3 - 4.6 (yellow to blue) a colour change gradient was not observed during trials. Moreover, no colour changes were also observed for the ionogel doped with bromothymol blue since the estimated pK_a of 8.82 is over the range of the pH measurements carried out during the on-body trial shown in Figure 4.7-a. Nevertheless, these two dyes (BPB, BTB) are potentially useful for picking up anomalous variations of the pH in the sweat during real-time analysis.

A more sophisticated approach to quantify the colour variations within the sweat's pH can be achieved using wearable device such as SMD-LED technology as previously reported.[26] However, a colorimetric electronic-free device can be easily read by the individual during the physical activity, considerably decreasing the complexity of the detection system (electronic part of the device) but improving the wearability and the read-out approach. Furthermore, the micro-fluidic platform has a major advantage in performance with respect to commercially available systems since they measure the pH of sweat from where it emerges and within an almost enclosed package therefore it minimises the interaction with carbon dioxide of the atmosphere, which can cause a lowering of the pH values.

In the presented system, a particular colour pattern of the barcode corresponds to a defined pH of the sweat where the captured images were analysed as explained earlier in Section 4.2.4 using OpenCV. Here, each pH prediction of each dye is calculated by normalisation with respect to the reference patches and then applied to the calibration model ascertained earlier. To achieve a single pH prediction from sensor barcode, each dye was considered equally with a weight of 1 and cumulative pH prediction was determined via their average value; this is shown in Figure 4.7-b and values are presented in Table 4.1. It can be seen that by combining the two dyes a low relative percentage error was achieved with the exception of the first measurement (7.68 %) in where the dyes pH's values might differ slightly from the ones of the pH meter due to residual conditioning of the activation solution in the ionogel. In addition, the Figure 4.7-b does show a similar trend by both measurement methods. It should be noted however that the accuracy of 0.49 of a pH unit ascertained in this study may need further investigation. For instance, a study may be needed to determine the correct weights when combining the dyes predictions to increase accuracy.

Table 4.1. Time series measurements of pH from the reference instrument (pH meter) and the predictions of the dyes when combined and weighted equally.[i]

Time / min	pH Meter	Dyes Prediction (pH)	% RE
20	6.38	5.89	7.68
30	5.8	5.56	4.14
40	5.67	5.67	0.00
50	5.95	5.6	5.38

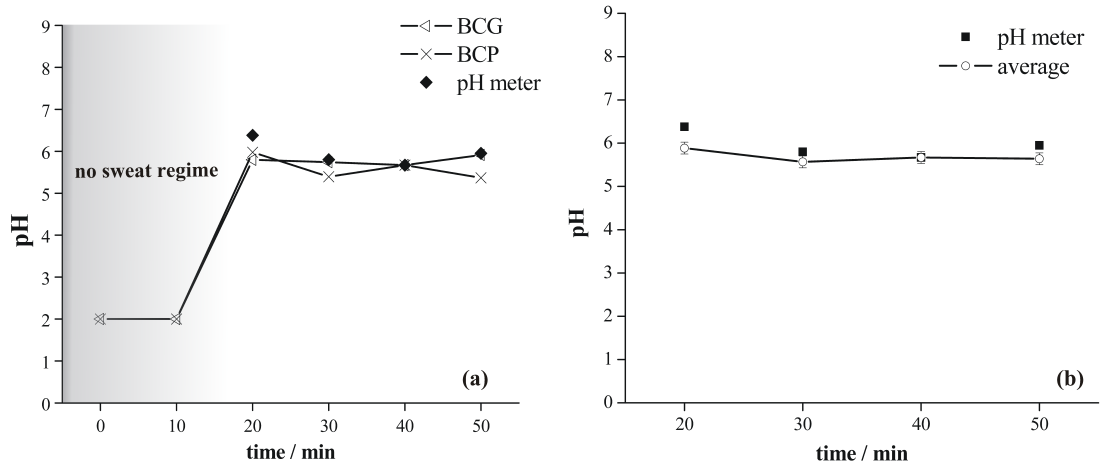

Figure 4.7. pH determination of sweat using the micro-fluidic system during a 50 min training period. (a) Plot showing the reference instrument in conjunction with the individual predictions of each dye when normalised with respect to the reference patches and predicted using the calibration model. (b) Plot of the reference measurement and the average of all the dye predictions when weighted equally.

However, to the best of our knowledge the micro-fluidic device described in this work is the only wearable electronic-free sensor capable to perform real-time measurements during active exercise period, with non-standardise light conditions. Similar work in the literature by Byrne *et al.*[34] have reported an accuracy of ± 0.5 pH units when using a digital colour camera but under controlled lighting conditions.

[i] The percentage relative error (%RE) is defined as $\frac{|A-B|}{A}\times 100$, where A and B are the values obtained using the pH-meter and the combined predictive values of the dyes, respectively.

4.5 Conclusions

In this chapter, the fabrication, characterisation and the performance of a wearable, electronic-free and flexible micro-fluidic system based on ionic liquid polymer gels (ionogels) for monitoring in real-time the pH of the sweat generated during an exercise period has been presented.

The ionogel matrix is very robust even at harsh pH conditions and the pH indicators bromophenol blue, bromocresol green, bromocresol purple and bromothymol blue retain their pH indicator properties when incorporated onto the ionogel. The ionogel-dye interactions ensure no leaching of the dyes occurs during experiments, providing long durability of the device and acceptable accuracy for the pH of sweat measurements over time. The approach presented here can provide immediate feedback regarding sweat composition, *i.e.* pH, to individuals during exercise period. A particular colour pattern of the barcode corresponds to a particular pH of the sweat with an accuracy of ~ 0.49 pH units after applying standard image processing and analysis techniques to the pictures, which were captured during exercise trials when the sensor was applied on the skin.

Future work will focus on the development of a more robust code for image processing, aiming a better resolution and accuracy in the pH prediction. Moreover, through a systematic comparison and correlation of pH of sweat with pH and lactate from blood, it will provide an easy, non-invasive and cheap tool to perform pH sweat analysis, improving sport performance and health.

Acknowledgment

This work was supported by Science Foundation Ireland under grant 07/CE/I1147 and the Research Career Start Programme 2010 fellowship from Dublin City University. Thanks to Cytec Industry for supplying the tetraalkylphosphonium Ionic Liquid.

Appendix B. Supporting information

Figure B1 of appendix B shows the four layers of the micro-fluidic device.

4.6 References

1. Diamond, D.; Coyle, S.; Scarmagnani, S.; Hayes, J., Wireless Sensor Networks and Chemo-/Biosensing. *Chemical Reviews* **2008,** *108*, 652-679.
2. Beauchamp, M.; Lands, L. C., Sweat-testing: A review of current technical requirements. *Pediatric Pulmonology* **2005,** *39*, 507-511.
3. Jonsdottir, B.; Bergsteinsson, H.; Baldursson, O., Cystic fibrosis - Review. *Laeknabladid* **2008,** *94*, 831-837.
4. Weber, J.; Kumar, A.; Bhansali, S., Novel lactate and pH biosensor for skin and sweat analysis based on single walled carbon nanotubes. *Sensors and Actuators B-Chemical* **2006,** *117*, 308-313.
5. Casa, D. J.; Armstrong, L. E.; Hillman, S. K.; Montain, S. J.; Reiff, R. V.; Rich, B. S. E.; Roberts, W. O.; Stone, J. A., National Athletic Trainers' Association Position Statement: Fluid Replacement for Athletes. *Journal of Athletic Training* **2000,** *35*, 212-224.
6. Schmid-Wendtner, M. H.; Korting, H. C., The pH of the Skin Surface and Its Impact on the Barrier Function. *Skin Pharmacology and Physiology* **2006,** *19*, 296-302.
7. Patterson, M. J.; Galloway, S. D. R.; Nimmo, M. A., Effect of induced metabolic alkalosis on sweat composition in men. *Acta Physiologica Scandinavica* **2002,** *174*, 41-46.
8. Granger, D.; Marsolais, M.; Burry, J.; Laprade, R., Na+/H+ exchangers in the human eccrine sweat duct. *American Journal of Physiology - Cell Physiology* **2003,** *285*, C1047-C1058.
9. Patterson, M. J.; Galloway, S. D. R.; Nimmo, M. A., Variations in regional sweat composition in normal human males. *Experimental Physiology* **2000,** *85*, 869-875.
10. Morgan, R. M.; Patterson, M. J.; Nimmo, M. A., Acute effects of dehydration on sweat composition in men during prolonged exercise in the heat. *Acta Physiologica Scandinavica* **2004,** *182*, 37-43.
11. Whitesides, G., Solving problems. *Lab on a Chip* **2010,** *10*, 2317-2318.
12. Benito-Lopez, F.; Coyle, S.; Byrne, R.; Smeaton, A.; O'Connor, N. E.; Diamond, D., Pump Less Wearable Microfluidic Device for Real Time pH Sweat Monitoring. *Procedia Chemistry* **2009,** *1*, 1103-1106.
13. Diamond, D., Internet-Scale Sensing. *Analytical Chemistry* **2004,** *76*, 278 A-286 A.
14. O'Toole, M.; Shepherd, R.; Wallace, G. G.; Diamond, D., Inkjet printed LED based pH chemical sensor for gas sensing. *Analytica Chimica Acta* **2009,** *652*, 308-314.
15. Smyth, C. n.; Lau, K. T.; Shepherd, R. L.; Diamond, D.; Wu, Y.; Spinks, G. M.; Wallace, G. G., Self-maintained colorimetric acid/base sensor using polypyrrole actuator. *Sensors and Actuators B: Chemical* **2008,** *129*, 518-524.
16. Safavi, A.; Maleki, N.; Bagheri, M., Modification of chemical performance of dopants in xerogel films with entrapped ionic liquid. *Journal of Materials Chemistry* **2007,** *17*, 1674-1681.
17. Seddon, K., Ionic liquids: Designer solvents for green synthesis. *Chemical Engineer* **2002**, 33-35.
18. Byrne, R.; Coleman, S.; Fraser, K. J.; Raduta, A.; MacFarlane, D. R.; Diamond, D., Photochromism of nitrobenzospiropyran in phosphonium based ionic liquids. *Physical Chemistry Chemical Physics* **2009,** *11*, 7286-7291.
19. Byrne, R.; Fraser, K. J.; Izgorodina, E.; MacFarlane, D. R.; Forsyth, M.; Diamond, D., Photo- and solvatochromic properties of nitrobenzospiropyran in ionic liquids

containing the [NTf2]- anion. *Physical Chemistry Chemical Physics* **2008,** *10*, 5919-5924.

20. Coleman, S.; Byrne, R.; Minkovska, S.; Diamond, D., Investigating Nanostructuring within Imidazolium Ionic Liquids: A Thermodynamic Study Using Photochromic Molecular Probes. *The Journal of Physical Chemistry B* **2009,** *113*, 15589-15596.
21. R.D. Rogers; Seddon, K. R., Ionic Liquids: Industrial Applications For Green Chemistry. *Proceedings of ACS Symposium Series, 1-5 April 2001 San Diego, CA* **2002**, 818.
22. Wasserscheid, P., Recent Developments in Using Ionic Liquids as Solvents and Catalysts for Organic Synthesis. In *Organic Synthesis Highlights V*, Wiley-VCH Verlag GmbH: 2008; pp 105-117.
23. Benito-Lopez, F.; Byrne, R.; Raduta, A. M.; Vrana, N. E.; McGuinness, G.; Diamond, D., Ionogel-based light-actuated valves for controlling liquid flow in micro-fluidic manifolds. *Lab on a Chip* **2010,** *10*, 195-201.
24. Neouze, M.-A.; Bideau, J. L.; Gaveau, P.; Bellayer, S.; Vioux, A., Ionogels, New Materials Arising from the Confinement of Ionic Liquids within Silica-Derived Networks. *Chemistry of Materials* **2006,** *18*, 3931-3936.
25. Tamada, M.; Watanabe, T.; Horie, K.; Ohno, H., Control of ionic conductivity of ionic liquid/photoresponsive poly(amide acid) gels by photoirradiation. *Chemical Communications* **2007,** *0*, 4050-4052.
26. Benito-Lopez, F.; Coyle, S.; Byrne, R.; O'Toole, C.; Barry, C.; Diamond, D. In *Simple Barcode System Based on Inonogels for Real Time pH-Sweat Monitoring*, Body Sensor Networks (BSN), 2010 International Conference on, 7-9 June 2010, 2010; 2010; pp 291-296.
27. Curto, V. F.; Coyle, S.; Byrne, R.; Angelov, N.; Diamond, D.; Benito-Lopez, F., Concept and development of an autonomous wearable micro-fluidic platform for real time pH sweat analysis. *Sensors and Actuators B: Chemical* **2012,** *175*, 263-270.
28. Ramnial, T.; Taylor, S. A.; Bender, M. L.; Gorodetsky, B.; Lee, P. T. K.; Dickie, D. A.; McCollum, B. M.; Pye, C. C.; Walsby, C. J.; Clyburne, J. A. C., Carbon-Centered Strong Bases in Phosphonium Ionic Liquids. *The Journal of Organic Chemistry* **2008,** *73*, 801-812.
29. O'Neill, S.; Conway, S.; Twellmeyer, J.; Egan, O.; Nolan, K.; Diamond, D., Ion-selective optode membranes using 9-(4-diethylamino-2-octadecanoatestyryl)-acridine acidochromic dye. *Analytica Chimica Acta* **1999,** *398*, 1-11.
30. MacFarlane, D. R.; Pringle, J. M.; Johansson, K. M.; Forsyth, S. A.; Forsyth, M., Lewis base ionic liquids. *Chemical Communications* **2006**, 1905-1917.
31. Soller, B. R., Design of intravascular fiber optic blood gas sensors. *Engineering in Medicine and Biology Magazine, IEEE* **1994,** *13*, 327-335.
32. Rehrer, N. J.; Burke, L. M., Sweat losses during various sports. *Aust J Nutr Diet* **1996,** *53*, S13-S16.
33. Morris, D.; Coyle, S.; Wu, Y.; Lau, K. T.; Wallace, G.; Diamond, D., Bio-sensing textile based patch with integrated optical detection system for sweat monitoring. *Sensors and Actuators B: Chemical* **2009,** *139*, 231-236.
34. L., B.; K., L.; S., E.; D., D., *Digital imaging as a detector for quantitative colorimetric analyses*. Society of Photo-Optical Instrumentation Engineers: Bellingham, WA, ETATS-UNIS, 2001; Vol. 4205, p 11.

Chapter 5

Organic Electrochemical Transistor Incorporating an Ionogel as Solid State Electrolyte for Lactate Sensing

Dion Khodagholy†[1], Vincenzo F. Curto†[2], Kevin J. Fraser[2], Moshe Gurfinkel[1], Robert Byrne[2], Dermot Diamond[2], George G. Malliaras[1], Fernando Benito-Lopez[2] and Roisin M. Owens[1]*

Journal of Material Chemistry 22 (2012), 4440–4443

ISSN: 1364-5501; DOI: 10.1039/C2JM15716K

[1]Department of Bioelectronics, Ecole Nationale Superieure des Mines, CMP-EMSE, MOC, F-13541 Gardanne, France
[2]CLARITY: Centre for Sensor Web Technologies, National Centre for Sensor Research, School of Chemical Sciences, Dublin City University, Dublin 9, Ireland

† Both authors contributed equally to this work.

* Author to whom correspondence should be addressed;

Abstract

The bulk of currently available biosensing techniques often require complex liquid handling, and thus suffer from problems associated with leaking and contamination. This chapter demonstrates the use of an Organic Electrochemical Transistor (OECT) for detection of lactate (an essential analyte in physiological measurements of athlete performance) by integration of a RTIL in a gel-format, as a solid-state electrolyte.

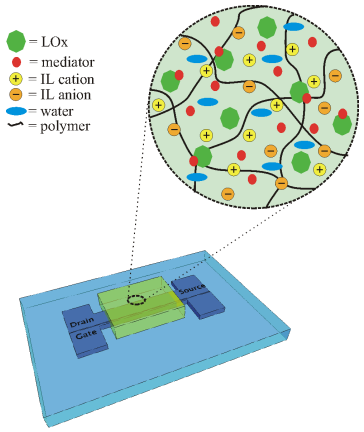

Keywords: lactate; OECTs; ionogel; wearable system, sweat analysis

5.1 Introduction

The detection of lactate (deprotonated form of lactic acid) in blood provides a biochemical indicator of anaerobic metabolism in patients with circulatory failure.[1] In addition to its presence in blood, lactate can be found in sweat (concentration range between 9 and 23 mM), reflecting, in an indirect way, eccrine gland metabolism.[2] It is well known that lactate concentration increases during physical exercise, making it a useful parameter to monitor wellness, physical fitness and the effects of exercise.[3]

Detection in sweat offers a less invasive and dynamic way of measuring lactate concentration, particularly during exercise. Current methods of detection of lactate include fibre optics,[4] conducting polyaniline films,[5] carbon nanotubes,[6] screen printed Prussian blue electrodes,[7] and biosensors based on electrochemiluminescent detection.[8] Commercial lactate sensors are also available,[9] based on standard electrochemical methods. One example is the lactate SCOUT (Senslab), which, however, samples from blood, making real-time detection impractical. Therefore, the possibility of a fast, reliable, robust, miniaturised and cheap way of measuring lactate concentration in physiological fluids will open the way to lactate biosensors for health and sport applications. Flexibility plays an important role, here also, as biosensors for lactate sensing in sweat are in demand as wearable sensors, integrated for example on textiles.

Conducting polymers are interesting biosensing materials owing to their low-cost, mechanical flexibility, and ionic conductivity. Such materials have been exploited in the field of organic electronics to fabricate biosensors. One such device is the organic electrochemical transistor (OECT). OECTs have been utilised in a variety of biosensing applications such as the detection of metabolites,[10, 11] ions,[12, 13] neurotransmitters,[14] cells,[15] antibodies[16] and DNA.[17] The OECT was first described by White *et al.* in 1984.[18] OECTs are three terminal devices containing source and drain electrodes that measure the current across the conducting polymer film (the transistor channel), and a gate electrode. The channel and the gate electrode are in ionic contact via an electrolyte. The working mechanism of the OECT relies on changing the doping state of the conducting polymer channel by application of a positive potential at the gate electrode. Such potential forces

cations from the electrolyte to penetrate into the channel and decreases the number of charge carriers (holes), consequently decreasing the channel current.[19] The vast majority of OECTs are based on poly(3,4-ethylenedioxythiophene) doped with poly(styrene sulfonate) (PEDOT : PSS), a commercially available polymer with high conductivity, which is also biocompatible.[20]

Room Temperature Ionic Liquids (RTILs) are low temperature molten salts that are entirely composed of cations and anions. Due to their unique properties such as large electrochemical stability window, high conductivity and thermal stability, ionic liquids have received increasing attention from the scientific community for applications in green chemistry[21] and electrochemistry,[22] among others. For instance, RTILs provide an attractive alternative to conventional organic solvents to solubilise and stabilise biomolecules such as enzymes and proteins.[21] There are three main strategies to solubilise biomolecules in RTILs: firstly by direct dispersion, secondly, through surface protein modification by PEGylation (covalent attachment of polyethylene glycol polymer chains to the protein) and thirdly by creating a hydrated RTIL.[22] The last method seems to be the most suitable for biosensors, because the addition of small amounts of water to ionic liquids strongly influences the protein solubility while retaining the properties of the selected ionic liquid. Fujita *et al.*[23] have demonstrated that certain proteins are, in fact, soluble, stable and remain active for up to 18 months in RTILs.

The integration of an OECT with a RTIL to make a glucose sensor was recently demostrated, in which the glucose oxidase enzyme was dispersed in the ionic liquid.[24] In the current chapter it is reported the development of a simple, yet robust biosensor that measures lactic acid, an important metabolite involved in several biological mechanisms. The novelty rests with the use of an ionogel which enables the development of a fully solid state yet flexible sensor, suitable for analysis of lactate in sweat. Ionogels are solid or gel-like polymeric materials that endow room temperature ionic liquids (RTILs) with structure and dimensional stability. Le Bideau *et al.*[25] summarised this new class of hybrid materials, in which the properties of the IL are hybridised with those of various components, which may be organic (low molecular weight gelator, (bio)polymer), inorganic (*e.g.* carbon nanotubes, silica, etc.) or hybrid organic–inorganic (*e.g.* polymer and inorganic fillers). These materials are thought to inherit all of the desirable RTIL properties whilst maintaining a gel-like structure.

The chapter presents the first step towards achieving a fast, flexible, miniaturised and cheap way of measuring lactate concentration in sweat through development of a biosensor based on an OECT that uses an ionogel as a solid-state electrolyte both to immobilise the enzyme and to serve as a supporting electrolyte.

5.2 Materials and methods

The OECT fabrication started with the deposition of a 2 mm thick sacrificial parylene C layer on a glass wafer. This parylene layer was subsequently patterned by standard lithography followed by a dry etch using O_2 plasma, defining a contact mask for the PEDOT : PSS channel and gate electrode. A 200 nm thick PEDOT : PSS film was then spin-coated from dispersion (PH-500 from H. C. Stark) and annealed at 140 °C for 60 min. To improve the PEDOT : PSS conductivity, 5 mL of ethylene glycol and 50 mL of dodecyl benzene sulfonic acid (DBSA) were added per 20 mL of PEDOT : PSS dispersion. Additionally, 0.25 g of the cross-linker 3-glycidoxypropyltrimethoxysilane (GOPS) was added to the above dispersion to render the PEDOT : PSS film insoluble. Finally the parylene layer was peeled off mechanically to reveal the PEDOT : PSS channel and the gate electrode. A similar process was followed to make transistors on parylene: the glass wafer was coated with a 2 mm thick parylene film (which would become the OECT support), and was treated with a detergent in order to enable the peel-off of the sacrificial parylene layer. A scheme of the fabrication steps is provided in Figure C1 of Appendix C.

The ionogel consists of two monomeric units: *N*-isopropylacrylamide (NIPAAm) and *N,N'*-methylene-bis(acrylamide) (MBAAm) in the molar ratio of 100 : 2, respectively (the chemical structure is shown in Figure 5.1-a). 1-Ethyl-3-methylimidazolium ethyl-sulfate ionic liquid, $[C_2mIm][EtSO_4]$ (Sigma-Aldrich, used as received), was chosen because of its miscibility with water, thus avoiding mixing problems with the phosphate buffer solution (PBS) containing the analyte. The reaction mixture was prepared by dissolving a ferrocene mediator [bis(n-5-cyclopentandienyl) iron] (Fc, 10 mM) (Sigma-Aldrich) in the IL and subsequently mixing the NIPAAm monomer, the crosslinker MBAAm and the photo-initiator dimethoxy-phenylacetophenone DMPA in 0.8 mL of $[C_2mIm]$ $[EtSO_4]$. A significant advantage was found in the solubility of the Fc in the ionic liquid, as Fc shows very

poor solubility in aqueous solutions such as PBS. Although it is possible that Fc may not be suitable as a mediator in a wearable device due to toxicity concerns, this may be addressed by ensuring that it is covalently bound to the ionogel and thus will not leach out. Alternative redox mediators also exist and have been used for example for subcutaneous glucose sensors which are FDA (U S Food and Drug Administration) approved.[26] The mixture was then sonicated at 45 °C for 10 min and a clear and monophasic solution was obtained. Additionally, stock solutions of 100 mM Lactate Oxidase (LOx) (Sigma Aldrich) and 1 M lactic acid (Sigma Aldrich) were prepared, both in PBS.

By mixing the RTIL mixture and the PBS solution containing the LOx enzyme with a ratio of 4 : 1 (17 % w/w of water) a clear liquid was obtained. The hydrated IL completely dissolved the protein and no precipitation was observed. 20 μL of the final solution was placed at the centre of the device where a polydimethylsiloxane (PDMS) well of a diameter of 8 mm was previously attached to avoid solution leakage after drop casting. Then, the monomers were photo-polymerised within the ionic liquid matrix using a UV irradiation source (three LED array at wavelength 365 nm, UV light intensity ~ 330 μW cm^{-2}) for 1 min. It should be noted that UV exposure time was kept short to avoid denaturation of the protein.

5.3 Results and discussion

Figure 5.1-b shows the layout of the planar OECT, consisting of two parallel stripes of PEDOT : PSS, with widths of 100 μm and 1 mm, serving as the gate electrode and channel of the OECT, respectively (it has been shown that for enzymatic sensing the area of the channel must be larger than the gate electrode[27]). The hydrated ionogel, which contains the LOx enzyme and the Fc mediator (schematic representation Figure 5.1-b), covers part of the channel and the gate of the OECT, as defined by the well.

Measurements were carried out by applying -0.3 V across the channel while triggering the gate electrode at 0.4 V by 3 min long square pulses. Figure 5.2-a shows the modulation of the drain current before ($t < 15$ min) and after the introduction of 20 μL of a PBS solution with the desired lactate concentration.

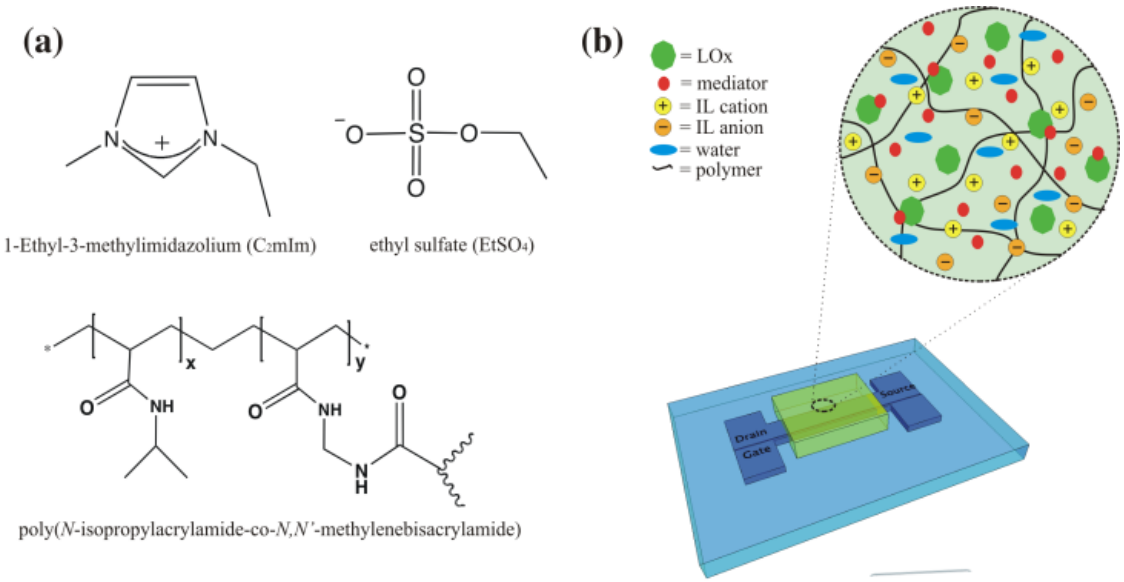

Figure 5.1. (a) Ionogel components and (b) a schematic representation of the OECT device with ionogel / enzyme mixture.

The introduction of the analyte is shown to lead to an increase in the modulation of the drain current, consistent with the mode of operation of OECT-based enzymatic sensors.[10] Figure 5.3-a depicts the series of reactions that take place upon introduction of the lactate. As lactic acid is oxidised to pyruvate, lactate oxidase is reduced and cycles back by the Fc/Ferricenium ion (Fc^{+}) couple, which carries electrons to the gate electrode. This leads to a decrease in the potential across the gate/electrolyte interface and a concomitant increase of the potential at the channel/electrolyte interface. As a result, more cations from the solution enter and dedope the channel (Figure 5.3-b) and the modulation of the drain current in response to a voltage pulse at the gate increases.

The modulation in the drain current is much larger than the gate current due to the inherent amplification characteristics of the OECT. This is demonstrated in Figure 5.2-b, where approximately 100 nA of current at the gate results in 11 mA modulation at the drain current. Figure 5.4-a shows the normalised response of the transistor ($\Delta I/I$) as a function of lactate concentration in the range 10–100 mM.

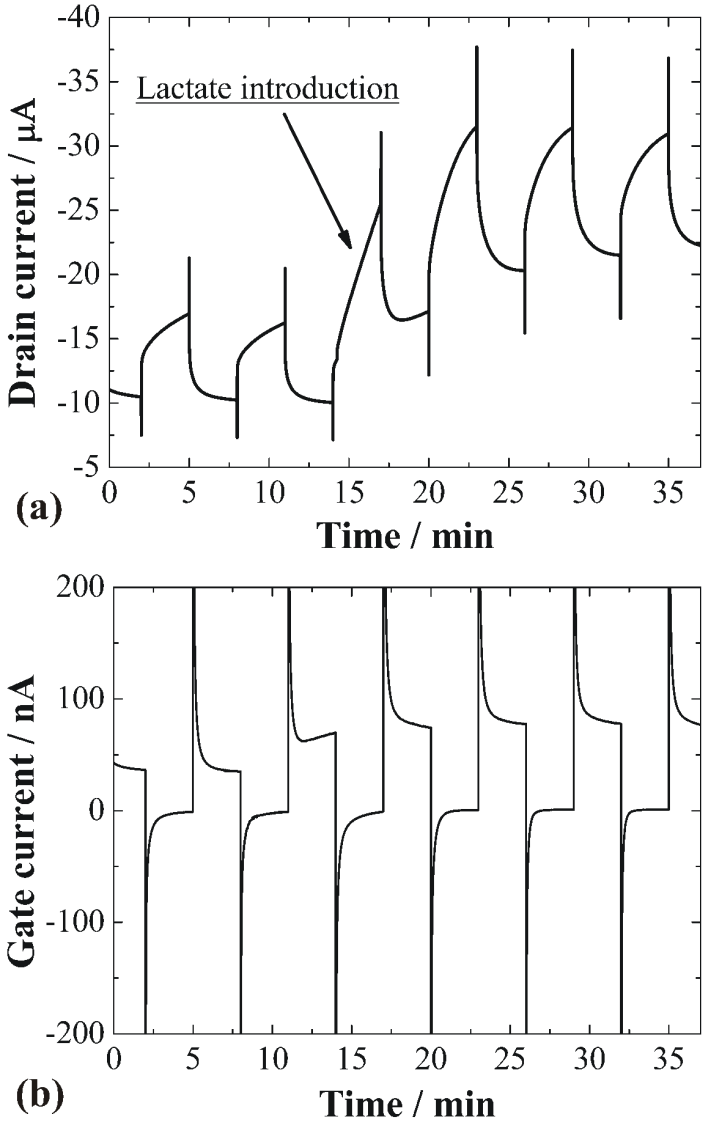

Figure 5.2. (a) Drain current *vs*. time (b) corresponding gate current *vs*. time

The response of the transistor is defined as the difference in the modulation level of the drain channel during application of a gate voltage in the absence and presence of the analyte. The data shown represent the average of three measurements, and the error bars represent the standard deviation from the mean. The time required for the sensor to reach steady-state after addition of analyte is approximately 10 min. This is most likely due to the time it takes for the analyte to diffuse to the enzyme through the gel and may thus be improved by increasing the enzyme concentration, decreasing the gel thickness, *etc*.

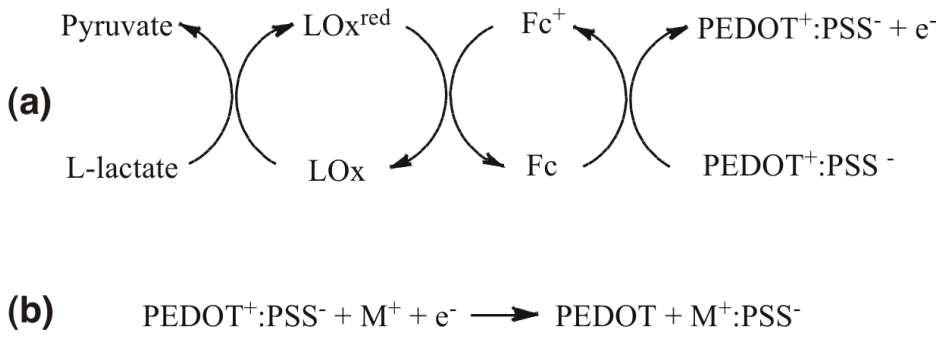

Figure 5.3. Reactions at the gate electrode (a) and at the channel (b) of the OECT

The data clearly show the detection of lactate in the relevant physiological range, covering the relevant range of lactate present in sweat, and suggesting the potential application of this device in the field of sport science as well as in healthcare. It should be noted that the sensor would also be compatible with the detection of lactate in blood (normal physiological range 0.3–1.3 mM, up to 25 mM during exercise).[28] Physiological testing is an important tool for athletes and coaches to check the athlete's health and develop individualised training strategies. While laboratory testing may be increasingly widespread, there is a great demand for wearable sensors to be used in the field.[29] Today's wearable technologies are based on physical sensors, such as electrocardiograph (ECG) electrodes, thermistors and accelerometers.[30] These sensors respond to physical changes in their environment *e.g.* heat, movement and light. Wearable chemo-sensors, in contrast, have the potential to measure many more variables relating to the individual's wellbeing and safety. The integration of chemical sensors (such as lactate) into a textile substrate is a challenging task, as a chemical reaction must happen for these devices to generate a signal and the sensors must be robust, non-invasive, low-power and straightforward to use. The OECT sensor presented here is a step forward towards such devices.

Figure 5.4-b shows a prototype of an array of these sensors (deposited on parylene) in a conformal configuration on a human forearm, demonstrating their wearability. The integration of this prototype with a wireless working platform, previously demonstrated for sweat analysis for non-invasive real time measurements,[29] is currently ongoing.

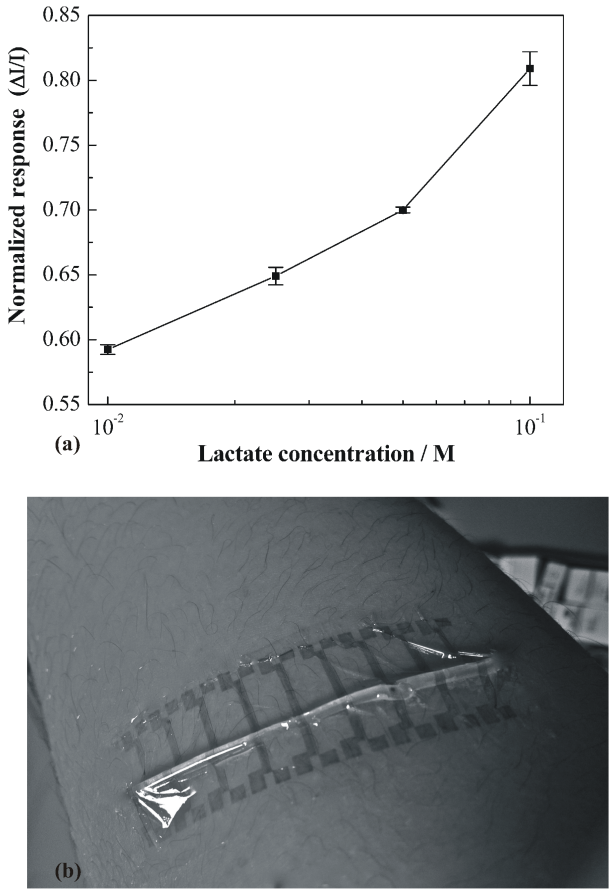

Figure 5.4. (a) Normalised response of the OECT *vs.* lactate concentration and (b) conformal OECT with gel shown on a forearm

5.4 Conclusions

In summary, this chapter demonstrated the detection of lactate in a relevant physiological range using an OECT sensor with an ionogel solidstate electrolyte. The significance of this work for sensing applications lies in the configuration of the sensor; we show for the first time a solid state electrolyte on a flexible transistor-based biosensor. This has implications for the wearability of the sensor and the storage of the sensor due to the enhanced stability of the enzyme in the ionogel. The aim is the use of this sensor as a wearable bandage-type sensor, which can be worn during exercise or health monitoring, allowing sweat to diffuse into the sensor with consequent detection of the lactate analyte. This could also have application for the detection of other sweat components such as pH, see Chapters 3 and 4.

Acknowledgment

F.B.L., V.F.C. and D.D. acknowledge funding from Science Foundation Ireland (SFI) under the CLARITY CSET award (grant 07/CE/I1147). V.F.C. acknowledges the Research Career Start Programme 2010 fellowship from Dublin City University. K.J.F. acknowledges the European Commission for financial support through a Marie Curie Actions International Re-inte- gration Grant (IRG) (PIRG07-GA-2010-268365) and Irish Research Council for Science, Engineering and Technology. R.M.O. acknowledges the European Commission for financial support through a Marie Curie International Reintegration Grant (grant PIRG06-GA-256367 CELLTOX).

Appendix C. Supporting information

Figure C1 of appendix C shows the three steps involved in the realisation of the conformal OECTs.

5.5 References

1. Weil, M. H.; Afifi, A. A., Experimental and Clinical Studies on Lactate and Pyruvate as Indicators of the Severity of Acute Circulatory Failure (Shock). *Circulation* **1970,** *41*, 989-1001.
2. Green, J. M.; Pritchett, R. C.; Crews, T. R.; McLester, J. R.; Tucker, D. C., Sweat lactate response between males with high and low aerobic fitness. *European Journal of Applied Physiology* **2004,** *91*, 1-6.
3. Billat, L. V., Use of Blood Lactate Measurements for Prediction of Exercise Performance and for Control of Training: Recommendations for Long-Distance Running. *Sports Medicine* **1996,** *22*, 157-175.
4. Liu, X. J.; Tan, W. H., Development of an optical fiber lactate sensor. *Mikrochimica Acta* **1999,** *131*, 129-135.
5. Chaubey, A.; Pande, K. K.; Singh, V. S.; Malhotra, B. D., Co-immobilization of lactate oxidase and lactate dehydrogenase on conducting polyaniline films. *Analytica Chimica Acta* **2000,** *407*, 97-103.
6. Weber, J.; Kumar, A.; Bhansali, S., Novel lactate and pH biosensor for skin and sweat analysis based on single walled carbon nanotubes. *Sensors and Actuators B-Chemical* **2006,** *117*, 308-313.
7. Yashina, E. I.; Borisova, A. V.; Karyakina, E. E.; Shchegolikhina, O. I.; Vagin, M. Y.; Sakharov, D. A.; Tonevitsky, A. G.; Karyakin, A. A., Sol-Gel Immobilization of Lactate Oxidase from Organic Solvent: Toward the Advanced Lactate Biosensor. *Analytical Chemistry* **2010,** *82*, 1601-1604.
8. Cai, X.; Yan, J. L.; Chu, H. H.; Wu, M. S.; Tu, Y. F., An exercise degree monitoring biosensor based on electrochemiluminescent detection of lactate in sweat. *Sensors and Actuators B-Chemical* **2009,** *143*, 655-659.

9. Wang, Y.; Xu, H.; Zhang, J.; Li, G., Electrochemical Sensors for Clinic Analysis. *Sensors* **2008,** *8*, 2043-2081.
10. Bernards, D. A.; Macaya, D. J.; Nikolou, M.; DeFranco, J. A.; Takamatsu, S.; Malliaras, G. G., Enzymatic sensing with organic electrochemical transistors. *Journal of Materials Chemistry* **2008,** *18*.
11. Yang, S. Y.; DeFranco, J. A.; Sylvester, Y. A.; Gobert, T. J.; Macaya, D. J.; Owens, R. M.; Malliaras, G. G., Integration of a surface-directed microfluidic system with an organic electrochemical transistor array for multi-analyte biosensors. *Lab on a Chip* **2009,** *9*, 704-708.
12. Bernards, D. A.; Malliaras, G. G.; Toombes, G. E. S.; Gruner, S. M., Gating of an organic transistor through a bilayer lipid membrane with ion channels. *Applied Physics Letters* **2006,** *89*, 053505.
13. Lin, P.; Yan, F.; Chan, H. L. W., Ion-Sensitive Properties of Organic Electrochemical Transistors. *Acs Applied Materials & Interfaces* **2010,** *2*, 1637-1641.
14. Yang, S. Y.; Kim, B. N.; Zakhidov, A. A.; Taylor, P. G.; Lee, J.-K.; Ober, C. K.; Lindau, M.; Malliaras, G. G., Detection of Transmitter Release from Single Living Cells Using Conducting Polymer Microelectrodes. *Advanced Materials* **2011,** *23*, H184-H188.
15. Lin, P.; Yan, F.; Yu, J.; Chan, H. L. W.; Yang, M., The Application of Organic Electrochemical Transistors in Cell-Based Biosensors. *Advanced Materials* **2010,** *22*, 3655-3660.
16. Kim, D.-J.; Lee, N.-E.; Park, J.-S.; Park, I.-J.; Kim, J.-G.; Cho, H. J., Organic electrochemical transistor based immunosensor for prostate specific antigen (PSA) detection using gold nanoparticles for signal amplification. *Biosensors and Bioelectronics* **2010,** *25*, 2477-2482.
17. Lin, P.; Luo, X.; Hsing, I. M.; Yan, F., Organic Electrochemical Transistors Integrated in Flexible Microfluidic Systems and Used for Label-Free DNA Sensing. *Advanced Materials* **2011,** *23*, 4035-4040.
18. White, H. S.; Kittlesen, G. P.; Wrighton, M. S., Chemical derivatization of an array of three gold microelectrodes with polypyrrole: fabrication of a molecule-based transistor. *Journal of the American Chemical Society* **1984,** *106*, 5375-5377.
19. Bernards, D. A.; Malliaras, G. G., Steady-State and Transient Behavior of Organic Electrochemical Transistors. *Advanced Functional Materials* **2007,** *17*, 3538-3544.
20. Owens, R. i. n. M.; Malliaras, G. G., Organic Electronics at the Interface with Biology. *MRS Bulletin* **2010,** *35*, 449-456.
21. Seddon, M. J. E. a. K. R., Ionic liquids. Green solvents for the future. *Pure Appl. Chem.* **2000,** *72*, 1391-1398.
22. Armand, M.; Endres, F.; MacFarlane, D. R.; Ohno, H.; Scrosati, B., Ionic-liquid materials for the electrochemical challenges of the future. *Nature Materials* **2009,** *8*, 621-629.
23. Fujita, K.; MacFarlane, D. R.; Forsyth, M.; Yoshizawa-Fujita, M.; Murata, K.; Nakamura, N.; Ohno, H., Solubility and Stability of Cytochrome c in Hydrated Ionic Liquids: Effect of Oxo Acid Residues and Kosmotropicity. *Biomacromolecules* **2007,** *8*, 2080-2086.
24. Yang, S. Y.; Cicoira, F.; Byrne, R.; Benito-Lopez, F.; Diamond, D.; Owens, R. M.; Malliaras, G. G., Electrochemical transistors with ionic liquids for enzymatic sensing. *Chemical Communications* **2010,** *46*.
25. Le Bideau, J.; Viau, L.; Vioux, A., Ionogels, ionic liquid based hybrid materials. *Chemical Society Reviews* **2011,** *40*, 907-925.

26. Heller, A.; Feldman, B., Electrochemical Glucose Sensors and Their Applications in Diabetes Management. *Chemical Reviews* **2008,** *108*, 2482-2505.
27. Tarabella, G.; Santato, C.; Yang, S. Y.; Iannotta, S.; Malliaras, G. G.; Cicoira, F., Effect of the gate electrode on the response of organic electrochemical transistors. *Applied Physics Letters* **2010,** *97*, 123304.
28. Phypers, B.; Pierce, J. T., Lactate physiology in health and disease. *Continuing Education in Anaesthesia, Critical Care & Pain* **2006,** *6*, 128-132.
29. Coyle, S.; Benito-Lopez, F.; Byrne, R.; Diamond, D., On-Body Chemical Sensors for Monitoring Sweat. In *Wearable and Autonomous Biomedical Devices and Systems for Smart Environment*, Lay-Ekuakille, A.; Mukhopadhyay, S., Eds. Springer Berlin Heidelberg: 2010; Vol. 75, pp 177-193.
30. Fabrice, A.; Schmitt, P. M.; Gehin, C.; Delhomme, G.; McAdams, E.; Dittmar, A., Flexible technologies and smart clothing for citizen medicine, home healthcare, and disease prevention. *Information Technology in Biomedicine, IEEE Transactions on* **2005,** *9*, 325-336.

Chapter 6

Probing the Specific Ion Effects of Biocompatible Hydrated Choline Ionic Liquids on Lactate Oxidase Biofunctionality

Vincenzo F. Curto,[1] Stefan Scheuermann,[2] Roisin Owens,[3] Vijayaraghavan Ranganathan,[4] Douglas R. MacFarlane, [4] Fernando Benito-Lopez [4, 5, *] and Dermot Diamond[1]

Physical Chemistry Chemical Physics – Submitted

[1] CLARITY: Centre for Sensor Web Technologies, National Centre for Sensor Research, Dublin City University, Dublin, Ireland.
[2] Department of Bioelectronics, Ecole Nationale Superieure des Mines, CMP-EMSE, MOC, 880 Rue de Mimet, Gardanne 13541, France
[3] School of Chemistry, Monash University, Wellington Road, Clayton, Australia
[4] CIC microGUNE, Arrasate-Mondragón, Spain.

* Author to whom correspondence should be addressed;

Abstract

This chapter presents an extended study on the ion effect of a series of biocompatible hydrated choline base Ionic Liquids (ILs) on Lactate Oxidase (LOx), an important enzyme in biosensing technology for the *in vitro* detection of lactic acid. Secondary structural analysis revealed changes on the protein conformation in hydrate ILs, while thermal unfolding/aggregation dynamic showed different profiles in the presence or absence of ILs. Moreover, LOx thermally denaturised at 90 °C showed residual activity in the presence of chloride and dihydrogenphosphate anion. Kinetic and lifetime studies were also performed, providing better understanding of the ion effect of ILs on the biocatalytic activity of the enzyme.

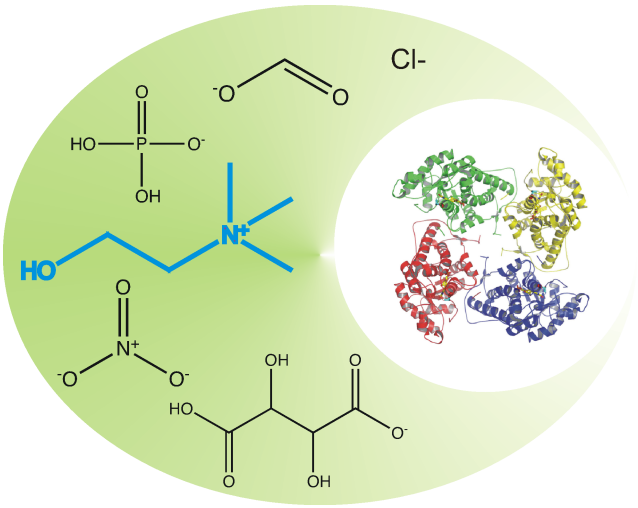

Keywords: hydrated Ionic Liquids; Lactate Oxidase; secondary structure; kinetic; long-term stability

6.1 Introduction

Preserving the native state of proteins plays a vital role in maintaining their biofunctionality and activity. Retaining of protein functionality over time is a key factor in the pharmaceutical field, as it determines the stability of protein-based drugs.[1] In this regard, a shelf life between 18 – 24 months is required for economic practicability. At the same time, with the exponential growth of point-of-care technologies, there is an increasing demand for physically and chemically stable enzyme formulations for biosensing, as this determines device lifetime.[2]

In general, irreversible changes to the folded state enzyme conformation can be induced by factors such as temperature, pH and specific ion interactions.[3] Approaches to improve the enzyme stability can be classified in two main categories: (1) the modification of enzyme state or (2) the optimisation of the solvent environment.[4] The modification of the enzyme state can be achieved in several ways: by isolation of structural variants extracted from natural organisms capable of existing in extreme environments, by rationale-based mutagenesis (bioengineering), by directed evolution of the enzyme and by PEGylation.[5, 6] The optimisation of the solvent environment, on the other hand, involves the use of surfactants and additives, changes of pH and/or the ionic strength of aqueous media.[3] Parallel to this, the use of organic (non-aqueous) media in enzymology has been explored in recent years since this can improve enzyme performance in certain cases.[7] Ionic Liquids (ILs) have recently emerged as a new class of organic solvents that may have considerable potential for enzyme stabilisation.[8]

ILs are molten salts having melting points below that of water. They have made considerable impact in several research areas, such as catalysis,[9] electrochemistry,[10] biosensing[11] and biochemistry.[12] The properties of ILs depend dramatically on the cation-anion combination and in this sense, properties such as polarity, viscosity, thermal stability and conductivity can be tailored *via* the appropriate cation/anion combination.[13] This is an attractive proposition, since it is therefore possible to design a solvent that has the optimum characteristics to improve, for example, the limited temperature and pH range under which many enzymes are stable when solubilised in water.[8]

An increasing number of publications have reported improvements to the

stability of proteins in the presence of ILs. A common strategy in this regard is to use a controlled amount of water in the IL (between 20% - 30% *w/w*), to produce so-called hydrated ILs (HyILs), which provide the required hydrogen-bonding environment for protein solubilisation.[8] For example, extended stability of cytochrome C was observed in hydrated choline dihydrogenphosphate (HyCDHP).[14] Several other studies have reported similar beneficial effects for mushroom tyrosinase,[15] ribonuclease A,[16] interleukin-2[17] and even DNA in hydrated choline ILs.[18] Moreover, ILs based on the choline cation are now commonly used in many applications for which biocompatibility is an essential requirement, *i.e.* cell cultures or *in vivo* applications.[19, 20]

The use of ILs in bioelectrochemistry has been summarised in a recent review by Fujita *et al.*[21], showing how ILs are now widespread in many electrochemical applications, *e.g.* as biofuel cell electrolytes for which more stable matrices are needed. Another growing field for ILs is biosensing, where they are used for the modification of electrodes, acting as a binder for carbon matrix (bucky gel) electrodes or for the immobilisation of bioreceptors.[22] In this regard, in Chapter 5 it was demonstrated the application of ILs in the ionogel format, to achieve a solid-state electrolyte for the development of organic electrochemical transistors (OECTs) for sensing of lactic acid (LA).

Lactic acid is an important metabolic analyte involved in many physiological processes[24] and in sports performance.[25] Consequently, there is considerable interest in lactate biosensors, but despite substantial body of research, the relatively poor stability of *L*-Lactate Oxidase (LOx) limits the effectiveness of current devices.[26, 27] LOx is a flavin mononucleotide (FMN) enzyme that catalyzes the oxidation of *L*-lactic acid into pyruvate, producing H_2O_2 in the process. LOx from the *Aerococcus viridans* contains two tightly packed tetramers, in which each enzyme monomer holds a non-covalently bound FMN group.[28]

In this chapter the use of hydrated choline cation-based ionic liquids on the stabilisation of Lactate Oxidase is presented. In particular, this work focuses on the effect of different HyILs on the biofunctionality of LOx, with particular emphasis on the influence of the HyILs on the enzyme secondary structure, and on the biocatalytic activity. The outcome of long-term stability studies of LOx in several HyILs is also presented.

6.2 Materials and Methods

6.2.1 Chemicals

Lactate Oxidase from *Aerococcus viridans* Grade I (EC 1.13.12.4) for sensor technology was kindly provided by Roche Diagnostics Deutschland GmbH as a lyophilised yellow powder. Choline Formate (CF), Choline Levulinate (CL), Choline Nitrate (CN), Choline Tartrate (CT), Choline Valporate (CV), Choline Aminoacetate (CAAc) and Choline Gallate (CG) were synthesised by neutralisation reaction of the selected acidic form of the anion with choline hydroxide, following the procedure described elsewhere.[19, 29] Choline dihydrogenphosphate Ionic Liquid buffer (CDHP/B) was synthesised as described.[30] It typically involves the addition of 6.30 g (0.5 mol) of Choline hydroxide (20 wt % in water) was added to a beaker containing 4.02 g of dry CDHP (1 mol), with stirring at room temperature until it becomes a clear solution. The water content (calculated) in this buffer mixture at this stage is 48 % and the remaining 52 % is ionic liquid. Choline dihydrogenphosphate (CDHP) was purchased from IOLITEC (Denzlingen, Germany). CF, CL and CG are liquid at room temperature while the other ILs are solids at ambient conditions. Choline Chloride (CCl), Horseradish peroxidase (HRP), 4-Aminoantipyrine (4APP), hydroxybenzoic acid (HBA), lactic acid, pH phosphate tablets pH 7.40, potassium phosphate monobasic and dibasic were obtained from Sigma-Aldrich (San Diego, USA) and used as received.

6.2.2 Preparation of LOx Solutions

HyILs solutions for circular dichroism spectroscopy (CD), long-term and residual activity studies were prepared with final water content of 25 % *w/w*, except for CT where a 35 % *w/w* solution was employed. Generally, HyILs/LOx solutions were prepared starting from 20 % *w/w* (30 % *w/w* for CT) water content in HyILs, where the right amount of water with LOx was added in order to reach the desired final water weight percentage and protein concentration. LOx solutions in the presence of CCl and CG were prepared by dissolving CCl and CG in PBS (pH 7.40; 10 mM) at a final concentration of 1 M. Hereafter they will be referred to CG and CCl solutions.

Moreover, LOx/IL-free solution (PBS 7.40; 10mM) was also studied for comparison.

6.2.3 Circular Dichroism Spectroscopy

The secondary structure of the enzyme was investigated by circular dichroism spectroscopy in the far-UV region (190-250 nm) using a JASCO CD J-810 Spectropolarimeter. CD spectra were recorder with a 0.1 cm path length quartz cuvette loaded with 300 µL of sample at the final concentration of 0.25 mg ml^{-1} of LOx. Temperature induced denaturation of the protein was performed from 25 °C to 90 °C at the scan rate of 1 °C min^{-1} at 222 nm. Quantitative secondary structure analysis of LOx in solution was determined by fitting the far-UV CD data using the published analysis algorithms CDSSTR (reference set 4) of the online server DICHROWEB.[31, 32]

6.2.4 Colorimetric Assays

Colorimetric assays for residual activity, kinetic and long-term stability studies were performed using TECAN Infinite M200 96 well plate reader. All the experiments were run at 25 °C. The red chromogenic dye (λ_{max} = 510 nm) is formed from the following cascade of reactions upon addition of lactic acid:

$$Lactic\ acid + O_2 \xrightarrow{LO_x} Pyruvate + H_2O_2$$

$$2\,H_2O_2 + 4AAP + HBA \xrightarrow{HRP} quinoneimine\ dye + 4\,H_2O$$

The composition of the assay was: 0.2 mM of 4AAP, 6 mM of HBA, 0.4 Unit per well (300 µL) and 50 nM of LOx in PBS pH 7.00 (0.15 M).

6.2.4.1 Long-term Stability and Residual Activity

Long-term stability and residual activity studies were performed by adding to the final assay solution only 5 µL of LOx solution (IL-free, CCl, CG and HyILs). The

dissolution of a small amount of HyILs/LOx and the relatively high molarity of the PBS of the colorimetric assay guarantee a minimal pH shift from neutrality, which might be caused by the acid/base character of some of the studied ILs. A lactic acid concentration of 10 mM was used to start the cascade of reactions. Long-term stability of the protein was investigated using LOx stock solutions stored at 5 °C and 37 °C, which were periodically tested over a period of 140 days. Residual activity test upon conditioning of the LOx solutions at 90 °C were similarly performed. Denaturation was induced by incubation of the samples in a thermostatic standard silicon oil bath.

6.2.4.2 Kinetic Studies

To determine the kinetic parameters of LOx, solutions at the concentration of 0.5 M in ILs were employed. This IL molarity guarantees the dominance of ion-specific effects on the enzyme rather than electrostatic forces.[33] Due to the higher IL concentrations, the pH of the PBS assay was affected and so its variation was recorded using a standard glass membrane pHmeter (VWR, sympHony SP70P). Kinetic constants (K_M, V_{max}) were obtained from the data through a nonlinear fitting of the Michaelis−Menten equation using an in-house Excel developed macro.[ii] *Turnover* numbers (k_{cat}) were calculated from V_{max} using the relationship, $k_{cat} = V_{max}/[E]$ where [E] is the molar enzyme concentration, *i.e.* 50 nM.

6.3 Results and Discussion

6.3.1 Effect of the Ionic Liquids on LOx Structure and Conformation

Figure 6.1-a presents the CD spectra at 25 °C (solid line) for lactate oxidase when in IL-free aqueous solution. The spectrum clearly shows the three characteristic peaks at 195 nm, 208 nm and 222 nm originating from the folded secondary structure of the

[ii] Non linear fitting was performed through minimisation of the sum of the square residuals (SSR) using *Solver* function.

enzyme. However, for CCl, the CD spectrum presents only two of these characteristic peaks at 208 nm and ~ 220 nm, as shown in Figure 6.1-b (solid line).

The high absorbance due to CCl in solution in the region 200-190 nm, made any quantitative analysis difficult. In the case of the different HyILs/LOx solutions and CG, high absorbance in most of the far-UV region was observed, making any CD spectral recording impractical. Blank experiments using enzyme-free HyILs revealed that the HyILs are responsible for the high absorbance (data not shown). Nevertheless, in the case of LOx dissolved in HyCDHP it was possible to record the full spectrum over the entire far-UV region (Figure 6.1-c – solid line), from which useful information about the secondary structure of LOx in HyCDHP can be extracted. [iii]

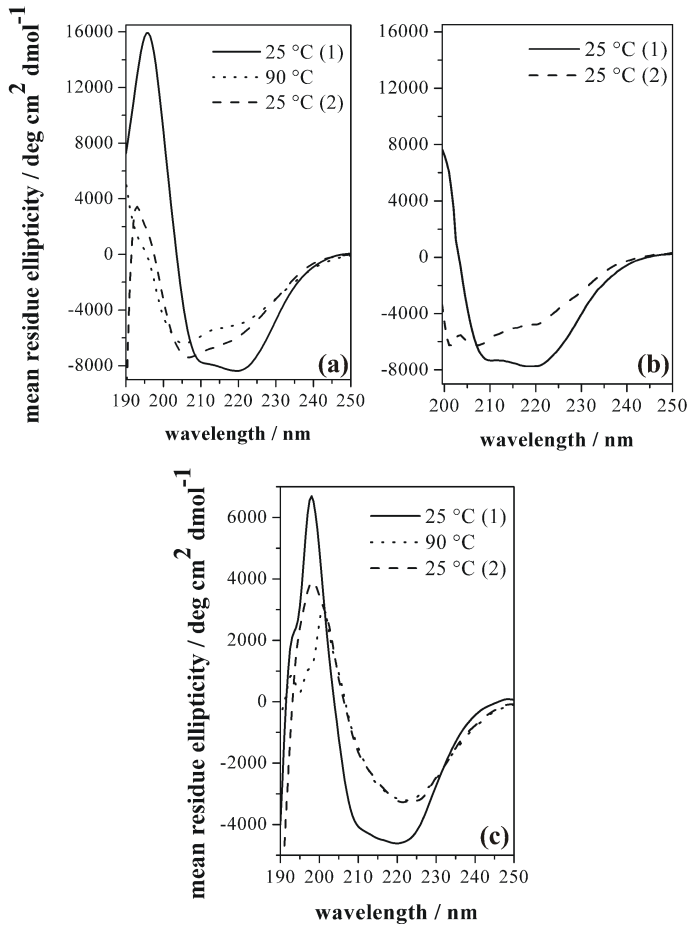

Figure 6.1. CD spectra of LOx dissolved in IL-free (a), CCl (b) and HyCDHP (c). The spectra were first recorded at 25 °C (1) (—), then thermal denaturation of the LOx was performed at 1 °C min^{-1} till 90 °C, followed by the recording of spectrum at 90 °C (····). Once the sample was cooled down the spectrum at 25 °C (2) (---) was recorded. The LOx concentration is 0.25 mg mL^{-1} in all the cases.

[iii] The less intense CD signal for HyCDHP/LOx is possibly due to the higher refractive index of HyCDHP (RI_{HyCDHP} = 1.49) compared to CCl and IL-free.

Comparing the three spectra in Figure 6.1, some differences on the secondary structure of LOx at 25 °C (1) are observed, especially for HyCDHP where a less pronounced peak at 208 nm is observed, which implies structural changes are occurring in the secondary structure of LOx. This is verified by the quantitative analysis (Table 6.1), which shows substantial differences in the α-helix and β-sheet content for HyCDHP compared to IL-free. For instance, LOx in HyCDHP presents only 11 % of α-helices, compared to the 28 % in IL-free. Conversely, a higher content of β-sheets and turns are observed for LOx when dissolved in HyCDHP. In this case, they represent 34 % and 24 % of the secondary structure, respectively, suggesting a change in the conformation of the enzyme in HyCDHP arises due to the different ionic environment.

It is known that a stabilising solvent often will produce an increase in the melting point of proteins, which implies that unfolding is less favorable at room temperature.[16, 17] Figure 6.1-a and Figure 6.1-c show the CD spectra recorded at 90 °C (no useful data at this temperature was obtained for CCl) compared with equivalent spectra obtained at 25 °C after denaturation, Figure 6.1 dash line. At 90 °C, both spectra present less intensive peak signals around 200 nm, and a substantial wavelength shift for the three peak maxima. Moreover, the peak at ~ 195 nm in the IL-free spectrum (predominantly given by the α-helices) has significantly reduced at 90 °C. On the other hand, the same peak in the HyCDHP spectrum (Figure 6.1-c) is still substantially present at 90 °C, implying that recovery of the original structure occurs once the sample is cooled down to 25 °C.

This conclusion is supported by the data in Table 6.1, where the decrease in the α-helix content of LOx in HyCDHP is only ca. 3 %, much smaller than the 10 % decrease observed in the IL-free sample. In addition, for IL-free samples, the concomitant increment in β-sheets, turns and unordered content that occurs upon thermal denaturation suggest that irreversible aggregation of the enzyme is happening. In fact, high levels of intermolecular β-sheet structures typically indicate aggregation.[3]

In addition, for IL-free samples, the concomitant increment in β-sheets, turns and unordered content that occurs upon thermal denaturation can suggest irreversible aggregation of the enzyme is happening. In fact, high levels of intermolecular β-sheet structures typically indicate aggregation.[3]

Table 6.1. Secondary structure analysis of LOx in IL-free and HyCDHP, with reported values in percentage. Quantitative CD analysis was performed for spectra recorded at 25 °C before (1) and after (2) thermal denaturation at 1 °C min^{-1} till 90 °C of the LOx. NRMSD states for normalised root mean square deviation.

	25 °C (1)		**25 °C (2)**	
	IL-free	**HyCDHP**	**IL-free**	**HyCDHP**
α-helices	28	11	18	8
ß-sheets	23	34	30	37
Turns	20	24	28	25
Unordered	30	30	23	30
NRMSD	*0.011*	*0.087*	*0.039*	*0.116*

The formation of aggregates in the IL-free case is verified by the change in the photomultiplier voltage value (High Tension - HT) of the spectropolarimeter during the thermal denaturation of LOx, Figure 6.2-a (solid line). In fact, Benjwal *et al.*[34] proposed an easy method to monitor real-time aggregation of proteins, by following changes in light scattering, as this correlates with variations in the particle size (aggregates). Alternatively, monitoring the CD-signal at 222 nm can provide information about the unfolding of proteins. Figure 6.2-a shows a sharp transition of the signal (solid black line) starting at 68 °C, with a similar effect occurring at 222 nm (solid light grey line), suggesting that unfolding and aggregation of LOx proceed simultaneously. For CCl, a sharp variation of the MRE (Mean Residual Ellipticity) signal at 222 nm suggests unfolding of LOx but the HT value *versus* temperature does not clearly support aggregation, although it does increase. This behavior can be attributed to aggregation of the unfolded enzyme being less favoured aggregation of the unfolded enzyme due to the presence of CCl. In contrast, both the HT and MRE curves for the HyCDHP/LOx do not present any similar transitions.

The decrease of the MRE signal may suggest some unfolding of LOx is happening, as is also indicated in 6.1 from the quantitative analysis of the CD spectra for HyCDHP. With regard to the HT value for HyCDHP (Figure 6.2-c), a less well-defined step increase is observed starting at ca. 72 °C, which implies that aggregation of the enzyme is inhibited compared to IL-free and CCl LOx solutions, due to the ionic effect and the greater viscosity of HyCDHP.

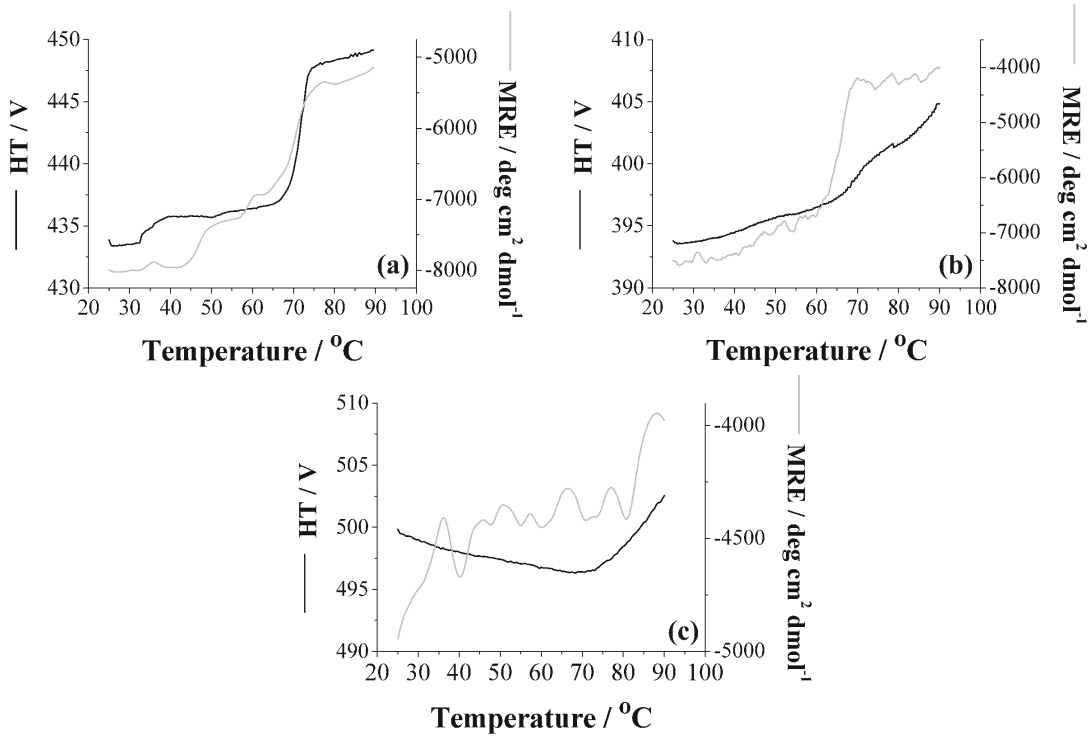

Figure 6.2. Thermal denaturation of LOx dissolved in IL-free (a), CCl (b) and HyCDHP (c). The (—) HT value and the (—) MRE (Mean Residual Ellepticity at λ = 222 nm were recorded from 25 °C to 90 °C at 1 °C min^{-1}. LOx concentration is 0.25 mg ml^{-1} in all cases.

The structural analysis does not provide any information on the capability of the enzyme to retain its catalytic activity after thermal denaturation. Therefore, the residual activity was characterised by incubating the LOx solutions at a constant temperature of 90 °C for different times, as explained in the experimental section. Choline Valporate, Choline Aminoacetate and Choline Gallate were found to be strong denaturating agents for the enzyme. In fact when LOx was dissolved in those HyILs and tested, no catalytic activity was observed. For this reason CV, CAAc and CG were not studied any further.

In contrast, LOx exhibited catalytic activity when dissolved in HyILs, *i.e.* HyCF, HyCL, HyCN and HyCT. However, upon incubation of these HyILs/LOx solutions at 90 °C, their residual activity was negligible after 5 min. Similar behaviour was also observed for the IL-free/LOx solution. These results indicate that thermal induced denaturation of LOx in those solutions is irreversible, leading to the entire loss of biocatalytic activity. This behaviour is expected for the LOx/IL-free solution, considering the aggregation dynamics shown in Figure 6.2-a. Unfortunately, the lack of CD data obtained for the LOx solutions in HyCF, HyCL,

HyCN and HyCT do not allow us to predict whether unfolding is occurring, with loss of bioactivity, regardless of enzyme aggregation.

For CCl and HyCDHP the thermal deactivation profiles are quite different. Figure 6.3 displays the residual activity of LOx *versus* incubation time, showing how the most of the activity loss occurs during the first 5 minutes of incubation (~ 75 %), followed by a progressive decrease, which becomes completely irreversible between 25 and 30 min. These results correlate well with the previous observations on the conformational changes of LOx when dissolved in CCl and HyCDHP. Although enzyme unfolding occurs in all cases, it appears that this process is quite reversible when denaturation conditions are applied for a short period of time (5-30 min). This is a clear demonstration that the presence of CDHP and CCl enhances the stability of LOx when it is thermally stressed.

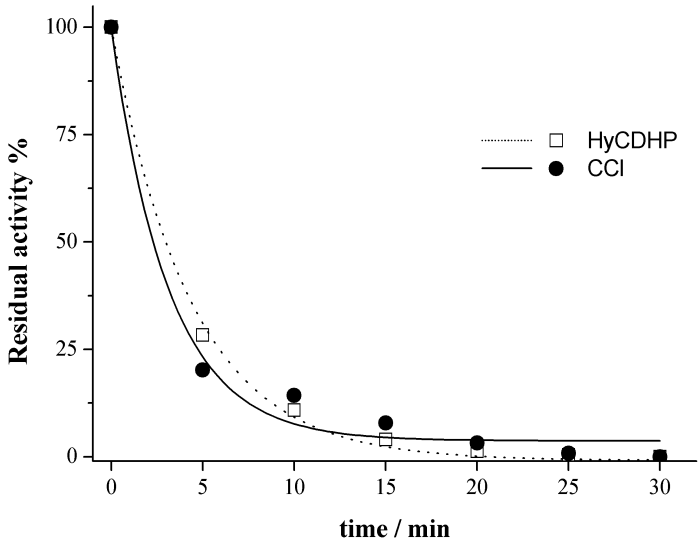

Figure 6.3. Residual activity of LOx dissolved in CCl 1 M in PBS pH 7.40 (●) and HyCDHP (□) upon thermal denaturation at 90 °C.

6.3.2 Effect of the Ionic Liquids on the LOx Biofunctionality

In order to obtain more information on the effect of the different ILs on the Lactate Oxidase function, kinetic characterisation of the enzyme aqueous solutions in the presence of ILs (0.5 M) was carried out. Figure 6.4 shows the experimental data points fitted using the Michaelis−Menten non-linear model[35] and table 6.2 summarises the calculated kinetic parameters K_M, k_{cat} and the catalytic efficiency given by the ratio k_{cat}/K_M.

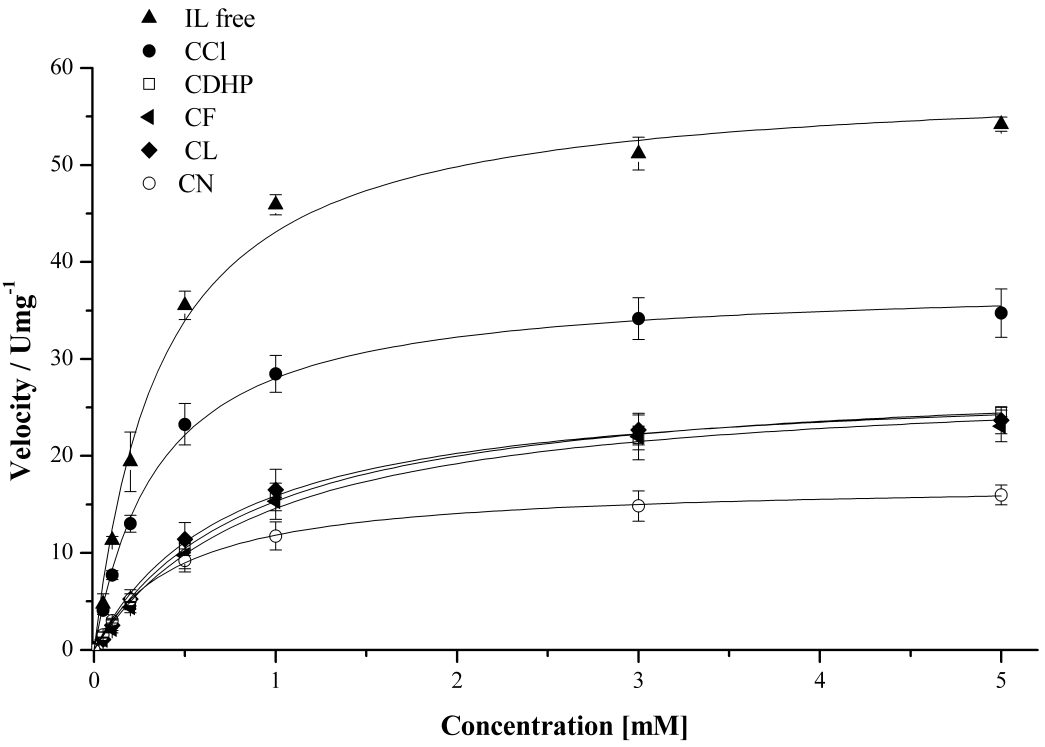

Figure 6.4. Initial velocity of LOx *versus* lactic acid concentration (n = 3). CCl and ILs concentration in the final assay is equal to 0.5 M. Fitting curves result from exponential Michaelis−Menten non-linear fitting.

Table 6.2. Kinetic parameters and pH values of LOx solutions in the absence (IL-free) and presence of ILs and CCl (final concentration 0.5 M).

	K_M [mM]	k_{cat} s^{-1}	k_{cat}/K_M [s^{-1} mM^{-1}]	pH no LA
IL-free	0.370	78.80	210.81	6.95
CCl	0.356	50.66	142.30	6.86
CDHP	0.872	38.26	43.88	5.98
CF	0.926	37.47	40.46	7.22
CL	0.757	37.23	49.18	7.16
CN	0.465	23.10	49.68	6.83

Moreover, experimental pH measurements of the final assay solutions in the absence and presence of lactic acid are also reported in table 6.2. It was found that addition of the IL causes a change in the pH, in some cases producing an increase (*e.g.* CF, pH 7.00 → 7.20) or a decrease (*e.g.* CDHP, pH 7.00→ 6.00) depending on

whereas the anion behaves as a Brønsted acid (DHP) or base (formate). Addition of lactic acid (5 mM) in the presence of the ILs in all the cases reduces the pH, typically by *ca.* 0.1 pH unit or less.

It should be noted that it was not possible to measure any kinetic parameters for choline tartrate, probably because of the significant degree of dissociation of the dicarboxylic anion, which generates an environment which is too acidic (pH = 3.60) for the enzyme to retain its functionality, as LOx has optimum pH activity between 6.5 and 7.5, as suggested by the enzyme supplier.

Table 6.2 presents results obtained for K_M and k_{cat} values in the various aqueous environments studies. K_M represents the affinity of the enzyme for the substrate, therefore for a given reaction velocity a low value of K_M indicates a better affinity between the two, whereas k_{cat} represents the *turnover* number of the enzyme (number of substrate molecules converted into product by the enzyme). The catalytic efficiency (overall effectiveness of the biocatalytic behaviour of the enzyme) is given by the ratio k_{cat}/K_M. Taking the catalytic efficiency first, it is clear that this is significantly reduced (approximately 5 fold) for all ILs compared to IL-free, except for CCl, which is reduced by *ca.* 30 %; *i.e.*, the catalytic activity of CCl is about 3 times greater than the other ILs tested. This relates closely to the k_{cat} values, which are always lower for the ILs and CCl compared to IL-free. The picture for variation in K_M is a little more complex, as the values for IL-free and CCl are closely matched (0.37 mM, 0.36 mM, respectively), CN is slightly higher (0.47 mM), while the other ILs are higher again, in the range 0.8-0.9 mM. These results suggest that in the presence of ILs, the enzyme and substrate interactions are weakened and it is believed that such effect can be mainly attributed to the anions of the tested ILs.

Considering the catalytic efficiency values as the key parameter, the following relationship can be expressed for the anion influence on the biocatalytic activity of lactate oxidase in choline-based ILs;

$$Cl^- > \text{nitrate}^- > \text{Levulinate}^- > DHP^- > \text{Formate}^-$$

Since the first observation by Hofmeister, the effect of ions on protein stability has been mostly attributed to their ability to modify the water distribution around and within protein hydration environment.[36] In order to understand the cause of this effect, the kosmotropic (‘structure-making’) and chaotropic (‘structure-breaking’)

nature of ions must be considered, as these are important parameters in terms of stabilising or destabilising ion specific effects on proteins. Several studies have revealed that the best stabilising conditions are normally provided by chaotropic cations and kosmotropic anions.[36-39] Choline is well known as a chaotropic cation for the stabilisation of proteins when coupled with a kosmotropic anion, such as DHP.[37] According to the Hofmeister anion series, DHP is considered a stabilising anion, while nitrate and chloride anions are normally considered strong and slightly destabilising anions, respectively.[36] No relevant data could be found for the levulinate anion, while several reports suggest that formate ILs can produce positive stabilisation effects,[40] [41] although this has not been specifically related to either its stabilising or destabilising nature.

Maeda-Yorita *et al*.[42] described an enhanced stabilisation effect on the bioactivity of LOx from chloride anions, which is broadly in accordance with our findings. However, the result for nitrate and DHP is not so easy to interpret. In fact, in the established anion series, the relative position of DHP compared with nitrate is not in line with previous reported works.[16, 36]

CDHP is known as a slightly acidic IL, due to the acidic character of the DHP anion ($H_2PO_4^-$).[43] This is supported by the pH values reported in table 6.2, which show a decrease of the solution pH in the presence of CDHP (pH 6.00 compared to 7.00 for IL-free). The other IL solutions generate a less pronounced pH shift (± 0.2 pH units) compared to IL-free. Together with the ions specific effect, the pH variation of the solution when adding CDHP, could possibly explain the lower catalytic efficiency of Lactate Oxidase (LOx optimum pH activity between 6.5 and 7.5)

MacFarlane *et al.*[30] reported the possibility of controlling proton activity in HyILs, obtaining an intrinsic proton buffering behavior of CDHP, denoted here as CDHP/B. Table 6.3 reports the kinetic parameters when CDHP/B is used in solution instead of CDHP and Figure 6.5 shows the kinetic curves for CDHP/B, with CDHP and IL-free for comparison. Firstly, the pH increases substantially (~ 0.80 pH units) when CDHP/B was added to the assay solution, reaching the optimum pH window for LOx; this is due to the inherent equilibrium of the dihydrogenphosphate and monohydrogenphosphate groups in CDHP/B.

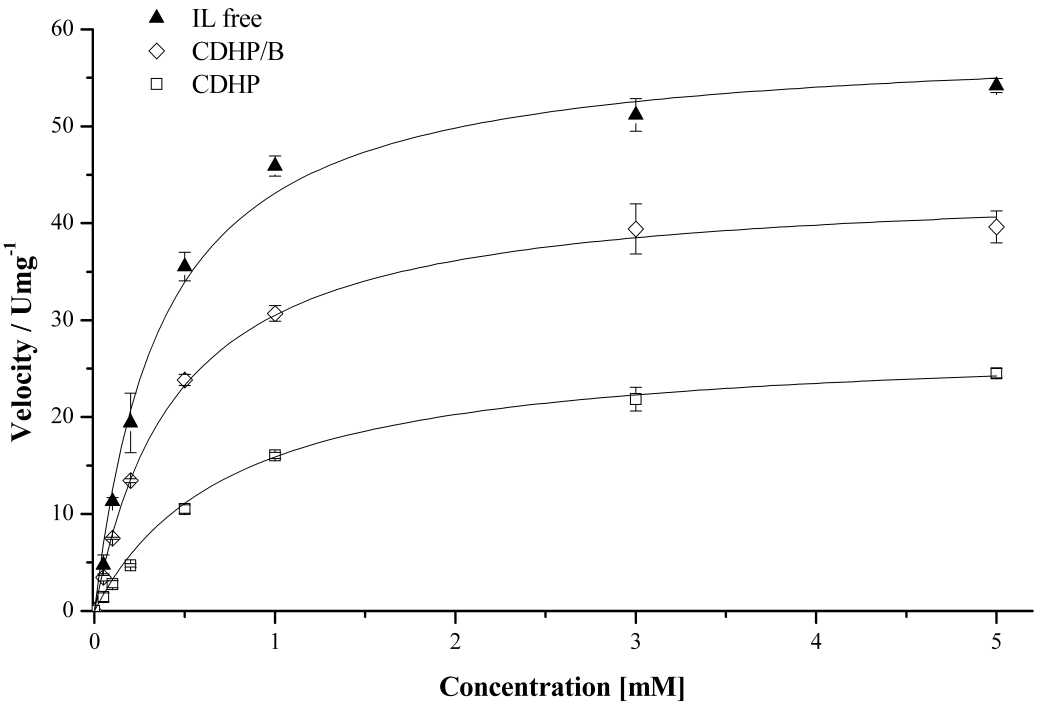

Figure 6.5. Initial velocity of LOx *versus* substrate concentration for IL-free, CDHP and CDHP/B (n = 3). IL-free and CDHP curves are reported from Figure 6.4 just for comparison. ILs concentration in the final assay is equal to 0.5 M. Fitting curves result from exponential Michaelis−Menten non-linear fitting.

Table 6.3. Kinetic parameters and pH values of LOx in IL-free and in the presence of CDHP/B and CDHP at the final concentration of 0.5 M.

	K_M	k_{cat}	k_{cat}/K_M	pH
	[mM]	s^{-1}	[s^{-1} mM^{-1}]	no LA
IL-free	0.370	78.80	210.81	7.00
CDHP/B	0.452	59.05	130.64	6.80
CDHP	0.872	38.26	43.88	6.00

Secondly, K_M decreases and k_{cat} increases in comparison to CDHP, which contributes to a substantial improvement in the catalytic efficiency of LOx, increasing to 130.64 s^{-1} mM^{-1} (*ca.* 3 times greater than CDHP) but still less than IL-free/LOx (210.81 s^{-1} mM^{-1}). Considering these results, it would appear that the catalytic behavior of LOx in CDHP is strongly influenced by pH. These results also enable the effect of the choline cation and the DHP anion to be discriminated from that of pH. As LOx is tested at the same pH as the other ILs (7.0 ± 0.2), it is possible now to assert that the specific ion effect of choline cation and DHP anion on LOx is

analogous to the other ILs, since similar reduction on the catalytic efficiency of LOx compared to the IL-free solution, with respect to the other HyILs, is observed. Following these observations, the previous anion series for LOx can be now amended to:

$$Cl^- > DHP^- > nitrate^- > Levulinate^- > Formate^-$$

6.3.3 Effect of the Ionic Liquids on LOx Lifetime

Enzyme lifetime/stability is critically important for the development of a practically useful lactate biosensor.[23] In order to test this, the catalytic function of the enzyme in the various ILs was tested and compared to similar experiments performed under IL-free conditions. The experiments were performed by periodical testing of LOx solutions stored at 5 °C and 37 °C, which correspond to standard storage temperature of home chilling units and average body temperature, respectively. Figure 6.6 shows the variation in initial velocity v of LOx over a period of 140 days. The y-axis reports the percentage ratio (i.e., $v/v_0 \times 100$), where v_0 is the initial velocity of the enzyme immediately (day 0) after dissolution in HyILs, CCl or IL-free solutions (pre-incubated at 25 °C for 2 h).

The insert graphs of Figure 6.6 shows the trend during the first 21 days at each temperature. In both cases, the fastest loss occurs with HyCL, HyCN, HyCT and HyCF. The decrease is particularly pronounced at 37 °C, with the enzyme activity in these ILs collapsing to almost zero within a few days.

Over the longer time period, enzyme activity was best preserved in CCl, when stored at 5 °C, with over 90 % of the original day 0 activity retained for 100 days, dropping to *ca.* 80% after 140 days. It is worth mentioning that this is significantly better than the results obtained in IL-free solution under the same conditions, which were *ca.* 65 % (day 100) and *ca.* 40 % (day 140). Next to CCl, the best results at 5 °C were obtained with HyCDHP, for which the performance was very similar to IL-free. For the other ILs, the decrease in stability was much more marked, the best being HyCDHP/B, in which the LOx was still reasonably active (*ca*. 85%) after 30 days.

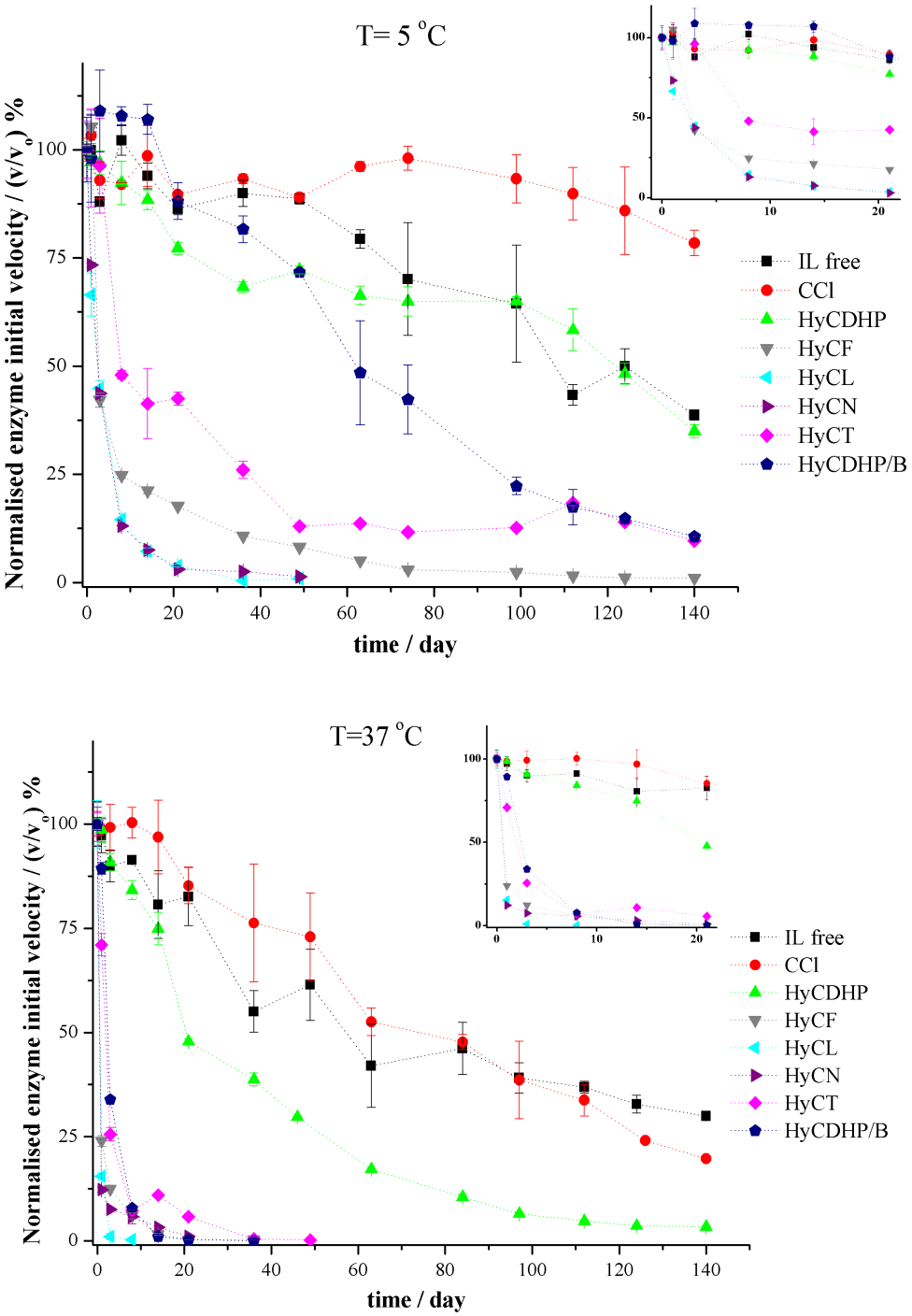

Figure 6.6. Long term stability of LOx when stored at 5 °C (top) and 37 °C (bottom) in the HyILs, IL-free and CCl solutions. The normalised enzyme initial velocity on the y-axis represents the ratio between the initial velocity v of the tested sample divided by the initial velocity v_0 of the fresh made stock LOx solutions. Insert graphs show the collected data points during the first 21 days of the study (n = 3).

At 37 °C, the decrease in enzyme stability was more pronounced, as would be expected because the energetic barrier for the enzymatic deactivation is lower compared to 5 °C. The best performing solution was again CCl, with results very

similar to those obtained under IL-free conditions, with both retaining *ca.* 80 % of the day 0 activity for 20 days (inset). Next best was HyCDHP (*ca.* 50 % day 0 activity after 20 days). Over the longer period, the trend was similar, with CCl ≈ IL-free (both retaining *ca.* 25 % day 0 activity), followed by CDHP (effectively reaching zero after *ca.* 120 days).

These results confirmed the beneficial effect of CCl for LOx long time stability, especially when it is stored at 5 °C with less than 25 % loss in activity after the period of test. This result confirms the stabilising effect of CCl observed in the residual activity study (Figure 6.3). HyCDHP is confirmed as the best stabilising of the tested HyILs, although does not give any better conditions compared to the IL-free solution. For the latter, LOx showed an unexpectedly extended lifetime and further investigation will be necessary to elucidate the cause.

It is also worth noting that, although HyCT cannot be considered to stabilise LOx to the same extent as HyCDHP, at 5 °C an improved stabilisation effect on LOx was observed compared to the HyILs CL, CN and CF. These results suggested that the specific ion effect of ILs on proteins can be, in general, quite different when in HyILs or in solution at high concentration of ILs, *e.g.* 0.5 M concentration.

For instance, it was not possible to obtain any kinetic parameter in the presence of CT, due to the low pH given by the tartrate anion in solution, as explained before; however, in HyCT Lactate Oxidase retained about 10 % of its initial activity after 140 days, as shown in Figure 6.6 at 5 °C. The origin of this result is not particularly clear but it might be attributed to the different water activity (a_w) of the two systems, which can influences the overall effective-pH in solution. In fact with the variation of a_w the dissociation equilibrium of tartrate anion can shift, with the final result of significant differences of the enzyme environment where it is dissolved. In this regard, in addition to the ion specific effects of CT, a_w/effective-pH can play a crucial role on the preservation of the biofunctionality of the enzyme. Very recent findings from Thompson *et al*.[44] showed for HyCDHP the influence of a_w on the effective-pH in solution, which here was proven as an important parameter for the retention of the enzyme biofunctionality.

Finally, the stability of LOx when stored in HyCDHP/B (52 % *w/w* ionic liquid) was also investigated. At 37 °C the loss of activity has a similar trend to with HyCN, HyCF and HyCL, reaching zero just after 14 days. Nevertheless, at 5 °C, the LOx deactivation during the first 20 days was found to be less pronounced, perhaps

indicating the beneficial effect of the choline DHP. Thereafter, a faster loss occurred, retaining only 10 % of its initial velocity after 140 days.

6.4 Conclusions

This work reports the influence of several biocompatible choline HyILs on the native structure and bioactivity of Lacate Oxidase, an important enzyme for the realisation of lactate biosensors. The study of the secondary structure of the enzyme showed differences in the α-helix and β-sheet content in HyCDHP; with a marked decrease of α-helices and increase of β-sheet. However, this does not seem to affect the enzyme activity, which overall is more stable when thermal denaturation is induced. Moreover, irreversible enzyme deactivation is diminished when using HyCDHP and CCl solutions.

The kinetic parameters also revealed a significant IL effect on the catalytic efficiency, which is strongly influenced by the nature of the anion. Interestingly, the acid character of the DHP anion had a negative influence on the biocatalysis of lactic acid, most likely due to the associated increased acidity, a critical parameter for optimising enzyme stability and performance. However, by using an IL "buffer", such as CDHP/B, it was possible to study the real ion effect of the choline cation and the DHP anion on the enzyme performance, as this allowed precise control of the solution pH.

In addition, long-term stability studies showed a remarkable ion specific effect on the enzyme, especially for choline chloride, for which *ca.* 80 % of the initial (day 0) activity is retained after 140 days when stored at 5 °C. Finally, HyCDHP performs as well as IL-free (PBS buffer) solutions in terms of LOx stabilisation. Therefore we believe that, the advantages on using HyILs, such as HyCDHP, as solvent in replacement of buffer solutions could drive the current research toward the realisation of more robust lactate biosensors, by using ILs to replace aqueous media.

Acknowledgements

This work was supported by Science Foundation Ireland under grant 07/CE/I1147 and the Research Career Start Programme 2010 fellowship from Dublin City University. Thanks to Roche Diagnostics Deutschland GmbH for providing the LOx

protein. Thanks also to the Conway Institute (University College of Dublin – Dublin) for access to the Circular Dichroism Spectropolarimeter.

6.5 Refernces

1. Frokjaer, S.; Otzen, D. E., Protein drug stability: a formulation challenge. *Nature Reviews Drug Discoveries* **2005,** *4*, 298-306.
2. Gibson, T., D., Biosensors: the stability problem. *Analysis* **1999,** *27*, 630-638.
3. Chi, E.; Krishnan, S.; Randolph, T.; Carpenter, J., Physical stability of proteins in aqueous solution: mechanism and driving forces in nonnative protein aggregation. *Pharmaceutical Research* **2003,** *20*, 1325-1336.
4. Weingartner, H.; Cabrele, C.; Herrmann, C., How ionic liquids can help to stabilize native proteins. *Physical Chemistry Chemical Physics* **2012,** *14*, 415-426.
5. Eijsink, V. G. H.; Gaseidnes, S.; Borchert, T. V.; Van den Burg, B., Directed evolution of enzyme stability. *Biomolecular Engineering* **2005,** *22*, 21-30.
6. Veronese, F. M., Peptide and protein PEGylation: a review of problems and solutions. *Biomaterials* **2001,** *22*, 405-417.
7. Klibanov, A. M., Improving enzymes by using them in organic solvents. *Nature* **2001,** *409*, 241-246.
8. Armand, M.; Endres, F.; MacFarlane, D. R.; Ohno, H.; Scrosati, B., Ionic-liquid materials for the electrochemical challenges of the future. *Nature Materials* **2009,** *8*, 621-629.
9. Welton, T., Room-temperature ionic liquids. Solvents for synthesis and catalysis. *Chemical Reviews* **1999,** *99*, 2071-2083.
10. MacFarlane, D. R.; Forsyth, M.; Howlett, P. C.; Pringle, J. M.; Sun, J.; Annat, G.; Neil, W.; Izgorodina, E. I., Ionic Liquids in Electrochemical Devices and Processes: Managing Interfacial Electrochemistry. *Accounts of Chemical Research* **2007,** *40*, 1165-1173.
11. Yang, S. Y.; Cicoira, F.; Byrne, R.; Benito-Lopez, F.; Diamond, D.; Owens, R. M.; Malliaras, G. G., Electrochemical transistors with ionic liquids for enzymatic sensing. *Chemical Communications* **2010,** *46*.
12. Jain, N.; Kumar, A.; Chauhan, S.; Chauhan, S. M. S., Chemical and biochemical transformations in ionic liquids. *Tetrahedron* **2005,** *61*, 1015-1060.
13. Ohno, H., Electrochemical aspects of ionic liquids. In John Wiley & Sons, Inc.: **2005**.
14. Fujita, K.; Forsyth, M.; MacFarlane, D. R.; Reid, R. W.; Elliott, G. D., Unexpected improvement in stability and utility of cytochrome c by solution in biocompatible ionic liquids. *Biotechnology and Bioengineering* **2006,** *94*, 1209-1213.
15. Lai, J.-Q.; Li, Z.; Lu, Y.-H.; Yang, Z., Specific ion effects of ionic liquids on enzyme activity and stability. *Green Chemistry* **2011,** *13*, 1860-1868.
16. Constatinescu, D.; Herrmann, C.; Weingartner, H., Patterns of protein unfolding and protein aggregation in ionic liquids. *Physical Chemistry Chemical Physics* **2010,** *12*, 1756-1763.
17. Weaver, K. D.; Vrikkis, R. M.; Van Vorst, M. P.; Trullinger, J.; Vijayaraghavan, R.; Foureau, D. M.; McKillop, I. H.; MacFarlane, D. R.; Krueger, J. K.; Elliott, G. D., Structure and function of proteins in hydrated choline dihydrogen phosphate ionic liquid. *Physical Chemistry Chemical Physics* **2012,** *14*, 790-801.

18. Vijayaraghavan, R.; Izgorodin, A.; Ganesh, V.; Surianarayanan, M.; MacFarlane, D. R., Long-term structural and chemical stability of DNA in hydrated ionic liquids. *Angewandte Chemie International Edition* **2010,** *49*, 1631-1633.

19. Vijayaraghavan, R.; Thompson, B. C.; MacFarlane, D. R.; Kumar, R.; Surianarayanan, M.; Aishwarya, S.; Sehgal, P. K., Biocompatibility of choline salts as crosslinking agents for collagen based biomaterials. *Chemical Communications* **2010,** *46*, 294-296.

20. Weaver, K. D.; Kim, H. J.; Sun, J.; MacFarlane, D. R.; Elliott, G. D., Cyto-toxicity and biocompatibility of a family of choline phosphate ionic liquids designed for pharmaceutical applications. *Green Chemistry* **2010,** *12*, 507-513.

21. Fujita, K.; Murata, K.; Masuda, M.; Nakamura, N.; Ohno, H., Ionic liquids designed for advanced applications in bioelectrochemistry. *RSC Advances* **2012,** *2*, 4018-4030.

22. Opallo, M.; Lesniewski, A., A review on electrodes modified with ionic liquids. *Journal of Electroanalytical Chemistry* **2011,** *656*, 2-16.

23. Khodagholy, D.; Curto, V. F.; Fraser, K. J.; Gurfinkel, M.; Byrne, R.; Diamond, D.; Malliaras, G. G.; Benito-Lopez, F.; Owens, R. M., Organic electrochemical transistor incorporating an ionogel as a solid state electrolyte for lactate sensing. *Journal of Materials Chemistry* **2012,** *22*, 4440-4443.

24. Phypers, B.; Pierce, J. T., Lactate physiology in health and disease. *Continuing Education in Anaesthesia, Critical Care & Pain* **2006,** *6*, 128-132.

25. Green, J. M.; Pritchett, R. C.; Crews, T. R.; McLester, J. R.; Tucker, D. C., Sweat lactate response between males with high and low aerobic fitness. *European Journal of Applied Physiology* **2004,** *91*, 1-6.

26. Lillis, B.; Grogan, C.; Berney, H.; Lane, W. A., Investigation into immobilisation of lactate oxidase to improve stability. *Sensors and Actuators B: Chemical* **2000,** *68*, 109-114.

27. Minagawa, H.; Yoshida, Y.; Kenmochi, N.; Furuichi, M.; Shimada, J.; Kaneko, H., Improving the thermal stability of lactate oxidase by directed evolution. *Cellular and Molecular Life Sciences* **2007,** *64*, 77-81.

28. Leiros, I.; Wang, E.; Rasmussen, T.; Oksanen, E.; Repo, H.; Petersen, S. B.; Heikinheimo, P.; Hough, E., The 2.1 A structure of aerococcus viridans L-lactate oxidase (LOx). *Acta Crystallogr.,Sect.F* **2006** 1185.

29. Winther-Jensen, O.; Vijayaraghavan, R.; Sun, J.; Winther-Jensen, B.; MacFarlane, D. R., Self polymerising ionic liquid gel. *Chemical Communications* **2009**, 3041-3043.

30. MacFarlane, D. R.; Vijayaraghavan, R.; Ha, H. N.; Izgorodin, A.; Weaver, K. D.; Elliott, G. D., Ionic liquid "buffers"-pH control in ionic liquid systems. *Chemical Communications* **2010,** *46*, 7703-7705.

31. Whitmore, L.; Wallace, B. A., Protein secondary structure analyses from circular dichroism spectroscopy: Methods and reference databases. *Biopolymers* **2008,** *89*, 392-400.

32. Whitmore, L.; Wallace, B. A., DICHROWEB, an online server for protein secondary structure analyses from circular dichroism spectroscopic data. *Nucleic Acids Research* **2004,** *32*, W668-W673.

33. Weibels, S.; Syguda, A.; Herrmann, C.; Weingartner, H., Steering the enzymatic activity of proteins by ionic liquids. A case study of the enzyme kinetics of yeast alcohol dehydrogenase. *Physical Chemistry Chemical Physics* **2012,** *14*, 4635-4639.

34. Benjwal, S.; Verma, S.; Röhm, K.-H.; Gursky, O., Monitoring protein aggregation during thermal unfolding in circular dichroism experiments. *Protein Science* **2006,** *15*, 635-639.

35. Berg, J. M.; Tymoczko, J. L.; Stryer, L., Biochemistry. *Section 8.4* - The Michaelis-Menten Model Accounts for the Kinetic Properties of Many Enzymes, W. H. Freeman**, 2002.,** *5th edition*.

36. Yang, Z., Hofmeister effects: an explanation for the impact of ionic liquids on biocatalysis. *Journal of Biotechnology* **2009,** *144*, 12-22.

37. Fujita, K.; MacFarlane, D. R.; Forsyth, M.; Yoshizawa-Fujita, M.; Murata, K.; Nakamura, N.; Ohno, H., Solubility and stability of cytochrome c in hydrated ionic liquids: effect of oxo acid residues and kosmotropicity. *Biomacromolecules* **2007,** *8*, 2080-2086.

38. Zhao, H., Methods for stabilizing and activating enzymes in ionic liquids - a review. *Journal of Chemical Technology and Biotechnology* **2010,** *85*, 891-907.

39. Zhao, H.; Olubajo, O.; Song, Z.; Sims, A. L.; Person, T. E.; Lawal, R. A.; Holley, L. A., Effect of kosmotropicity of ionic liquids on the enzyme stability in aqueous solutions. *Bioorganic Chemistry* **2006,** *34*, 15-25.

40. Mann, J. P.; M c Cluskey, A.; Atkin, R., Activity and thermal stability of lysozyme in alkylammonium formate ionic liquids-influence of cation modification. *Green Chemistry* **2009,** *11*, 785-792.

41. Hekmat, D.; Hebel, D.; Joswig, S.; Schmidt, M.; Weuster-Botz, D., Advanced protein crystallization using water-soluble ionic liquids as crystallization additives. *Biotechnology Letters* **2007,** *29*, 1703-1711.

42. Maeda-Yorita, K.; Aki, K.; Sagai, H.; Misaki, H.; Massey, V., L-lactate oxidase and L-lactate monooxygenase: Mechanistic variations on a common structural theme. *Biochimie* **1995,** *77*, 631-642.

43. MacFarlane, D. R.; Pringle, J. M.; Johansson, K. M.; Forsyth, S. A.; Forsyth, M., Lewis base ionic liquids. *Chemical Communications* **2006**, 1905-1917.

44. Thompson, B. C.; Winther-Jensen, O.; Winther-Jensen, B.; MacFarlane, D. R., A Solid-state pH Sensor for nonaqueous media including ionic liquids. *Analytical Chemistry* **2013,** *85*, 3521-3525.

Chapter 7

Fast Prototyping of Paper-based Micro-fluidic Devices by Contact Stamping Using Indelible Ink

Vincenzo F. Curto[‡1], Nuria Lopez-Ruiz[‡2], L.F. Capitan-Valley[3], A.J. Palma[2], F. Benito-Lopez[1,4*] and D. Diamond[1]

Lab on a Chip – Submitted

[1]CLARITY: Centre for Sensor Web Technologies, National Centre for Sensor Research, School of Chemical Sciences, Dublin City University, Dublin 9, Ireland
[2] ECSENS, Dept. of Electronics and Computer Technology, ETSIIT, University of Granada, Granada, Spain.
[3] ECSENS, Dept. of Analytical Chemistry, Faculty of Sciences, University of Granada, Granada, Spain.
[4] CIC microGUNE, Arrasate-Mondragón.

*Author to whom correspondence should be addressed;

Abstract

This chapter presents a fast and cheap prototyping technique for the realisation of paper-based micro-fluidic devices simply by using a stamp and indelible ink. The proposed mechanism implies contact stamping of indelible ink to laboratory filter paper using a PDMS stamp, which defines the micro-fluidic structure. It is a cleanroom and washing steps-free method which provides a reproducible way for the production of functional paper-based micro-fluidic devices in a single step in less than 10 seconds. The method is fully characterised and the concept has been applied, as a proof-of-principle, for the realisation of a low-cost colorimetric glucose sensor.

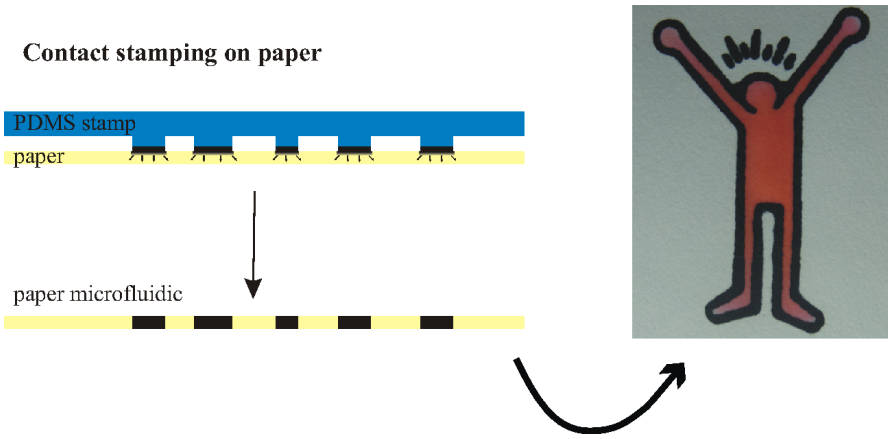

Keywords: paper-base micro-fluidic; contact stamping; indelible ink; glucose.

7.1 Introduction

This chapter describes the development of a single step technology for the realisation of paper-based micro-fluidic devices, where indelible ink is transferred from a PDMS stamp to laboratory filter paper by contact stamping, generating a micro-fluidic structure in less than 10 seconds. The indelible ink acts as a barrier for the liquid, which is forced to move inside the stamped micro-fluidic structure.

Paper-based micro-fluidics have been identified as an ideal approach for preparing low-cost and easy/ready-to-use analytical platforms for Point of care (POC) diagnostic devices.[1] In particular, there are important opportunities for paper-based micro-fluidic devices for fast health screening of large numbers of individuals in developing countries, for instance, where sophisticated technologies are poor or non-existent.[2, 3] Paper-based micro-fluidics could also have a positive impact on monitoring medical disorders such as diabetes and AIDS among others, for which early diagnosis is crucial.[4] Moreover, paper-based micro-fluidic devices could also play an important role on the development of sensors for on-site environmental monitoring at the point-of-need.[5] For example, fresh water management is of crucial importance for pre-risk assessment of fresh water stream in developing countries, as poor environmental conditions can cause the development of severe human disorders like cholera.[6]

Another interesting aspect of paper-based micro-fluidic technology is the high compatibility of nitrocellulose with many chemical reagents and biological relevant substances,[7] making paper a suitable substrate for its integration with different analytical techniques, such as electrochemical,[8] electrochemiluminescence,[9] chemilumines-cence[10] and colourimetric.[11] Ideally, the most interesting way of detection could imply a colour or light intensity variation monitored by means of a mobile phone camera.[12] The coupling of such technologies would open new opportunities toward the realisation of a wireless sensor network (WSN) in the field of chemical and biochemical sensing for environmental and health monitoring.[13]
On the fabrication side, new paper micro-fluidic fabrication protocols continuously appear in the literature. Shen *et al.*[7] recently summarised the *pros* and *cons* of many of these protocols. Photolithography[14] and CO_2 laser treatment[15] techniques, for instance, provide high resolution patterning of paper but, on the other

hand, the final devices are not flexible and compatible with lateral flow assays, respectively. Whitesides *et al.*[16] also proposed a FLASH photolithography method where there is no need for a clean room, reducing substantially the production costs. However, while the use of wax for the hydrophibisation of paper normally needs an extra heating step, *e.g.* wax diffusion in paper, which can increase fabrication costs.[17, 18]

This Chapter describes a fast and reproducible, one-step fabrication method for the production of paper-based micro-fluidic devices on laboratory filter paper. The innovation of this technique lies on the simplicity of its fabrication method, as it requires only a PDMS stamp with the designed features along with the paper and ink. In contrast to the view that ink printing techniques are not suitable for the fabrication of paper-based micro-fluidic devices,[16] it is demonstrated that by taking advantage of the absorbing capability of filter paper it is possible to create paper-based micro-fluidics by simple contact stamping. While the use of indelible ink to create micro-fluidic structures has been reported previously,[19, 20] to the best of our knowledge this is the first time that direct contact stamping of paper-based micro-fluidics has been performed using commercially available ink.

7.2 Materials and Methods

The micro-fluidic platform was fabricated using standard laboratory filter paper (Whatman© grades 1 and 595), which adsorbs the ink through its full thickness and defines the borders and so the flow channels of the micro-fluidic structure. Three different inks were examined: Black fountain pen ink from Noodler's Ink™ (*Product Code: 19001),* Black *214 Stamp Ink* from HITT Marking Devices Inc. and Lumocolor© Permanent Universal Black Ink (kindly provided by Staedtler Mars GmbH & Co. KG). Lumocolor© ink viscosity was reduced by using a solvent mixture made of a 1:1 *v/v* ethanol-n-propanol, 10:1 ink-solvent mixture. The main attractive characteristics of the listed inks are their hydrophobic nature when dry, and short drying times.

The contact stamping is performed using PDMS stamps (10:3 *w/w* monomer-curing agent), cured at 60 °C for 8 h. In order to control the volume of ink transferred from the PDMS stamp to the filter paper, the inking of PDMS is performed using a

stone ink-pad (2" x 4" rectangle from HITT Marking Devices©). Based on the company specifications, the ink-pad is capable of providing a constant ink flow from the porous stone when in contact with the stamp. Moreover, the ink-pad can be used with solvent/acid based industrial inks, which cannot be employed with standard pads. The PDMS stamp was incorporated onto a custom made rectangular prism made of aluminum and a layer of a black ceramic material (see Figure 1D, Appendix D). The dimensions of the prism are 4.35 x 5.1 x 7.6 cm (H x W x L) with a total weight of 440 g. The stamping device (PDMS stamp/rectangular prism) will be referred to as 'PDMS stamp' from now on.

The PDMS negative molds were fabricated through a micromiller (CAT3D, Datron, UK) using 4 mm thick PMMA (poly methyl metacrylate) as substrate, although other materials could be employed. First, a 3 mm flat endmill was used to shave off 300 μm of material in order to flatten the PMMA surface. Following this, a 600 μm deep pocket of suitable *x* and *y* dimensions was milled out. Using flat endmills of appropriate dimensions, the required negative mold was milled out starting from the bottom of the pocket. All designs were performed using Solid Works© Student version 2012 and converted to the final toolpaths using AutoDesk© HSMxpress.

The inking process was performed by gently pushing the PDMS stamp three times against the ink saturated stone pad. This step was followed by exposing the inked PDMS to air for 5 seconds, in order to remove any air bubbles formed on top of the PDMS stamp. The presence of air bubbles on the surface of the inked PDMS occurs as a consequence of the air that is expelled from the pores of the stone during the inking process. Finally the PDMS stamp was placed in contact with the laboratory filter paper for three seconds, without the application of any force.

The glucose paper based assay was performed by spotting 2 μL of a fresh PBS solution (pH = 7.4) containing 67 U mL^{-1} of Glucose Oxidase (GOx), 100 U $mL^{-1}$of Horseradish Peroxidase (HRP), 0.3 mM Trehalose, 6 mM 4AAP and 12 mM HBA. Functionalised paper-based micro-fluidic devices were dried at RT and used the same day. Photographs of the paper-based micro-fluidic devices were taken using a Canon PowerShot G7 camera in a controlled light intensity area. After transferring the images to the computer, the analysis of the sensing area colour change was performed using a script and functions on Matlab R2007b© (The MathWorks, Inc., Natick, MA, USA).

7.3 Results and Discussion

7.3.1 Ink Selection

During the evaluation of the most suitable ink for the stamping process, the three selected inks (see above) were tested by simply drop casting a 1 μL of each onto Whatman© filter paper grade 1. The Noodler's Ink™ sample was found to be unsuitable for stamping the filter paper for two reasons. Firstly, a yellowish ring (most probably due to separation of components in the ink) formed around the outer rim of the ink spot (see Figure 2D, Appendix D) and secondly, despite its hydrophobic nature, this ink did not coherent hydrophobic barriers in the paper (see Video 1 ESI†). For these two reasons it was decided not to use Noodler's™ Black Ink for further experiments. In contrast, neither the Black *214* nor the Black Lumocolor© showed this yellowish ring after being drop cast on paper.

After the ink stains were dried at room temperature for 5 minutes (enough time to assume that the solvent of the inks is completely evaporated), the hydrophobicity of the two inked papers was then characterised by placing a 2 μL drop of DI water on top. Black *214* is described by the manufacturer as a "*waterproof ink with excellent adhesion",* while Black Lumocolor© ink is similarly claimed to be a water- and weather-proof ink with drying time of seconds. However, Black *214* did not make the paper hydrophobic enough, displaying similar behaviour to Noodler's™ Black Ink. Furthermore, a yellowish substance leached out from the inked area just after the DI water droplet was absorbed by the paper during testing, Figure 7.1-a. In contrast, Black Lumocolor© ink makes the stained regions of the paper very hydrophobic, as the water droplet was able to sit on top of it for several minutes without being absorbed, as shown in Figure 7.1-b. These results demonstrated that only the Black Lumocolor© ink is capable of making stained areas of paper suitably hydrophobic, and therefore it was selected for fabrication of the paper-based micro-fluidic devices. Videos 2 and 3 of the ESI† show the behaviour of the papers when water droplets are placed on inked-regions.

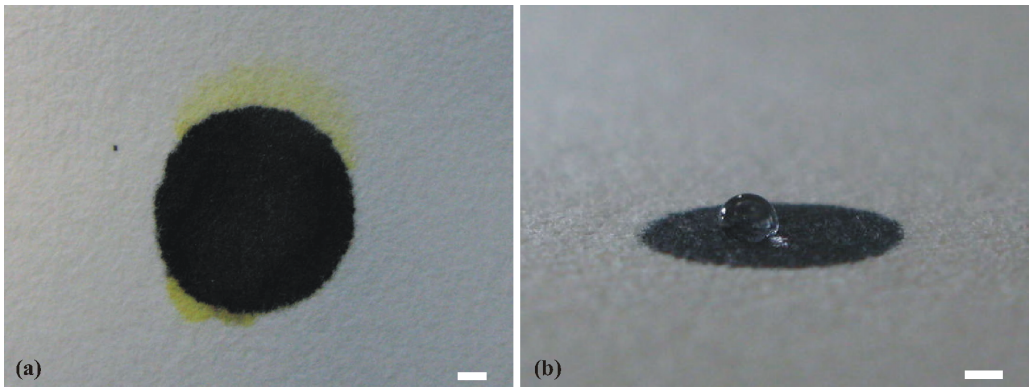

Figure 7.1. Whatman filter paper grade 1 spotted with 1 µL of (a) Black *214* and *(b)*Black Lumocolor© inks. The two pictures show the different behavior of the paper upon placing a 2 µL DI water droplet on top of the ink spots. Coloured components can be clearly seen leaching from the Black 214 sample as the droplet is absorbed and passes from the centre to the outer edge of the droplet by capillary action. In contrast, the droplet sits in a stable manner on top of the Black Lumocolor spot and is still clearly visible after 5 minutes (Scale bar: 1 mm).

It is well known that a functional paper-based micro-fluidic device will be produced only if the patterned hydrophobic barrier (normally polymers) penetrates the entire thickness of the paper to the distal surface, otherwise the liquid flow may continue beneath the micro-fluidic borders making the paper-based micro-fluidic channel inoperative.[16] Therefore, while these initial tests had confirmed that Black Lumocolor© ink provides a sufficient hydrophobic barrier, it was particularly important to establish if the stamping process was capable of generating a continuous barrier that could fully retain water across the entire thickness of the paper.

Figure 7.2-a and c show stamped rings generated using a PDMS stamp with an internal diameter of 3 mm and outer diameter of 4.1 mm, where two different viscosities of Black Lumocolor© ink were used. The ring shown in Figure 5.2a was generated using Black Lumocolor© ink as received by Staedtler Mars GmbH & Co. KG, while the ring in Figure 7.2-c was stamped using a 10:1 *v/v* solution of the Black Lumocolor© ink and a thinning solvent (see materials and methods), in order to obtain a less viscous formulation, without losing substantial ink hydrophobicity for the pattering of paper.

The two inset pictures on the top right of Figure 7.2-a and c show the reverse (distal) side of the stamped ink rings. Comparing these two images, it appeared that the transferred ink ring on the reverse side of the paper was not as effective for the commercial ink formulation.

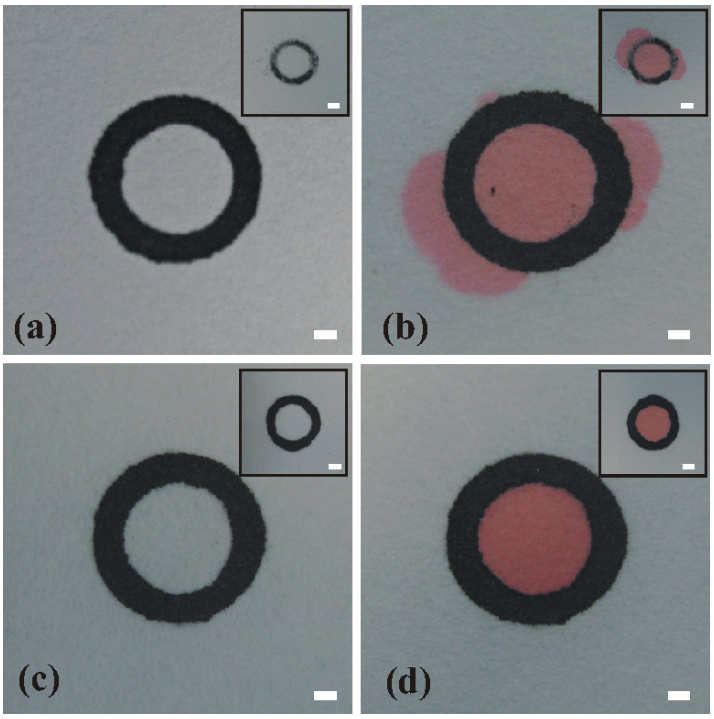

Figure 7.2. Rings stamped in Whatman filter paper grade 1 using Black Lumocolor© ink of two different viscosities: used as received from Staedtler Mars GmbH & Co. KG (a, b) and diluted 10:1 to decrease viscosity with the thinning solvent (c, d). Pictures b and d show the rings after the addition of 4 μL of red food dye aqueous solution was placed inside the rings. Insertion pictures show the reverse side of the inked paper (Scale bars: 1 mm for the main pictures and 2 mm for inset pictures)

In fact, the inset of Figure 7.2-a shows the ink was not completely absorbed throughout the thickness of the paper, since a less intense and somewhat patchy black colour ring can be seen when compared to the inset picture of Figure 7.2-c. Performing contact stamping with the ink as provided does not ensure appropriate fabrication conditions. On the other hand, using only a 10:1 *v/v* formulation of ink/thinning solvent[iv], suitable contact stamping fabrication conditions achieved a continuous barrier against the diffusion of water from the interior region is provided. This is verified by comparing Figure 7.2-b and Figure 7.2-d where, upon the addition of 4 μL of a red food dye water solution, the liquid can be contained inside the stamped ring just when the less viscous ink formulation is employed.

[iv] Experiments using higher volume ratio of ink/thinning solvent, *e.g.* 10:2 and 10:3 *v/v*, still provided a hydrophobic barrier against water but, at the same time, higher dimensional deviations of transferred ink features were observed as the increment of available solvent induced a faster flow of the ink through and across the paper fibres (data not shown).

7.3.2 Contact Stamping Performance

In order to explore the functionality of the paper-based micro-fluidic devices made using this technique, a series of open straight channels (L x W = 6 x 1.5 cm) were stamped on paper using several PDMS stamps with varying dimensions. In order to define the open channel structures on paper, a pair of borders of equal width was employed. For instance, the channel border pairs were varied from 200 μm to 1200 μm, in steps of 100 μm. This range of border widths was chosen to find the minimum channel border width required to make effective fluidic structures. In addition, Whatman grade 1 and 595 laboratory filter papers were employed throughout these experiments, in order to understand if their different flow rates (respectively medium and medium fast) influence the ink stamping effectiveness.

Two main parameters were considered to be particularly critical for the realisation of useful paper-based micro-fluidic devices, such as the width of the stamped borders and the final width of the micro-fluidic channel. Figure 7.3 shows the percentage increment of the stamped border width (W_b - left hand side *y* axis) and the percentage of the achieved channel width (W_c - right hand side *y* axis) *versus* the width of the employed PDMS stamp. W_b and W_c can be defined as follows:

$$\%W_b = (W_{sb}/W_{PDMS})\, x\, 100$$

$$\%W_c = (W_{sc}/W)\, x100$$

where W_{sb} is the stamped border width on the paper, W_{PDMS} is the width of the border of the employed PDMS stamp, W_{SC} is the stamped channel width on the paper obtained using a stamp channel width of W, in this case 1.5 cm (schematic representation Figure 3D, Appendix D).

The results show that W_b decreases as the stamp width increases. For instance, for both paper types, a 200 μm border of the PDMS stamp, produced features on paper that were over 300 % the initial value, *i.e.* > 600 μm. Larger channel border pairs produced wider stamped features in absolute terms, but smaller in relative terms. This effect can be explained as the ink loaded on the PDMS stamp, when in contact with the paper, is preferentially absorbed by the fibers of the paper perpendicularly to the applied stamp pressure in an isotropic manner along the paper-

air interface. However, this behaviour is less pronounced when the border stamp width is increased. In fact from 900 μm onward a plateau region (between ~ 137 % and ~ 125 %) can be observed for both paper types. In this case the loaded ink still spreads along the paper-air interface, but an increasing proportion of it is also absorbed through the paper thickness, as more ink is available. As consequence of the increase of the feature border width W_{sb} on paper, the final size of the micro-fluidic channel width is affected as well, *i.e.* W_c in Figure 7.3. In particular as W_{PDMS} increases, the decrease on the stamped channel width is less pronounced.

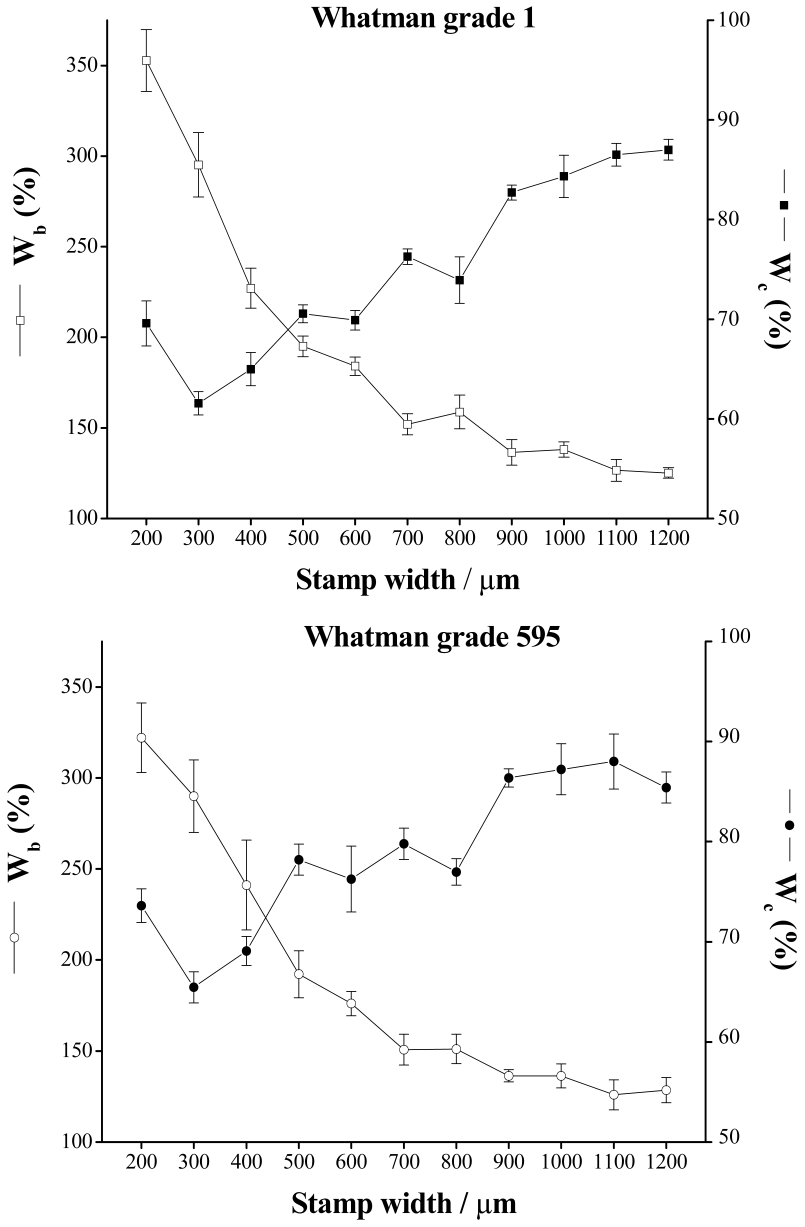

Figure 7.3. Percentage of border width variation (W_b) and final channel width (W_c) for open straight channels with different border width on Whatman grade 1 *(top)* and grade 595 *(bottom)* filter papers (n = 5).

Moreover, this effect gradually levels off when the PDMS stamp is > *ca.* 900 µm. This result is particularly critical if paper-based micro-fluidic devices of well defined channel widths are required. Therefore during fabrication of paper-based micro-fluidics using this approach, the effective channel reduction factor has to be taken into account when designing the micro-fluidic structure. An interesting outcome of these results is that no substantial differences in the behaviour of the two different paper grades was observed, except for slightly higher reproducibility of the features generated with the Whatman grade 1 paper, as the average of the standard deviation is 8.36 % and 11.35 % for Whatman grade 1 and 595, respectively (smaller error bars, Figure 7.3). Therefore, for the rest of the experiments, only Whatman grade 1 was used.

It is important to appreciate that functional fluidic channels were not obtained for all conditions used in these experiments. As mentioned previously, when smaller micro-fluidic borders are used, most on the ink spreads along the top surface of the paper, without penetrating completely to the reverse side, which allows liquid to leak across the boundary of the defined fluidic channel (for example, see the inset image, Figure 7.2-b). Therefore the volume of ink that can be loaded onto the surface of the PDMS stamp during the inking step is crucial for producing functional structures.

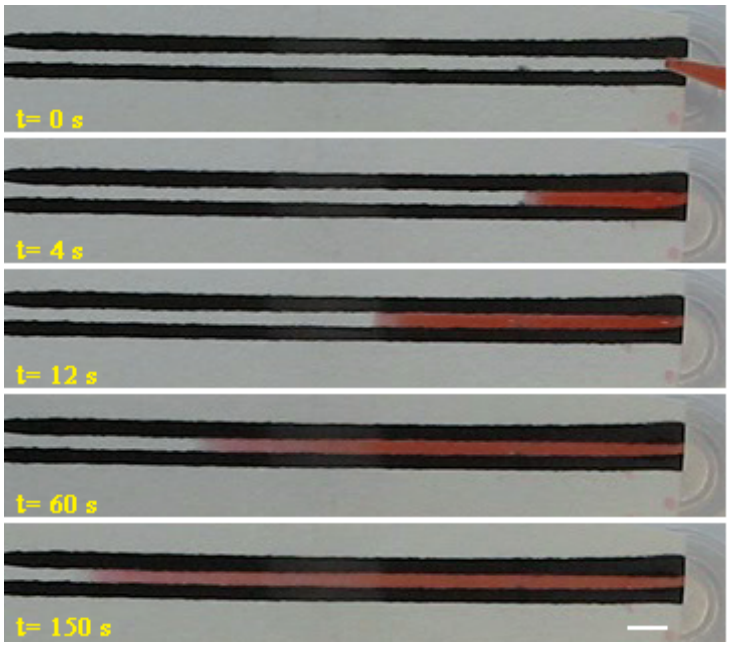

Figure 7.4. Sequence of video frames from a µPAD formed on Whatman grade 1 paper tracking the movement of 20 µL of a red food dye solution. Stamping conditions: PDMS stamp border width 1100 µm, Black Lumocolor© ink thinned formulation, average flow speed = 1.3 mm s^{-1} (Scale bar: 3.5 mm).

Higher volumes of ink are retained with increasing the PDMS stamp width and it was observed that only stamps with borders ≥ 1100 μm have an acceptable performance. Figure 7.4 shows a set of video frames recorded when 20 μL of an aqueous solution of a red food dye was placed at the right end of a channel. No leakage was observed over the entire length of the channel, demonstrating the applicability of this technique for the fabrication of paper-based micro-fluidic devices.

7.3.3 Stamping of Cheap Paper-based Micro-fluidic Glucose Sensors

Since the first development of paper-based micro-fluidic devices, the main explored application has been in the field of clinical diagnosis, where the demand for low cost, robust and reliable systems is very high. As proof of concept, a colourimetric glucose sensor was designed and fabricated using contact stamped paper- based micro-fluidic device composing of a straight channel of dimensions 10 x 2 mm (L x W) followed by a circular sensing area of diameter equal to 1.9 mm.

The colourimetric glucose assay was performed utilising 4-aminoantipyrine (4AAP) and 4-hydroxybenzoic acid (HBA) chromogenic system in the presence of HRP and GOx. All the chemical were purchased form Sigma-Aldrich and used as received. The stoichiometry of the chromogenic reaction is as follows:

$$Glucose + O_2 \xrightarrow{GO_x} Gluconic\ acid + H_2O_2$$

$$2\,H_2O_2 + 4AAP + HBA \xrightarrow{HRP} quinoneimine\ dye + 4\,H_2O$$

leading to the formation of a red coloured dye with λ_{max} = 510 nm.

The developed detection code allows cropping of the area of interest for a given photograph in order to extrapolate the red, green and blue components of the RGB colour space for the area of interest. Once the area is selected, a zeros and ones mask of the whole picture is stored and used as a reference to register the position of the pixels of interest (non-zero values of the mask). Using the mask, the red, blue and green components are obtained for each pixel of the region of interest and stored in

R, G and B matrixes. Each matrix keeps the corresponding component information for the whole cropped area. From these data, the mode of each matrix is calculated, which is the value that appears most frequently. Finally, mode values are taken as the three final RGB components of the whole area.[21] Figure 7.5 shows the variation in the R/B ratio (red and blue component) for digital images taken of the sensor *versus* concentration of glucose, in the relevant physiological range. A linear model was used to fit the experimental data points. The inset pictures show the difference in the colour (red) of the assay obtained with 0.05 mM, 4.0 mM and 20 mM glucose samples. In the current manifestation of the sensor, the red coloured dye generated an even colour across the detection area without leaching beneath the paper-based micro-fluidic device border, proving the feasibility of the proposed fabrication method and indicating its potential application for a wide range of potential applications.

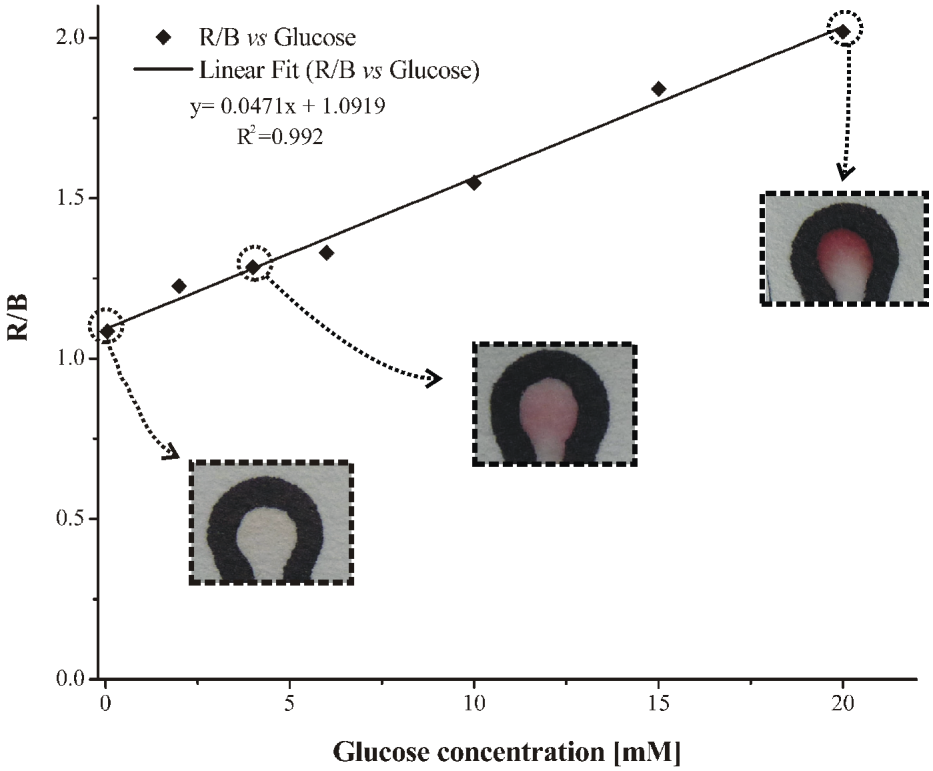

Figure 7.5. Calibration curve of the colourimetric paper-based micro-fluidic glucose sensor device.

Considering only the price of the materials used *i.e.* paper and ink, the estimate unit production cost is as follows. The laboratory filter paper Whatman grade 1 (VWR international) is ~ €1.74 per sheet (460 x 570 mm), of which only a small portion (15 x 10 mm) was required per unit ~ €0.001. Black Lumocolor© costs €30

per litre (commercial value provided by Staedtler Mars GmbH & Co. KG); the volume of ink employed for the stamping of the glucose paper-based micro-fluidic device was calculated to be ~ 10 μL, which gives a cost of only ~ €0.0003. Therefore the average total cost of production of one paper-based micro-fluidic device was estimated to be as little as ~ €0.0015.

7.4 Conclusions

A fast (10s) and simple method to produce paper-based micro-fluidic devices by contact stamping using a PDMS stamp has been developed. Black Lumocolor© ink can form effective hydrophobic barriers that constrain the diffusion of water within the boundaries of the ink pattern. The contact stamping performance was characterised using open straight channels, revealing that operative micro-fluidic device can be obtained only using stamps with borders ≥ 1100 μm.

Compared to other reported paper-based micro-fluidic device fabrication technologies, contact stamping is capable of providing an easy way to produce paper-based micro-fluidic structures without sophisticated infrastructural requirements. Furthermore, this approach can be used for mass production of paper-based micro-fluidic device sensors by non-specialist staff, which could be important for producing diagnostic devices in developing countries.

Acknowledgements

This work was supported by Science Foundation Ireland under grant 07/CE/I1147 and a Research Career Start Programme 2010 fellowship from Dublin City University. Thanks to Staedtler Mars GmbH & Co. KG. (Germany) for supplying the Lumocolor© Permanent Universal Ink Black.

Appendix D. Supporting information

Electronic Supplementary Information (ESI) (appendix D) available: Figure D1 shows the contact stamping apparatus, Figure D2 the yellowish ring generated from the staining of Whatman grade 1 using Black Noodler's Ink and Figure D3 scheme of the fabrication of paper-based micro-fluidics using the contact stamping. Video 1, Video 2 and Video 3 (ESI of the published version) show the behaviour of the inked

papers when water is drop cast on top, respectively for Black Fountain Pen Ink from Noodler's InkTM, Black *214 Stamp Ink* from HITT Marking Devices Inc. and Lumocolor© Permanent Universal Ink Black from Staedtler Mars GmbH & Co. KG.

7.5 References

1. Gubala, V.; Harris, L.; Ricco, A.; Tan, M.; Williams, D., Point of care diagnostics: status and future. *Analytical Chemistry* **2012,** *84*, 487-1002.
2. Martinez, A. W.; Phillips, S. T.; Whitesides, G. M.; Carrilho, E., Diagnostics for the Developing World: Microfluidic Paper-Based Analytical Devices. *Analytical Chemistry* **2009,** *82*, 3-10.
3. Govindarajan, A. V.; Ramachandran, S.; Vigil, G. D.; Yager, P.; Bohringer, K. F., A low cost point-of-care viscous sample preparation device for molecular diagnosis in the developing world; an example of microfluidic origami. *Lab on a Chip* **2012,** *12*, 174-181.
4. Mao, X.; Huang, T. J., Microfluidic diagnostics for the developing world. *Lab on a Chip* **2012,** *12*, 1412-1416.
5. Mentele, M. M.; Cunningham, J.; Koehler, K.; Volckens, J.; Henry, C. S., Microfluidic Paper-Based Analytical Device for Particulate Metals. *Analytical Chemistry* **2012,** *84*, 4474-4480.
6. Bunyakul, N.; Edwards, K.; Promptmas, C.; Baeumner, A., Cholera toxin subunit B detection in microfluidic devices. *Analytical and Bioanalytical Chemistry* **2009,** *393*, 177-186.
7. Li, X.; Ballerini, D. R.; Shen, W., A perspective on paper-based microfluidics: Current status and future trends. *Biomicrofluidics* **2012,** *6*, 011301.
8. Dungchai, W.; Chailapakul, O.; Henry, C. S., Electrochemical Detection for Paper-Based Microfluidics. *Analytical Chemistry* **2009,** *81*, 5821-5826.
9. Wang, S.; Ge, L.; Zhang, Y.; Song, X.; Li, N.; Ge, S.; Yu, J., Battery-triggered microfluidic paper-based multiplex electrochemiluminescence immunodevice based on potential-resolution strategy. *Lab on a Chip* **2012,** *12*, 4489-4498.
10. Yu, J.; Ge, L.; Huang, J.; Wang, S.; Ge, S., Microfluidic paper-based chemiluminescence biosensor for simultaneous determination of glucose and uric acid. *Lab on a Chip* **2011,** *11*, 1286-1291.
11. Dungchai, W.; Chailapakul, O.; Henry, C. S., Use of multiple colorimetric indicators for paper-based microfluidic devices. *Analytica Chimica Acta* **2010,** *674*, 227-233.
12. Garcia, A.; Erenas, M. M.; Marinetto, E. D.; Abad, C. A.; de Orbe-Paya, I.; Palma, A. J.; Capitan-Vallvey, L. F., Mobile phone platform as portable chemical analyzer. *Sensors and Actuators B: Chemical* **2011,** *156*, 350-359.
13. Diamond, D., Internet-Scale Sensing. *Analytical Chemistry* **2004,** *76*, 278 A-286 A.
14. Martinez, A. W.; Phillips, S. T.; Butte, M. J.; Whitesides, G. M., Patterned Paper as a Platform for Inexpensive, Low-Volume, Portable Bioassays. *Angewandte Chemie International Edition* **2007,** *46*, 1318-1320.
15. Chitnis, G.; Ding, Z.; Chang, C.-L.; Savran, C. A.; Ziaie, B., Laser-treated hydrophobic paper: an inexpensive microfluidic platform. *Lab on a Chip* **2011,** *11*, 1161-1165.

16. Martinez, A. W.; Phillips, S. T.; Wiley, B. J.; Gupta, M.; Whitesides, G. M., FLASH: A rapid method for prototyping paper-based microfluidic devices. *Lab on a Chip* **2008,** *8*, 2146-2150.
17. Carrilho, E.; Martinez, A. W.; Whitesides, G. M., Understanding Wax Printing: A Simple Micropatterning Process for Paper-Based Microfluidics. *Analytical Chemistry* **2009,** *81*, 7091-7095.
18. Songjaroen, T.; Dungchai, W.; Chailapakul, O.; Laiwattanapaisal, W., Novel, simple and low-cost alternative method for fabrication of paper-based microfluidics by wax dipping. *Talanta* **2011,** *85*, 2587-2593.
19. Nie, J.; Zhang, Y.; Lin, L.; Zhou, C.; Li, S.; Zhang, L.; Li, J., Low-Cost Fabrication of Paper-Based Microfluidic Devices by One-Step Plotting. *Analytical Chemistry* **2012,** *84*, 6331-6335.
20. Fang, X.; Chen, H.; Jiang, X.; Kong, J., Microfluidic Devices Constructed by a Marker Pen on a Silica Gel Plate for Multiplex Assays. *Analytical Chemistry* **2011,** *83*, 3596-3599.
21. Cantrell, K.; Erenas, M. M.; de Orbe-PayaÃÅ, I.; CapitaÃÅn-Vallvey, L. F., Use of the Hue Parameter of the Hue, Saturation, Value Color Space As a Quantitative Analytical Parameter for Bitonal Optical Sensors. *Analytical Chemistry* **2009,** *82*, 531-542.

Chapter 8

Future Work and Perspectives

Wearable Chemo/bio-sensors for Sweat Sensing in Sports Applications: Combining Micro-fluidics and Novel Materials

In recent years point-of-care technology has seen growing interest since the possibility to integrate and link this technology with every day devices (*e.g.* mobile phone) is becoming a reality and this will have a huge impact on the future of home-based health management. Advances in wearable technologies will make a critical contribution to achieving the ultimate goal of a truly functional Body Sensor Network (BSN) capable of providing continuous information about an individual's personal health status.

Micro-fluidic devices will also play a key role with regard to the chemo/bio-sensing of bodily fluids. In these systems, a simplified and a more user-friendly fluid handling technology must be achieved such as low/zero power passive pumps or capillary force driven micro-fluidics. Moreover, the integration of reliable high-performance sensing materials will have a significant impact on the future expansion of the point-of-care market.

The work presented in Chapters 3 to 7 of this thesis followed two main streams: the technological development of wearable micro-fluidic devices and the study of materials suitable for the realisation of such systems.

Chapters 3 and 4 described the development and the performance of wearable micro-fluidic devices for measuring the pH of sweat in a real scenario. Although both systems had simple colorimetric read-out capabilities, an electronics-free sensor, *i.e.* micro-fluidic barcode, provides a more user-friendly method of performing the same type of analysis. In fact, since the colorimetric detection can be remotely monitored by means of recording systems such as cameras, there is no need to wear electronics of any kind. In addition to this, there are other reasons why the micro-fluidic barcode gives better performance compared to the system presented in chapter 3. Firstly, the use of ionogels for the sensing of pH was found to be particularly convenient as ionogels are easy to pattern inside the micro-fluidic structure, giving a high reproducibility in the fabrication/performance of the sensor when compared to the micro-fluidic device in which a cotton thread was integrated inside the micro-channel. In fact, in the latter wearable sensor, the alignment of the cotton thread was found to be particularly critical to the reproducibility of the sensor, as revealed in the data presented in figure 3.6 (pumping rate *vs.* time), in which the pumping rate presented significant device-to-device variation (large error bars). Moreover, ionogels doped with pH dyes provide improved chemical and mechanical stability of the sensing material over time. For instance, micro-fluidic barcodes

stored at ambient conditions over a year, showed virtually identical response when re-tested. The high performance of this sensing material most likely arises from the encapsulation of the IL within the pNIPAAm hydrogel. The IL provides a suitable microenvironment for the immobilisation of the pH dyes, while also conferring mechanical flexibility to the final soft material, which does not become brittle under low-humidity conditions (in contrast to hydrogels).

The conclusion is that both the proposed micro-device platform and the sensing material, employed for the study presented in chapter 4, represent a valid and appropriate approach for addressing the aims of this thesis. Nevertheless, further optimisation of the wearable sensor is desirable, and therefore in the following chapter, section 8.1, it is proposed to further develop the colorimetric detection method by processing the video data with the HSV (Hue Sharpness Value) colour space, rather than the more common RGB.

In chapters 5 and 6, respectively, the development of an organic electrochemical transistor (OECTs) for lactate detection and the study of a stable formulation for its bioreceptor (Lactate Oxidase) were discussed, with the ultimate goal being the real-time monitoring of lactic acid in sweat, during exercise. This is a particularly important target species, as lactate concentration increases in sweat during physical exercise, and it is a useful parameter to monitor wellness, physical fitness and the effectiveness of exercise.[1]

The use of OECTs for lactate sensing represents an interesting and novel strategy for future integration of this biosensor into a wearable platform. There are several advantages on the use of OECTs compared to more conventional sensor platforms, such as easy integration into electronic circuits and operation at low potentials. In addition to this, the OECTs presented in chapter 5 were entirely made of PEDOT:PSS, which makes them very low-cost and compatible with industrial stamping processes, such as roll-to-roll production. The following section 8.2 presented preliminary results of attempts to improve the performance of the OECTs through reduction of the sensor dimensions, which could also make it possible to be incorporated into a completely wearable configuration.

However, further improvements could also be made to the incorporation of the ionogel solid-state electrolytes into the transistor structure. An issue that should be addressed in future generations of these wearable biosensors is the delamination of the ionogel from the top of the transistor upon the addition of the sweat samples. In

the current configuration the ionogel swells and curls when multiple additions of the analyte are performed, causing the detachment of the ionogel, which compromises the proper operability of the organic electrochemical transistor.

Several approaches can be pursued to address this problem. As high definition features can now be easily manufactured using photolithography, the ionogels could be patterned onto a defined compartment of the transistor, such as the gate electrode, in which the enzymatic reaction takes part and is detected. Moreover, in order to avoid delamination of the ionogel from the PEDOT:PSS gate surface, it would be possible to form an interpenetrating network between the CPs and the ionogel polymeric matrices. In fact, a valuable study would be to try to understand the conditions, *e.g.* temperature and time, necessary for the ionogel precursor solution to swell and diffuse into the PEDOT:PSS layer, so as to obtain a robust contact between the ionogels with the CPs. Alternatively, other materials could also be employed for the modification of the gate electrode. For example a redox hydrogel may further improve the biosensor performance presented in chapter 5, in which a freely diffusing electrochemical mediator, *i.e.* ferrocene, had to be employed. In fact, it would be highly desirable to perform the immobilisation of the electrochemical mediator onto the polymeric matrix of the ionogel backbone in order to avoid leaching of active components from the sensor. This in turn may lead to a more stable and reproducible biosensor response over longer periods of time, for example sweat analysis during the course of an athlete training session.

However, the strategy proposed here should also consider the results obtained in chapter 6. In fact, although the use of hydrated ILs did not provide improved long-term stability compared to PBS and choline chloride, those results suggest that a further enhancement the biosensor performance may be possible. In fact, the use of ILs in these type sensors is desirable for the same reasons presented for the barcode micro-fluidics: the chemical and mechanical stability of the resulting ionogel matrix over a prolonged period of time will be greatly improved. In fact, it is difficult to create mechanically stable hydrogels even with a plasticiser, and many ILs inherently provide this function (so no additional plasticiser is needed).

Finally, it is worth highlighting that other approaches can be pursued for the development of wearable biosensors. For instance, integration of nanomaterials onto fabrics can give new opportunities for the development of wearable lactate sensors. In this regard, section 8.2 will discuss new approaches in which graphene and the

contact stamping technique discussed in chapter 7 could open new possibilities for the realisation of very low-cost, wearable chemical sensors and biosensors.

8.1 Wearable Micro-fluidic pH Sweat Sensing: a Promising Improvement

8.1.1 Introduction

Chapter 4 described a wearable micro-fluidic barcode for real-time sweat sensing using a camera and the RGB (Red Green Blue) colour space. The promising performance of this system makes additional development of the micro-fluidic barcode sensor an interesting option, in order to explore whether its performance can be further enhanced.

In terms of the wearability of the sensor, the second generation of the micro-fluidic barcode presents a more compact and flexible format which increases the freedom for the wearer during exercise and reduces discomfort to a minimum.

Improvements to the performance of the micro-fluidic system have also been undertaken, through the use of a more accurate algorithm for colorimetric image analysis. In fact, the system presented in chapter 4 had limited accuracy ~ 0.49 pH units, when used during exercise. It is envisioned that the new sensor configuration will improve the accuracy of the pH analysis towards 0.2 pH units.

8.1.2 Results and Future Work

To improve the wearability of the barcode, the sharp corners of the old device were replaced by round edges, achieving a more circular configuration, as shown in Figure 8.1. This small modification reduces the discomfort for the wearer and at the same time it does not affect the operability of the sensor.

In addition, the sweat absorbing patch area was re-engineered in order to make it reusable. In this new configuration the absorbing material of the passive pump system can be replaced at the end of each trial and, once substituted with new one, the device is ready to be used again.

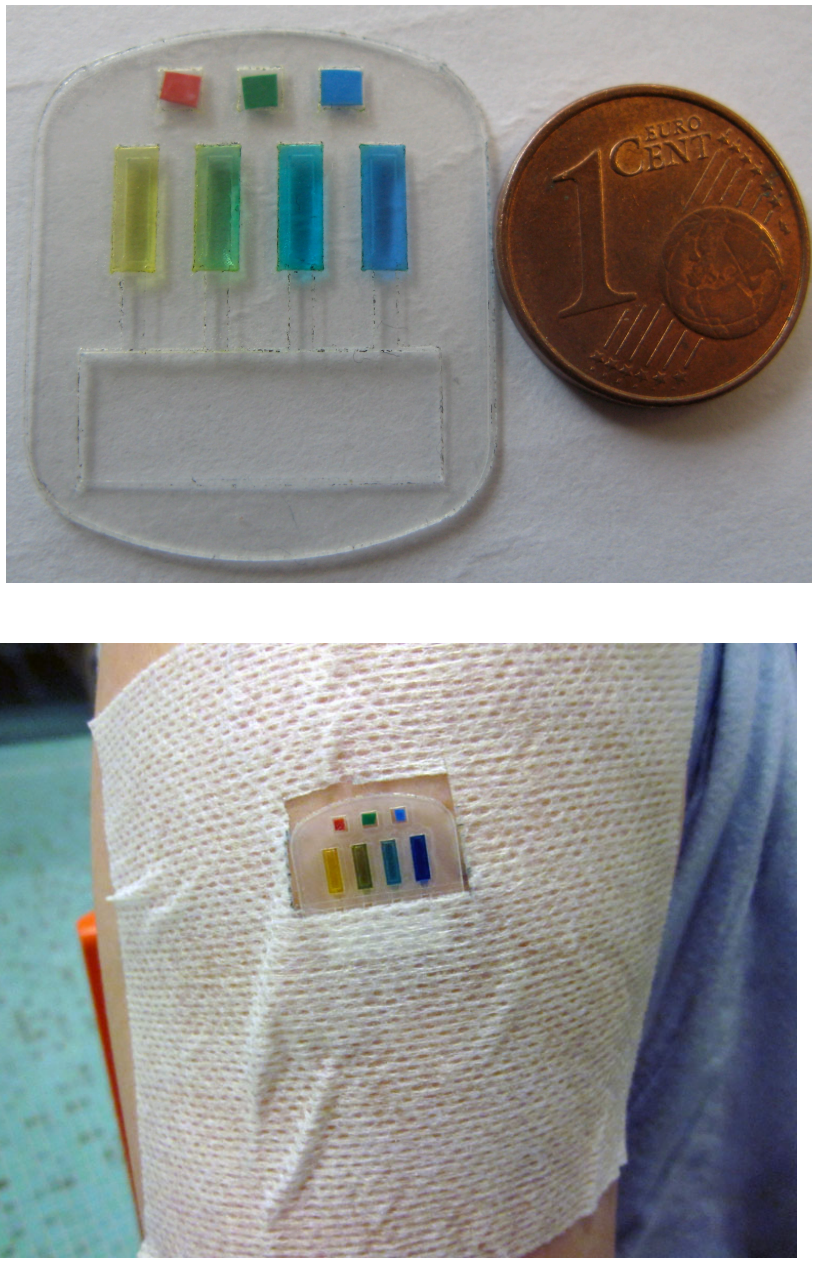

Figure 8.1. Redesigned configuration of the micro-fluidic barcode with improved wearability (top) and its integration on the forearm of an athlete (bottom).

In order to further develop the performance of the device, a different colour space than RGB was explored, specifically the HSV colour space. Recently, it has been shown that better performance in remote colorimetric detection may be possible using the Hue component of the cylindrical HSV colour space instead of the three components of the RGB space.[2] In particular, the RGB components do not respond uniformly to induced light variation, such as shadow and changes in the ambient light conditions, while the Hue component appears to be much less impacted by such effects. These advantages can be particularly important if the device is to be used

under different lighting conditions, for instance under variable indoor or outdoor conditions during exercise.

Preliminary studies have been carried out on the performance of coupling this image processing approach with the wearable micro-fluidic barcode sensor. The calibration curves for the four ionogels that form the sensor detection area were obtained by exposing each of the ionogels for five minutes to solutions of known pH from 3.0 to 10.0 in 0.5 pH steps. The analysis of the colour changes of the ionogel barcode was performed by means of an OpenCV computer vision library.

Figure 8.2 presents the calibration response curves of each pH dye-doped ionogel when analysed using the Hue component of the HSV colour space. Considering the great variation of the Hue values for the four ionogels, it appears that the proposed method might be successfully applied for pH estimation in a real scenario. Moreover, each pH dye doped-ionogel shows excellent correlation to a sigmoidal regression model with a R^2 value greater than 0.995.

Further improvements will focus on the development of an automated code through which varying environmental light conditions can be normalised in order to enable auto-compensation of light fluctuations, and minimisation of the noise in the picture, which mainly arises from the athlete's movements. For the latter issue it has been shown that the Hue value is able to perform reliable measurements even when pictures are taken completely out of focus, a particular characteristic that can assist pH monitoring via the device during physical activity.[3]

More recently it was decided to develop a new technique for colorimetric detection in real time, through the use of a video camera instead of a still-image camera. The main advantages of using video cameras are the higher frame recording capability, which can dramatically improve the overall performance of the system as more data can be collected and averaged.

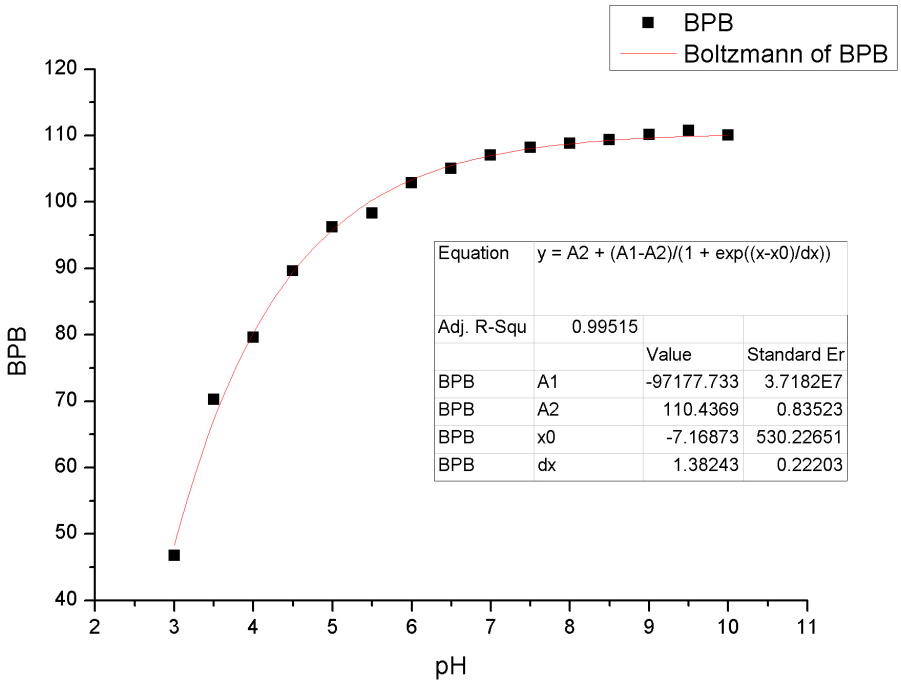

Equation	y = A2 + (A1-A2)/(1 + exp((x-x0)/dx))		
Adj. R-Squ	0.99515		
		Value	Standard Er
BPB	A1	-97177.733	3.7182E7
BPB	A2	110.4369	0.83523
BPB	x0	-7.16873	530.22651
BPB	dx	1.38243	0.22203

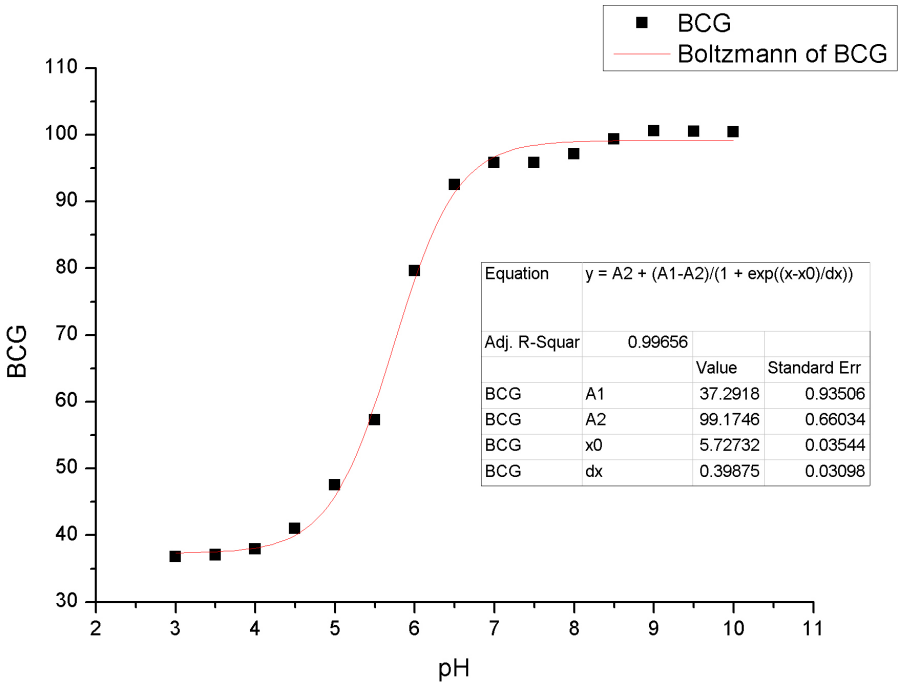

Equation	y = A2 + (A1-A2)/(1 + exp((x-x0)/dx))		
Adj. R-Squar	0.99656		
		Value	Standard Err
BCG	A1	37.2918	0.93506
BCG	A2	99.1746	0.66034
BCG	x0	5.72732	0.03544
BCG	dx	0.39875	0.03098

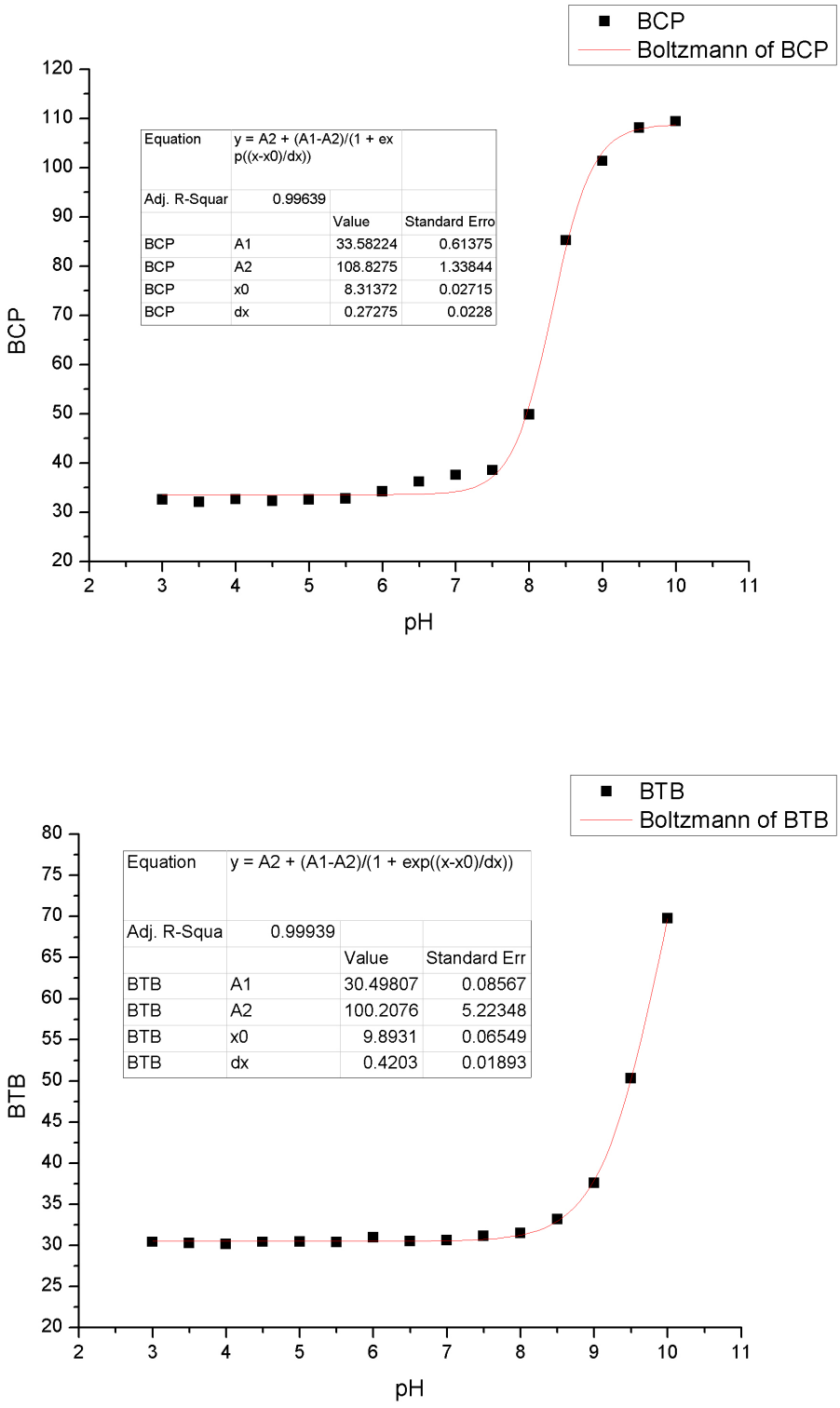

Figure 8.2. Calibration curves, camera's response, to colorimetric changes of the pH dyes/ionogel: from top to bottom Bromophenol Blue (BPB), Bromodresol Green (BCG), Bromocresol Purple (BCP), Bromothymol Blue (BTB) in the micro-fluidic device.

Preliminary studies have been already undertaken, as shown in Figure 8.3 during a cycling trial.

Figure 8.3. Cycling trial where video camera was used to simultaneously monitor the colour changes of 4 different the barcode in real-time *(left)*. 4 different barcode placed on the lower back and shoulder during recording *(right)*.

Finally, it should be appreciated that using a video camera for continuous colorimetric detection could provide a route to a more integrated BSN for sport applications. In fact, state-of-the-art video cameras used to record sport events (*e.g.* Olympic games 2012) [4] have been used to track the movements of the athletes and, therefore, it is believed that they could be potentially used for the detection of on-body chemical and biochemical colorimetric sensors. Continuing technological advances in this field have witnessed the development of gigapixel resolution cameras, which could offer extraordinary capacity for image-based remote sensing, including colorimetric chemical sensing and biosensing.[5]

8.2 Electrochemical Sensing of Lactate: Opportunities and Challenges

For the realisation of the next generation of sweat wearable sensors, lactate should be considered as one of the main analytical targets. Based on the results presented in chapter 6, future research with these devices should focus on the integration of the lactate sensors into a wearable platform using a form of LOx that is stable in hydrated Ionic Liquids (HyILs/LOx).

Initial work in this regard has been carried out in order to explore ways to improve upon the performance of the first generation solid-state electrolyte OECT sensors. For example, improved response time has been achieved through reduction of the electrode dimensions (Figure 8.4-a). These improved OECTs also have improved lifetimes in comparison to the system described in chapter 5. Moreover, the parallel integration of a pump-less configuration [6] through a de-gas driven micro-fluidic system is under investigation. In fact, taking advantage of the high solubility of air in PDMS it is possible to generate spontaneous sweat movement through micro-channels, by simply degassing the PDMS before use.

Chapter 2 gave a wide overview of novel materials that have great potential for biomedical applications, such as ionic liquids and ionogels, metal nanoparticles, nanocomposites and carbon-based nanomaterials. Since the discovery of graphene in 2004,[7] interest has risen exponentially in applications for this promising material, mainly driven by its exceptional electrocatalytic, mechanical and electronic properties. However, graphene is not normally water dispersible but its oxide form, graphene oxide (GO), does form stable water dispersions.[8] Such stable GO dispersions can be used as an ink for patterning onto plastic substrates and can subsequently be reduced to graphene (reduced graphene oxide – rGO).[9]

Using a similar approach, Molina *et al.*[10] showed it was possible to functionalise polyester fibers by dip-coating with rGO, achieving a conductivity of 23.15 Ω cm^{-2} just with three rGO coatings. The possibility of obtaining highly conductive fabrics, yet flexible, opens new routes for the development of wearable sensors and biosensors. Very recently, a similar approach was employed to generate pH, K^+ and NH_4^+ sensors using cotton yarn coated with carbon nanotubes. [11]

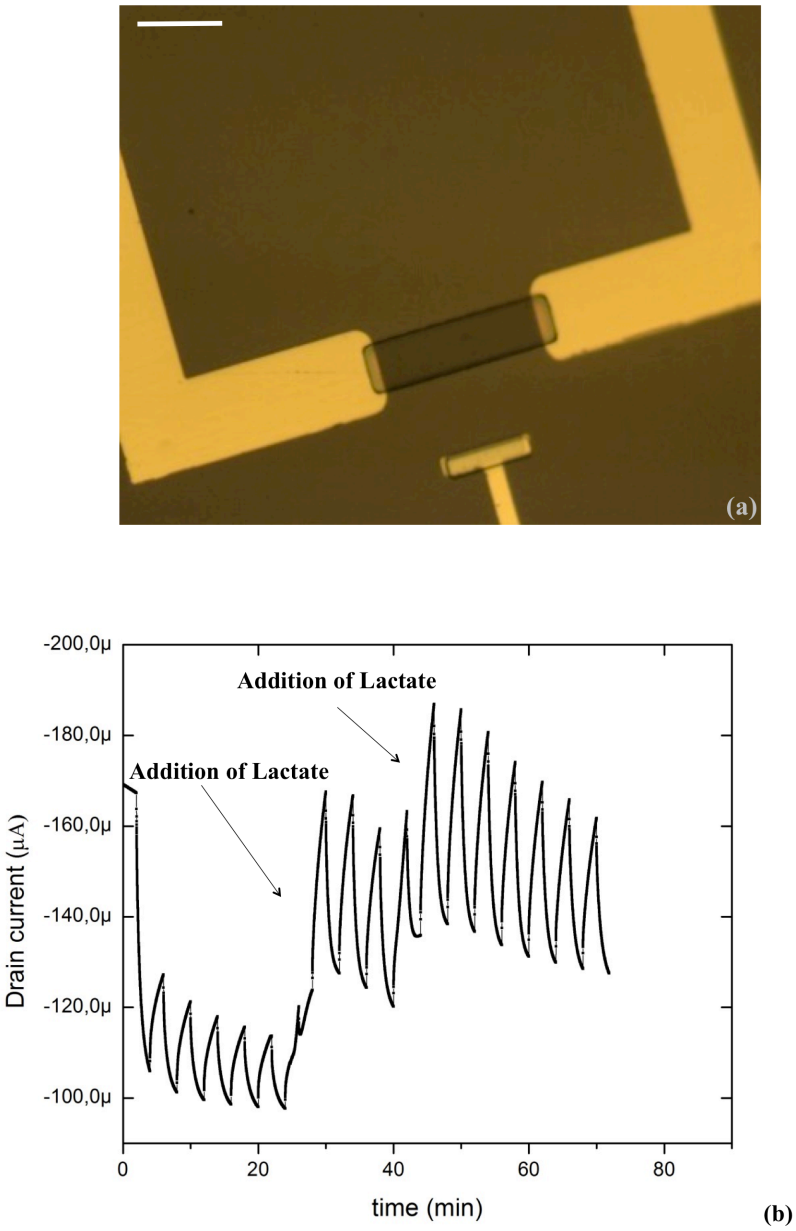

Figure 8.4. Picture of the improved generation of the OECTs, with reduced geometry (channel 100 × 25 µm and gate 10 × 25 µm; scale bar 50 µm) *(a)* and initial experiments for multiple detection of lactate *(b)*. The two additions of lactate were performed using 2 µL of PBS (pH 7.00) carrying 5 mM of the substrate.

Using this approach, initial work has been undertaken toward the functionalisation of lycra fabric with rGO to obtain a flexible electrode material which can be used for the realisation of an electrochemical lactate sensor on textile. In particular, using state-of-the-art machinery, such as spray coater, it is possible to

selectively functionalise lycra, as shown in Figure 8.5. The characterisation of the material is currently under investigation.

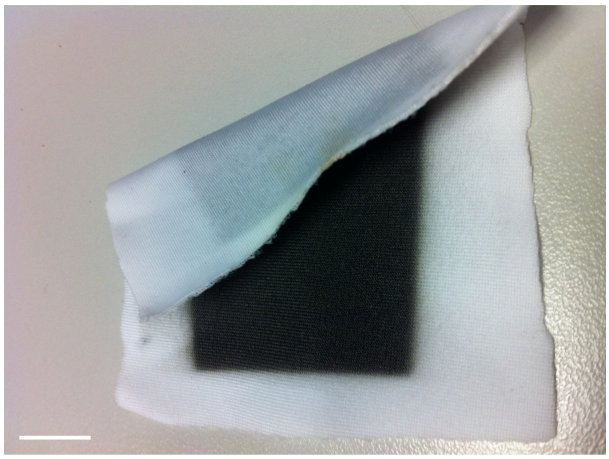

Figure 8.5. Commercially available lycra fabric spray coated only on one side with rGO. Spray coating was performed using water dispersible GO, which was reduced to rGO using hydrazine (scale bar 1 cm).

The integration of such sensors in a wearable platform is one of the main challenges still to be achieved following from the work described in this thesis. The stamping technique for generating paper-based micro-fluidics presented on chapter 7 could be used to create micro-fluidic structures on textiles in which the electrochemical lactate sensor would be integrated within the area of the micro-fluidic channel (ink uncovered area). A similar micro-fluidic device was recently produced by Xing *et al.*[12], through the micropattering of textile using a fluorinate based superhydrophobic coating. This promising approach of selectively pattering textiles could provide a simple means for the future fabrication and integration of sensors in off-the-shelf T-shirts.

8.3 Conclusions

The strategies discussed and explored in this chapter offer exciting opportunities for the future progress of the area of body (chemo/bio)sensor networks. Fully functional wearable chemo/bio-sensors are still beyond the current state of the art, but developments in materials chemistry do offer new approaches to advancing the

concept. In addition to the technical challenges of performing remote on-body monitoring of key chemical and biological markers, emphasis must also be given to the device wearability, and to the physical interface of the sensor with the wearer. In that regard, integration of chemo/bio-sensors on textiles can provide better performing devices, as they can be held in tight contact with the skin, which is important for valid sweat sampling. Additionally, their physiological relevance of the monitored sweat target parameters should be also established, for example, through parallel studies of sweat and blood samples.

8.4 References

1. Green, J.M.; Pritchett, R.C.; Crews, T.R.; McLester, J.R.; Tucker, D.C., Sweat lactate response between males with high and low aerobic fitness. *Eur. J. Appl. Physiol.* **2004**, *91*, 1-6.
2. Fay, C.; Lau, K.-T.; Beirne, S.; Conaire, C.; McGuinness, K.; Corcoran, B.; O'Connor, N.E.; Diamond, D.; McGovern, S.; Coleman, G.*, et al.*, Wireless aquatic navigator for detection and analysis (wanda). *Sensors Actuators B: Chem.* **2010**, *150*, 425-435.
3. Garcia, A.; Erenas, M.M.; Marinetto, E.D.; Abad, C.A.; de Orbe-Paya, I.; Palma, A.J.; Capitan-Vallvey, L.F., Mobile phone platform as portable chemical analyzer. *Sensors Actuators B: Chem.* **2011**, *156*, 350-359.
4. http://www.techradar.com/news/television/bbc-talks-super-hi-vision-plans-for-london-2012-1068914, Seen june 11th 2013 **2012**, *March 6th*.
5. Brady, D.J.; Gehm, M.E.; Stack, R.A.; Marks, D.L.; Kittle, D.S.; Golish, D.R.; Vera, E.M.; Feller, S.D., Multiscale gigapixel photography. *Nature* **2012**, *486*, 386-389.
6. Dimov, I.K.; Basabe-Desmonts, L.; Garcia-Cordero, J.L.; Ross, B.M.; Ricco, A.J.; Lee, L.P., Stand-alone self-powered integrated microfluidic blood analysis system (simbas). *Lab on a Chip* **2011**, *11*, 845-850.
7. Novoselov, K.S.; Geim, A.K.; Morozov, S.V.; Jiang, D.; Zhang, Y.; Dubonos, S.V.; Grigorieva, I.V.; Firsov, A.A., Electric field effect in atomically thin carbon films. *Science* **2004**, *306*, 666-669.
8. Lerf, A.; He, H.; Forster, M.; Klinowski, J., Structure of graphite oxide revisited‚äñ. *The Journal of Physical Chemistry B* **1998**, *102*, 4477-4482.
9. He, Q.; Sudibya, H.G.; Yin, Z.; Wu, S.; Li, H.; Boey, F.; Huang, W.; Chen, P.; Zhang, H., Centimeter-long and large-scale micropatterns of reduced graphene oxide films: Fabrication and sensing applications. *ACS Nano* **2010**, *4*, 3201-3208.
10. Molina, J.; Fernandez, J.; Ines, J.C.; del Rio, A.I.; Bonastre, J.; Cases, F., Electrochemical characterization of reduced graphene oxide-coated polyester fabrics. *Electrochim. Acta* **2013**, *93*, 44-52.
11. Guinovart, T.; Parrilla, M.; Crespo, G.A.; Rius, F.X.; Andrade, F., Potentiometric sensors using cotton yarns, carbon nanotubes and polymeric membranes. *Analyst* **2013**, 138, 5208-5215.
12. Xing, S.; Jiang, J.; Pan, T., Interfacial microfluidic transport on micropatterned superhydrophobic textile. *Lab on a Chip* **2013**, *13*, 1937-1947.

Appendix A

Supporting information for

Concept and Development of an Autonomous Wearable Micro-fluidic Platform for Real Time pH Sweat Analysis

Vincenzo F. Curto[1], S. Coyle[1], R. Byrne[1], N. Angelov[1], D. Diamond[1], F. Benito-Lopez[1*]

Sensors and Actuators B: Chemical 175 (2012) 263–270

ISSN: 0925-4005; http://dx.doi.org/10.1016/j.snb.2012.02.010

[1]CLARITY: Centre for Sensor Web Technologies, National Centre for Sensor Research, School of Chemical Sciences, Dublin City University, Dublin 9, Ireland

* Author to whom correspondence should be addressed;

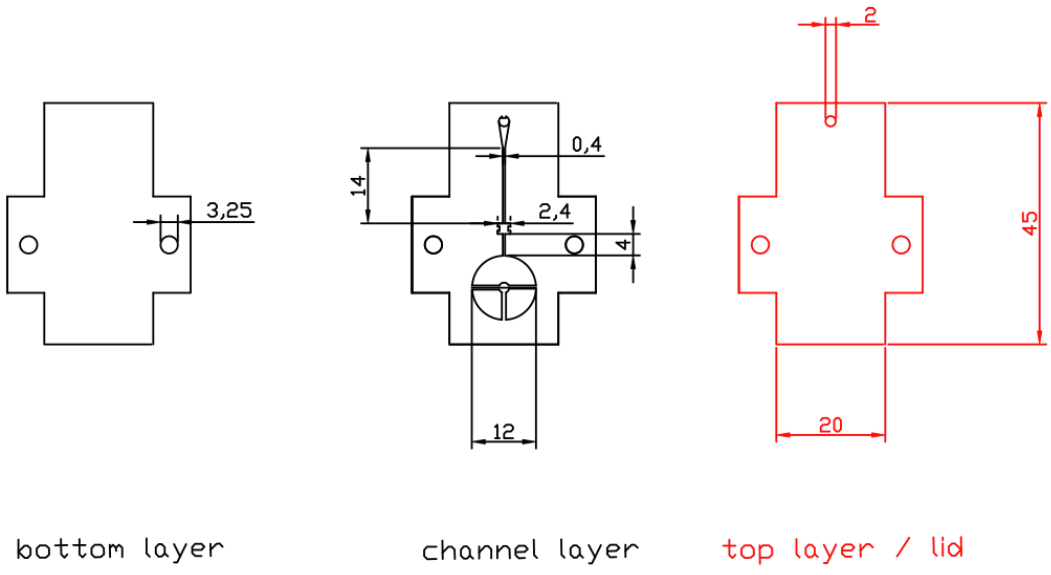

Figure A1. Scheme of the micro-fluidic layout made in AutoCAD (© 2010 Autodesk, Inc.). Bottom layer (left), microchannel layer (center) and top layer (right). All dimensions in mm.

Appendix B

Supporting information for

Real-Time Sweat pH Monitoring Based on a Wearable Chemical Barcode Micro-fluidic Platform Incorporating Ionic Liquids

Vincenzo F. Curto[1], C. Fay[1], S. Coyle[1], R. Byrne[1], C. O'Toole[1], C. Barry[1], S. Hughes[2], N. Moyna[2], D. Diamond[1], F. Benito-Lopez[1*]

Sensors and Actuators B: Chemical 171-172 (2012) 1327–1334

ISSN: 0925-4005; http://dx.doi.org/10.1016/j.snb.2012.06.048

[1]CLARITY: Centre for Sensor Web Technologies, National Centre for Sensor Research, School of Chemical Sciences, Dublin City University, Dublin 9, Ireland

[2]School of Health and Human Performance, Dublin City University, Dublin, Ireland

* Author to whom correspondence should be addressed;

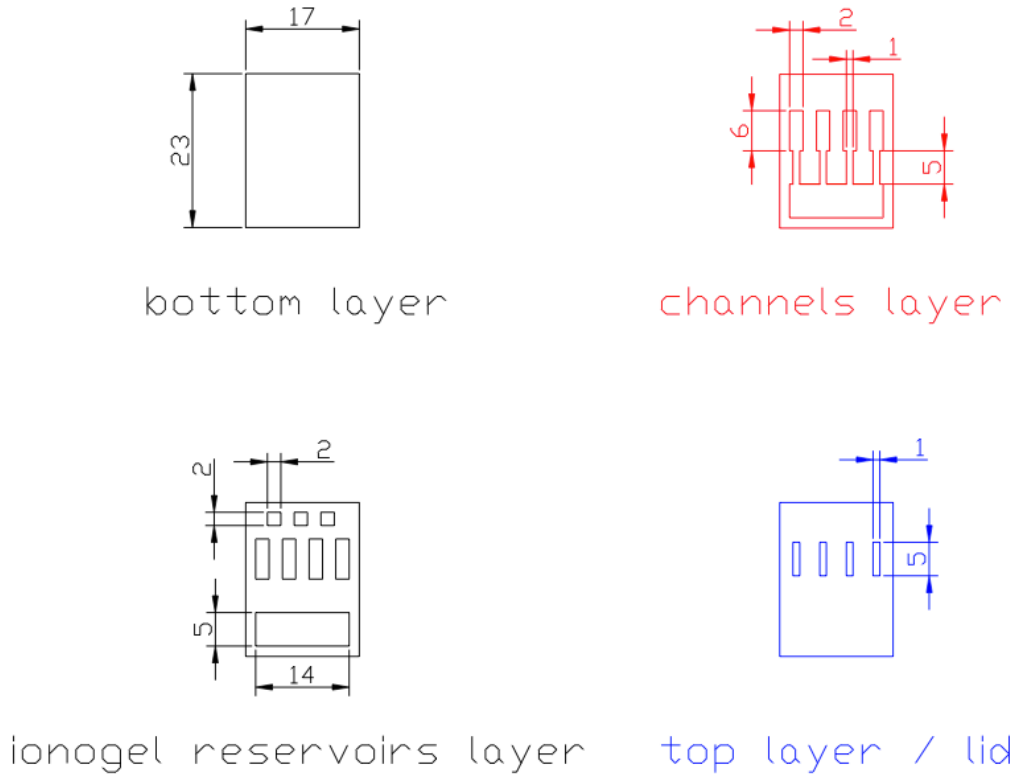

Figure B1. Scheme of the micro-fluidic layout made in AutoCAD (© 2010 Autodesk, Inc.). Bottom layer (*top left*), microchannel layer (*top right*), ionogel reservoir layer *(bottom left)* and top layer *(bottom right)*. All dimensions in mm.

Appendix C

Supporting information for

Organic Electrochemical Transistor Incorporating an Ionogel as Solid State Electrolyte for Lactate Sensing

Dion Khodagholy†[1], Vincenzo F. Curto†[2], Kevin J. Fraser[2], Moshe Gurfinkel[1], Robert Byrne[2], Dermot Diamond[2], George G. Malliaras[1], Fernando Benito-Lopez[2] and Roisin M. Owens[1]*

Journal of Material Chemistry 22 (2012), 4440–4443

ISSN: 1364-5501; DOI: 10.1039/C2JM15716K

[1]Department of Bioelectronics, Ecole Nationale Superieure des Mines, CMP-EMSE, MOC, F-13541 Gardanne, France

[2]CLARITY: Centre for Sensor Web Technologies, National Centre for Sensor Research, School of Chemical Sciences, Dublin City University, Dublin 9, Ireland

† Both authors contributed equally to this work.

* Author to whom correspondence should be addressed;

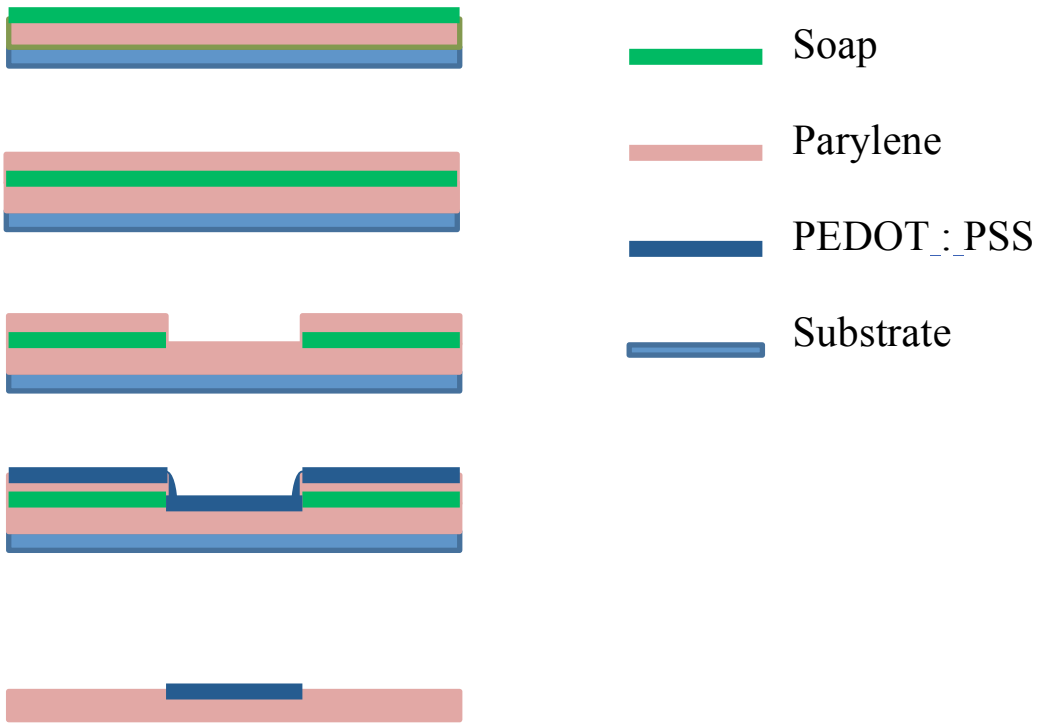

Figure C1. Schematic representation of the steps involved in the realisation of the conformal transistor. From top to bottom: (1) deposition of parylene C (main substrate) and a layer of soap, (2) deposition of a second layer of parylene C (sacrificial), (3) dry etch using O_2 plasma to define the OECT structure, (4) spin-coating of PEDOT:PSS and (5) peeling off of sacrificial parylene C layer to reveal the PEDOT : PSS channel and the gate electrode.

Appendix D

Supporting information for

Fast Prototyping of Paper-based Micro-fluidic Devices by Contact Stamping Using Indelible Ink

Vincenzo F. Curto[‡1], Nuria Lopez-Ruiz[‡2], L. F. Capitan-Valley[3], A. J. Palma[2], F. Benito-Lopez[1, 4, *] and D. Diamond[1]

Lab on a Chip – Submitted

[1]CLARITY: Centre for Sensor Web Technologies, National Centre for Sensor Research, School of Chemical Sciences, Dublin City University, Dublin 9, Ireland

[2] ECSENS, Dept. of Electronics and Computer Technology, ETSIIT, University of Granada, Granada, Spain.

[3] ECSENS, Dept. of Analytical Chemistry, Faculty of Sciences, University of Granada, Granada, Spain.

[4] CIC microGUNE, Arrasate-Mondragón, Spain.

* Author to whom correspondence should be addressed;

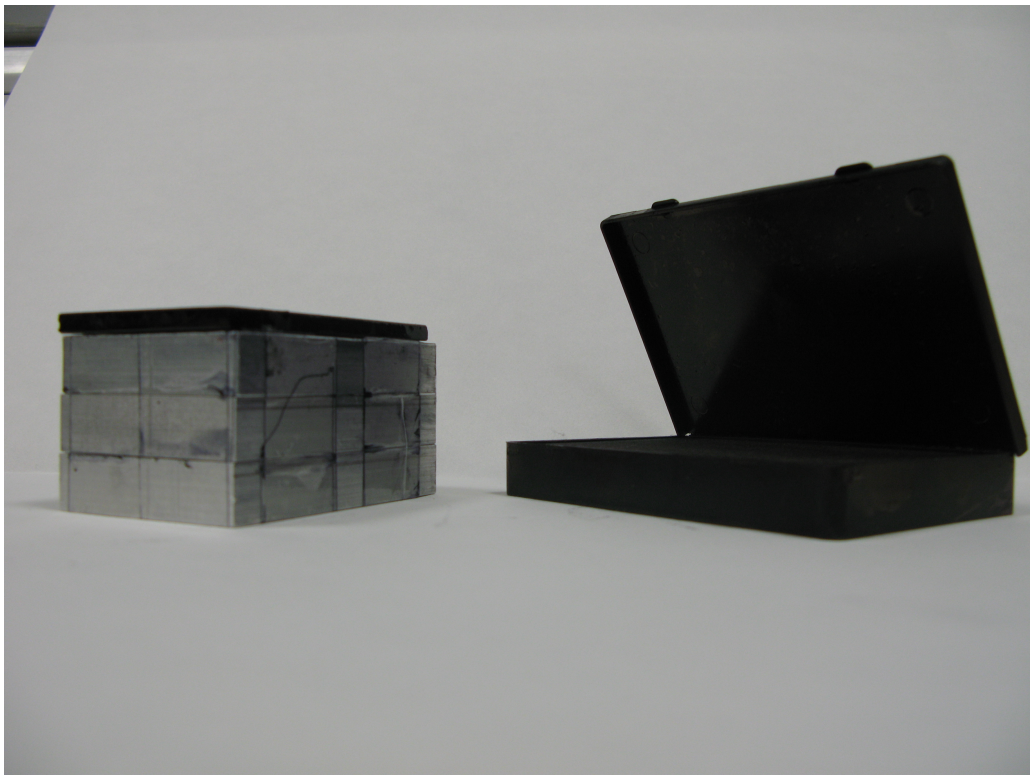

Figure D1. Picture of the contact stamping apparatus. Rectangular prism made of aluminum and a layer of a black ceramic material (left), stone pad saturated with ink (right).

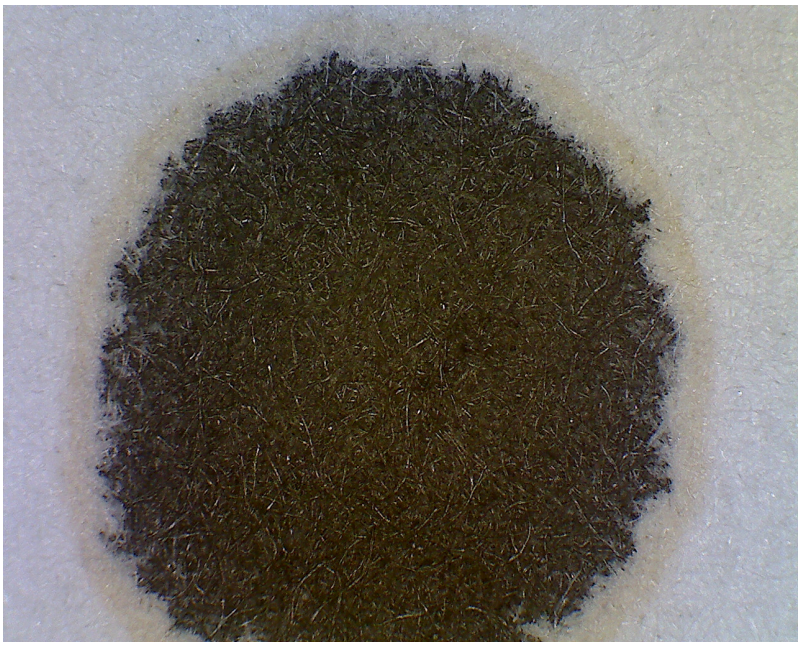

Figure D2. Yellowish ring generated from the staining of Whatman grade 1 using Black Noodler's Ink™.

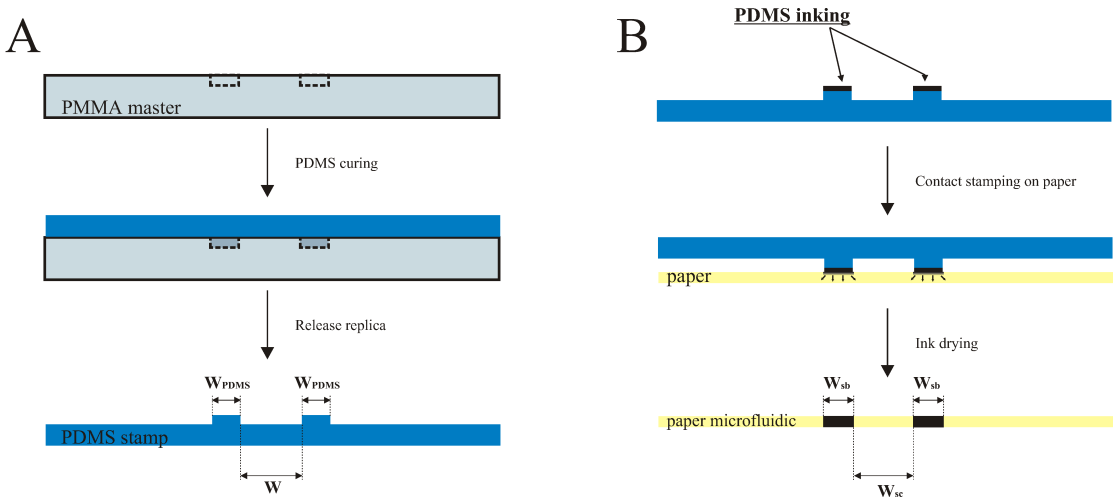

Figure D3. A) Scheme of the fabrication of the PDMS stamp and B) steps involved on the contact stamping of open straight channels for the experiments describe on Figure 3. W_{PDMS} represents the width of the PDMS stamp features, while W is the designed channel width. After performing the contact stamping on paper, the generated fluidic structures are characterised by W_{sb}, which is the stamped border width on the paper (with $W_{sb} > W_{PDMS}$) and W_{sc}, which is the stamped channel width on the patterned paper (with $W_{sc} < W$).